B 会場 : 11/26 PM2(14:50-16:20)

14:50~15:05:00

グローバルシミュレーションによる LLBL の成因と構造の解明

#田中 高史 ¹⁾
(¹REPPU 研

Origin and structure of the LLBL elucidated by the global simulation

#Takashi Tanaka¹⁾
(1REPPU code institute

Adopting REPPU (REProduce Plasma Universe) code level 8, we reproduced the solar wind-magnetosphere-ionosphere (S-M-I) interaction when the interplanetary magnetic field (IMF) is obliquely northward, and investigated the relationship between the low-latitude boundary layer (LLBL) and the projection structure of ionospheric convection cells. When the IMF is obliquely northward, the ionospheric convection cells consist of a central lobe + round merging cell (which constitutes the exchange cycle), a reciprocal cell on the opposite side in the morning and evening, a nighttime cell, and two viscous cells at low latitudes. In the magnetosphere, the medium-speed LLBL is formed between the high-speed solar wind and the low-speed magnetospheric interior. From the connection of magnetic field lines, the outer half of the LLBL is projected onto the lobe cell, and the inner half onto the round-merging cell. From the origin of the lobe + round merging cell, it is estimated that both the open and closed magnetic field lines in the LLBL have been the IMF until recently, and especially the open magnetic field lines in the outer half have been the solar wind until more recently. It is not surprising that the LLBL contains particles similar to solar wind particles. Such projection structure is consistent with satellite observations which show that the outer half of the LLBL only appears when the IMF is northward, and that the nature of the particles is more similar to magnetosheath particles. These results indicate that the LLBL is a passway for anti-sunward convection involving an open magnetic field. The LLBL is Kevin-Helmholtz (KH) unstable, and KH waves propagating along the inner boundary of the LLBL penetrate deep into the magnetosphere. This wave can drive two viscous cells, one in the morning side and one in the evening side, which consist only of closed magnetic field.

REPPU (REProduce Plasma Universe) コードレベル8によって、interplanetary magnetic field (IMF) 斜め北向きの時の太陽風一磁気圏一電離圏(S-M-I)相互作用を再現し、low-latitude boundary layer (LLBL) と電離圏対流セルの投影関係を調べた。IMF 斜め北向きの時、電離圏対流セルは中央のローブ+(交換サイクルを構成する)round merging セル、それと朝夕反対側にある reciprocal セル、夜間セル、低緯度の2つの粘性セルの計5つからなる。磁気圏では高速の太陽風と低速の磁気圏内部の間に、中速度のLLBL が形成される。磁力線の接続から、LLBL の外半分はローブセルに、内半分は round-merging セルに投影される。ローブ+ round merging セルの成因から推定すると、LLBL にある開磁力線と閉磁力線は、共に最近まで IMF であったものであり、特に外半分の開磁力線はより最近まで太陽風であったものと推定される。LLBL に太陽風粒子に似た粒子が存在するのは当然である。この投影構造は、LLBL の外半分は IMF 北の時のみ現れ、粒子の性質はよりマグネトシース粒子に近いという衛星観測とも、consistent である。これらの結果は、LLBL とは開磁場を含む反太陽向き対流のルートであることを示している。LLBL は Keivin-Helmholtz (KH) 不安定であり、LLBL の内側境界に沿って伝搬する KH 波は、磁気圏内部に深く浸透する。これによって、閉磁場のみからなる、朝夕2つの粘性セルが駆動される。

B 会場 : 11/26 PM2(14:50-16:20)

15:05~15:20:00

準定常磁気圏対流における定常性の維持、空間電荷分布、エネルギー輸送

#海老原 祐輔 $^{1)}$, 平原 聖文 $^{2,3)}$, 田中 高史 $^{3)}$ $^{(1)}$ 京都大学生存圈研究所, $^{(2)}$ 名古屋大学宇宙地球環境研究所, $^{(3)}$ 九州大学

Stationarity, space charge distribution, and energy transfer in the quasi-steady magnetospheric convection electric field

#Yusuke Ebihara¹⁾, Masafumi HIRAHARA^{2,3)}, Takashi TANAKA³⁾
⁽¹Kyoto University, ⁽²Nagoya University, ⁽³Kyushu University

The dawn-dusk electric field on the dayside is known to persist in the magnetosphere when the interplanetary magnetic field (IMF) is southward. Two fundamental questions arise regarding the queasy-steady convection electric field. First, is the quasi-steady dawn-dusk convection electric field in the magnetosphere caused by space charge that deposits in the magnetosphere? Secondly, how is the quasi-steady electric field sustained? Using the basis of global MHD simulations, we obtained the following results and inferences. (1) Near the equatorial plane, positive space charge dominates the duskside magnetosphere, while the negative space charge dominates the dawnside magnetosphere. (2) Space charge accumulation in the magnetosphere alone cannot account for the dawn-dusk electric field. Instead, plasma motion plays a primary role in generating the dawn-dusk electric field as previously suggested. (3) Steady convection electric field can be established when plasma flow remains steady. Even under such steady conditions, magnetic energy is continuously transferred from the solar wind to the polar ionosphere, as manifested by integral curves of the Poynting flux vector. This unidirectional energy flow is associated with the convective plasma motion that produces the steady dawn-dusk electric field. (4) The magnetosphere basically maintains equilibrium through a balance of unidirectional energy flow from the solar wind to the ionosphere. (5) When the equilibrium is partially disrupted (for example, in the near-Earth tail region during the substorm growth phase), the electric field becomes inductive. For the large-scale convection electric field, whether the electric field is electrostatic or inductive depends on the state of equilibrium.

B 会場 : 11/26 PM2(14:50-16:20)

15:20~15:35:00

水星磁気圏夜側領域に見られる特徴的な磁場構造を用いた電流構造の解析

#小川 琢郎 $^{1)}$, 篠原 育 $^{2)}$, 村上 豪 $^{2)}$ $^{(1)}$ 東大, $^{(2)}$ 宇宙航空研究開発機構

Current structures from magnetic field configurations in Mercury's nightside magnetosphere

#Takuro Ogawa¹⁾, Iku SHINOHARA²⁾, Go MURAKAMI²⁾

(1The University of Tokyo, (2Japan Aerospace Exploration Agency/Institute of Space and Astronautical Science

It is widely known that Mercury's magnetosphere is like Earth's. There may be many structures that are unique or like Earthe's but are different in time scale and spatial scale since the strength of Mercury's magnetic field and physical parameters such as solar wind are different. MESSENGER is the only satellite that orbited and observed Mercury's magnetosphere for a long time. However, its details are still unknown because there were many constraints on the MESSENGER observation.

Focusing on the magnetic field observation of MESSENGER, we find a characteristic depression structure in the nightside magnetosphere. Even in a series of orbits where the satellites pass over almost the same region, this depression structure may or may not be observed. This observational feature suggests that this structure changes on a time scale of a few hours. The structure is observed over a wide region in the nightside magnetosphere. Several previous studies have concluded that this structure is due to the tail current sheet crossing, and no in-depth studies have been conducted. However, when we focus on the magnetic field components that create this depression structure, we find that the main components are different between those observed near Mercury and those observed on the magnetospheric structure other than the tail current sheet.

In this study, we refer to this structure as a "dip" and conduct an analysis using both magnetic field and plasma data. Our results indicate that the dip is closely related to nightside currents, previously unresolved in detail, based on magnetic field-derived current calculations, plasma temperature, and its dependence on solar wind dynamic pressure. These findings suggest that the ring current in Mercury's nightside magnetosphere plays a crucial role.

In this presentation, I will report on the status of our research.

水星には磁気圏があることは広く知られている。地球磁気圏とよく似た磁気圏構造も有している一方で、磁場固有磁場の強さや受ける太陽風の強さといった物理条件の違いによって、水星磁気圏特有の現象が起こることや、地球磁気圏によく似た現象であっても空間・時間スケールが大きく異なり得ることがわかっている。過去水星磁気圏を周回探査した衛星は MESSENGER のみである。しかし、MESSENGER は様々な制約を抱えていたため、その詳細は明らかになっていないことが多く残っている。

MESSENGER で観測された磁場データに注目すると、磁気圏夜側領域に特徴的な窪み構造が確認できる。衛星がほとんど同じ領域を通過する連続した周回においても、この窪み構造が観測される場合と観測されない場合がある。このことから、この構造は数時間程度の時間スケールで変化していると考えられる。

本構造は先行研究では plasma sheet によるものであると結論付けられており、それ以上の踏み込んだ研究はされてこなかった.しかし、この窪み構造の磁場成分に注目すると、水星近傍で観測されるものと尾部で観測されるものでは特徴が異なっている.このことから特に水星近傍で観測される構造は plasma sheet 以外の何らかの磁気圏構造の影響を受けていると考えられる.

本研究ではこの構造を「dip」とよび、磁場及びプラズマデータからの解析を行った。その結果、dip が磁場を用いた電流計算、プラズマの温度・太陽風動圧との関係から、従来その詳細が明らかになっていない夜側領域での ring current が重要な役割を果たしていることを示唆する結果を得た.

本講演では研究の現状について報告する.

B 会場 : 11/26 PM2(14:50-16:20)

15:35~15:50:00

かぐや衛星が捉えた月ミニ磁気圏における「電子のみ」磁気リコネクションの兆候

#荻野 晃平 $^{1)}$, 原田 裕己 $^{1)}$, 齋藤 義文 $^{2)}$, 西野 真木 $^{2)}$, 横田 勝一郎 $^{3)}$, 高橋 太 $^{4)}$, 清水 久芳 $^{5)}$, 笠原 禎也 $^{6)}$, 熊本 篤志 $^{7)}$ (1 京都大学大学院理学研究科, $^{(2)}$ 国立研究開発法人宇宙航空研究開発機構, $^{(3)}$ 大阪大学大学院理学研究科, $^{(4)}$ 九州大学理学研究院, $^{(5)}$ 東京大学地震研究所, $^{(6)}$ 金沢大学学術メディア創成センター, $^{(7)}$ 東北大学大学院理学研究科

Kaguya observations of potential electron-only magnetic reconnection signatures on the lunar mini-magnetosphere

#Kohei Ogino¹⁾, Yuki Harada¹⁾, Yoshifumi Saito²⁾, N. Masaki Nishino²⁾, Shoichiro Yokota³⁾, Futoshi Takahashi⁴⁾, Hisayoshi Shimizu⁵⁾, Yoshiya Kasahara⁶⁾, Atsushi Kumamoto⁷⁾

⁽¹Department of Geophysics, Graduate School of Science, Kyoto University, ⁽²Institute of Space and Astronautical Science, Japan Aerospace Exploration Agency, ⁽³Graduate School of Science, Osaka University, ⁽⁴Department of Earth and Planetary Sciences, Kyushu University, ⁽⁵Earthquake Research Institute, University of Tokyo, ⁽⁶Information Media Center, Kanazawa University, ⁽⁷Graduate School of Science, Tohoku University

Magnetic reconnection is a fundamental process in space plasma that causes particle acceleration by converting electromagnetic energy into charged particle energy. Recent observations by the MMS mission first reported electron-only magnetic reconnection in a thin current sheet (thinner than the ion inertial length) in the Earth's turbulent magnetosheath region, accompanied by electron outflow jets in the absence of ion outflow jets (Phan et al., 2018). Since the lunar crustal magnetic anomalies (LMAs) also exhibit spatial scales smaller than the ion characteristic scales, recent ARTEMIS observations (Sawyer et al., 2023), numerical simulations (Stanier et al., 2024), and laboratory experiences (Rovige et al., 2024) suggested that the electron-only magnetic reconnection can also occur on LMAs. However, direct observations of electron-only magnetic reconnection on LMAs have not been reported partly because the time resolution of the instruments onboard typical lunar orbiters is not sufficient to resolve such an electron-scale phenomenon. In this study, we focus on Kaguya's low-altitude (~30 km) and high-time resolution data of charged particles and electromagnetic fields. We identified an electron-scale current sheet crossing from magnetic field data, as well as simultaneous super-ion-Alfvénic electron acceleration in the minimum variance L direction, Hall magnetic fields with polarity consistent with the electron jet direction, and a flux-rope-like signature, which suggests the occurrence of multiple X-line magnetic reconnection. Our observational results reinforce the ideas that electron-only magnetic reconnection can occur in the plasma environment near LMAs and that LMAs offer interesting plasma-physics laboratories to investigate the fundamental nature of electron-only magnetic reconnection.

B 会場 : 11/26 PM2(14:50-16:20)

15:50~16:05:00

あらせ衛星の PWE/EFD を用いた衛星帯電と光電子がつくる擬似電場の推定

#今野 翼 $^{1)}$, 中川 朋子 $^{2)}$, 堀 智昭 $^{3)}$, 笠羽 康正 $^{4)}$, 松田 昇也 $^{5)}$, 笠原 禎也 $^{5)}$, 三好 由純 $^{6)}$, 土屋 史紀 $^{4)}$, 熊本 篤志 $^{4)}$, 新堀 淳樹 $^{6)}$, 松岡 彩子 $^{7)}$

 $^{(1)}$ 東北工業大学, $^{(2)}$ 東北工業大学, $^{(3)}$ 名古屋大学・宇宙地球環境研究所, $^{(4)}$ 東北大学, $^{(5)}$ 金沢大学, $^{(6)}$ 名古屋大学, $^{(7)}$ 京都大学

Estimation of a spurious electric field arising from spacecraft charging and photoelectron cloud using PWE/EFD onboard ARASE

#Tsubasa Konno¹⁾, Tomoko NAKAGAWA²⁾, Tomoaki HORI³⁾, Yasumasa KASABA⁴⁾, Shoya MATSUDA⁵⁾, Yoshiya KASAHARA⁵⁾, Yoshizumi MIYOSHI⁶⁾, Fuminori TSUCHIYA⁴⁾, Atsushi KUMAMOTO⁴⁾, Atsuki SHINBORI⁶⁾, Ayako MATSUOKA⁷⁾

⁽¹Tohoku Institute of Technology, ⁽²Tohoku Institute of Technology, ⁽³Institute for Space-Earth Environmental Research, Nagoya University, ⁽⁴Tohoku University, ⁽⁵Kanazawa University, ⁽⁶Nagoya University, ⁽⁷Kyoto University)</sup>

The most commonly used spaceborne technique for electric field measurement is the double probe method, which measures the potential difference between a pair of identical probes extending from the spacecraft. The potential of a sunlit probe in a tenuous plasma becomes positive due to the balance of photoelectron current and the ambient electron current. A bias current applied to the probe reduces its potential to be lower than that of the spacecraft potential. In a tenuous plasma, the electric field measurement using double probes can suffer from a spurious sunward electric field due to photoelectrons emitted from the spacecraft and the positive charging of the spacecraft body. The photoelectrons are emitted from the sunlit side of the spacecraft and the center of the photoelectron cloud is thought to be shifted toward the sun, attracting the surface charge of the spacecraft. The resultant pair of charges localized on the sunlit side induce a dipole-like electric field pointing sunward. This local electric field is registered as a sinusoidal curve of the potential difference between the two probes as a function of the phase of the satellite's spin motion. Imbalance of the sheath potentials between the two probes can also be detected as a sunward spurious field. The sunward-side probe collects more photoelectrons emitted from the spacecraft, decreasing the probe potential, while the anti-sunward probe loses more escaping photoelectrons due to the positively charged spacecraft body, increasing the probe potential.

For a precise analysis of the ambient (natural) electric field, it is desirable to estimate the spurious electric field and then subtract it from a measured electric field. In this study, an attempt is made to estimate the spurious electric field from the potential difference obtained by Plasma Wave Experiment (PWE) / Electric Field Detector (EFD) onboard the Arase satellite. Our estimation of the spurious electric field was based on the following assumptions: 1) an observed electric field is a sum of natural and spurious fields, 2) the natural electric field is perpendicular to the background magnetic field, and 3) the spurious electric field points sunward. For selected cases in which the background magnetic field was parallel to the spin plane, we estimated the x-component (sunward in the spin plane) of the spurious electric field.

Monthly statistics starting from April 2017 to March 2024 revealed the presence of the spurious electric field during periods in which the electron density was less than $100~\rm cm^{-3}$. A linear relationship is identified between the x-component of the spurious electric field and the log of electron density ($\log n_e$) in the range $10 < n_e < 100~\rm cm^{-3}$ in 2/3 of the months in which the estimation was available. Using the linear relationship, the spurious electric field was estimated as a function of the electron density. In some cases, the x-component of the spurious electric field followed that of the observed electric field. Subtraction of the spurious component from the observation improved the ratio of the sunward component with respect to the magnitude of the electric field. In some other cases, however, the estimation was not successful and over-subtraction occurred. We investigated a possibility that the spurious electric field deviated from the sun direction due to the photoelectron cloud guided by the background magnetic field, but there was no clear correlation found between the over-subtraction and the direction of the background magnetic field.

The relationship between the spurious electric field and $\log n_e$ disappeared in 2018-2020. The fitting parameters of the regression line were examined to see if there is any correlation with F10.7 intensity as an indicator of the solar UV, but the reason for the loss of the linear relation in 2018-2020 is not yet understood.

衛星による電場観測にて多く用いられるダブルプローブ法では、衛星から伸展させた一対のプローブ間の電位差を計測する。日照中でのプラズマ中にある衛星の電位は、周辺プラズマからの流入電子電流と衛星からの流出光電子電流とのつり合いで決まり、前者が少ない低密度域では正に定まる。プローブに電子を注入するバイアス電流を供給すると、プローブの電位はよりプラズマ電位に近く安定するため、2つのプローブの電位差は宇宙空間の電場を反映することになる。

この方法で計測された電場は、電子密度の低いときに太陽方向の成分が強まる問題がある。これは自然電場と考えにくく、計測によって生じた人工的な擬似電場と考えられる。その原因として、衛星からの光電子雲と正の衛星帯電が考えられている。光電子雲は衛星から太陽方向に偏って放出され、衛星帯電の中心も衛星表面が等電位になるようスピン軸から

太陽方向にずれると予想される。その結果生じる双極子電場はプローブ間の電位差波形に正弦波をつくり、太陽方向の擬似電場として検出される。もう一つの原因として、太陽方向のプローブでは光電子雲からの電子電流によって電位が下がり、反対側のプローブでは日照側から放出された光電子が逃走するためのポテンシャル障壁が衛星のつくる電位のために下がり、正味の光電子電流が増加するためプローブ電位が上がる結果、 プローブのシース電位の違いが太陽方向の電位差として検出されることも考えられる。

これらの影響を排した電場解析のためには、擬似成分を推定して観測値から差し引くことが求められる。本研究では、あらせ衛星のプラズマ波動・電場観測器 (Plasma Wave Experiment / Electric Field Detector, PWE/EFD) のデータから擬似電場の推定を試みる。ここで、観測される電場は自然の成分と擬似成分からなり、自然電場は外部磁場と直交し、擬似電場は太陽方向を指すと仮定する。これらを踏まえると、外部磁場が衛星のスピン面と平行の場合には、擬似電場の太陽方向成分が推定できる。2017 年 4 月から 2024 年 3 月までのデータを 1 か月ごとに調査したところ、電子密度 100 cm $^{-3}$ 以下 で擬似電場の発生が確認された。なお、この電子密度は PWE/HFA によって UHR 周波数から求められたものである。推定ができた月のうち 2/3 は、電子密度が $10~{\rm cm}^{-3}$ - $100~{\rm cm}^{-3}$ の範囲で電子密度の対数と擬似電場の間に線形性がみられた。線形回帰式から擬似電場を電子密度の関数として試算したところ、観測された電場の太陽方向成分に近い値となる場合もあった。試算した擬似成分を観測電場から差し引くと、太陽向き成分の卓越が改善された。しかしこれはいつもうまくいくわけではなく、過剰に差し引いてしまう場合もあった。光電子雲が背景磁場にガイドされて擬似電場が太陽方向を指さない可能性を考えたが、背景磁場の方向と電場の差し引き結果に関連性はなかった。

擬似電場の推定値と電子密度の対数との間に線形性がみられないケースは 2018 年 - 2020 年に集中していた。太陽紫外線と比較したものの、原因はわかっていない。

B会場: 11/26 PM2 (14:50-16:20)

16:05~16:20:00

UHR 電子密度データ更新後の Arase 衛星における衛星電位一電子密度の相関

#川潟 桂也 1), 笠羽 康正 1), 新堀 淳樹 2), 城 剛希 1), 土屋 史紀 1), 風間 洋一 3), 中川 朋子 4), 加藤 雄人 1) (1 東北大学, $^{(2}$ 名古屋大学, $^{(3}$ 台湾中央研究院天文及天文物理研究所, $^{(4}$ 東北工業大学

Correlation of spacecraft potential to the latest electron density data observed by Arase

#Keiya KAWAGATA¹⁾, Yasumasa KASABA¹⁾, Atsuki SHINBORI²⁾, Koki TACHI¹⁾, Fuminori TSUCHIYA¹⁾, Yoichi KAZAMA³⁾, Tomoko NAKAGAWA⁴⁾, Yuto KATOH¹⁾

⁽¹Tohoku University, ⁽²Nagoya University, ⁽³Academia Sinica Institute of Astronomy and Astrophysics, Taiwan, ⁽⁴Tohoku Institute of Technology

Recently, the electron density derived from the upper hybrid resonance (UHR) frequency onboard the Arase has been fully updated, leading to a significant improvement in reliability. Using this latest data, we have re-examined the correlation between spacecraft potential and electron density, with low-energy electron data.

Since March 2017, Arase has been orbiting in Geospace for about 7 years, continuously providing diverse datasets that contribute to determining electron density and temperature. These plasma parameters are fundamental for understanding the structure of the ionosphere, plasmasphere, and magnetosphere. Those are also important to control wave dispersion, growth, damping, and propagation paths. On Arase, UHR frequencies are identified by a combination of automated detection and visual inspection from the PWE/HFA (Plasma Wave Experiment/High-Frequency Analyzer) electric field spectra (10 kHz – 10 MHz), with a time resolution of 1 min. Electron density is derived from UHR frequency with the background magnetic field strength measured by MGF. This method enables accurate determination of electron density, including low-temperature electrons below 37 eV(the lower detection limit of the LEPe set from May 2017). However, difficulties arise in regions where strong waves appear near the UHR frequency, or in low-density environments with weak UHR signals. Other previous satellites have used direct particle measurements of low-energy ions (and electrons), but such instruments are generally hard to capture cold populations. Cold plasma dominates in the inner magnetosphere, so the density estimation by particle instuments require some assumptions for cold populations below the detection limit.

Spacecraft potential itself can serve as a rough indicator of electron density. The floating potential in plasma is determined by the balance between photoelectron emission due to solar UV radiation and incoming plasma electron current. As it depends on surface materials, secondary electron yield, spacecraft geometry and attitude, as well as ambient electron temperature, the accuracy of density inferred from spacecraft potential is limited. However, it offers a useful density proxy except in eclipse conditions as a direct measurement at 1-spin (~ 8 s) resolution without assumptions or visual identification. Moreover, it may provide estimates of the temperature of cold electrons not measured by LEPe.

Previously, correlations between spacecraft potential and UHR-derived density appeared excessively poor in the low-density regions (<1 /cc; corresponding to electron plasma frequencies below ~10 kHz). Consequently, the UHR electron density data was comprehensively updated in 2024, yielding significantly improved reliability. In this study, we use the updated datasets (April 2017 - December 2024) to re-evaluate potential – density correlations, incorporating low-energy electron data.

First, we re-evaluated the correlation between spacecraft potential and UHR density after the update. Specifically, we divided the MLT into 8 sectors and are investigating the correlations in each sector. Whereas the previous data showed large scatter in the low-density regime (<1 /cc), the updated densities display much stronger convergence. A robust correlation between spacecraft potential and log (electron density) is clearer in the dayside where hot electrons are not so many. Nevertheless, in the nightside and outside the plasmasphere, deviations persist at low densities, where spacecraft potential tends to appear lower than expected. This could be explained by enhanced inflowing electron currents in the plasma sheet.

Accordingly, we started the quantitative evaluation with LEPe moment data for electron density and temperature above 37 eV, for the influence of thermal conditions on spacecraft potential. Furthermore, we intend to investigate the relationship with solar UV flux, which can affect the photoelectron outflow current.

The stability of probe potential is critical for the accurate electric field measurements in magnetospheric and ionospheric plasmas. The present study will also provide a basis for the measurement accuracy of electric field and electron density observations by similar probes onboard the BepiColombo/Mio Mercury orbiter, which commenced its orbital observations in 2026. Both Arase and Mio are equipped with relatively short antennas (15 m, compared with 50 m on Geotail and Cluster). In low-density regions where the Debye length exceeds the antenna length, the probe potential may become biased toward the spacecraft potential rather than the ambient plasma potential, leading to an apparent underestimation of the spacecraft potential. Furthermore, the operational strategy of Arase, in which the bias current supplied to the probes had been limited to 50% of the photoelectron emission current, may have enhanced this effect. Since June 2025, the bias current has increased to 80% of the photoelectron emission current, and a reassessment of these effects will be conducted once the updated UHR electron density data become available.

最近 Arase 衛星における UHR(高域ハイブリッド共鳴波動)周波数を用いた電子密度は全面更新され、その信頼性が大きく向上した。このデータを用いて、衛星電位一電子密度の相関について低エネルギー電子データも併せた再評価を行った。

Arase 衛星は、2017 年 3 月以降、約 7 年間に渡りジオスペースを飛翔し、この領域の電子密度・温度決定に資する多様なデータを取得し続けている。密度・温度は電離圏・プラズマ圏・磁気圏の構造を決める基本情報であり、波動の分散関係やその成長・減衰、伝搬経路をも左右する。Arase 衛星では、PWE/HFA(プラズマ波動計測器/高周波受信部)の電場スペクトル(10 kHz~10 MHz)から UHR 周波数を自動判定と目視の組み合わせで同定し(時間分解能:1 min)、背景磁場強度と併せて電子密度を決定してきた。この方法は、電子計測器(LEPe)の下限エネルギー(2017/5 以降:37 eV)の低温成分を含む電子密度を高精度で決定できるが、UHR 周波数近傍に他の強い波動が見られる領域や UHR 強度が弱い低密度領域の場合にはその決定は難しい。他衛星ではプラズマ密度として低エネルギーイオン・電子の直接計測データが併用されてきたが、粒子計測器では低温粒子の検出が難しい。特に内部磁気圏域では低温プラズマが多く、Arase の静電プラズマ計測器 LEPe・LEPi では計測対象にならない低エネルギーの分布関数に仮定が必要となる。

衛星電位も電子密度の指標となる。プラズマ中における衛星の浮動電位は、太陽紫外線による光電子流出と周辺プラズマからの電子流入のバランスで決定される。衛星表面材料に依存する光電子流出・二次電子放出効率、衛星の形状・姿勢、および周辺電子温度に影響されることから、衛星電位から演繹される電子密度の精度は低い。しかし、目視決定や特定の仮定に依存することなく 1-spin(8 sec 程度)の分解能で観測量を取得できるため、光電子放出が無い日陰時を除き、ある程度の信頼性を持った電子密度を導出することが潜在的に可能であり、また低エネルギー電子の温度情報も推定できる可能性がある。

これまで、Arase 衛星は 1/cc 以下(電子プラズマ周波数: $\sim 10kHz$ 以下)で、UHR 由来電子密度の精度が低く、衛星電位との相関が過剰に悪く見えていた。幸い、UHR 電子密度データは 2024 年に全面更新され、より信頼性が高くなった。本研究では最新電子密度データ(2017 年 4 月 ~ 2024 年 12 月)を用いて、衛星電位一電子密度の相関について低エネルギー電子データも併せた再評価を行った。

はじめに、衛星電位と UHR 電子密度との相関について再評価を行った。具体的には、MLT を 8 つに分割し、それぞれの領域での UHR 由来電子密度一衛星電位の相関およびその経年変化の確認を進めている。これまでこの相関は低密度域(1 /cc 以下)で過剰にばらついていたが、電子密度データの全面更新に伴ってかなりの収束をみた。特に hot 電子の少ない昼側では、 $\log(電子密度)$ と衛星電位の間によい精度を見出している。とはいえ、hot 電子の多いプラズマ圏外・夜側では、依然として低密度域でこの関係から逸脱し、想定される相関よりも衛星電位が小さく出るデータが散見される。プラズマシートの影響で電子密度がより高くなる夜側ではより流入電子電流量が大きくなることがあり、衛星電位がより下がってバランスすることによると考えうる。

この検証に向け、LEPe による~37eV 以上の電子の密度・温度モーメントデータを併用し、プラズマ温度が与える衛星電位への定量的な影響評価に着手した。光電子電流量に影響しうる太陽 UV flux との相関も確認予定である。

プローブ電位の安定度は、磁気圏・電離圏電場及び低周波電場波動の精度決定要因でもある。本研究は、2026 年から周回観測を開始する BepiColombo/Mio 水星探査機における同型プローブを用いた電子密度・電場計測の精度保障の基礎ともなる。Arase 衛星・Mio 探査機はアンテナ長が 15 m と短く(Geotail・Cluster:50 m)、低密度域で Debye 長>アンテナ長となりやすい。このため、プローブ電位が Debye 長以内の「周辺プラズマ電位より衛星電位に近いポテンシャル」を拾うことで、擬似的に低衛星電位にみえる可能性もある。これまで Arase 衛星はプローブに与えるバイアス電流量を光電流流出量の \sim 50% 程度に抑えて運用してきたことも、この影響を助長している可能性がある。2025 年 6 月からは光電流流出量の \sim 80% 程度にバイアス電流量を向上させており、UHR 由来電子密度データが更新され次第この評価も進めていく。

B 会場 : 11/26 PM3(16:40-18:25)

16:40~16:55:00

ハイパースペクトルカメラ (HySCAI) による N_2 1PG の回転温度子午線分布の観測

#居田 克巳 $^{1)}$, 吉沼 幹朗 $^{1)}$, 海老原 祐輔 $^{2)}$ (1 核融合研, $^{(2)}$ 京大生存圏

Observation of rotational temperature meridian distribution of N_2 1PG using hyperspectral camera (HySCAI)

#Katsumi Ida¹⁾, Mikirou Yoshinuma¹⁾, Yusuke Ebihara²⁾

(1) National Institute for Fusion Science, (2) Research Institute for Sustainable Humanosphere, Kyoto University

A hyperspectral camera for auroral imaging (HySCAI) has been installed at the KEOPS (Kiruna Esrange Optical Platform Site) of the Swedish Space Corporation (SSC) in Kiruna, Sweden, and observations have been underway since 2023. HySCAI features two gratings: one with 500 grooves per millimeter (mm) covering a broad spectral range of 400 – 800 nm with a spectral resolution of 2.1 nm (full width at half maximum, FWHM), and another with 1,500 grooves per mm capable of covering a narrow spectral range of 123 nm with a high spectral resolution of 0.73 nm.

We focused on the auroral breakup that began around 17:30 UT on January 1, 2025. This breakup was associated with a large substorm with minimum SML index exceeding -2000 nT, and is characterized by intense red color. During this breakup, HySCAI measured the red region (620-720 nm), including the OI (1D) 630.0 nm line, which is the cause of the red aurora, and the vibrational-rotational levels of the N_2 1PG molecule at the following bands: (8,5) 646.7 nm, (7,4) 654.5 nm, (6,3) 662.6 nm, (5,2) 670.1 nm, (4,1) 679.0 nm, (3,0) 687.6 nm, and the Meinel system (3,0) 685 – 690 nm, (4,1) 705 – 710 nm. HySCAI can distinguish them individually. In the red region, prior to the breakup of the red aurora (approximately 6 minutes before), an increase in N_2 1PG was observed. During the breakup of the red aurora, the OI (1D) 630.0 nm line was much brighter than N_2 1PG. This aurora breakup with intense red color lasted approximately 50 minutes. The ratio of each band of the molecular vibrational-rotational levels of N_2 1PG was not constant during this period, and a clear temporal variation was observed. From the spectral shapes of each band of the molecular vibrational-rotational levels of N_2 1PG during the red aurora breakup, the meridional distribution of nitrogen's rotational temperature was obtained.

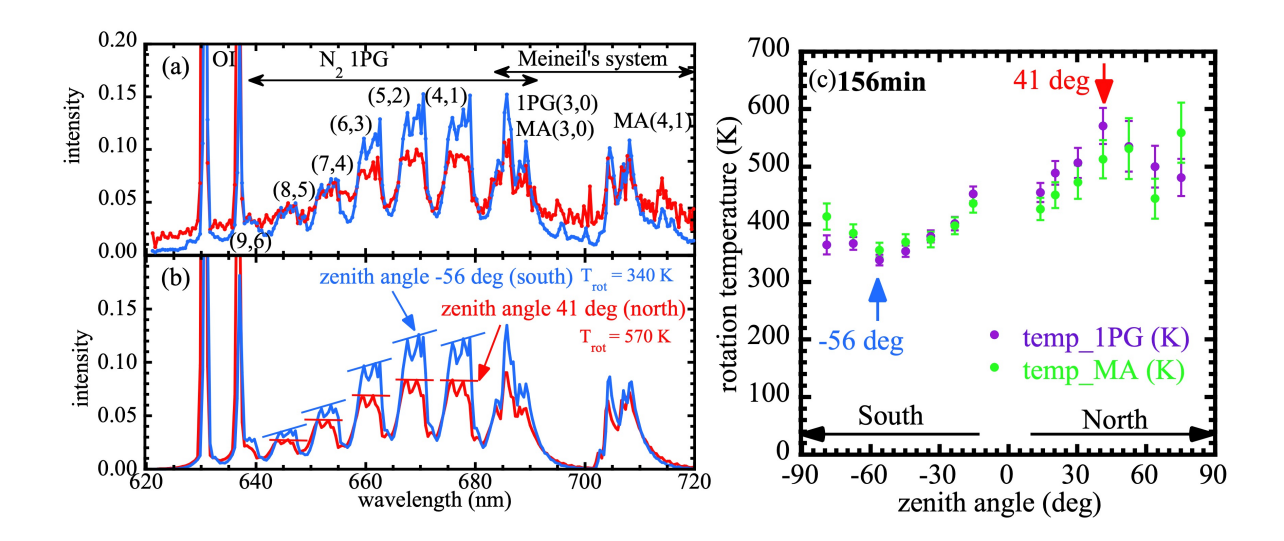
The figure shows (a) the nitrogen spectrum observed at zenith angles of -56° (south) and 41° (north), (b) the nitrogen spectrum calculated using rotational temperature and vibration temperature as parameters, and (c) the meridional distribution of rotational temperature. The shape of the spectrum changes with rotational temperature, becoming upward-sloping at low rotational temperatures but flattening or downward-sloping as rotational temperature increases. By comparing with model calculations, rotational temperatures can be estimated at each point. As a result, significant differences in rotational temperature were observed, with a minimum of 340 K on the south side and a maximum of 570 K on the north side. Subsequently, this temperature difference decreased over time, and during the latter half of the breakup, the distribution of rotational temperatures became nearly flat.

オーロラ観測用ハイパースペクトルカメラ(Hyperspectral Camera for Auroral Imaging: HySCAI)をスウェーデンのキルナにある SSC(スウェーデン宇宙公社)の KEOPS(キルナ・エスレンジ・オプティカル・プラットフォーム・サイト)に設置、2023 年から観測を行っている。HySCAI には 2 つのグレーティングがあり、1 つは 500 溝/mm で 400-800 nm の広いスペクトルを 2.1 nm のスペクトル分解能 (FWHM) でカバーし、もう 1 つは 1500 溝/mm で 0.73 nm の高いスペクトルを 123 nm の狭いスペクトルでカバーすることができる。

2025 年 1 月 1 日 17:30 UT 頃に始まったオーロラのブレイクアップに着目する。このブレイクアップは SML 指数が-2000 nT を超える大規模なサブストームに伴うもので、赤色が強いという特徴が見られた。このとき、HySCAI はオーロラの赤色光領域 (620 – 720nm) を計測した。この波長領域には OI (1D) 630.0nm のライン、 N_2 1PG の分子の振動回転準位の各バンド (8,5) 646.7nm, (7,4) 654.5nm, (6,3) 662.6nm, (5,2) 670.1nm, (4,1) 679.0nm, (3,0) 687.6nm および Meinel system の (3,0) 685-690nm, (4,1) 705-710nm が含まれ、HySCAI はこれらを分離計測できる。赤色光領域において、オーロラのブレークアップの直前(6分前)では N_2 1PG が先行して強くなり、ブレークアップ中では OI (1D) 630.0nm のラインが N_2 1PG よりもはるかに強く光っていた。この赤色が強いオーロラのブレークアップは約 50 分程度続いた。 N_2 1PG の分子の振動回転準位の各バンドの比は、その間一定ではなく明瞭な時間変化が観測された。赤いオーロラのブレークアップ中の N_2 1PG の分子の振動回転準位の各バンドのスペクトル形状から窒素の回転温度の子午線分布を得た。

図は、天頂角-56 度(南側)と 41 度(北側)において (a) 観測された窒素のスペクトル、(b) 回転温度・振動温度をパラメータとして計算した窒素のスペクトル,(c) 回転温度の子午線分布である。スペクトルの形状はその回転温度によって変化し、回転温度が低い場合には右肩上がりとなるが、回転温度が上昇するとフラットまたは右肩下がりになる。モデル

計算と比較することで、各点での回転温度を評価することができる。その結果、回転温度は南側では最低 340K, 北側では最高 570K と大きな差が観測された。その後、時間と共にこの温度差は小さくなって、ブレークアップ後半では、回転温度の分布はほぼフラットになることが観測された。



B 会場 : 11/26 PM3(16:40-18:25)

16:55~17:10:00

#平原 聖文 $^{1)}$, 海老原 祐輔 $^{2)}$, 坂野井 健 $^{3)}$ $^{(1)}$ 名大・宇地研、 $^{(2)}$ 京大・生存研、 $^{(3)}$ 東北大・理

Space plasma precipitation and repelling processes by field-aligned electrostatic potential in auroral arc and hole

#Masafumi HIRAHARA¹⁾, Yusuke EBIHARA²⁾, Takeshi SAKANOI³⁾
(¹ISEE, Nagoya Univ., (²RISH, Kyoto Univ., (³PPARC, Tohoku Univ.)

Electric fields along local magnetic field line are one of effective mechanisms for accelerating space plasmas, as represented by the cases of neutron stars and planetary auroras. In the terrestrial polar regions, anti-earthward electrostatic fields along geomagnetic field lines can accelerate electrons in space plasmas into the Earth's upper atmosphere, generating bright and dynamic auroras characterized by arcs, curtains, curls, etc. One of the acceleration mechanisms producing "inverted V"-shaped features in energy-time/latitude distributions of precipitating auroral electrons, as observed in low-altitude space missions, is due to anti-earthward parallel electrostatic fields. The field-aligned electrostatic potentials, ranging from tens of volts to tens of kilo volts, are a consequence of the dynamo process generated in the dynamically changing magnetosphere. Our satellite instruments observed clear ion flux depletion in the energy range corresponding to localized field-aligned electrostatic potential above the satellite, which was coincidental with the electron precipitation forming the inverted-Vs. With advanced instruments onboard a microsatellite in low-altitude polar orbit, we detected recurring ion precipitation signatures accelerated by earthward parallel electrostatic fields, coinciding with electron flux depletion in the energy range smaller than the electrostatic potential. These precipitating ion signatures were observed in aurora-void regions, which we call "auroral holes" here, a conception newly defined after "coronal hole" of the Sun. These signatures provide persuasive double clues for the earthward electrostatic fields that accelerate ions toward the Earth and prevent electrons from penetrating the upper atmosphere although results in the past satellite missions might show the similar signatures.

B 会場 : 11/26 PM3(16:40-18:25)

17:10~17:25:00

#八島 和輝 $^{1)}$, 田口 聡 $^{1)}$, 小池 春人 $^{1)}$, 細川 敬祐 $^{2)}$ $^{(1)}$ 京大理, $^{(2)}$ 電気通信大学

Temporal evolution of low-energy electron precipitation in longitudinally elongated moving cusp auroras

#Kazuki Yashima¹⁾, Satoshi Taguchi¹⁾, Haruto Koike¹⁾, Keisuke Hosokawa²⁾

⁽¹Department of Geophysics, Graduate School of Science, Kyoto University, ⁽²Graduate School of Communication Engineering and Informatics, University of Electro-Communications

When the interplanetary magnetic field has a southward component, precipitation of low-energy electrons is enhanced in the cusp region above the ionosphere. Within the cusp, particularly in its high-latitude portion, the precipitation is further intensified in elongated structures that extend longitudinally. These regions often exhibit dynamic motion lasting several minutes, with some drifting poleward. Ground-based observations of the 630-nm aurora show that such longitudinally elongated precipitation regions typically extend a few hundred kilometers, and can occasionally reach lengths of 400 km or more. Lowaltitude satellite observations have demonstrated that enhanced precipitation of electrons with energies below a few hundred eV is responsible for the intensification of the 630-nm cusp aurora. However, the temporal evolution of the moving electron precipitation region remains difficult to resolve from only satellite measurements. We have recently developed a methodology that incorporates the GLOW model (including the Meier model of electron precipitation) with 630-nm all-sky auroral images to derive the two-dimensional distribution of the differential energy flux of low-energy electrons within a roughly circular region with a diameter of approximately 1400 km centered on the aurora observation point. In the present study, this methodology is applied to moving cusp auroras that extend longitudinally over ~400 km. We analyzed 630-nm auroral images obtained from an all-sky imager at Svalbard and identified several events of longitudinally elongated moving cusp auroras. Using the aforementioned method, we investigated the temporal evolution of the electron differential energy flux within these regions. The results consistently revealed a characteristic temporal sequence: a rapid enhancement of the flux, followed by a quasi-stable phase, and then a monotonic decrease. The significance of this temporal sequence is discussed in the context of Alfvénic electron acceleration processes occurring in higher-altitude regions above the aurora.

B 会場 : 11/26 PM3(16:40-18:25)

17:25~17:40:00

サブオーロラ帯の高感度大気光カメラで観測される波長 557.7 nm の弱いディフューズ発光領域のあらせ衛星との共役観測:複数例解析

#五味 優輝 $^{1)}$, 塩川 和夫 $^{1)}$, 三好 由純 $^{1)}$, 大塚 雄一 $^{1)}$, 大山 伸一郎 $^{1)}$, Connors Martin $^{2)}$, 新堀 淳樹 $^{1)}$, 堀 智昭 $^{1)}$, Jun ChaeWoo $^{1)}$, 山本 和弘 $^{1)}$, 篠原 育 $^{3)}$, 浅村 和史 $^{3)}$, 笠原 慧 $^{4)}$, 桂華 邦裕 $^{4)}$, 横田 勝一郎 $^{5)}$, 土屋 史紀 $^{6)}$, 熊本 篤志 $^{6)}$, 笠原 禎也 $^{7)}$, 風間 洋一 $^{8)}$, Wang Shiang-Yu $^{8)}$, Tam Sunny W.Y. $^{9)}$, 松岡 彩子 $^{10)}$

 $^{(1)}$ 名古屋大学, $^{(2)}$ アサバスカ大学, $^{(3)}$ 宇宙航空研究開発機構, $^{(4)}$ 東京大学, $^{(5)}$ 大阪大学, $^{(6)}$ 東北大学, $^{(7)}$ 金沢大学, $^{(8)}$ 中央研究院天文及天文物理研究所, $^{(9)}$ 国立成功大学, $^{(10)}$ 京都大学

Conjugate Observations of Faint Diffuse Emission at Subauroral Latitudes Using Arase and Ground Cameras: Multiple Event Analysis

#Masaki Gomi¹⁾, Kazuo SHIOKAWA¹⁾, Yoshizumi MIYOSHI¹⁾, Yuichi OTSUKA¹⁾, Shin-ichiro OYAMA¹⁾, Martin Connors²⁾, Atsuki SHINBORI¹⁾, Tomoaki HORI¹⁾, Chaewoo JUN¹⁾, Kazuhiro YAMAMOTO¹⁾, Iku SHINOHARA³⁾, Kazushi ASAMURA³⁾, Satoshi KASAHARA⁴⁾, Kunihiro KEIKA⁴⁾, Shoichiro YOKOTA⁵⁾, Fuminori TSUCHIYA⁶⁾, Atsushi KUMAMOTO⁶⁾, Yoshiya KASAHARA⁷⁾, Yoichi KAZAMA⁸⁾, Shiang-Yu Wang⁸⁾, Sunny W.Y. Tam⁹⁾, Ayako MATSUOKA¹⁰⁾

⁽¹Institute for Space-Earth Environmental Research, Nagoya University, ⁽²Athabasca University, ⁽³Japan Aerospace Exploration Agency, ⁽⁴Tokyo University, ⁽⁵Osaka University, ⁽⁶Tohoku University, ⁽⁷Kanazawa University, ⁽⁸Academia Sinica Institute of Astronomy and Astrophysics, Taiwan, ⁽⁹National Cheng Kung University, ⁽¹⁰Kyoto University)</sup>

Discrete auroras such as STEVE and SAR arcs, typically observed at subauroral latitudes, have extensively been studied using all-sky imagers on the ground. On the other hand, diffuse emissions at subauroral latitudes have not well been studied. In this study, using high-sensitivity all-sky airglow cameras installed in Canada and Alaska, we have newly identified faint diffuse emissions at a wavelength of 557.7 nm with intensities of 300-1000 Rayleighs, which spread equatorward of the conventional auroral oval. We have analyzed 11 events of these faint diffuse emissions with conjugate plasma and field measurements by the Arase satellite in the inner magnetosphere. Conjugate observations of such diffuse emissions at subauroral latitudes and their corresponding magnetospheric source region have not been previously reported. These diffuse emission regions exhibited patchy structures in one case, while in the others they showed no distinct spatial structures but instead spread longitudinally with almost the same brightness across the field of view of the all-sky imager. In all 11 analyzed events, the magnetospheric conjugate regions corresponding to the emissions were located inside the plasmasphere, where plasma-sheet electrons with energies of several keV were simultaneously observed. At the same time, no plasma-sheet ions with such energies were detected. Plasma waves were observed in 8 events, including narrow-band plasmaspheric hiss (1 event) and lower-band chorus waves (1 event), both of which can cause cyclotron resonance scattering of plasma-sheet electrons. In the events without wave activity, emission intensifications associated with substorm onsets were observed (1 event). These results suggest that precipitation of plasma-sheet electrons into the ionosphere, driven by substorms and pitch angle scattering due to wave-particle interactions in the plasmasphere, is responsible for the formation of faint diffuse 557.7-nm emission regions equatorward of the auroral oval. However, in two events no corresponding waves or substorms were identified, and the cause of the emission remains unclear.

オーロラ帯のすぐ低緯度側に位置するサブオーロラ帯では、STEVE や SAR アークのような特有なディスクリートオーロラが報告されている。しかし、サブオーロラ帯のディフューズオーロラについては十分に研究されていない。本研究では、北米のサブオーロラ帯に設置された高感度全天カメラを用いて、これまでに観測されていたオーロラオーバルよりも低緯度側に広がる波長 557.7 nm で 300-1000 R の弱いディフューズな発光領域を新しく見出した。さらに、あらせ衛星によってその発光領域に対応する磁気圏領域を 11 例観測した。このようなサブオーロラ帯に広がるディフューズな発光に対応する磁気圏領域の同時観測はこれまで行われていない。これらのディフューズな発光領域は、1 例ではパッチ構造を示し、それ以外でははっきりとした構造を持たず、全天カメラの視野内で経度方向に同じ明るさの領域が広がる特徴を示した。解析した 11 例のすべてのイベントで、発光領域に対応する磁気圏領域はプラズマ圏内に位置しており、エネルギーが数 keV のプラズマシート電子群を同時に観測した。このとき、数 keV/q のプラズマシートイオンは観測されなかった。また、同時にプラズマ波動が観測される例は 8 例あり、とくにプラズマシート電子とサイクロトロン共鳴を引き起こす狭帯域プラズマ圏ヒス(1 例)や lower-band chorus 波動(1 例)を観測する例も存在した波動が観測されなかった例では、サブストームの発生にともなう増光が見られた(1 例)。これらのことから、プラズマシート電子がサブストームや波動によるピッチ角散乱による電離圏への降り込みが、オーロラオーバルよりも低緯度側の領域で引き起こされており、弱いディフューズな波長 557.7 nm の発光領域が形成されていると考えた。ただし、対応する波動やサブストームが見られない例も 2 例あり、その原因はわかっていない。

B 会場 : 11/26 PM3(16:40-18:25)

17:40~17:55:00

非線形アンペール力による低プラズマ密度領域の形成と位相混合: IAW 発展への寄与

#川上 航典 $^{1)}$, 吉川 顕正 $^{2)}$, 深沢 圭一郎 $^{3)}$, 樋口 颯人 $^{4)}$ $^{(1)}$ 九州大学, $^{(2)}$ 九州大学, $^{(3)}$ 総合地球環境学研究所, $^{(4)}$ 株式会社 QunaSys

Phase Mixing and Formation of Low Plasma Density Region by Nonlinear Ampere Force: Implication for IAWs Development

#Kosuke KAWAKAMI¹), Akimasa YOSHIKAWA²), Keiichiro FUKAZAWA³), Hayato HIGUCHI⁴) (¹Kyusyu univeristy, ⁽²Kyushu university, ⁽³Research Institute for Humanity and Nature, ⁽⁴QunaSys

Ionospheric Alfven Resonators (IARs), located in the upper terrestrial ionosphere, play crucial roles: they confine Alfven waves due to the background Alfven velocity gradient and serve as acceleration regions for inertial or dispersive Alfven waves. Thus, they have been regarded as one of the key regions for understanding the formation processes of auroral acceleration regions. Previous observations in IARs have revealed the presence of low-density plasma structures, extending several kilometers in the perpendicular direction and organizing in the altitude direction according to the resonance frequency, accompanied by electron and ion acceleration [Aikio et al., 2004; Chaston et al., 2006]. Among these findings, two aspects - (1)the development of perpendicular fine structures and (2)the decrease in plasma density - are essential conditions for the significant development of inertial Alfven waves. Based on this, a previous study [Lysak and Song, 2008] assumed the presence of density cavity regions and simulated Alfven wave propagation, demonstrating that phase mixing leads to the evolution of perpendicular structures. Furthermore, other studies [Streltsov and Lotko, 2008; Sydorenko et al., 2008] focused on the formation processes of low-density plasma regions via parallel nonlinear Lorentz force. Their simulations showed that the parallel nonlinear force associated with standing Alfven waves in the IAR expels plasma from the antinodes of the standing wave, thereby forming altitude-dependent density structures partially consistent with observations.

In this study, we extend these works by considering not only the parallel but also the perpendicular nonlinear Ampere force. We hypothesize that this additional contribution can more efficiently generate low-density plasma structures that are consistent with observations, both in the perpendicular and altitude directions. We perform two-dimensional multi-fluid MHD simulations [Toth et al., 2009] to investigate the self-consistent process from formation of low-density plasma regions to the subsequent development of perpendicular structures through phase mixing. Our results show that low-density regions formed by the perpendicular nonlinear Ampere force play the similar role as the assumed density-depleted regions in previous studies, leading to phase mixing and the perpendicular fine structures. In this presentation, we will report these results and discuss future perspectives.

地球電離圏上空に存在する IAR(Ionospheric Alfven Resonator) は、背景 Alfven 速度の勾配により Alfven 波を閉じ込める役割を持つ領域かつ、Inertial Alfven 波や Dispersive Alfven 波による加速領域であるため、オーロラ加速領域形成過程解明の鍵を握る領域としても注目されてきた。これまでの観測では、IAR 領域内において垂直方向に数 km 程度、高度方向に IAR の共鳴周波数に従う構造を持つ低プラズマ密度領域と、それに伴う電子・イオンの加速が生じていることが明らかにされている [Aikio et al., 2004. Chaston et al., 2006]。特に、(1) 垂直方向に発達した構造を持つこと、(2) 背景プラズマ密度の減少、の 2 つは Inertial Alfven 波が発達する上で不可欠な条件である。このことを元に、先行研究 [Lysak and Song 2008] では、プラズマ密度減少領域を仮定した上で Alfven 波の伝播について数値実験を行ったところ、位相混合によって垂直方向の構造が発展することを確認している。また先行研究 [Streltsov and Lotko 2008, Sydorenko et al., 2008] では、特に低プラズマ密度領域の形成過程に焦点を当てた数値シミュレーションから、IAR 中での定在 Alfven 波構造において働く平行方向の非線形ローレンツ力が定在波構造の腹からプラズマを押し出すことによって、高度方向に観測と部分的に類似する密度構造が形成されることを確認した。

そこで本研究では、平行方向だけでなく垂直方向の非線形アンペール力も考慮することで、垂直方向も含めて観測と一致し、かつより効率的に低プラズマ密度構造が形成されると着想し、低プラズマ密度領域の形成から位相混合によって垂直方向の構造が発展するまでを self-consistent な発展を解明すること目的として、2次元 multi-fluid MHD シミュレーションを用いた検証を行った。その結果、垂直方向の非線形アンペール力によって形成された低プラズマ密度領域の存在が、先行研究で仮定されていた低プラズマ密度領域と同じ働きをすることで、位相混合が生じ、垂直方向の構造が発展することを確認した。本発表ではこれらの結果について報告しつつ、今後の展望について概説する予定である。

B 会場 : 11/26 PM3(16:40-18:25)

17:55~18:10:00

#野田 大晨 $^{1)}$, 三好 由純 $^{1)}$, 細川 敬祐 $^{2)}$, 浅村 和史 $^{3)}$, 坂野井 健 $^{4)}$, 齋藤 慎司 $^{5)}$, Lessard Marc $^{6)}$, Jaynes Alison $^{7)}$, Shumko Mike $^{8)}$, Alexa Halford $^{9)}$, 滑川 拓 $^{5)}$, 三谷 烈史 $^{3)}$, 能勢 正仁 $^{10)}$, McHarg Geoff $^{11)}$, Ledvina Vincent $^{12)}$, Hampton Don $^{12)}$ (1 名古屋大学, (2 電気通信大学, (3 宇宙航空研究開発機構, (4 東北大学, (5 国立研究開発法人 情報通信研究機構, (6 ニューハンプシャー大学, (7 アイオワ大学, (8 ジョンズ・ホプキンズ大学, (9 ゴダード宇宙飛行センター, (10 名古屋市立大学, (11 アメリカ合衆国空軍士官学校, (12 アラスカ大学

Pulsating aurora electrons observed by LAMP sounding rocket

#Taisei NODA¹⁾, Yoshizumi MIYOSHI¹⁾, Keisuke HOSOKAWA²⁾, Kazushi ASAMURA³⁾, Takeshi SAKANOI⁴⁾, Shinji SAITO⁵⁾, Marc Lessard⁶⁾, Alison Jaynes⁷⁾, Mike Shumko⁸⁾, Halford Alexa⁹⁾, Taku NAMEKAWA⁵⁾, Takefumi MITANI³⁾, Masahito NOSE¹⁰⁾, Geoff McHarg¹¹⁾, Vincent Ledvina¹²⁾, Don Hampton¹²⁾

⁽¹Nagoya University, ⁽²University of Electro-Communications, ⁽³Institute of Space and Astronautical Science, JAXA, ⁽⁴Tohoku University, ⁽⁵National Institute of Information and Communication Technology, ⁽⁶University of New Hampshire, ⁽⁷University of Iowa, ⁽⁸Johns Hopkins University, ⁽⁹Goddard Space Flight Center, NASA, ⁽¹⁰Nagoya City University, ⁽¹¹The United States Air Force Academy, ⁽¹²University of Alaska

Pulsating aurora is a type of diffuse aurora characterized by quasi-periodic variations, typically with periods ranging from a few to a few tens of seconds. The over-darkening, a decrease in brightness by several tens of percent relative to the background, which often occurs immediately after an increase in brightness during the pulsation "ON" phase.

We investigated pulsating aurora and associated over-darkening phenomena using electron data from EPLAS and optical data from AIC, both onboard the LAMP sounding rocket, launched on March 5, 2022 from the Poker Flat Research Range, US. EPLAS measured electrons in the 5 eV-15 keV energy range, while AIC observed optical emissions in the 667-680 nm and 844-848 nm wavelength ranges. During the flight, multiple pulsating aurora and over-darkening events were observed. Near the rocket apex, the optical aurora emission at the magnetic footprint decreased from 3,000 Rayleigh to 1,300 Rayleigh. At the same time, EPLAS detected a ~50% reduction in downward energy flux, particularly at energies above 5 keV. An energy dispersion of precipitating electrons was also detected during the darkening phase. The inverse energy dispersion at the lowest energy of precipitating electrons around 5 keV was found, which is consistent with Miyoshi-Saito model that considers the propagation effects of chorus waves. To better understand the mechanism, we performed numerical simulations of wave-particle interactions. In this presentation, we will show detailed variations of precipitating electron spectra and pitch-angle distributions during the over-darkening events and compare the observations with numerical simulations to discuss possible mechanisms responsible for the over-darkening.

B 会場 : 11/26 PM3(16:40-18:25)

18:10~18:25:00

あらせ衛星・DMSP衛星観測データを用いたコーラス波動由来の降下電子と低軌道衛星の表面帯電に関するイベント解析

#荒木 大智 $^{1)}$, 寺本 万里子 $^{1)}$, 升野 颯人 $^{1)}$, 笠原 禎也 $^{2)}$, 熊本 篤志 $^{3)}$, 土屋 史紀 $^{3)}$, 松田 昇也 $^{2)}$, 笠原 慧 $^{4)}$, 風間 洋一 $^{5)}$, 松岡 彩子 $^{6)}$, 堀 智昭 $^{7)}$, 新堀 淳樹 $^{7)}$, 山本 和弘 $^{7)}$, 三好 由純 $^{7)}$, 篠原 育 $^{8)}$, 奥村 哲平 $^{8)}$, 古賀 清一 $^{8)}$, 岡本 博之 $^{8)}$, 北村 健太郎 $^{1)}$

(1 九工大, (2 金沢大学, (3 東北大学, (4 東京大学, (5 中央研究院, (6 京都大学, (7 名古屋大学, (8 宇宙航空研究開発機構

Event Analysis of Chorus-Wave-Induced Electrons with LEO Satellite Surface Charging Using Arase and DMSP Satellite Data

#Daichi Araki¹⁾, Mariko TERAMOTO¹⁾, Hayato MASUNO¹⁾, Yoshiya KASAHARA²⁾, Atsushi KUMAMOTO³⁾, Fuminori TSUCHIYA³⁾, Shoya MATSUDA²⁾, Satoshi KASAHARA⁴⁾, Yoichi KAZAMA⁵⁾, Ayako MATSUOKA⁶⁾, Tomoaki HORI⁷⁾, Atsuki SHINBORI⁷⁾, Kazuhiro YAMAMOTO⁷⁾, Yoshizumi MIYOSHI⁷⁾, Iku SHINOHARA⁸⁾, TEPPEI OKUMURA⁸⁾, KIYOKAZU KOGA⁸⁾, HIROYUKI OKAMOTO⁸⁾, Kentaro KITAMURA¹⁾

⁽¹Kyushu Institute of Technology, ⁽²Kanazawa University, ⁽³Tohoku University, ⁽⁴Tokyo University, ⁽⁵Academia Sinica Institute of Astronomy and Astrophysics, Taiwan, ⁽⁶Kyoto University, ⁽⁷Nagoya University, ⁽⁸JAXA

Satellites operating in space can experience surface charging depending on the surrounding plasma environment (e.g., Gussenhoven et al., 1985). Electrostatic Discharge (ESD) caused by surface charging can seriously affect satellite operations, such as by damaging solar panels. Therefore, assessing and preventing risks due to charging and discharging is an important issue for the safe operation of satellites, and future realization of satellite surface charging prediction is anticipated. Previous studies (Gussenhoven et al., 1985; Frooninckx and Sojka, 1992; Anderson, 2012) have confirmed that surface charging mainly occurs in the premidnight region, caused by high-energy precipitating electrons that also drive discrete aurora in the same region. On the other hand, recent studies have confirmed that surface charging also occurs, albeit rarely, in the morning region (e.g., Xuejie et al., 2017), where the regions do not overlap with discrete aurora. Therefore, this study focuses on surface charging of low-altitude satellites during diffuse aurora in the morning region.

To detect surface charging events of low-Earth orbit (LEO) satellites, plasma observation data from the DMSP F16 satellite are used. On May 06, 2022, from 17:31:21 to 17:31:44UT, surface charging occurred on the DMSP F16 satellite, where electron fluxes increased in the 1 – 20 keV energy range, showing characteristics of diffuse aurora. At this time, the Arase satellite, which was located about 1 hour in magnetic local time (MLT) away from DMSP F16, observed chorus waves in the magnetosphere. The resonant electron energy at the magnetic equator when chorus waves were observed was estimated to be 8.874 – 26.93 keV. These electrons are consistent with the diffuse auroral electrons that caused surface charging of the satellite. From this, a scenario can be considered in which high-energy electrons, pitch-angles scattered by chorus waves, precipitate from the magnetosphere into the ionosphere along magnetic field lines, and when a low-Earth orbit satellite passes through the precipitation region, surface charging occurs. These results suggest that chorus waves excited in the morning magnetosphere may contribute to the occurrence of surface charging on low-Earth orbit satellites.

宇宙空間を飛行する人工衛星は、周辺のプラズマ環境に応じて表面帯電が起こることがある (e.g., Gussenhoven et al., 1985)。表面帯電によって引き起こされる静電放電:ESD(Electro Static Discharge) は、太陽電池の損傷のように衛星運用に深刻な影響を与える可能性がある。そのため、人工衛星を安全に運用する上で、帯電・放電によるリスクとそれを未然に防ぐことは重要な課題であり、将来的な衛星表面帯電予測の実現が期待される。これまでの研究 (Gussenhoven et al., 1985; Frooninckx and Sojka, 1992; Anderson, 2012;) において、表面帯電は主に夜側領域で発生することが確認されており、これらは同じく夜側領域で発生するディスクリートオーロラを駆動する高エネルギー降下電子が原因である。一方で近年、朝側領域においても表面帯電が少数発生することが確認されており (e.g., Xuejie et al., 2017)、これらはディスクリートオーロラの発生領域と重ならない。そこで本研究は、朝側領域のディフューズオーロラ時の低高度衛星の表面帯電に着目した。

低軌道衛星の表面帯電イベントを検出するために、DMSP 衛星 F16 のプラズマ観測データを用いている。2022/05/06 17:31:21~17:31:44 において、DMSP 衛星 F16 で表面帯電が発生し、電子のフラックスは 1 keV~20 keV のエネルギー帯で増加しておりディフーズオーロラの特徴を示していた。このとき、DMSP 衛星から MLT~1 h 程度離れていたあらせ衛星は、磁気圏でコーラス波動を観測していた。コーラス波動が観測された際の磁気赤道における共鳴電子エネルギーを推定した結果、8.874~26.93 keV であった。これらの電子は、衛星の表面帯電の原因となったディフーズオーロラ電子と一致している。これらより、コーラス波動のピッチ角散乱によって高エネルギー電子が磁力線沿いに磁気圏から電離圏へ降り込むとき、その降り込み先を低軌道衛星が通過することで表面帯電が発生するシナリオが考えられる。以上の結果は、朝側磁気圏に励起されたコーラス波動が、低軌道衛星の表面帯電の発生に寄与する可能性を示している。

B 会場 : 11/27 AM1(9:15-10:45)

9:15~9:30:00

周波数上昇を伴った電磁イオンサイクロトロン放射波束の非線形発展過程

#大村 善治 $^{1)}$, Chen Huayue $^{2)}$, Wang Xueyi $^{2)}$, 謝 怡凱 $^{1)}$ $^{(1)}$ 京大生存研, $^{(2)}$ オーバーン大学

Nonlinear Evolution of Wave Packets of EMIC Rising-tone Emissions

#Yoshiharu Omura¹⁾, Huayue Chen²⁾, Xueyi Wang²⁾, Yikai Hsieh¹⁾
⁽¹Research Institute for Sustainable Humanosphere, Kyoto University, ⁽²Auburn University)

Electromagnetic ion cyclotron (EMIC) waves with rising tone frequency are frequently observed in the inner magnetosphere. They play a critical role in the loss process of the radiation belt electrons. We performed a one-dimensional hybrid simulation in a dipole magnetic field in the presence of energetic protons with temperature anisotropy. Through interaction between the protons and thermal fluctuations of the transverse electromagnetic fields, a coherent wave gradually grows at the frequency and wavenumber with the maximum linear growth rate. The interaction between the coherent wave and the energetic protons in the presence of positive gradient of the dipole magnetic field results in formation of a proton hole in the velocity phase space, giving rise to the resonant current JE (<0) parallel to the wave electric field. As reported in our previous study [1], the wave amplitude and the JE maximize at the same location. Along with the formation of JE, the JB (>0) parallel to the wave magnetic field also formed which contributes to variation of the wave frequency and wave number through the nonlinear dispersion relation. As observed at a fixed position, the frequency and the wavenumber do not change in the growing phase of the wave packet. Both frequency and wavenumber start to change after the wave amplitude is maximized. The wave packet with the increased frequency and the wavenumber propagates slower than the foregoing wave packet with the original frequency, because the group velocity decreases with the increasing frequency. There arises a spatial gap between the original wave packet and the new wave packet with the increased frequency, resulting in formation of two distinct wave packets. The frequency increase and the separation process of the wave packet are repeated through space-time evolution of the wave packets, resulting in formation of several subpackets of an EMIC rising-tone emission. The wave growth with frequency increase is interpreted with the nonlinear wave growth theory [2, 3]

- [1] Chen, H., Wang, X., Lin, Y., Zhao, H., et al. (2025). Nonlinear proton dynamics in the formation of rising tone EMIC wave subpackets. Geophysical Research Letters, 52, e2025GL115834
- [2] Omura, Y., J. Pickett, B. Grison, O. Santolik, et al. (2010), Theory and observation of electromagnetic ion cyclotron triggered emissions in the magnetosphere, J. Geophys. Res., 115, A07234, doi:10.1029/2010JA015300
- [3] Shoji, M., and Y. Omura (2013), Triggering process of electromagnetic ion cyclotron rising tone emissions in the inner magnetosphere, J. Geophys. Res. Space Physics, 118, 5553 5561, doi:10.1002/jgra.50523.

B 会場 : 11/27 AM1(9:15-10:45)

9:30~9:45:00

MMS 衛星によって得られたフォアショック構造内でのホイッスラーモード波動の 観測的証拠

#北村 成寿 $^{1)}$, 天野 孝伸 $^{2)}$, 大村 善治 $^{3)}$, 三好 由純 $^{4)}$, 加藤 雄人 $^{5)}$, 小嶋 浩嗣 $^{6)}$, Lee Sun-Hee^{7,8)}, 北原 理弘 $^{9)}$, Boardsen Scott A. $^{8,10)}$, 中村 るみ $^{1,11)}$, Gershman Daniel J. $^{8)}$, 齋藤 義文 $^{12)}$, 横田 勝一郎 $^{13)}$, Pollock Craig J. $^{14)}$, Le Contel Olivier $^{15,16)}$, Russell Christopher T. $^{17)}$, Strangeway Robert J. $^{17)}$, Lindqvist Per-Arne $^{18)}$, Ergun Robert E. $^{19)}$, Burch James L. $^{20)}$

(1 名古屋大学, (2 東京大学, (3 京都大学, (4 名古屋大学, (5 東北大学, (6 京都大学, (7 Catholic University of America, (8 NASA ゴダード宇宙飛行センター, (9 東北大学, (10 University of Maryland in Baltimore County, (11 Space Research Institute, Austrian Academy of Sciences, (12 宇宙航空研究開発機構, (13 大阪大学, (14 Denali Scientific, (15 Laboratoire de Physique des Plasmas, CNRS/Ecole Polytechnique, (16 Institut Polytechnique de Paris/Sorbonne Université/Université Paris-Saclay/Observatoire de Paris, (17 University of California, Los Angeles, (18 Royal Institute of Technology, (19 University of Colorado, Boulder, (20 Southwest Research Institute

Observational evidence of nonlinear growth of whistler-mode waves in foreshock structures obtained by the MMS spacecraft

#Naritoshi Kitamura¹⁾, Takanobu AMANO²⁾, Yoshiharu OMURA³⁾, Yoshizumi MIYOSHI⁴⁾, Yuto KATOH⁵⁾, Hirotsugu KOJIMA⁶⁾, Sun-Hee Lee^{7,8)}, Masahiro KITAHARA⁹⁾, Scott A. Boardsen^{8,10)}, Rumi NAKAMURA^{1,11)}, Daniel J. Gershman⁸⁾, Yoshifumi SAITO¹²⁾, Shoichiro YOKOTA¹³⁾, Craig J. Pollock¹⁴⁾, Olivier Le Contel^{15,16)}, Christopher T. Russell¹⁷⁾, Robert J. Strangeway¹⁷⁾, Per-Arne Lindqvist¹⁸⁾, Robert E. Ergun¹⁹⁾, James L. Burch²⁰⁾

(¹Nagoya University, (²The University of Tokyo, (³Kyoto University, (⁴Nagoya University, (⁵Tohoku University, (⁶Kyoto University, (⁷Catholic University of America, (⁸NASA Goddard Space Flight Center, (⁹Tohoku University, (¹⁰University of Maryland in Baltimore County, (¹¹Space Research Institute, Austrian Academy of Sciences, (¹²JAXA, (¹³The University of Osaka, (¹⁴Denali Scientific, (¹⁵Laboratoire de Physique des Plasmas, CNRS/Ecole Polytechnique, (¹⁶Institut Polytechnique de Paris/Sorbonne Université/Université Paris-Saclay/Observatoire de Paris, (¹⁷University of California, Los Angeles, (¹⁸Royal Institute of Technology, (¹⁹University of Colorado, Boulder, (²⁰Southwest Research Institute

To demonstrate observational evidence of nonlinear wave growth, we present an electron distribution function exhibiting significant nongyrotropy near the cyclotron resonance velocity during a whistler-mode wave event in a foreshock structure. This nongyrotropic electron distribution function is predicted by a nonlinear wave-particle interaction theory for coherent large-amplitude waves [e.g., Omura, EPS, 2021]. An electron phase space hole is generated in the distribution functions due to the phase trapping motion of cyclotron resonant electrons around the resonance velocity in the presence of an appropriate magnitude of inhomogeneity. Electrons with such a nongyrotropic distribution function exchange energy and momentum efficiently with whistler-mode waves. The Magnetospheric Multiscale (MMS) spacecraft observed whistler-mode waves in a foreshock structure, which is called the Short Large-Amplitude Magnetic field Structures (SLAMS). By applying the method of wave-particle interaction analyzer (WPIA) to data obtained with the Fast Plasma Investigation Dual Electron Spectrometer (FPI-DES) and the search-coil magnetometer (SCM), we identified an electron phase space hole, which was suitable for wave growth; the hole appeared at an appropriate gyro phase angle relative to the whistler-mode wave magnetic field only near the cyclotron resonance velocity. The gradient of the magnetic field intensity along the magnetic field line during the time intervals was suitable for wave growth due to the phase trapping motion of resonant electrons. A loss cone of heated electrons escaping from the high-pressure part of the foreshock structure played an important role in generating temperature anisotropy for wave growth. When such a distribution function encounters a gradient of magnetic field intensity with an appropriate magnitude, whistler-mode waves grow rapidly due to the nonlinear growth mechanism. Because fluctuations in magnetic field intensity exist in foreshock structures, it is probably common for electrons to encounter such a magnetic field gradient, and there must be many opportunities for nonlinear whistler-mode wave growth in foreshock structures.

B 会場 : 11/27 AM1(9:15-10:45)

9:45~10:00:00

#松岡 彩子 $^{1)}$, 寺本 万里子 $^{2)}$, 笠原 禎也 $^{3)}$, 尾崎 光紀 $^{3)}$, 松田 昇也 $^{3)}$, 三好 由純 $^{4)}$, 堀 智昭 $^{5)}$, 玉村 優剛 $^{1)}$, 篠原 育 $^{6)}$ $^{(1)}$ 京都大学, $^{(2)}$ 九州工業大学, $^{(3)}$ 金沢大学, $^{(4)}$ 名古屋大学, $^{(5)}$ 名古屋大学・宇宙地球環境研究所, $^{(6)}$ 宇宙航空研究開発機構

Characteristics of the low-frequency magnetic field variations coincided with whistler chorus observed by Arase

#Ayako Matsuoka¹⁾, Mariko TERAMOTO²⁾, Yoshiya KASAHARA³⁾, Mitsunori OZAKI³⁾, Shoya MATSUDA³⁾, Yoshizumi MIYOSHI⁴⁾, Tomoaki HORI⁵⁾, Yugo Tamamura¹⁾, Iku SHINOHARA⁶⁾

⁽¹Graduate School of Science, Kyoto University, ⁽²Kyushu Institute of Technology, ⁽³Kanazawa University, ⁽⁴Nagoya University, ⁽⁵Institute for Space-Earth Environmental Research, Nagoya University, ⁽⁶JAXA

We are investigating the magnetic field variations in association with the relativistic electrons in the inner magnetosphere. It is known that the acceleration and loss of the energetic particles in the radiation belts are deeply related with the energy transfer by electromagnetic waves. The frequencies of whistler chorus waves are generally ranging 0.1 - 0.8 fce (fce is the equatorial electron cyclotron frequency) but often dramatically dropped and became much lower than the commonly observed frequencies of whistler chorus waves.

Our statistical result on the spacial distribution of the low-frequency whistler chorus waves shows that it occures more frequently near the magnetic equator on the nightside, which is consistent with the mechanism proposed in previous studies, in which whistler chorus waves are excited by energy supplied by high-energy electrons injected from the plasma sheet. Meanwhile, we found that the low-frequency whistler chorus waves were also observed on the dayside, and it would be suggested that those chorus waves are excited by non-thermal electrons that reached the dayside from the nightside plasma sheet. Moreover, the low-frequency whistler chorus waves substantially often occur even at low magnetic activities (Dst <40nT). Our statistical results show that the low-frequency whistler chorus is more common phenomena than already reported.

In our presentation we focus on the wave activities also at further lower frequencies. In the low-frequency whistler chorus events, the frequencies at which the waves have substantial intensity extends to the frequencies lower than proton cyclotron frequency. We will discuss the characteristics of the low-frequency whistler chorus waves associated with the magnetospheric disturbance phenomena, e.g., dipolarization and bursty bulk flow from the night-side plasma sheet.

B 会場 : 11/27 AM1(9:15-10:45)

10:00~10:15:00

#城 剛希 1), 加藤 雄人 1), 熊本 篤志 1), 笠原 禎也 2), 松田 昇也 2), 新堀 淳樹 3), 吹澤 瑞貴 4), 小川 泰信 4), 細川 敬祐 5), 松 岡 彩子 6), 寺本 万里子 7), 山本 和弘 3), 笠原 慧 8), 横田 勝一郎 9), 桂華 邦裕 10), 堀 智昭 3), 三好 由純 3), 篠原 育 11) $^{(1}$ 東北大学, $^{(2}$ 金沢大学, $^{(3}$ 名古屋大学, $^{(4)}$ 国立極地研究所, $^{(5)}$ 電気通信大学, $^{(6)}$ 京都大学, $^{(7)}$ 九州工業大学, $^{(8)}$ 東京大学, $^{(9)}$ 大阪大学大学院, $^{(10)}$ 東京大学, $^{(11)}$ 宇宙航空研究開発機構

ULF-Modulated Whistler Mode Wave and Electron Precipitation Observed by EISCAT and Arase

#Kohki Tachi¹⁾, Yuto KATOH¹⁾, Atsushi KUMAMOTO¹⁾, Yoshiya KASAHARA²⁾, Shoya MATSUDA²⁾, Atsuki SHINBORI³⁾, Mizuki FUKIZAWA⁴⁾, Yasunobu OGAWA⁴⁾, Keisuke HOSOKAWA⁵⁾, Ayako MATSUOKA⁶⁾, Mariko TERAMOTO⁷⁾, Kazuhiro YAMAMOTO³⁾, Satoshi KASAHARA⁸⁾, Shoichiro YOKOTA⁹⁾, Kunihiro KEIKA¹⁰⁾, Tomoaki HORI³⁾, Yoshizumi MIYOSHI³⁾, Iku SHINOHARA¹¹⁾

⁽¹Department of Geophysics, Graduate School of Science, Tohoku University, ⁽²Emerging Media Initiative, Kanazawa University, ⁽³Institute for Space-Earth Environement Research, Nagoya University, ⁽⁴National Institute of Polar Research, ⁽⁵University of Electro-Communications, ⁽⁶Graduate School of Science, Kyoto University, ⁽⁷Kyushu Institute of Technology, ⁽⁸Tokyo University, ⁽⁹Osaka University, ⁽¹⁰Department of Earth and Planetary Science, Graduate School of Science, The University of Tokyo, ⁽¹¹Japan Aerospace Exploration Agency/Institute of Space and Astronautical Science

We report analysis results of ULF waves observed by the Arase satellite, whistler-mode waves modulated by ULF oscillations, and precipitating electrons with ULF-period modulation observed by EISCAT during a conjugate event. Although ULF-period modulations of whistler-mode waves and precipitating electrons have been reported previously, conjugate observations have not yet been presented. Whistler-mode waves are thought to play an important role in the acceleration and loss processes of high-energy particles in the inner magnetosphere, and have been actively discussed in recent years. Recent studies also suggest that ULF waves influence the generation and propagation of whistler-mode waves, leading to phenomena such as whistler-mode waves enhanced at ULF periods and ducted propagation of whistler-mode waves guided by ULF waves. In this study, we investigate whether the flux of precipitating electrons is modulated at the ULF period through whistler-mode waves modulated by ULF oscillations.

The target event occurred between 02:00 and 03:00 UT on 23 October 2024. During this interval, the Arase satellite was traversing the dawn sector at magnetic local time 05:00 and L=7.2, where it observed Pc5-band ULF waves with a period of about 300 s, as well as lower-band whistler-mode chorus waves whose intensity varied in synchrony with the ULF period. Simultaneously, electron fluxes in the 12-100 keV range exhibited periodic variations with the same timescale. At the same time, the EISCAT radar, located near the magnetic footprint of Arase, detected periodic enhancements of ionospheric electron density above 60 km altitude. This indicates intermittent precipitation of electrons with energies up to 100 keV from the magnetosphere into the ionosphere. Data analysis revealed a strong positive correlation between the intensity of whistler-mode waves observed by Arase and the electron density variations observed by EISCAT.

The observed electron precipitation is considered to be caused by pitch angle scattering due to whistler-mode waves. For whistler-mode waves to resonate with electrons in the observed energy range, they need to propagate to high latitudes along a field line at least the magnetic latitude of 18 degrees apploximately. While the resonance energy near the loss cone is below 10 keV at the magnetic equator, it increases to several hundred keV at the observed latitude. To discuss the resonance energy in more detail, we perform ray-tracing calculations to evaluate the propagation angle and location of the waves along their ducted paths, and calculate the resonance energy at each point. These results are then directly compared with the energy characteristics of precipitating electrons observed by EISCAT. Furthermore, we use ground magnetometer data from IMAGE stations to examine the spatial extent of this event. This study contributes to advancing our understanding of wave – wave and wave – particle interactions among ULF waves, whistler-mode waves, and high-energy electrons.

B 会場 : 11/27 AM1(9:15-10:45)

10:15~10:30:00

コーラス波動による非線形電子加速における不均一性パラメータの直接評価

#德田 晴哉 $^{1)}$, 笠原 禎也 $^{1)}$, 松田 昇也 $^{1)}$, 栗田 怜 $^{2)}$, 頭師 孝拓 $^{3)}$, 小嶋 浩嗣 $^{2)}$, 笠原 慧 $^{4)}$, 横田 勝一郎 $^{5)}$, 堀 智昭 $^{6)}$, 桂華 邦裕 $^{4)}$, 松岡 彩子 $^{7)}$, 寺本 万里子 $^{8)}$, 山本 和弘 $^{6)}$, 三好 由純 $^{6)}$, 篠原 育 $^{9)}$

 $^{(1)}$ 金沢大学, $^{(2)}$ 京都大学, $^{(3)}$ 奈良工業高等専門学校, $^{(4)}$ 東京大学, $^{(5)}$ 大阪大学大学院, $^{(6)}$ 名古屋大学・宇宙地球環境研究所, $^{(7)}$ 京都大学, $^{(8)}$ 九州工業大学, $^{(9)}$ 宇宙航空研究開発機構

Direct Evaluation of the Inhomogeneity Parameter as Evidence of Nonlinearity in Chorus Wave – Induced Electron Acceleration

#Seiya Tokuda¹⁾, Yoshiya KASAHARA¹⁾, Shoya MATSUDA¹⁾, Satoshi KURITA²⁾, Takahiro ZUSHI³⁾, Hirotsugu KOJIMA²⁾, Satoshi KASAHARA⁴⁾, Shoichiro YOKOTA⁵⁾, Tomoaki HORI⁶⁾, Kunihiro KEIKA⁴⁾, Ayako MATSUOKA⁷⁾, Mariko TERAMOTO⁸⁾, Kazuhiro YAMAMOTO⁶⁾, Yoshizumi MIYOSHI⁶⁾, Iku SHINOHARA⁹⁾

⁽¹Graduate School of Natural Science and Technology, Kanazawa University, ⁽²Research Institute for Sustainable Humanosphere, Kyoto University, ⁽³Nara College, National Institute of Technology, ⁽⁴Graduate School of Science, The University of Tokyo, ⁽⁵Graduate School of Science, Osaka University, ⁽⁶Institute for Space - Earth Environmental Research, Nagoya University, ⁽⁷Graduate School of Science, Kyoto University, ⁽⁸Graduate School of Engineering, Kyushu Institute of Technology, ⁽⁹Institute of Space and Astronautical Science, Japan Aerospace Exploration Agency

Whistler-mode chorus waves play important roles in the acceleration and loss of energetic electron populations in the Earth's inner magnetosphere. Previous studies have reported that the generation of chorus waves, a type of whistler-mode waves, is accompanied by rapid variations in electron pitch angle distributions [Fennel et al., 2014; Kurita et al., 2018]. This phenomenon is characterized by the deformation of electron distribution in the velocity space where effective wave-particle interaction is expected and the electron flux drastically increases within the resonance range of cyclotron resonance.

In this study, we analyzed variations in electron flux associated with chorus waves using observation data from PWE, MEP-e, and MGF onboard the Arase satellite in order to deepen our understanding of such phenomena. During the observation period from March 2017 to October 2018, 46 events were visually identified, and we compared the range of deformations in electron pitch angle distributions with the resonance range calculated from the observed chorus waves for each event. As a result, it was found that the observed deformations in electron pitch angle distributions can be explained by first-order cyclotron resonance with the chorus waves in many of the identified events.

It is also noted that rapid variations in the electron pitch angle distribution, occurring on time scales ranging from a few seconds to several tens of seconds, are not always adequately explained by conventional quasi-linear diffusion theory [Kurita et al., 2018, 2025; Saito et al., 2021]. In this study, we further investigated to clarify whether these rapid variations are associated with nonlinear wave – particle interactions. Specifically, we calculate the ratio of wave-induced effects to background inhomogeneity effects ρ γ [Saito et al., 2016] and classify the electron scattering processes for each event, thereby quantitatively evaluating the degree of nonlinearity. In the presentation, we discuss the results of this nonlinearity evaluation and their implications.

ホイッスラーモード波は、地球内部磁気圏における高エネルギー電子の加速や消失に重要な役割を果たしていることが知られている。先行研究では、ホイッスラーモード波の一種であるコーラス波動の発生に伴い、電子ピッチ角分布が変動する現象が報告されている [Fennel et al., 2014; Kurita et al., 2018]。この現象では、速度空間において波動粒子相互作用が有効に働く領域でピッチ角分布の変動が観測されており、特にサイクロトロン共鳴条件を満たす領域で電子フラックスの増加が示されている。

本研究では、このような現象の理解を深めることを目的として、あらせ衛星に搭載された PWE、MEP-e、MGF の観測データを用いて、コーラス波動に伴う電子フラックス変動現象の解析を行った。2017 年 3 月から 2018 年 10 月までの観測期間において、目視により 46 件のイベントを同定し、各イベントにおける電子ピッチ角分布の変動範囲と、コーラス波動から計算される共鳴範囲との比較を行った。その結果、多くのイベントにおいて、観測されたピッチ角分布の変動はコーラス波動との一次サイクロトロン共鳴によって説明可能であることが明らかとなった [Tokuda et al., 2025]。

また、電子ピッチ角分布の変動は数秒から数十秒という短時間スケールで発生しており、従来の準線形拡散理論では十分に説明できない場合がある [Kurita et al., 2018, 2025; Saito et al., 2021]。そこで本研究では、これらの急激な変動が非線形波動粒子相互作用によって生じているかどうかをさらに詳細に解析した。具体的には、波動誘起効果と背景不均一性効果の比 ρ γ [Saito et al., 2016] を算出し、各イベントについて電子の散乱過程を分類することで、非線形性の程度を定量的に評価した。本発表では、この非線形性評価の結果とその解釈について議論する。

B 会場 : 11/27 AM1(9:15-10:45)

10:30~10:45:00

#字井 瞭介 $^{1)}$, マルチネス・カルデロン クラウディア $^{1)}$, Kolmašová Ivana $^{2,3)}$, Santolík Ondřej $^{2,3)}$, 塩川 和夫 $^{1)}$, 篠原 育 $^{4)}$, 三好 由純 $^{1)}$, 笠原 慧 $^{5)}$, 桂華 邦裕 $^{5)}$, 横田 勝一郎 $^{6)}$, 堀 智昭 $^{1)}$, 三谷 烈史 $^{4)}$, 高島 健 $^{4)}$, Wang Shiang-Yu $^{7)}$, 風間 洋一 $^{7)}$, Jun ChaeWoo $^{1)}$, 笠原 禎也 $^{8)}$, 松田 昇也 $^{8)}$, 新堀 淳樹 $^{1)}$, Bortnik Jacob $^{9)}$, Rodger Craig J $^{10)}$

(1) 宇宙地球環境研究所,名古屋大学,(2) Department of Space Physics, Institute of Atmospheric Physics CAS,(3) Faculty of Mathematics and Physics, Charles University,(4) 宇宙航空研究開発機構,(5) 東京大学,(6) 大阪大学大学院,(7) Academia Sinica Institute of Astronomy and Astrophysics,(8) 金沢大学,(9) University of California Los Angeles,(10) Department of Physics,University of Otago

Lightning-Generated Whistler wave coupling and its effects on electrons in the inner magnetosphere using ERG and WWLLN

#Ryosuke Ui¹⁾, Claudia Martinez-Calderon¹⁾, Ivana Kolmašová^{2,3)}, Ondřej Santolík^{2,3)}, Kazuo SHIOKAWA¹⁾, Iku SHINOHARA⁴⁾, Yoshizumi MIYOSHI¹⁾, Satoshi KASAHARA⁵⁾, Kunihiro KEIKA⁵⁾, Shoichiro YOKOTA⁶⁾, Tomoaki HORI¹⁾, Takefumi MITANI⁴⁾, Takeshi TAKASHIMA⁴⁾, Shiang-Yu Wang⁷⁾, Yoichi KAZAMA⁷⁾, Chaewoo JUN¹⁾, Yoshiya KASAHARA⁸⁾, Shoya MATSUDA⁸⁾, Atsuki SHINBORI¹⁾, Jacob Bortnik⁹⁾, Craig J Rodger¹⁰⁾

⁽¹Institute for Space Earth Environmental Research, Nagoya University, ⁽²Department of Space Physics, Institute of Atmospheric Physics CAS, ⁽³Faculty of Mathematics and Physics, Charles University, ⁽⁴ISAS, ⁽⁵Tokyo University, ⁽⁶Osaka University, ⁽⁷Academia Sinica Institute of Astronomy and Astrophysics, ⁽⁸Kanazawa University, ⁽⁹University of California Los Angeles, ⁽¹⁰Department of Physics, University of Otago

Lightning discharges in the Earth's atmosphere emit electromagnetic waves over a broad frequency spectrum. In the Very Low Frequency (VLF) range, energy can penetrate upwards into the ionosphere, propagating as whistler-mode waves into the inner magnetosphere. These waves are known to cause pitch-angle scattering of radiation belt electrons, leading to their precipitation into the atmosphere. While one-to-one correlations between single lightning events and subsequent electron precipitation have been established, the long-term impact of global lightning activity on the total trapped electron population remains an open question. Martinez-Calderon et al. (2020) conducted a year-long comparison of global lightning activity, measured by the World Wide Lightning Location Network (WWLLN), with trapped electron fluxes observed by the Van Allen Probes. They did not find the expected clear long-term connection between increased lightning activity and decreased radiation belt fluxes. A more recent analysis incorporating WWLLN, Van Allen Probes, and Arase data for 2018 yielded similar results (manuscript in preparation).

To explain the above, we assumed that the propagation efficiency of whistler waves from the atmosphere to the magneto-sphere is highly variable and potentially low. This study statistically quantifies this efficiency using data from Arase (PWE, MEP-e, HEP) and WWLLN. Focusing on the 30 days of peak global lightning activity in 2018, we applied the methodology of Zheng et al. (2016) to determine the correspondence rate between whistlers and lightning strokes. For exceptionally large-amplitude whistler events, we also conducted targeted case studies on concurrent electron data to identify direct signatures of pitch-angle scattering. Our approach provides key observational data on lightning-whistler coupling efficiency, addressing the inconsistencies between models and long-term observations.

B 会場 : 11/27 AM2(11:05-12:35)

11:05~11:20:00

ダクト伝搬する波動と粒子の相互作用観測のための超小型電子計測技術の開発

#田中 寿典 $^{1)}$, 笠原 慧 $^{2)}$, 三谷 烈史 $^{3)}$, 三好 由純 $^{4)}$, 加藤 雄人 $^{5)}$ $^{(1)}$ 東京大学, $^{(2)}$ 東京大学, $^{(3)}$ 宇宙航空研究開発機構, $^{(4)}$ 名古屋大学, $^{(5)}$ 東北大学

Development of a CubeSat Electron Measurement Technology for Observing Ducted Wave-Particle Interactions in Low Earth Orbit

#Toshinori TANAKA¹⁾, Satoshi KASAHARA²⁾, Takefumi MITANI³⁾, Yoshizumi MIYOSHI⁴⁾, Yuto KATOH⁵⁾
⁽¹The University of Tokyo, ⁽²The University of Tokyo, ⁽³Japan Aerospace Exploration Agency, ⁽⁴Institute for Space-Earth Environemental Research, Nagoya University, ⁽⁵Tohoku University

Plasma waves in the Earth's magnetosphere play a significant role in space environment dynamics by accelerating and scattering charged particles. For example, whistler-mode chorus waves are generated near the magnetic equator and are known to cause pitch-angle scattering of energetic electrons. As these waves propagate to higher latitudes, their resonance energy with electrons increases, leading to the precipitation of quasi-relativistic and relativistic electrons into the atmosphere. It has been suggested that such waves can be guided by field-aligned density enhancements, or "ducts," enabling efficient propagation to higher latitudes without significant scattering. However, direct observational evidence of this process remains scarce. To test the hypothesis of high-energy electron precipitation driven by ducted waves, we are developing the Low-Earth Orbit Electron Sensor (LEON) for the IMPACT project. LEON is a compact detector capable of covering a wide energy range of 10 - 1000 keV with a single instrument, enabling observations from seed electrons before interaction to quasi-relativistic/relativistic electrons afterward. In-situ measurements of precipitating electrons from low-Earth orbit (500 - 600 km) will provide decisive evidence of wave - particle interactions occurring within ducts. Few detectors can achieve such wide energy coverage within the 1U CubeSat form factor. LEON employs a hybrid configuration, using an Avalanche Photodiode (APD) for low energies and a Solid-State Detector (SSD) for high energies. In this presentation, we report on the performance evaluation of a 1.5-mm thick SSD and noise-mitigation simulations. Laboratory tests with 57Co and 207Bi sources confirmed that the SSD provides sufficient energy resolution (eg. FWHM = 7.8 keV at 122 keV). Monte Carlo simulations were also conducted to design aluminum shielding against background from sunlight and protons. The results demonstrate that, with optimized shielding, LEON can effectively measure electrons from 25 to 1600 keV, covering the target science range while suppressing proton contamination.

地球磁気圏に存在するプラズマ波動は、荷電粒子の加速や散乱を引き起こすことで、宇宙環境の変動に中心的な役割を 果たしている。例えば、ホイッスラーモード・コーラス波動は、磁気赤道付近で発生後、高エネルギー電子のピッチ角散 乱を引きおこす。高緯度に伝搬したプラズマ波動は、電子との共鳴エネルギーが高くなることで、準相対論的/相対論的 電子の降下を引き起こす。このようなプラズマ波動は、周囲よりプラズマ密度が高い「ダクト」構造に捕捉されること で、散乱することなく高緯度へと伝搬することが示唆されているが、その直接的な観測証拠は未だ限られている。本研究 の目的は、この「ダクト伝搬波動による高エネルギー電子の降下」という仮説をその場観測によって実証する IMPACT プロジェクトで使用する、「超小型高エネルギー電子計測器(LEON; Low-earth Orbit Electron Sensor)」の開発である。 LEON は、波動による加速・散乱前のシード電子から、相互作用後の準相対論・相対論的電子までを包括する 10~1000 keV のエネルギー帯域を単一の機器で捉える。高度 500~600 km の低軌道において、大気へ降下してくるこれらの電子 を計測することは、ダクト内波動との相互作用の決定的な証拠となる。しかし、この広帯域なエネルギー範囲をカバーす る電子計測器の中で、超小型衛星に搭載可能な 1U サイズのものは少ない。LEON は、低エネルギー側をアバランシェ フォトダイオード(APD)、高エネルギー側を固体検出器(SSD)で分担するハイブリッド構成を用いている。本発表で は、LEON 開発の一環として行った、高エネルギー側を担う厚さ 1.5 mm の SSD の性能評価と、ノイズ対策シミュレー ションについて報告する。性能評価実験では、放射線源として 57Co および 207Bi を用い、SSD が十分なエネルギー分 解能を持つことを確認した(FWHM=7.8keV@122keV)。また、計測ノイズ源となる太陽光や高エネルギー陽子をアルミ ニウムを用いて遮蔽するため、モンテカルロシミュレーションを実施した。その結果、最適な厚さのアルミニウム遮蔽材 を施すことで、電子の計測結果に陽子の影響を抑えて、目標エネルギー範囲を包含する 25~1600 keV の電子を計測可能 であることを示す予定である。

B 会場 : 11/27 AM2(11:05-12:35)

11:20~11:35:00

磁気圏 ELF/VLF 波動解析における時系列に着目した空電ノイズ除去プログラムの 開発

#伊藤 優斗 $^{1)}$, 塩川 和夫 $^{1)}$, マルチネス・カルデロン クラウディア $^{1)}$, マニネン ユルキ $^{2)}$, コナーズ マーティン $^{3)}$ $^{(1)}$ 名大 ISEE, $^{(2)}$ オウル大学, $^{(3)}$ アサバスカ大学

Development of a Time-Series-Based Software for Sferic Noise Removal in Magnetospheric ELF/VLF Wave Analysis

#Yuto Ito¹⁾, Kazuo SHIOKAWA¹⁾, Claudia Martinez-Calderon¹⁾, Jyrki Manninen²⁾, Martin Connors³⁾
⁽¹Institute for Space-Earth Environmental Research, Nagoya University, ⁽²University of Oulu, Finland, ⁽³Athabasca University, Canada

Analyzing dynamic spectra of magnetospheric ELF/VLF waves, generated through interactions in the magnetospheric plasma, offers useful information for understanding the plasma state However, when these waves are received on the ground using antennas, noise by sferics produced by lightning makes it difficult to identify magnetospheric waves on the dynamic spectra. In this study, we developed software to remove the noise from sferics while preserving the waveforms of magnetospheric ELF/VLF signals as much as possible. We used data with a 40-kHz sampling rate obtained in 2024 at Athabasca, Canada, and Oulujärvi, Finland, through the PWING project. Since sferics appear as short pulses lasting only a few hundred milliseconds, they are detected as broadband features in the spectrum, particularly at higher frequencies, and frequently overlap with magnetospheric ELF/VLF waves. In contrast, magnetospheric ELF/VLF waves vary over several milliseconds or seconds, much more slowly than sferics. Therefore, we considered it more appropriate to address sferic noise in the time domain rather than in the frequency domain. Our method detects sferics as noise in the time domain and attempts to remove them through interpolation. A simple method of setting values to zero when amplitudes exceed a threshold was found to spread spectral contamination into the low-frequency range. Furthermore, when interpolation was performed by averaging spectra before and after the removed intervals, we found that using intervals that were too long led to removal of more than 50% of the data. To address this, we attempted to optimize the procedure to minimize the removed intervals. In this presentation, we will report these results, including noiseremoval approaches using machine learning, and discuss the validity of the proposed sferic-removal methods.

磁気圏プラズマの相互作用によって発生する磁気圏 ELF/VLF 波動についてダイナミックスペクトルを通じて解析することは磁気圏プラズマの状態を知る上で有用な情報である。しかし、これらの波動を地上に建設したアンテナを用いて傍受する際、落雷により発生する空電がノイズとなり、ダイナミックスペクトル上で磁気圏からの波動が見えづらくなってしまうことが度々ある。そこで、本研究では磁気圏 ELF/VLF 波動の信号波形をなるべく壊すことなく空電ノイズを除去するソフトウェアの開発に取り組んだ。使用したデータは、カナダの Athabasca 及びフィンランドの Oulujarvi で PWING プロジェクトで 2024 年に取得された 40kHz サンプルのデータである。空電は数百 ms 程度のごく短時間でパルス状に振動するので、スペクトル上では広い帯域に、とりわけ高周波側に顕著に現れて、磁気圏 ELF/VLF 波動と重なることが多い。一方、磁気圏 ELF/VLF 波動は空電と比較して数ミリから数秒程度の長い時間をかけて波形が変化する。したがって、空電ノイズの除去は周波数領域ではなく時間領域で考えるのが妥当だと考えた。そこで本研究では空電を時間領域でノイズとして検知して、補間することで除去を試みた。単純に振幅が閾値を超えた場合に値をゼロにする手法は、低周波側のスペクトルにも除去によるスペクトル汚染が広がることが分かった。また、除去後のデータを前後のデータのスペクトルを平均して補間する場合、時系列波形における空電ノイズの判定区間を長くしすぎると、除去率 50% 以上の大きな割合のデータが除去されてしまうことが分かった。このため、除去する部分をできるだけ短くするように最適化を試みている。講演では、機械学習によるノイズ除去の手法を含めてこれらの結果を報告し、空電除去の方法の妥当性を議論する。

B会場: 11/27 AM2(11:05-12:35)

11:35~11:50:00

#田中 友啓 $^{1,2)}$, 田中 良昌 $^{1,2,3)}$, 小川 泰信 $^{1,2)}$, 門倉 昭 $^{2,3)}$, 村瀬 清華 $^{4)}$, 細川 敬祐 $^{5)}$, 大山 伸一郎 $^{2,6,7)}$, Kero Antti $^{7)}$ $^{(1)}$ 総研大, $^{(2)}$ 国立極地研究所, $^{(3)}$ データサイエンス共同利用基盤施設, $^{(4)}$ 北見工業大学, $^{(5)}$ 電気通信大学, $^{(6)}$ 名古屋大学宇宙地球環境研究所, $^{(7)}$ オウル大学ソダンキュラ観測所

Hardness of precipitating particle energy spectrum revealed by spectral riometer: May 2024 storm event

#Tomotaka Tanaka^{1,2)}, Yoshimasa TANAKA^{1,2,3)}, Yasunobu OGAWA^{1,2)}, Akira KADOKURA^{2,3)}, Kiyoka MURASE⁴⁾, Keisuke HOSOKAWA⁵⁾, Shin-ichiro OYAMA^{2,6,7)}, Antti Kero⁷⁾

⁽¹The Graduate University for Advanced Studies, SOKENDAI, ⁽²National Institute of Polar Research, NIPR, ⁽³Joint Support-Center for Data Science Research, ROIS, ⁽⁴Kitami Institute of Technology, KIT, ⁽⁵The University of Electro-Communications, ⁽⁶Institute for Space-Earth Environmental Research, Nagoya University, ⁽⁷Sodankyla Geophysical Observatory, University of Oulu

Spectral riometers in Finland observe cosmic noise in the frequency range of 20 – 55 MHz, and the frequency spectra of cosmic noise absorption (CNA) derived from the observations are expected to provide estimates of the altitude distribution of electron density enhancements in the ~50 – 100 km region. However, only one case study has attempted to derive altitude distributions of electron density enhancements using a spectral riometer, in which the results during an electron precipitation event showed good agreement with simultaneous EISCAT radar observations. This indicates that, although the spectral riometer has sufficient capability to capture the characteristics and temporal variations of mesospheric electron density enhancements, our understanding of these processes remains limited.

In May 2024, an extreme magnetic storm occurred, during which the Dst index reached – 400 nT. During the 16-day period from May 1, which included this storm, frequent enhancements of mesospheric electron density were observed by the spectral riometer at Kilpisjärvi, Finland. These enhancements were caused by phenomena such as high-energy electron precipitation associated with substorms, X-ray emissions associated with solar flares, and high-energy proton precipitation during proton events.

In this study, we focused on the fact that the slope of the CNA frequency spectrum obtained by the spectral riometer is expected to serve as an indicator of the hardness of the energy spectrum of precipitating particles, i.e., the characteristic altitude of electron density enhancements. More specifically, the key parameter is the spectral index, defined as the absolute value of the slope in the relation $\mathbf{CNA} \propto \mathbf{f}^{-n}$, where f is the frequency of cosmic radio noise and n is the spectral index. The CNA spectrum is known to follow a curve with $\mathbf{n} = \mathbf{2}$ when electron density enhancements occur only above an altitude of 70 km. In contrast, when enhancements occur below 70 km, the spectral index decreases toward 0 as the characteristic altitude becomes lower.

In this presentation, we will show that the temporal variation of the spectral index during proton and electron precipitation events agreed well with the features expected from other observations and previous studies. For proton precipitation events, the spectral index became smaller when the flux of >10 MeV protons relative to >50 MeV protons observed by the GOES-18 satellite was smaller, i.e., when the precipitating proton energy spectrum was harder. For electron precipitation events associated with substorms, the MLT distribution of the spectral index showed that the value was around 2 near midnight, while it tended to be smaller than 2 in the morning side. This tendency is consistent with previous studies reporting that precipitating electron spectra become harder in the morning side. In contrast, the number of flare events was too small to obtain sufficient results.

These results demonstrate that the spectral index can serve as an indicator of the hardness of the energy spectrum of precipitating particles and suggests that the spectral riometer is a useful tool for elucidating the characteristics of mesospheric electron density enhancements.

B 会場 : 11/27 AM2(11:05-12:35)

11:50~12:05:00

マルチ観測網で捉えた特異な高周波 VLF バーストパッチの出現統計と伝搬特性

#マルチネス・カルデロン クラウディア $^{1)}$, マニネン ユルキ $^{2)}$, 塩川 和夫 $^{1)}$, 笠原 禎也 $^{3)}$, 松田 昇也 $^{3)}$, 篠原 育 $^{4)}$, 三好由純 $^{1)}$, 新堀 淳樹 $^{1)}$, ハンセルカ ミロスラフ $^{5)}$, ピシャ ダビッド $^{6)}$

 $^{(1)}$ 名古屋大学 ISEE、 $^{(2)}$ オウル大学、 $^{(3)}$ 金沢大学、 $^{(4)}$ 宇宙科学研究所 JAXA、 $^{(5)}$ ドイツ地球科学研究センター、 $^{(6)}$ IAP CAS

Statistics and propagation of unusual 'high frequency' VLF bursty-patches from multi-point observations

#Claudia Martinez-Calderon¹⁾, Jyrki Manninen²⁾, Kazuo Shiokawa¹⁾, Yoshiya Kasahara³⁾, Shoya Matsuda³⁾, Iku Shinohara⁴⁾, Yoshizumi Miyoshi¹⁾, Atsuki Shinbori¹⁾, Miroslav Hanzelka⁵⁾, David Pisa⁶⁾

⁽¹Institute for Space-Earth Environmental Research, Nagoya University, Japan, ⁽²Sodankyla Geophysical Observatory, Sodankyla, Finland, ⁽³Graduate School of Natural Science and Technology, Kanazawa University, Kanazawa, Japan, ⁽⁴Institute of Space and Astronautical Science, Japan Aerospace Exploration Agency, Sagamihara, Japan, ⁽⁵GFZ Helmholtz Centre for Geosciences, Potsdam, Germany, ⁽⁶Institute of Atmospheric Physics, Prague, Czech Republic

In the magnetosphere, Extremely Low (ELF) and Very Low Frequency (VLF) plasma waves occur naturally in the 3 Hz to 30 kHz frequency range. Through wave-particle interactions they influence radiation belt dynamics, accelerating electrons or scattering them into the atmosphere. Bursty-patches are a recently identified class of VLF emissions, occurring at frequencies above half the equatorial electron gyrofrequency (fce/2) at the corresponding L-shell of observation. Usual VLF waves should not be able to propagate to the ground at these frequencies and locations. However, they have been observed at multiple ground-based stations with little information on their occurrence rates or propagation characteristics.

In this study, we use data from VLF receiver stations in Finland to discuss the properties and specific propagation of bursty-patches to the ground. We mainly analyzed 1 year of data from Kannushleto (KAN, MLAT=65.0N, L=5.5) and Oulujarvi (OUJ, MLAT=61.3N, L=4.4) to assess overall occurrence rates, as well as investigate simultaneous and conjugated observations. We also present preliminary results from the Angeli station (ANG, MLAT=66.1N, L=6.3). From a unique conjugate event (showing one-to-one correspondence) observed by KAN, OUJ, and the Arase satellite in the magnetosphere, we also investigated the wave propagation characteristics using polarization and ray tracing analysis.

B 会場 : 11/27 AM2(11:05-12:35)

12:05~12:20:00

磁気嵐時の CNA 変化に関するシミュレーション

#三好 由純 ^{1,2)}, PR Shreedev¹⁾, Jordanova Vania³⁾, Tang Linhui⁴⁾, 齊藤 慎司 ⁵⁾, 塩川 和夫 ¹⁾, 大山 伸一郎 ¹⁾, 細川 敬祐 ⁶⁾
⁽¹ 名古屋大学宇宙地球環境研究所, ⁽²Kyung Hee University, ⁽³ ロスアラモス国立研究所, ⁽⁴Beihang University, ⁽⁵ 情報通信研究機構, ⁽⁶ 電気通信大学

Global CNA response to a magnetic storm: a simulation study

#Yoshizumi Miyoshi^{1,2)}, Shreedev PR¹⁾, Vania Jordanova³⁾, Linhui Tang⁴⁾, Shinji SAITO⁵⁾, Kazuo SHIOKAWA¹⁾, Shinichiro OYAMA¹⁾, Keisuke HOSOKAWA⁶⁾

⁽¹Institute for Space-Earth Environemental Research, Nagoya University, ⁽²Kyung Hee University, ⁽³Los Alamos National Laboratory, ⁽⁴Beihang University, ⁽⁵NICT, ⁽⁶The University of Electro-Communications

Cosmic Noise Absorption (CNA) is caused by enhancements in electron density in the D-region ionosphere through energetic electron precipitation (EEP). It has been widely used as a reliable tracer of EEP from the ground. Recent global network observations (Kato et al., 2024) revealed the longitudinal evolution of EEP; CNA enhancements typically expand eastward in association with particle injections. To investigate the global evolution of CNA during a magnetic storm, we employ the global simulation RAM-SCBE (Jordanova et al., 2023), which models the evolution of the electron distribution function, the plasmasphere, and wave – particle interactions. The GLOW model (Solomon, 2017) is then used to calculate the ionization profiles driven by electron precipitation obtained from RAM-SCBE. Our results show that CNA first appears in the morning sector and subsequently drifts toward the dayside, reflecting the drift motion of energetic electrons and the distribution of whistler-mode wave activity. In this presentation, we will present simulation results on the global evolution of CNA and discuss how CNA variations depend on the energetic electron distribution and whistler-mode waves in the magnetosphere.

Cosmic Noise Absorption(CNA)は、高エネルギー電子降下(EEP)によって D 領域電離圏の電子密度が増加することで引き起こされ、地上から観測可能な EEP の信頼できる指標として広く利用されてきている。近年の全球ネットワーク観測(Kato et al., 2024)により、EEP の経度方向への発達過程も明らかになっており、CNA の増加は通常、電子のドリフトに伴って東向きに広がることが示されている。この磁気嵐時における CNA の発達過程を調べるために、本研究では、RAM-SCBE(Jordanova et al., 2023)と GLOW(Solomon, 2017)によって、磁気嵐時の電子分布関数、熱的プラズマ、また波動粒子相互作用によるピッチ角散乱、そして EEP に伴う超高層大気の電離過程のシミュレーションを行った。その結果、磁気嵐時主相において、CNA はまずサブオーロラ帯の朝側で出現し、その後昼側へと拡大していくことが示さた。これは磁気圏における高エネルギー電子のドリフト、ホイッスラーモード波動によるピッチ角散乱の空間発展を反映していると考えられる。本報告では、この CNA の時間空間変化に関するシミュレーション結果を示すとともに、電離圏で起こる CNA 変動が磁気圏における高エネルギー電子の分布、およびホイッスラーモード波の時空間発展にどのように依存するかを議論する。

B 会場 : 11/27 AM2(11:05-12:35)

12:20~12:35:00

2024年5月巨大地磁気嵐時の ULF 波動による放射線帯電子の拡散について

#山本 和弘 $^{1)}$, 三好 由純 $^{2)}$, 尾花 由紀 $^{3)}$, 松岡 彩子 $^{4)}$, 寺本 万里子 $^{5)}$, 笠羽 康正 $^{6)}$, 笠原 禎也 $^{7)}$, 堀 智昭 $^{8)}$, 新堀 淳樹 $^{8)}$, 熊本 篤志 $^{6)}$, 土屋 史紀 $^{6)}$, 篠原 育 $^{9)}$

 $^{(1)}$ 名古屋大学・宇宙地球環境研究所, $^{(2)}$ 名古屋大学・宇宙地球環境研究所, $^{(3)}$ 九州大学, $^{(4)}$ 京都大学, $^{(5)}$ 九州工業大学, $^{(6)}$ 東北大学, $^{(7)}$ 金沢大学, $^{(8)}$ 名古屋大学・宇宙地球環境研究所, $^{(9)}$ 宇宙航空研究開発機構

ULF wave radial diffusion of radiation belt electrons during the May 2024 super geomagnetic storm

#Kazuhiro Yamamoto¹⁾, Yoshizumi MIYOSHI²⁾, Yuki OBANA³⁾, Ayako MATSUOKA⁴⁾, Mariko TERAMOTO⁵⁾, Yasumasa KASABA⁶⁾, Yoshiya KASAHARA⁷⁾, Tomoaki HORI⁸⁾, Atsuki SHINBORI⁸⁾, Atsushi KUMAMOTO⁶⁾, Fuminori TSUCHIYA⁶⁾, Iku SHINOHARA⁹⁾

⁽¹Institute for Space-Earth Environmental Research ⁽¹ISEE), Nagoya University, ⁽²Institute for Space-Earth Environmental Research ⁽¹ISEE), Nagoya University, ⁽³International Research Center for Space and Planetary Environmental Science, Kyushu University, ⁽⁴World Data Center for Geomagnetism, Kyoto, Graduate School of Science, Kyoto University, ⁽⁵Faculty of Engineering Department of Space Systems Engineering, Kyushu Institute of Technology, ⁽⁶Planetary Plasma and Atmospheric Research Center, Graduate School of Science, Tohoku University, ⁽⁷Graduate School of Natural Science and Technology, Kanazawa University, ⁽⁸Institute for Space-Earth Environmental Research ⁽¹ISEE), Nagoya University, ⁽⁹Institute of Space and Astronautical Science, Japan Aerospace Exploration Agency

The acceleration mechanism of radiation belt electrons is a crucial research issue in magnetospheric plasma physics in terms of particle acceleration and space weather. While the local acceleration of radiation belt electrons by plasma waves has been extensively studied in recent years (Thorne, 2010; Reeves et al., 2013; Thorne et al., 2013), radial diffusion is also considered as an important factor that redistributes radiation belt electrons from the region of the local acceleration to other locations (Ma et al., 2018). Previous studies of the radial diffusion caused by ultralow frequency (ULF) waves developed empirical models of the radial diffusion coefficient under various geomagnetic activity levels (Brautigam and Albert, 2000; Brautigam et al., 2005; Ozeke et al., 2012, 2014; Sandhu et al., 2021; Murphy et al., 2023). However, these models do not cover the highest levels (Kp >7, where Kp is the Planetary K index), and thereby event analysis is required to obtain an accurate radial diffusion coefficient during the G4 (Kp = 8, 9-) and G5-class (Kp = 90) geomagnetic storms. Therefore, to understand the role of ULF waves in the radial diffusion of electrons during the highest geomagnetic activity, we investigated the ULF wave activity during the G5-class geomagnetic storm in May 2024. In the early recovery phase of this storm, the Arase satellite (Miyoshi et al., 2018) detected toroidal waves with a large amplitude (60 nT peak-to-peak) in the dawn sector (9-11 MLT hours) on May 11, 2024. Although the toroidal waves were detected deep in the magnetosphere at L > 2.5, their frequency ranges from 2 to 6 mHz, corresponding to the Pc 5 range. We also analyzed the geomagnetic field observed at the International Monitor for Auroral Geomagnetic Effect (IMAGE) stations near Arase's ionospheric footprint. Using the amplitude-phase gradient method (Pilipenko and Fedorov, 1994), we identified the frequencies of field line resonance (FLR) at the altitude-adjusted corrected geomagnetic (AACGM) latitudes between 47 to 59°. The FLR frequencies obtained from the ground-based observation were close to Arase's observation and gradually decreased with AACGM latitude. These results demonstrate that the toroidal Pc 5 waves observed by Arase are standing Alfvén waves excited through FLR. Using the formula derived by Ozeke et al. (2014), we calculated the radial diffusion coefficients of a 950 keV electron for the toroidal Pc 5 waves with an assumption of m = 3, where m is the azimuthal wave number. The diffusion coefficient of the electric field reached $^{\sim}10 \text{ day}^{-1}$ around L = 4.6, an order of magnitude larger than that of Kp = 6 calculated by Ozeke et al. (2014). Given that the local peak of the phase space density of ~1 MeV electrons is located at L <4, we suggest that the toroidal standing Alfvén waves transport the ~1 MeV electrons from the location of the local peak to an outer region within a few hours.

B会場: 11/27 PM1 (13:45-15:45)

13:45~14:00:00

#長田 知大 $^{1)}$, 関 華奈子 $^{1,2)}$, 山川 智嗣 $^{3)}$, 山本 和弘 $^{3)}$, 海老原 祐輔 $^{4)}$, 天野 孝伸 $^{1)}$, 桂華 邦裕 $^{1)}$ (1 東京大学大学院理学系研究科, $^{(2)}$ 東京大学先端科学技術研究センター, $^{(3)}$ 名古屋大学宇宙地球環境研究所, $^{(4)}$ 京都大学生存圏研究所

Influence of the Weak Intrinsic Magnetic Field on the Development of Magnetic Storms Based on Global Drift-Kinetic Simulations

#Kazuhiro Osada¹⁾, Kanako SEKI^{1,2)}, Tomotsugu YAMAKAWA³⁾, Kazuhiro YAMAMOTO³⁾, Yusuke EBIHARA⁴⁾, Takanobu AMANO¹⁾, Kunihiro KEIKA¹⁾

⁽¹Graduate School of Science, the University of Tokyo, ⁽²Research Center for Advanced Science and Technology, the University of Tokyo, ⁽³Institute for Space-Earth Environmental Research, Nagoya University, ⁽⁴Research Institute for Sustainable Humanosphere, Kyoto University

Earth's intrinsic magnetic field strength is one of the most critical parameters in geospace. It has decreased by ~30% over the past 2000 years [Olson and Amit, 2006]. The decrease will change quasi-static parameters of the magnetosphere-ionosphere-thermosphere system [e.g. Cnossen et al, 2012]. It will also change transient phenomena of magnetosphere like substorms and magnetic storms. A previous study examined the dependency of auroral substorms on the intrinsic magnetic field by global MHD simulations [Ebihara et al., 2020]. However, the effect of intrinsic magnetic field strength on the development of magnetic storms is still unclear, because in the inner magnetosphere, kinetic processes, which are not included in the MHD approximation, are dominant.

We investigated the development of magnetic storms and ring current and associated excitations of ULF waves, using a magnetosphere-ionosphere coupled model [Yamakawa et al. 2023] which combines GEMSIS-RC [Amano et al. 2011] and GEMSIS-POT [Nakamizo et al. 2012]. In GEMSIS-RC, the 5D drift-kinetic equation and Maxwell's equations are solved self-consistently. GEMSIS-POT solves ionospheric electric potential for the height-integrated ionosphere. In the coupled model, distribution of plasmaspheric cold plasma is also evolved based on a continuity equation. Simulations were conducted for three cases: the present Earth (Case 1), a planet with a weak (2/3 of Case 1) intrinsic magnetic field and high ionospheric conductivity (Case 2), and with the weak magnetic field and standard ionospheric conductivity (Case 3). Case 1, 2, and 3 correspond to Run 1, 3, and 5 of global MHD simulations (Ebihara et al. [2020]), respectively. For each case, we applied R1-FAC to the ionosphere and set the temperature and density of the plasma sheet according to the corresponding run.

From the obtained distributions of the ring current ions, SYM-H index with the Dessler-Parker-Sckopke relation is estimated to evaluate the development of magnetic storms. The minimum value of SYM-H index turned out to be in the following order: Case 3 <Case 2 <Case1, and SYM-H index declined more rapidly in Cases 2 and 3 than in Case 1. The total kinetic energy of the ring current was the smallest in Case 2, and almost the same in Cases 1 and 3. Although the total kinetic energy of the ring current decreases under weak intrinsic magnetic field cases, the decrease is smaller relative to the reduction of the intrinsic dipole magnetic energy in the denominator of the DPS relation, which results in a larger decrease of the estimated SYM-H index in Case 2 than in Case 1. We also found that in the weak intrinsic magnetic field cases, ring current azimuthal development is faster in the duskside. This is because ring current developed closer to Earth in the cases, which leads to larger drift frequencies of ring current ions. Excitations of fundamental ULF waves due to injection of ring current ions are identified in all cases: dayside Pc5 and dawnside Pc4. Under the weak intrinsic magnetic fields, the amplitude of excited ULF waves was smaller in the dayside and larger in the dawnside. In the presentation, we will also discuss the reason in detail.

B 会場 : 11/27 PM1(13:45-15:45)

14:00~14:15:00

あらせの衛星帯電について

#陶 由未加 $^{1)}$, 笠原 慧 $^{1)}$, 浅村 和史 $^{2)}$, 松岡 彩子 $^{3)}$, 髙原 璃乃 $^{1)}$, 三好 由純 $^{4)}$ (1 東京大学, $^{(2}$ 宇宙航空研究開発機構, $^{(3)}$ 京都大学, $^{(4)}$ 名古屋大学

Spacecraft charging of the Arase (ERG) satellite

#Yumika SUE¹⁾, Satoshi KASAHARA¹⁾, Kazushi ASAMURA²⁾, Ayako MATSUOKA³⁾, Rino TAKAHARA¹⁾, Yoshizumi MIYOSHI⁴⁾

(1 UTokyo, (2 JAXA, (3 Kyoto univ., (4 Nagoya Univ.

Spacecraft charging can cause satellite malfunctions; therefore, understanding the conditions under which charging occurs is crucial for the safe operation of satellites. Spacecraft charging arises from an imbalance between the inflow and outflow of charged particles. Previous studies have long investigated the conditions for spacecraft charging, suggesting correlations with the temperature and flux of ambient electrons [e.g., Davis et al., 2008]. In addition, during eclipse periods, photoelectron emission ceases due to the absence of solar illumination, making the spacecraft more prone to negative charging.

When charging occurs, ultra-low-energy ions (on the order of 0 - 10 eV) are attracted by the spacecraft potential. These ultra-low-energy ions are difficult to detect during non-charging periods because of the low sensitivity of particle instruments at the lowest energy range. In this study, we utilize the charging state of the Exploration of Energization and Radiation in Geospace (ERG; Arase) satellite to investigate the physical characteristics of ultra-low-energy ions, particularly oxygen ions, which are usually undetectable. This provides new insight into the circulation of oxygen in the Earth's magnetosphere.

We analyzed the ion density and temperature during spacecraft charging events observed by Arase in eclipse. Our results show that, in most cases, the H+ density during charging was significantly lower than the electron density derived from wave data. The contribution of ultra-low-energy H+ to the total H+ density was generally less than 5%, and at most 15%. Regarding the O+/H+ density ratio, values were typically below ~25%, but in some events exceeded unity. This is much higher than previously reported O+ fractions in the near-Earth magnetosphere (~0.4), suggesting the possibility that H+ measurements may have been saturated during these events. To validate the reliability of these observations, further analyses using independent diagnostics, such as wave data, are required.

衛星帯電は人工衛星の故障を引き起こすため、衛星を安全に運用していく上でその発生条件を明らかにすることは重要である。衛星帯電は、衛星に入流出する荷電粒子のバランスによって発生する。衛星帯電の発生条件に関する研究は長年にわたって行われており、衛星周囲の電子の温度やフラックスとの関係 [Davis et al.,2008 など] が示唆されている。また、日陰時は太陽光による光電子放出がなくなるため、衛星は負に帯電しやすい。

さらに帯電発生時には、超低エネルギー (0-10eV 程度) のイオンが衛星の帯電ポテンシャルによって引き寄せられる。これらの超低エネルギーイオンは、観測器の低エネルギー側の感度が低く、帯電非発生時には検出されにくい。本研究は、ジオスペース探査衛星あらせの帯電状態を用いて普段は検出できない超低エネルギー、特に酸素イオンの物理的様相を明らかにすることで、地球磁気圏の酸素循環を理解する手掛かりとなる。

今回、ジオスペース探査衛星あらせの日陰時の帯電現象について、帯電発生時のイオンの密度および温度について解析を行った。

その結果、帯電発生時の H+ 密度は波動データから得られた電子密度に比べてほとんどの場合で大きく下回っていた。 また、超低エネルギーの H+ のトータルの H+ 密度への寄与は多くても 15 % 以下で大体は 5% 以下であった。

O+/H+ の密度比については、大体のイベントで~25% 以下だが、一部イベントで 1 を超えていた。これは先行研究の地球磁気圏近傍の酸素イオンの存在割合 (たかだか~0.4) よりも極めて大きく、水素イオン計測が当イベントで飽和していた可能性が考えられる。この観測データの妥当性を検証するためには、波動データ等を用いた別視点の解析が必要である。

B会場: 11/27 PM1(13:45-15:45)

14:15~14:30:00

#西田 結衣 $^{1)}$, 三好 由純 $^{1)}$, 浅村 和史 $^{2)}$, Kistler Lynn $^{3)}$, 篠原 育 $^{2)}$ $^{(1)}$ 名大 ISEE、 $^{(2)}$ 宇宙航空研究開発機構、 $^{(3)}$ ニューハンプシャー大学

Long-term Variations of He++ Ions in the Inner Magnetosphere: Observations by Arase LEP-i

#Yui Nishida¹⁾, Yoshizumi MIYOSHI¹⁾, Kazushi ASAMURA²⁾, Lynn Kistler³⁾, Iku SHINOHARA²⁾ (¹ISEE/Nagoya University, ⁽²ISAS/JAXA, ⁽³University of New Hampshire

He++ ions in the inner magnetosphere primarily originate from the solar wind and can serve as a tracer of solar wind-origin ions. However, their spatial and temporal variations remain poorly understood due to the limited number of satellite observations with sufficient mass resolution. The Low-Energy Particle (LEP-i) instrument onboard the Arase satellite provides high mass resolution and enables clear discrimination among ion species, including He++. In this study, we analyzed Time-of-Flight (TOF) data from LEP-i with a 10-min time resolution to investigate the long-term variations of He++ ions in the inner magnetosphere and their dependence on L-shell. Our analysis covers the period from the declining phase of Solar Cycle 24 through the rising phase of Solar Cycle 25.

We found that the ratio of He++ and H+ (19 keV/q) has a clear solar cycle dependence. The ratio varies distinctly between the outer ($L \ge 4.5$) and inner (L < 4.5) magnetosphere, suggesting differences in loss time scales, likely due to charge exchange process. Furthermore, we found that the He++/H+ ratio observed by Arase LEP-i is correlated with solar wind speed, which is similar variation to the He++/H+ ratio in the solar wind. Unlike previous studies, observations by the Arase satellite's LEP-i instrument suggest that He++ counts depend on both solar activity and geomagnetic activity. These findings suggest that He++ ions in the inner magnetosphere retain signatures of their solar wind origin and serve as useful tracers of solar wind-origin plasma in the inner magnetosphere.

B会場: 11/27 PM1(13:45-15:45)

14:30~14:45:00

ジオコロナ水素原子密度:Arase 衛星の高エネルギーイオンデータを用いた推定

#家田 章正 $^{1)}$, 北村 成寿 $^{1)}$, 三好 由純 $^{1)}$, 堀 智昭 $^{1)}$, 山本 和弘 $^{1)}$, Jun ChaeWoo¹⁾, 横田 勝一郎 $^{2)}$, 笠原 慧 $^{3)}$, 桂華 邦裕 $^{3)}$, 篠原 育 $^{4)}$

(1 名大 ISEE, (2 阪大, (3 東大, (4 宇宙航空研究開発機構

Geocoronal atomic hydrogen number density: Estimation using energetic ions observed by the Arase satellite

#Akimasa Ieda¹⁾, Naritoshi KITAMURA¹⁾, Yoshizumi MIYOSHI¹⁾, Tomoaki HORI¹⁾, Kazuhiro YAMAMOTO¹⁾, Chaewoo JUN¹⁾, Shoichiro YOKOTA²⁾, Satoshi KASAHARA³⁾, Kunihiro KEIKA³⁾, Iku SHINOHARA⁴⁾

(¹Institute for Space-Earth Environmental Research, Nagoya University, (²Osaka university, (³University of Tokyo, (⁴JAXA)

The geocorona is a part of the neutral atmosphere of the Earth above an altitude of 2000 km. It consists of low-energy hydrogen atoms and plays a key role in controlling the decay rate of geomagnetic storms through charge-exchange reactions with high-energy ions. However, the number density of geocoronal hydrogen shows discrepancies of up to a factor of two among models based on ultraviolet satellite observations and numerical simulations, and its density during geomagnetic storms remains poorly understood. In this study, we estimate the geocoronal hydrogen density using high-energy (10 – 100 keV) ions measured by the Arase satellite. The apogee of Arase is 6 Earth radii, with an orbital period of 9.4 hours. Our method includes comparing ion fluxes between a given pass and subsequent passes one to two orbits later to calculate ion decay rates. The decay rates, together with charge-exchange cross-section models, are then used to derive the geocoronal density. Because this method requires the absence of ion injections, it is best suited for analyzing the recovery phase rather than the main phase of geomagnetic storms.

We analyzed the geomagnetic storm that began on May 10, 2024, with a particular focus on intervals when Arase stayed near the magnetic equatorial plane. At that time, the magnetic position of Arase corresponded to L*= 3 Earth radii. According to existing models, the geocoronal density at this location is estimated to be 5 - 10 x 10^8 m^-3. Our results show that during the early recovery phase (May 12), the geocoronal density reached 50 x 10^8 m^-3, several times higher than the model prediction. In contrast, during the late recovery phase (May 14), the density was 8 x 10^8 m^-3, consistent with the model. These findings suggest that the negative ionospheric storm occurring in the early recovery phase may have caused heating and expansion of the neutral atmosphere, thereby enhancing the hydrogen density.

ジオコロナは、地球の中性大気であり、高度 2000 km 以上に位置する。ジオコロナは低エネルギーの水素原子であり、高エネルギーイオンを電荷交換反応により消失させるために、磁気嵐の減衰率を支配している。しかし、ジオコロナ水素原子の数密度は、紫外線衛星観測や数値シミュレーションに基づいたモデルにおいて、一般に 2 倍程度の相違が有り、さらに、磁気嵐時には不明である。本研究では、ジオコロナ数密度を、あらせ衛星の高エネルギー (10-100 keV) イオン観測により求める。あらせ衛星の遠地点は 6 地球半径、軌道周期は 9.4 時間である。手法としては、あるパスと、1-2 周回後のパスのデータを比較して、イオンの減少率を算出する。この減少率と、電荷交換反応断面積モデルを用いて、ジオコロナ密度を算出する。本手法は、イオンの注入が無いことが望ましいため、磁気嵐の主相よりも回復相の解析に適している。

2024 年 5 月 10 日に開始した磁気嵐の解析を行った。特に、あらせ衛星が磁気赤道面付近に滞在する時間帯に着目した。この時間帯において、あらせ衛星の位置は、地球中心からの磁気的な距離 L*が地球半径の 3 倍であった。この位置において既存のモデルのジオコロナ密度は、5-10 (x $10^8/m^3$) であった。算出の結果、2024 年 5 月の磁気嵐回復相前半 (5 月 12 日) には、ジオコロナ密度は 50 (x $10^8/m^3$) であり、モデル値よりも数倍高かった。一方、回復相後半(5 月 14 日)では、ジオコロナ密度は 8 (x $10^8/m^3$) であり、モデル値と同等であった。これらの結果の解釈として、磁気嵐回復相前半に発生した負相電離圏嵐において、加熱により中性大気が膨張することにより、水素原子密度が増大した可能性がある。

B会場: 11/27 PM1(13:45-15:45)

14:45~15:00:00

2024年5月と10月に発生した巨大磁気嵐時のプラズマ圏電子密度の緩やかな回復 について

#新堀 淳樹 $^{1)}$, 北村 成寿 $^{2)}$, 山本 和弘 $^{3)}$, 熊本 篤志 $^{4)}$, 土屋 史紀 $^{4)}$, 松田 昇也 $^{5)}$, 笠原 禎也 $^{5)}$, 寺本 万里子 $^{6)}$, 松岡 彩子 $^{7)}$, 大塚 雄一 $^{2)}$, 惣宇利 卓弥 $^{7)}$, 西岡 未知 $^{8)}$, PERWITASARI Septi $^{9)}$, 三好 由純 $^{2)}$, 篠原 育 $^{10)}$

(1 名大宇地研, (2 名古屋大学, (3 名古屋大学宇宙地球環境研究所, (4 東北大学, (5 金沢大学, (6 九州工業大学, (7 京都大学,

 $^{(8)}$ (独) 情報通信研究機構, $^{(9)}$ N I C T, $^{(10)}$ 宇宙航空研究開発機構

Slow recovery of the plasmaspheric electron density during the May and October 2024 severe geomagnetic storms

#Atsuki Shinbori $^{1)}$, Naritoshi KITAMURA $^{2)}$, Kazuhiro YAMAMOTO $^{3)}$, Atsushi KUMAMOTO $^{4)}$, Fuminori TSUCHIYA $^{4)}$, Shoya MATSUDA $^{5)}$, Yoshiya KASAHARA $^{5)}$, Mariko TERAMOTO $^{6)}$, Ayako MATSUOKA $^{7)}$, Yuichi OTSUKA $^{2)}$, Takuya SORI $^{7)}$, Michi NISHIOKA $^{8)}$, Septi PERWITASARI $^{9)}$, Yoshizumi MIYOSHI $^{2)}$, Iku SHINOHARA $^{10)}$

⁽¹Institute for Space-Earth Environmental Research, Nagoya University, ⁽²Nagoya University, ⁽³Institute for Space-Earth Environmental Research, Nagoya University, ⁽⁴Tohoku University, ⁽⁵Kanazawa university, ⁽⁶Kyushu Institute of Technology, ⁽⁷Kyoto University, ⁽⁸NICT, ⁽⁹NICT, ⁽¹⁰JAXA)</sup>

The spatial distribution of electron density in the ionosphere shows a severe change during geomagnetic storms and substorms driven by solar wind disturbances. Electron density variations and irregularities can cause total signal blackouts during strong scintillation periods and enhance satellite positioning errors. We analyzed Global Navigation Satellite System (GNSS) - total electron content (TEC) and Arase satellite observation data to elucidate the slow recovery of the plasmaspheric electron density during the May and October 2024 geomagnetic storms. To identify the electron density variation in the ionosphere, we calculated the ratio of the TEC difference (rTEC), which is defined as the difference from the 10-quiet-day average TEC normalized by the average value. Additionally, we estimated the electron density in the plasmasphere and inner magnetosphere from the upper frequency limit of the upper hybrid resonance (UHR) waves observed by the Arase satellite. Consequently, an L-t plot of the electron density showed that the plasmasphere shrank up to L = 1.5-2.5 after a sudden commencement of both geomagnetic storms. During the storm recovery phase, the plasmapause gradually shifted to a higher L-shell. The electron density in the plasmasphere recovered the geomagnetically quiet-time level on a 3- or 4-day scale. The timescale of the plasmaspheric refilling was much longer than that of other coronal mass ejection (CME)-driven geomagnetic storms during the Arase era. The rTEC in the Northern Hemisphere showed that an enhancement in the rTEC value occurred at high latitudes (60° - 70° in magnetic latitude (MLAT)) in the daytime (10 - 14 in magnetic local time (MLT)), approximately 1 h after the storm onset. Subsequently, a tongue of ionization (TOI) formed in the polar cap owing to the enhancement of two-cell convection in the high-latitude ionosphere during the main phase of geomagnetic storms. Both geomagnetic storm events showed that the rTEC was globally depleted during the recovery phase. The depletion indicates the occurrence of a negative storm owing to a neutral composition (O/N2) change driven by the energy input from the magnetosphere in the high-latitude thermosphere. Furthermore, it took more than 3 days for the plasmaspheric electron density to recover the geomagnetically quiet-time level. The coincidence of the long refilling timescale of the plasmasphere and the depletion of the rTEC suggests that a strong negative storm impedes plasmaspheric refilling for the severe geomagnetic storms.

電離圏電子密度の空間分布は、太陽風擾乱によって駆動される磁気嵐やサブストーム中に顕著な変動を示す。特に、電 離圏の電子密度変動や不規則構造は、電波を散乱させ、信号の遮断を引き起こす可能性があり、衛星測位誤差を拡大させ る原因となりうる。本研究では、2024年5月と10月の磁気嵐中にプラズマ圏の電子密度がゆっくりと回復するメカニズ ムを解明するため、全球測位衛星システム(GNSS) - 全電子数(TEC)データとあらせ衛星の観測データの解析を行っ た。電離圏電子密度の変動を同定しやすくするため、10 日間の地磁気静穏日の平均 TEC 値から算出した差分 TEC 値を 計算し、この値を平均値で正規化した値を差分 TEC 比 (rTEC) として定義した。さらに、あらせ衛星が観測した高域混 成共鳴(UHR)波動の上限周波数から、プラズマ圏と内磁気圏の電子密度を推定した。その結果、電子密度の L-t プロッ トにおいて、磁気嵐開始後にプラズマ圏が L = 1.5-2.5 まで急速に収縮し、その後の磁気嵐の回復相においてプラズマ圏 が徐々に高L値側へ拡大していくことが示された。両磁気嵐イベントについてプラズマ圏の電子密度が地磁気静穏時の レベルに回復するまでに3日または4日間かかっていた。プラズマ圏の再充填の時間スケールは、あらせ衛星による観 測が実施している期間に発生した他のコロナ質量放出(CME)駆動の磁気嵐イベントに比べてはるかに長かった。北半 球における rTEC の磁気緯度―地方時の 2 次元マップにおいて、磁気地方時 10~14 時、磁気緯度 60°~70°の昼間側 の高緯度域で、磁気嵐の開始から約1時間後にrTEC値の増大が発生していたことがわかった。その後、磁気嵐の主相時 における高緯度電離圏の2セル対流の強化により、極冠域に伸びる高電子密度領域(TOI)が形成されていた。両方の磁 気嵐イベントの回復相において rTEC 値が全球的に減少し、静穏なレベルに戻るまでに 3 日以上も要した。この rTEC 値 の減少は、磁気圏からのエネルギー入力によって高緯度熱圏で中性大気組成(O/N 🛛)の変化が生じ、電離圏負相嵐が発 生したことを示している。プラズマ圏の長い再充填時間スケールと rTEC の減少している期間が一致することは、巨大磁 気嵐時に発生した強い電離圏負相嵐がプラズマ圏の再充填を妨げていることを示唆している。

B会場: 11/27 PM1(13:45-15:45)

15:00~15:15:00

#竹内 亘平 $^{1)}$, 浅村 和史 $^{2)}$, 横田 勝一郎 $^{3)}$, 三好 由純 $^{1)}$ $^{(1)}$ 名古屋大学 ISEE, $^{(2)}$ 宇宙航空研究開発機構, $^{(3)}$ 大阪大学

Development of ion energy-mass spectrometer "ULTIMA" for suprathermal ion observations.

#Kohei Takeuchi¹⁾, Kazushi ASAMURA²⁾, Shoichiro YOKOTA³⁾, Yoshizumi MIYOSHI¹⁾
⁽¹Institute for Space-Earth Environmental Research, Nagoya University, ⁽²Japan Aerospace Exploration Agency, ⁽³Osaka University

In the Earth's magnetosphere, ions of both solar wind origin and ionospheric origin coexist Ionospheric ions such as N+, O+, and molecular ions have energies of about 0.1 eV in the ionosphere and are accelerated to several tens of eV before escaping into the magnetosphere. However, the mechanism responsible for this acceleration remains unclear. To clarify this mechanism, we are developing a new ion energy-mass spectrometer "ULTIMA(Ultra Low energy Thermal Ion Mass Spectrometer Analyzer)". With this instrument, we aim to investigate variations in the ion distribution functions associated with ion heating at ionospheric altitudes and to analyze the interactions between ions and plasma waves. The instrument mainly consists of two components: an electrostatic energy-per-charge analyzer and a mass analyzer. For the mass analyzer, we employ a Time-of-Flight (TOF) method with a Linear Electric Field (LEF) system, enabling the high mass resolution necessary to distinguish N+ from O+. We are currently conducting performance evaluation tests of the mass analyzer using the engineering model. We report on the results of laboratory beam experiments.

B会場: 11/27 PM1 (13:45-15:45)

15:15~15:30:00

#Vanhamaki Heikki¹⁾, Pedersen Marcus¹⁾, Aikio Anita¹⁾, Cai Lei¹⁾, Myllymaa Milla¹⁾, Waters Colin²⁾, Gjerloev Jesper³⁾, Kunduri Bharat⁴⁾

⁽¹University of Oulu, Finland, ⁽²University of Newcastle, Australia, ⁽³The Johns Hopkins University, USA, ⁽⁴Virginia Tech, USA

Ionospheric Joule heating and neutral density variations at low Earth orbits during geomagnetic storms

#Heikki Vanhamaki¹⁾, Marcus Pedersen¹⁾, Anita Aikio¹⁾, Lei Cai¹⁾, Milla Myllymaa¹⁾, Colin Waters²⁾, Jesper Gjerloev³⁾, Bharat Kunduri⁴⁾

⁽¹University of Oulu, Finland, ⁽²University of Newcastle, Australia, ⁽³The Johns Hopkins University, USA, ⁽⁴Virginia Tech, USA

During geomagnetic storms intense Joule heating causes thermal expansion of the upper atmosphere, thus increasing satellite drag at low Earth orbits (LEO). This chain of events often begin when high-speed stream/stream interaction regions (HSS/SIR) or interplanetary coronal mass ejections (ICME) impact Earth's space environment. In the "Joule heating effects on ionosphere-thermosphere coupling and neutral density (JOIN)" project we determine the statistical distribution of the auroral Joule heating in the northern hemisphere during geomagnetic storms using SuperMAG, SuperDARN and AMPERE data. This is compared with the large-scale atmospheric density variations at LEO observed by the Swarm, GRACE and GRACE-FO satellites.

Based on superposed epoch analysis of 231 geomagnetic storms between 2014 and 2024, it is found that the Joule heating in the ionospheric E-region and neutral density enhancements at LEO show different characteristics depending on the geomagnetic storm driver. The Joule heating has a faster increase at the beginning of the storm main phase when the storm is initiated by a HSS/SIR or sheath region of ICMEs, while a more gradual and longer lasting increase is found in storms driven by magnetic clouds within ICMEs. The thermospheric density enhances gradually during the storm main phase and the enhancements are typically largest (median peak increase of 120%) and longest-lasting for storms driven by MC due to the prolonged interval of intense Joule heating.

B会場: 11/27 PM1(13:45-15:45)

15:30~15:45:00

地球磁気圏 X 線撮像計画 GEO-X の現状

#江副 祐一郎 1),船瀬 龍 2,3),三好 由純 4),中嶋 大 5),三石 郁之 4),布施 綾太 3),川端 洋輔 3),小泉 宏之 3),中島 晋太郎 2),石川 久美 1),沿澤 正樹 1),佐藤 佑樹 5),萩野 浩一 3),松本 洋介 6),細川 敬祐 7),伊師 大貴 2),上野 宗孝 2),山崎 敦 2),長谷 川 洋 2),三田 信 2),三谷 烈史 2),藤本 正樹 2),川勝 康弘 2),岩田 隆浩 2),米山 友景 8),満田 和久 9),平賀 純子 10),笠原 慧 3),佐原 宏典 1),金森 義明 11),森下 浩平 12)

 $^{(1)}$ 都立大, $^{(2)}$ JAXA 宇宙研, $^{(3)}$ 東大, $^{(4)}$ 名古屋大, $^{(5)}$ 関東学院大, $^{(6)}$ 千葉大, $^{(7)}$ 電気通信大学, $^{(8)}$ 中央大学, $^{(9)}$ 国立天文台, $^{(10)}$ 関西学院大, $^{(11)}$ 東北大, $^{(12)}$ 九州大

Status of GEO-X mission

#Yuichiro Ezoe¹⁾, Ryu Funase^{2,3)}, Yoshizumi MIYOSHI⁴⁾, Hiroshi Nakajima⁵⁾, Ikuyuki Mitsuishi⁴⁾, Ryota Fuse³⁾, Yosuke Kawabata³⁾, Hiroyuki Koizumi³⁾, Shintaro Nakajima²⁾, Kumi Ishikawa¹⁾, Masaki Numazawa¹⁾, Yuki Satoh⁵⁾, Koichi Hagino³⁾, Yosuke Matsumoto⁶⁾, Keisuke HOSOKAWA⁷⁾, Daiki ISHI²⁾, Munetaka Ueno²⁾, Atsushi Yamazaki²⁾, Hiroshi Hasegawa²⁾, Makoto Mita²⁾, Takefumi MITANI²⁾, Masaki FUJIMOTO²⁾, Yasuhiro Kawakatsu²⁾, Takahiro Iwata²⁾, Tomokage Yoneyama⁸⁾, Kazuhisa Mitsuda⁹⁾, Junko Hiraga¹⁰⁾, Satoshi KASAHARA³⁾, Hironori Sahara¹⁾, Yoshiaki Kanamori¹¹⁾, Kohei Morishita¹²⁾

⁽¹Tokyo Metropolitan University, ⁽²ISAS/JAXA, ⁽³University of Tokyo, ⁽⁴Nagoya University, ⁽⁵Kanto Gakuin University, ⁽⁶Chiba University, ⁽⁷University of Electro-Communications, ⁽⁸Chuo University, ⁽⁹NAOJ, ⁽¹⁰Kwansei Gakuin University, ⁽¹¹Tohoku University, ⁽¹²Kyushu University)</sup>

The interaction between the solar wind and Earth's magnetosphere, encompassing processes related to mass, momentum, and energy transportation, represents a critical scientific theme not only in solar-terrestrial science but also in astronomy and space weather research. To date, observations with solar wind monitors and in-situ satellites measuring plasma and electromagnetic fields within Earth's magnetosphere have investigated this phenomenon across a wide range of scales, from a few kilometers to tens of Earth radii. However, due to the limitations of point measurements, a comprehensive understanding of the global picture of the Earth's magnetosphere, including changes in the magnetospheric shape driven by transient solar wind variations, remains elusive, with current knowledge largely limited to averaged behaviors.

GEO-X is a novel small satellite mission designed to advance our understanding of solar wind-magnetosphere interactions through soft X-ray imaging of the dayside magnetospheric boundary, particularly the magnetosheath and cusp regions (Ezoe et al. 2023 JATIS). By using solar wind charge exchange (SWCX) X-ray emission, GEO-X will enable global imaging of the magnetosphere. Aimed for launch in 2027, the mission will utilize a rideshare opportunity followed by orbital maneuvers to conduct magnetospheric observations. The X-ray emission data will provide new insights into the Earth's magnetosphere. Complementary to XRISM, which conducts high-precision spectroscopy in low Earth orbit, GEO-X will offer a perspective through global imaging observations, contributing to a deeper understanding of the SWCX emission. Equipped with a propulsion system to perform orbital maneuvers, GEO-X holds engineering significance as a small exploration satellite. This presentation reports on the mission objectives of GEO-X, along with the latest developments in its observational instrument and satellite bus.

太陽風と地球の磁気圏がどのように相互作用するか、質量、運動量、エネルギーに関するプロセスを含むこの問題は太陽地球系科学のみならず、天文学や宇宙天気にも関連した重要な科学テーマの一つである。これまでに太陽風モニターや地球磁気圏のプラズマ・電磁場計測を行うその場観測衛星によって、数キロメートルから数十地球半径に渡る様々なスケールでこの問題は調べられてきた。しかし、太陽風の過渡的な変動による地球磁気圏の形状変化を含む、全球的な影響の把握は点観測の限界によって難しく、平均的な理解にとどまっている。

GEO-X は太陽風と地球磁気圏の相互作用を理解するための新しい超小型衛星ミッションであり、昼側磁気圏境界面、特にシースとカスプ領域の軟 X 線イメージングを行う (Ezoe et al. 2023 JATIS)。すざく衛星等で確立してきた太陽風電荷交換 X 線 (SWCX) によって、磁気圏のグローバル撮像を実現する。打ち上げは 2027 年を目指しており、相乗り打ち上げから軌道遷移を行って磁気圏観測を行う。X 線発光データから、地球磁気圏の新たな知見を得ることができると同時に磁気圏外からの俯瞰的な観測を行うため、地球周回での高精度分光を行う XRISM 衛星と相補的であり、SWCX プロセスの発光原理の理解にも繋がる。推進系を搭載して軌道遷移を行うため、超小型探査機の発展という工学的な意義も持つ。本講演では GEO-X の開発状況と科学検討の最新の進展について報告する。

Geotail 長期観測に基づく Micro Type III 太陽電波バーストの太陽活動依存性

#加藤 健丸 $^{1)}$, 栗田 怜 $^{2)}$, 小嶋 浩嗣 $^{2)}$ (1 京都大学生存圏, $^{(2}$ 京都大学

Solar Activity Dependence of Micro Type III Solar Radio Bursts Based on Longterm GEOTAIL Observations

#Takemaru Kato¹⁾, Satoshi KURITA²⁾, Hirotsugu KOJIMA²⁾

(1 Research Institute for Sustainable Humanosphere, Kyoto University, (2 Kyoto University

This study analyzes long-term observations from the Plasma Wave Instrument (PWI) aboard the GEOTAIL spacecraft to clarify the relationship between Micro Type III solar radio bursts and solar activity. GEOTAIL was launched in July 1992 as a Japan - U.S. joint mission and observed plasma waves in Earth's magnetotail for ~30 years. The PWI/SFA subsystem covers 5.62~Hz - 800~kHz (electric field) and 5.62~Hz - 12.5~kHz (magnetic field) with a temporal resolution of 8 - 64~s.

Previous studies indicate that Micro Type III bursts are a class of solar radio emission that differ from classical type III bursts in typical intensity and occurrence rate. Classical type III bursts are thought to arise when Langmuir waves driven by electron beams near the Sun convert to escaping electromagnetic waves that are then detected near Earth. Whereas classical type III bursts are commonly associated with solar flares, Micro Type III bursts are not; they are believed to result from continuous acceleration processes near active regions, with sources near the edges of closed-field coronal streamers [A. Morioka et al.,2015]

Using GEOTAIL's multi-decadal dataset, we examine variations in occurrence rate and statistical properties across the solar cycle that could not be captured in short-term studies. We first assess instrument noise in detail to verify data reliability over the full mission and to quantify how noise levels vary across years and antenna configurations. We then develop an automated detection pipeline to efficiently identify Micro Type III bursts and to characterize statistical trends such as occurrence rates and intensity distributions. This extends prior event-based analyses to a long-term, systematic evaluation. We further quantify correlations with the international sunspot number and assess spatial associations with active regions. Our results show that Micro Type III activity closely tracks solar-cycle variability, with pronounced changes in occurrence rate at specific activity phases. In this presentation, we report characteristics of the GEOTAIL/PWI dataset and the occurrence properties of Micro Type III bursts revealed by our long-term analysis, and we outline prospects for cycle-by-cycle characterization and for constraining the underlying generation mechanisms.

本研究では、人工衛星 GEOTAIL に搭載されたプラズマ波動観測器によって取得された長期観測データを解析し、Micro Type III 太陽電波バーストと太陽活動の関係を明らかにすることを目的とする。GEOTAIL 衛星は 1992 年 7 月に日本と米国の共同ミッションとして打ち上げられ、30 年間にわたり地球磁気圏尾部のプラズマ波動を観測した。搭載機器の PWI/SFA では電界 5.62 Hz~800 kHz、磁界 5.62 Hz~12.5 kHz の帯域を観測し、時間分解能は 8~64 秒である。

先行研究によると、Micro Type III 太陽電波バーストは太陽を起源とする電波放射の一種で、通常の Type III とは異なる強度、頻度をもつ。通常の Type III は、太陽周辺で発生したラングミュア波が自由空間波へ変換されて地球周辺で観測される現象である。通常の Type III では主にフレアによって引き起こされるのに対し、Micro Type III ではフレアが原因ではなく、はっきりはしていないが活動領域周辺で継続的に起こる加速過程が原因とされており、発生源については閉じた磁力線であるコロナストリーマの端付近で起きているとされている [A. Morioka et al.,2015]。

本研究では、GEOTAILの長期データ解析により、従来の短期間研究では把握できなかった太陽活動周期に伴う発生頻度や統計的特性の変動を解析した。

解析にあたっては、長期間のデータを用いて、観測器のノイズレベルなどを詳細に評価し、長期間にわたる観測データの信頼性を確認し、ノイズレベルが観測年次、アンテナの種類によってどのように変化するのかを明らかにした。その後、自動抽出手法を導入することで、膨大なデータから Micro Type III 太陽電波バーストを効率的に検出し、発生頻度や強度分布などの統計的傾向を明らかにした。これにより、従来の事例解析に留まっていた研究を拡張し、長期的かつ体系的な評価が可能となった。さらに、本研究では抽出した Micro Type III ボーストの統計解析を用いて太陽黒点数との相関を確認し、活動領域との対応を示した。その結果、Micro Type III 電波バーストは太陽活動の変動と密接に関連していることが示され、特定の太陽活動段階において放射の発生頻度が顕著に変化する傾向が確認された。本発表では、これまでの長期データ解析から明らかになった Geotail 衛星搭載 PWI のデータの特性や、Micro Type III 電波バーストの出現特性に関して報告する。また、長期間にわたるデータを利用し、太陽活動周期ごとにおける電波放射特性の詳細な評価や、発生メカニズムの解明に向けた研究に関しての展望も加えて議論する。

OCTAVE VLF/LF 帯標準電波で観測された高エネルギー電子降下の兆候

#吉井 駆 $^{1)}$, 大矢 浩代 $^{1)}$, 土屋 史紀 $^{2)}$, MARTIN Conner $^{3)}$, 西谷 望 $^{4)}$ $^{(1)}$ 千葉大学大学院融合理工学府, $^{(2)}$ 東北大学惑星プラズマ・大気研究センター $^{(2)}$ アサバスカ大学科学センター, $^{(4)}$ 名古屋大学宇宙地球環境研究所(ISEE)

Signatures of energetic electron precipitation observed with OCTAVE VLF/LF transmitter signals

#Kakeru YOSHII¹), Hiroyo OHYA¹), Fuminori TSUCHIYA²), Conner MARTIN³), Nozomu NISHITANI⁴)

(1) Graduate School of Science and Engineering, Chiba University, Japan, (2) Planetary Plasma and Atmospheric Research Center (PPARC), Tohoku University, Japan, (3) Center for Science, Athabasca University, Canada, (4) Institute for Space-Earth Environmental Research (ISEE), Nagoya University, Japan

Ultra low frequency (ULF, <5 Hz) -modulated energetic electron precipitation (EEP, 100 keV to 1 MeV) occurs during substorms in the Athabasca sub-auroral zone (Miyashita et al., 2018), and that ULF-modulated EEP also occurred by low-ering of mirror point during geomagnetically quiet time (Brito et al., 2012; Tanaka et al., 2022). However, the underlying mechanism remains unclear. In this study, we investigate oscillations in amplitude and phase of very low frequency (VLF, 3 – 30 kHz) and low frequency (LF, 30 – 300 kHz) transmitter signals due to EEPs. The aim is to elucidate their generation mechanisms by comparing with ground-based magnetic field data and ionospheric plasma dynamics observed by the Super Dual Auroral Radar Network (SuperDARN) HF radar. We investigated an EEP event that occurred during the recovery phase of a geomagnetic storm on May 29, 2017. VLF/LF amplitude oscillations with periods of 3 – 4 minutes were observed on multiple propagation paths over North America. In particular, anti-phase variations were found between the NDK (the frequency of transmitter: 25.2 kHz) – Athabasca (ATH) and WWVB (60.0 kHz) – ATH paths. Furthermore, SuperDARN observations showed significant Doppler velocity perturbations to the east of ATH, accompanied by moving echoes detected across multiple beams. Further details will be discussed in the session.

脈動オーロラの発光強度変化と降下電子エネルギースペクトルの相関: LAMP 観測ロケット,全天カメラ,れいめい衛星による観測

#平野 晶也 $^{1)}$, 細川 敬祐 $^{1)}$, 三好 由純 $^{2)}$, 浅村 和史 $^{3)}$, Lessard Marc $^{4)}$, Mcharg Matthew $^{5)}$, Jaynes Allison $^{6)}$, Shumko Mykhaylo $^{7)}$, Ledvina Vincent $^{8)}$, Hampton Don $^{8)}$, 坂野井 健 $^{9)}$, 三谷 烈史 $^{3)}$, 滑川 拓 $^{10)}$, 能勢 正仁 $^{11)}$, 小川 泰信 $^{12)}$, Halford Alexa $^{13)}$

 $^{(1)}$ 電通大, $^{(2)}$ 名大 ISEE, $^{(3)}$ 宇宙研, $^{(4)}$ ニューハンプシャー大学, $^{(5)}$ アメリカ合衆国空軍士官学校, $^{(6)}$ アイオワ大学, $^{(7)}$ ジョンズ・ホプキンズ大学応用物理研究所, $^{(8)}$ アラスカ大学フェアバンクス校, $^{(9)}$ 東北大学・理・PPARC, $^{(10)}$ NICT, $^{(11)}$ 名市大・DS 学部, $^{(12)}$ 極地研, $^{(13)}$ NASA ゴダード宇宙飛行センター

The correlation between the luminosity variation of pulsating aurora and energy spectra of precipitating electrons

#Masaya HIRANO¹⁾, Keisuke HOSOKAWA¹⁾, Yoshizumi MIYOSHI²⁾, Kazushi ASAMURA³⁾, Marc Lessard⁴⁾, Matthew Mcharg⁵⁾, Allison Jaynes⁶⁾, Mykhaylo Shumko⁷⁾, Vincent Ledvina⁸⁾, Don Hampton⁸⁾, Takeshi SAKANOI⁹⁾, Takefumi MITANI³⁾, Taku NAMEKAWA¹⁰⁾, Masahito NOSE¹¹⁾, Yasunobu OGAWA¹²⁾, Alexa Halford¹³⁾

(1 University of Electro-Communications, Tokyo, Japan, (2 Institute for Space – Earth Environmental Research, Nagoya Uni-

⁽¹University of Electro-Communications, Tokyo, Japan, ⁽²Institute for Space – Earth Environmental Research, Nagoya University, Nagoya, Japan, ⁽³Institute of Space and Astronautical Science, Sagamihara, Kanagawa, Japan, ⁽⁴University of New Hampshire, Durham, New Hampshire, USA, ⁽⁵Department of Physics, the United States Air Force Academy, Colorado, USA, ⁽⁶Department of Physics and Astronomy, University of Iowa, Iowa City, Iowa, USA, ⁽⁷Johns Hopkins University Applied Physics Laboratory, Maryland, USA, ⁽⁸Geophysical Institute, University of Alaska Fairbanks, Alaska, USA, ⁽⁹Department of Geophysics, Graduate School of Science, Tohoku University, Sendai, Japan, ⁽¹⁰National Institute of Information and Communications Technology, Tokyo, Japan, ⁽¹¹Nagoya City University, Nagoya, Japan, ⁽¹²National Institute of Polar Research, Tokyo, Japan, ⁽¹³NASA Goddard Space Flight Center, Greenbelt, Maryland, USA

Aurorae observed in the nightside auroral zone are primarily classified into two broad categories: discrete aurorae, which have clear and distinct spatial structures, and diffuse aurorae characterized by vague and indistinct patchy shapes. It is known that most of diffuse aurorae exhibit quasi-periodic luminosity modulations on timescales of a few to a few tens of seconds, and these are referred to as pulsating aurora (PsA). The energy of the precipitating electrons causing PsA tends to be higher than that of those causing typical discrete aurorae, and we refer to these precipitating electrons here as "PsA electrons". The tail of the energy spectra of PsA electrons often extends to a few tens/hundreds of keV. Such sub-relativistic electron precipitation can be explained by whistler-mode chorus waves, which are generated near the magnetospheric equatorial plane and propagate along magnetic field lines, scattering electrons through wave-particle interactions at high latitudes. Regarding the relationship between PsA electrons and auroral emissions, simultaneous observations by the Reimei satellite, using an electron detector and a multi-spectral auroral camera, suggest that a flux modulation, whose electrons energy is above a few keV, is the primary cause of the luminosity modulation of PsA (Miyoshi et al., 2015). However, the duration of those earlier observations was as short as a minute and focused on a small area. As a result, the detailed correlation between the luminosity modulation of PsA and the energy spectrum of PsA electrons during relatively longer intervals (e.g., over several minutes) has not yet been clarified. This issue fundamentally stems from the absence of a long-duration spacecraft mission capable of conducting continuous electron measurements in the regions where PsA occurs.

To address these issues, we conducted a correlation analysis between PsA electrons and auroral brightness over a period of several minutes and an area spanning more than 500 km. We used in-situ low-energy electron data obtained from the EPLAS (Electron PLASma Detector) onboard the LAMP (Loss through Auroral Microburst Pulsation) sounding rocket and PsA emission intensity data obtained from an EMCCD (Electron Multiplying Charge Coupled Devices) all-sky camera in Alaska during the launch window. The launch window of the LAMP sounding rocket window was from 11:29 to 11:38 UT on March 5, 2022, and the EPLAS instrument covered an energy range from 5 eV to 15 keV. Meanwhile, the EMCCD all-sky camera in Venetie, Alaska, observed the region containing the magnetic footprint of the rocket during the launch window with a temporal resolution of 100 Hz.

In this study, we focused specifically on the continuous transition of the characteristics of PsA electron precipitation and the corresponding optical morphology of the aurorae as the rocket flew in the latitudinal direction. In the initial phase of the flight, a clear quasi-periodic modulation was observed in the energy flux around 10 keV, and high-contrast PsA was observed by the ground-based all-sky imager. However, as the rocket moved to higher latitudes, this modulation gradually became indistinct, and the optical contrast of the PsA also decreased. Subsequently, the 10 keV modulation disappeared, while steady electron precipitation around 1 keV became prominent. During this period, the faint background emission became stronger than the pulsating component of the PsA. In the final phase of the flight, the steady precipitation of PsA electrons around 1 keV and the modulation of the energy flux around 10 keV occurred simultaneously, exhibiting a complex morphology where the PsA was superimposed on a bright background emission. The presence of such remarkable differences in the characteristics of precipitating electrons and corresponding optical emissions depending on latitude suggests the possibility that the

properties of chorus waves may systematically change with latitude (e.g. Lower Band Chorus and Upper Band Chorus occur simultaneously). In the presentation, we plan to discuss the factors that determine the correlation between PsA electrons and auroral emissions, including a comparison with past observations from the Reimei satellite.

夜側オーロラ帯で観測されるオーロラは、明瞭な空間構造を持つディスクリートオーロラと曖昧な空間構造を持つディフューズオーロラの二つに大別される。ディフューズオーロラの多くは、数秒から数十秒ほどの準周期的な輝度変調を示すことが知られており、脈動オーロラ(Pulsating Aurora: PsA)と呼ばれる。PsA を引き起こす降下電子のエネルギーは典型的なディスクリートオーロラを引き起こすものよりも高いことが知られており、それらの降下電子をここでは「PsA電子」と呼ぶ。PsA電子のエネルギースペクトルは、その裾野が数十から数百 keV にまで及ぶこともある。このような準相対論的な電子降下は、磁気赤道面付近で発生する自然電磁波「ホイッスラーモードコーラス波」が磁力線に沿って伝搬し、磁気圏の高緯度領域において波動粒子相互作用によって電子を散乱することによって説明できる。PsA電子とオーロラ発光の関連については、科学衛星「れいめい」に搭載された電子観測器と多波長オーロラカメラによる同時観測から数 keV 以上の変調が PsA の輝度変調の主原因であることが示唆されている (Miyoshi et al., 2015)。しかし、先行研究の観測時間は一分未満であり、狭い領域についてのみ着目しているため、長時間かつ広範囲にわたる PsA の輝度変調と PsA電子のエネルギースペクトルとの間の詳しい相関関係は明らかになっていない。この問題は、PsA が発生している領域において長時間継続的に電子計測を行う飛翔体ミッションが存在しなかったことに本質的に起因する.

この問題を解決するために、本研究では、LAMP (Loss through Auroral Microburst Pulsation) 観測ロケットに搭載された低エネルギー電子観測器 EPLAS (Electron PLASma Detector) のデータと、アラスカに設置されている EMCCD (Electron Multiplying Charge Coupled Devices) 全天カメラから得られた打ち上げウィンドウ中の PsA の発光強度データに対して、数分間におよぶ時間幅で、かつ 500 km 四方を超える広い領域にわたって相関解析を行った.LAMP 観測ロケットの打ち上げウィンドウは 2022 年 3 月 5 日 11:29-11:38 UT であり、搭載された低エネルギー電子観測器 EPLAS は 5 eV から 15 keV までのエネルギー範囲をカバーしている.また、アラスカのベネタイに設置されている EMCCD 全天カメラは、LAMP ロケットの打ち上げウィンドウ中のロケットのフットプリントを含む領域を 100 Hz の時間分解能で観測していた.

本研究では、特にロケットが緯度方向に飛翔するのに伴い、PsA 電子の降下特性とそれに対応するオーロラの光学的形態が連続的に遷移していく様子に着目した。飛翔初期には 10 keV 付近のエネルギーフラックスに明瞭な準周期的変調が見られ、地上ではコントラストの強い PsA が観測されたが、ロケットが高緯度側へ移動するにつれてこの変調は次第に不明瞭となり、PsA の光学的なコントラストも低下した。その後、10 keV の変調が消失する一方で 1 keV 付近の安定した電子降下が顕著になり、PsA の脈動成分よりも背景のぼんやりとした発光が全体的に増光する期間が観測された。飛翔終盤には、この 1 keV 付近の安定的な PsA 電子の降下と 10 keV 付近のエネルギーフラックスの変調が同時に発生し、明るい背景発光に PsA の明滅が重なるという複合的な様相を呈した。このように緯度によって降下電子および対応する光学発光の特性に顕著な違いが見られることは、コーラス波動の特性(例えば Lower Band Chorus と Upper Band Chorus が同時に発生しているかなど)が緯度によって系統的に変化している可能性を示唆する。発表では、れいめい衛星による過去の観測データとの比較も交え、PsA 電子とオーロラ発光の相関を決める要因について考察を行う予定である。

#伊藤 ゆり $^{1,2)}$, 小川 泰信 $^{1,2)}$, 田中 良昌 $^{1,2,3)}$, 門倉 昭 $^{2,3)}$, 吹澤 瑞貴 $^{1,2)}$, 三好 由純 $^{4)}$, 新堀 淳樹 $^{4)}$, 細川 敬祐 $^{5)}$, 堀 智 昭 $^{4)}$, 笠原 禎也 $^{6)}$, 松田 昇也 $^{6)}$, 土屋 史紀 $^{7)}$, 熊本 篤志 $^{7)}$, 松岡 彩子 $^{8)}$, 篠原 育 $^{9)}$ $^{(1)}$ 総研大, $^{(2)}$ 極地研, $^{(3)}$ ROIS-DS, $^{(4)}$ 名大 ISEE, $^{(5)}$ 電通大, $^{(6)}$ 金沢大, $^{(7)}$ 東北大, $^{(8)}$ 京都大, $^{(9)}$ 宇宙研

Statistical study of pulsating auroral types and high-latitude chorus waves based on Arase – ground conjugate observations

#Yuri ITO^{1,2}), Yasunobu OGAWA^{1,2}), Yoshimasa TANAKA^{1,2,3}), Akira KADOKURA^{2,3}), Mizuki FUKIZAWA^{1,2}), Yoshizumi MIYOSHI⁴), Atsuki SHINBORI⁴), Keisuke HOSOKAWA⁵), Tomoaki HORI⁴), Yoshiya KASAHARA⁶), Shoya MATSUDA⁶), Fuminori TSUCHIYA⁷), Atsushi KUMAMOTO⁷), Ayako MATSUOKA⁸), Iku SHINOHARA⁹)

(¹SOKENDAI, (²NIPR, (³ROIS-DS, (⁴ISEE/Nagoya Univ., (⁵UEC, (6Kanazawa Univ., (7Tohoku Univ., (8Kyoto Univ., (9ISAS/JAXA)

Pulsating aurora (PsA), which is characterized by quasi-periodic luminosity modulation of ~2 - 30 sec, is a common aurora associated with ~10 keV electron precipitation. During PsA, much higher energy (i.e., sub-relativistic/relativistic) electrons sometimes precipitate into the ionosphere. The highly energetic electrons penetrate into lower altitudes and induce ozone depletion in the mesosphere and upper stratosphere. In our previous study, we have observationally proposed a physical process in which wave propagation latitudes, the energy of scattered electrons, and patchy structure of PsA are controlled by "density ducts". However, no previous study has statistically investigated the relationship between chorus wave propagation, the energy of electron precipitation, and auroral types, which is necessary to understand importance of the density ducts.

In order to examine the relationship, we make a statistical analysis of simultaneous PsA and chorus wave observation data from 2017 to 2024. These simultaneous conjugate observations were archived with the Arase satellite and multi-point ground instruments in Scandinavia. We identified a total conjunction duration of 25.5 hours under the following conditions: 1) Arase was located at the absolute value of magnetic latitudes higher than 10°, 2) auroral structures related to magnetospheric plasma waves can be identified. The identified auroral structures were categorized into diffuse auroras, amorphous pulsating auroras (APA), patchy pulsating auroras (PPA), patchy auroras (PA). First, we compared auroral types with the presence or absence of chorus waves. When chorus waves were observed (Case 1), 84% of auroras included PPA/PA. In contrast, when chorus waves were not observed (Case 2), 86% of auroras were diffuse auroras or APA. In Case 1, the occurrence frequency increased toward the morning sector. In addition, we derived the background electron density from the UHR frequency measured with Arase for each event, and we found some events demonstrating a clear correlation between chorus wave intensity and background electron density variations. In this presentation, we show the observational results and discuss the background processes of energetic electron precipitation during PsA, focusing on density ducts.

#髙原 璃乃 $^{1,2)}$, 篠原 育 $^{2)}$, 笠原 慧 $^{3)}$, 浅村 和史 $^{2)}$, 横田 勝一郎 $^{4)}$, 桂華 邦裕 $^{3)}$, 風間 洋一 $^{5)}$, Wang Shiang-Yu $^{5)}$, Tam Sunny Wing-Yee $^{6)}$, Chang Tzu-Fang $^{6)}$, Wang Bo-Jhou $^{5)}$, Jun ChaeWoo $^{7)}$, 堀 智昭 $^{8)}$, 松岡 彩子 $^{9)}$, 寺本 万里子 $^{10)}$, 山本 和 弘 $^{11)}$, 笠原 禎也 $^{12)}$, 松田 昇也 $^{12)}$, 熊本 篤志 $^{13)}$, 新堀 淳樹 $^{14)}$, 土屋 史紀 $^{13)}$, 三好 由純 $^{14)}$

 $^{(1)}$ 東京大学, $^{(2)}$ 宇宙航空研究開発機構, $^{(3)}$ 東京大学, $^{(4)}$ 大阪大学大学院, $^{(5)}$ Academia Sinica Institute of Astronomy and Astrophysics, $^{(6)}$ National Cheng Kung University, $^{(7)}$ 名古屋大学, $^{(8)}$ 名古屋大学,宇宙地球環境研究所, $^{(9)}$ 京都大学, $^{(10)}$ 九州工業大学, $^{(11)}$ 名古屋大学宇宙地球環境研究所, $^{(12)}$ 金沢大学, $^{(13)}$ 東北大学, $^{(14)}$ 名古屋大学

Categorization of the Factors of Loss Cone Electron Input in Higher-Latitude Regions of the Inner Magnetosphere

#Rino TAKAHARA^{1,2)}, Iku SHINOHARA²⁾, Satoshi KASAHARA³⁾, Kazushi ASAMURA²⁾, Shoichiro YOKOTA⁴⁾, Kunihiro KEIKA³⁾, Yoichi KAZAMA⁵⁾, Shiang-Yu Wang⁵⁾, Sunny Wing-Yee Tam⁶⁾, Tzu-Fang Chang⁶⁾, Bo-Jhou Wang⁵⁾, Chaewoo JUN⁷⁾, Tomoaki HORI⁸⁾, Ayako MATSUOKA⁹⁾, Mariko TERAMOTO¹⁰⁾, Kazuhiro YAMAMOTO¹¹⁾, Yoshiya KASAHARA¹²⁾, Shoya MATSUDA¹²⁾, Atsushi KUMAMOTO¹³⁾, Atsuki SHINBORI¹⁴⁾, Fuminori TSUCHIYA¹³⁾, Yoshizumi MIYOSHI¹⁴⁾

⁽¹University of Tokyo, ⁽²ISAS/JAXA, ⁽³University of Tokyo, ⁽⁴Osaka University, ⁽⁵ASIAA, ⁽⁶National Cheng Kung University, ⁽⁷Nagoya University, ⁽⁸ISEE / Nagoya University, ⁽⁹Kyoto University, ⁽¹⁰Kyushu Institute of Technology, ⁽¹¹ISEE / Nagoya University, ⁽¹²Kanazawa University, ⁽¹³Tohoku University, ⁽¹⁴Nagoya University)</sup>

Whistler mode chorus waves are detected primarily outside the plasmapause from the nightside to the dayside in the inner and outer magnetosphere. They scatter electrons in pitch angles and cause electron precipitation into the Earth's upper atmosphere. While nightside chorus waves are frequently observed at geomagnetically disturbed times around the magnetic equator, dayside chorus waves are much more detected ranging from the equator to higher latitudes (e.g., Meredith et al., 2012). The resonance energy tends to become higher in the off-equatorial regions due to larger magnetic field intensity. Electron measurements with the sounding rockets and numerical simulations have suggested that "sub-relativistic electron precipitation is caused by interactions with chorus waves propagating to higher latitudes (Miyoshi et al., 2010; Namekawa et al., 2023). Furthermore, the previous statistical survey of loss cone electrons by Takahara et al. (2025) also indicates the contribution of higher-latitude chorus waves to tens of keV electron precipitation in the regions of MLT >3 h at L=5 - 6.

In situ loss cone electron observations have just recently been enabled by electron analyzers onboard the Arase satellite that is capable of electron measurement with high angular resolution enough to resolve small loss cone angles in the magnetosphere. Moreover, the Arase satellite performs electron measurements up to $|\text{MLAT}| = 40^{\circ}$, providing superior spatial coverage compared to other satellites. In this study, we investigated and categorized the loss cone input events for electrons with energies of 7 – 88 keV in the higher latitude regions ($10^{\circ} < |\text{MLAT}| < 40^{\circ}$) observed by the Arase satellite from March 2017 to March 2022. This study aims to reveal and quantify the contribution of each factor by examining direct measurements of loss cone electrons.

We found that chorus waves are the primary cause of loss cone input as for higher-energy (29 - 88 keV) electrons (Type 1), and the occurrence probability decreases as with increasing magnetic latitudes. This spatial distribution may result from the spatial distribution of the resonance energy defined by the ambient magnetic field intensity and electron density and/or the less occurrence of intense chorus waves at higher latitudes. Besides, we also found another category of event (Type 2) which are characterized by the simultaneous detection of chorus waves although the resonance energies of them are too high compared to the energy range of observed loss cone electrons. Type 2 events are found to frequently occur around the dawnside (MLT = 3 - 9 h) at $20^{\circ} < |\text{MLAT}| < 40^{\circ}$. They occur with reduced electron densities or fpe /fce (fpe and fce are the local electron plasma frequency and electron gyro frequency, respectively) values and are sometimes accompanied by Langmuir waves. We also found that Type 2 events occur more frequently for lower-energy (7 - 24 keV) loss cone electron input from the nightside to the dawnside (MLT=21 - 9 h). Additionally, contributions of whistler hiss waves were identified, and events with broadband electrostatic noise (BEN) were also detected. In this presentation, we present the results of a categorization of loss cone input factors for 7 - 88 keV electrons and discuss the possible factors contributing to Type 2 events.

R006-P06

ポスター1:11/25 AM1/AM2 (9:15-12:35)

#謝 怡凱 ¹⁾, 大村 善治 ¹⁾
⁽¹ 京大生存研

Short-term and long-term energetic electron precipitation induced by whistlermode chorus waves

#YIKAI HSIEH1), Yoshiharu Omura1)

(1 Research Institute for Sustainable Humanosphere, Kyoto University

Nonlinear wave-particle interaction with whistler-mode chorus waves is one of the processes that drive energetic electron precipitation in the Earth's inner magnetosphere. Using the Green's function method, we investigate the precipitation rates of electrons interacting with both parallel and oblique lower-band chorus emissions around the outer radiation belt. We analyze both short-term effects (within a single emission) and long-term evolution (~tens of minutes) of electron precipitation. Our results confirm that when chorus waves propagate obliquely to the background magnetic field, electrons are generally more likely to be precipitated than in the case of parallel chorus waves. For short-term precipitation, namely the one-to-one correspondence between electron precipitations and chorus elements, we demonstrate that the majority of precipitation arises from nonlinear scattering (phase bunching) of cyclotron resonance, while smaller fractions result from Landau resonance and 2nd cyclotron resonance in the oblique chorus cases. For long-term precipitation, referring to the evolution of precipitation during events with consecutive chorus emissions, we find that oblique chorus waves are more effective than parallel waves at driving electrons toward low equatorial pitch angles, ultimately leading to enhanced precipitation. Additionally, we derive pitch angle scattering rates and verify precipitation processes governed by nth-order cyclotron resonances for both parallel and oblique chorus waves. The pitch angle scattering rates provide valuable insights for improving the prediction of space weather phenomena such as pulsating auroras and microbursts.

#栗田 怜 $^{1)}$, 三好 由純 $^{2)}$, 加藤 雄人 $^{3)}$, 齊藤 慎司 $^{4)}$, 松田 昇也 $^{5)}$, 笠原 禎也 $^{5)}$, 松岡 彩子 $^{6)}$, 堀 智昭 $^{2)}$, 寺本 万里子 $^{7)}$, 山本 和弘 $^{2)}$, 新堀 淳樹 $^{2)}$, 篠原 育 $^{8)}$

 $^{(1)}$ 京都大·生存研, $^{(2)}$ 名古屋大学宇宙地球環境研究所, $^{(3)}$ 東北大学, $^{(4)}$ 情報通信研究機構, $^{(5)}$ 金沢大学, $^{(6)}$ 京都大学, $^{(7)}$ 九州工業大学, $^{(8)}$ 宇宙航空研究開発機構

Empirical wave power models of whistler-mode chorus waves deduced from the Arase observation

#Satoshi Kurita¹⁾, Yoshizumi MIYOSHI²⁾, Yuto KATOH³⁾, Shinji SAITO⁴⁾, Shoya MATSUDA⁵⁾, Yoshiya KASAHARA⁵⁾, Ayako MATSUOKA⁶⁾, Tomoaki HORI²⁾, Mariko TERAMOTO⁷⁾, Kazuhiro YAMAMOTO²⁾, Atsuki SHINBORI²⁾, Iku SHINOHARA⁸⁾

⁽¹Research Institute for Sustainable Humanosphere, Kyoto University, ⁽²ISEE, Nagoya University, ⁽³Tohoku University, ⁽⁴NICT, ⁽⁵Kanazawa University, ⁽⁶Kyoto University, ⁽⁷Kyushu Institute of Technology, ⁽⁸ISAS/JAXA

Whistler mode chorus waves play crucial roles in the Earth's inner magnetosphere dynamics through wave-particle interactions. In particular, stochastic acceleration by chorus waves is responsible for the creation of relativistic electrons in the Earth's outer radiation belt during geomagnetic disturbances. The quasi-linear diffusion regime can describe the stochastic acceleration, and modeling works based on that regime successfully reproduce observed flux increase in radiation belt electrons during geomagnetic disturbances. The quasi-linear diffusion model of chorus waves requires information on wave power and the normal angle of chorus waves, which significantly changes the timescale for the acceleration of relativistic electrons. The model describes the wave power distribution as a function of frequency using a Gaussian function. The magnetic latitude dependence of this distribution needs to be incorporated into the model to correctly evaluate stochastic acceleration of electrons during the propagation of chorus waves from the magnetic equator to higher latitudes.

We aim to develop the empirical chorus wave model based on the Arase satellite observation, which describes the wave power distribution as a function of L*, magnetic latitude, and magnetic local time. We have statistically investigated the frequency spectra of wave magnetic fields obtained by the Onboard Frequency Analyzer (OFA), a part of the Plasma Wave Experiment onboard the Arase satellite. The wave power of chorus waves is derived from the OFA-SPEC dataset, and the wave power is modeled so that the parameter can be used as input for the quasi-linear diffusion model. We report on the integrated wave power distributions of lower-band and upper-band chorus waves as a function of L*, MLAT, and MLT. We derived the wave power distributions of the waves with and without wave power close to the instrument noise level. The input parameters of the quasi-linear diffusion model are derived from the obtained distributions. We will discuss the use case of the chorus wave models with and without the wave power close to the instrument noise level, together with quasi-linear diffusion rates evaluated from the wave power obtained from the constructed models.

あらせ衛星で観測された静電波を伴うホイッスラーモード波の特性

#吉田 永遠 $^{1)}$, 栗田 怜 $^{2)}$, 小嶋 浩嗣 $^{2)}$, 笠原 禎也 $^{3)}$, 松田 昇也 $^{3)}$, 松岡 彩子 $^{4)}$, 三好 由純 $^{5)}$, 堀 智昭 $^{5)}$, 寺本 万里子 $^{6)}$, 山本 和弘 $^{5)}$, 篠原 育 $^{7)}$

 $^{(1)}$ 京都大学, $^{(2)}$ 京都大学生存圈研究所, $^{(3)}$ 金沢大学, $^{(4)}$ 京都大学理学研究科, $^{(5)}$ 名古屋大学宇宙地球環境研究所, $^{(6)}$ 九州工業大学, $^{(7)}$ 宇宙航空研究開発機構/宇宙科学研究所

Characteristics of whistler-mode waves that generate electrostatic emissions observed by the Arase satellite

#Towa Yoshida¹⁾, Satoshi KURITA²⁾, Hirotsugu KOJIMA²⁾, Yoshiya KASAHARA³⁾, Shoya MATSUDA³⁾, Ayako MATSUOKA⁴⁾, Yoshizumi MIYOSHI⁵⁾, Tomoaki HORI⁵⁾, Mariko TERAMOTO⁶⁾, Kazuhiro YAMAMOTO⁵⁾, Iku SHINOHARA⁷⁾

⁽¹Kyoto University, ⁽²Research Institute for Sustainable Humanosphere, Kyoto University, ⁽³Kanazawa University, ⁽⁴Graduate School of Science, Kyoto University, ⁽⁵Institute for Space-Earth Environmental Research, Nagoya University, ⁽⁶Kyushu Institute of Technology, ⁽⁷Japan Aerospace Exploration Agency/Institute of Space and Astronautical Science

Whistler-mode electromagnetic waves are observed in the Earth's magnetosphere. These waves are excited near the magnetic equator and propagate toward higher latitudes. Whistler-mode waves are typically observed in the frequency range 0.1-0.8fce, where fce is the equatorial electron cyclotron frequency. Whistler-mode waves are observed in two frequency bands with power gaps near 0.5 fce. Whistler-mode waves are associated with various nonlinear phenomena and the important role of acceleration processes in the magnetosphere. The STEREO satellite observed an oblique whistler-mode wave with distorted electric field. This distortion is from the plasma density fluctuations which driven by the electrostatic field of the whistler-mode wave [Kellogg et al., 2010]. In ISEE satellite, the beam mode electrostatic bursts modulated by chorus waves have been observed [Reinleitner et al., 1982], and this modulation is caused by the Landau resonance of electrons and the chorus wave [Reinleitner et al., 1983]. Van Allen Probes observed Langmuir waves modulated by chorus waves [Li et al., 2017]. However, in these previous studies, only a few cases have been analyzed.

To further examine the electrostatic emissions associated with chorus waves, we perform a statistical analysis based on plasma wave data obtained by the Arase satellite, which observes from equator to middle latitudes. As a result, in addition to the chorus-modulated electrostatic waves reported in previous studies, we found a new type of electrostatic waves modulated by longer periods. Furthermore, we found that differences in modulation are dependent on the parallel electric potential of the whistler-mode waves. The mechanism of chorus-related electrostatic waves is investigated through both observations and simulations [Xin An et al., 2019; Ma et al., 2024]. The electrostatic waves we found have not been examined by simulations. In this study, we will perform simulations to investigate the modulation characteristics of electrostatic waves. In this presentation, we will mainly report the analysis results on the Arase observations and also introduce plans for numerical simulations.

地球の内部磁気圏では、ホイッスラーモードの電磁波が多く観測されている。これらの波動は、地球の磁気赤道付近で励起され、高緯度方向へ伝搬する。周波数は発生領域の電子サイクロトロン周波数の $0.1\sim0.8$ 倍の範囲にあり、特に 0.5 倍付近で強度のギャップが現れることが多い。このホイッスラーモード波は、さまざまな非線形現象と関連しており、磁気圏における高エネルギー電子の形成に寄与している。STEREO 衛星においては、歪んだ電界成分をもつホイッスラーモード波が観測されており、この歪みはホイッスラーモード波の静電成分によって電子が捕捉されているためだと考えられている [Kellogg et al., 2010]。また、ISEE 衛星では、ホイッスラーモードコーラス波によって変調された静電バーストが観測されている [Reinleitner et al., 1982]。この静電バーストは磁力線平行方向に振動しており、コーラス波の位相速度と等しい速度をもつ電子がランダウ共鳴することによって生じていると考えられる [Reinleitner et al., 1983]。また、Van Allen Probes による観測においても、同様にコーラス波によって変調された静電波が観測されており、振動方向および周波数からラングミュア波であると考えられている [Li et al., 2017]。しかし、これらの先行研究は数例の事例解析にとどまり、現象の包括的な理解には至っていない。

そこで本研究では、磁気赤道付近から中緯度域まで広く周回し、本現象を多く観測しているあらせ衛星のデータを解析した。その結果、先行研究で報告されていたコーラス波に変調された静電波に加えて、より長周期で変調される静電波を新たに発見した。さらに、統計解析により、静電波の変調の違いはホイッスラーモード波の磁力線平行方向のポテンシャルに依存していることを明らかにした。ホイッスラーモード波に変調された静電波については、観測結果に加えてシミュレーションによって、物理メカニズムが検討されている [Xin An et al., 2019; Ma et al., 2024]。一方、あらせ衛星で観測されたより長周期で変調された静電波については、シミュレーションを用いた検証はこれまで行われていない。今後は、数値シミュレーションを実施し、これらの静電波の変調特性やホイッスラーモード波による励起過程についてさらに検討を進める予定である。本発表では、まずあらせ衛星の観測データに基づく解析結果を中心に報告し、併せてシミュレーションによる検証についても紹介する。

内部磁気圏における孤立静電ポテンシャルの統計解析

#藤田 結衣 $^{1)}$, 頭師 孝拓 $^{1)}$, 栗田 怜 $^{2)}$, 笠原 禎也 $^{3)}$, 松田 昇也 $^{3)}$, 堀 智昭 $^{4)}$, 松岡 彩子 $^{2)}$, 寺本 万里子 $^{5)}$, 山本 和弘 $^{6)}$, 三 好 由純 $^{7)}$, 篠原 育 $^{8)}$

 $^{(1)}$ 奈良高専, $^{(2)}$ 京都大学, $^{(3)}$ 金沢大学, $^{(4)}$ 名古屋大学・宇宙地球環境研究所, $^{(5)}$ 九州工業大学, $^{(6)}$ 名古屋大学宇宙地球環境研究所, $^{(7)}$ 名古屋大学, $^{(8)}$ 宇宙航空研究開発機構

Statistical analysis of the isolated electrostatic potentials in the inner magnetosphere

#Yui FUJITA¹⁾, Takahiro ZUSHI¹⁾, Satoshi KURITA²⁾, Yoshiya KASAHARA³⁾, Shoya MATSUDA³⁾, Tomoaki HORI⁴⁾, Ayako MATSUOKA²⁾, Mariko TERAMOTO⁵⁾, Kazuhiro YAMAMOTO⁶⁾, Yoshizumi MIYOSHI⁷⁾, Iku SHINOHARA⁸⁾

(1 National Institute of Technology, Nara College, (2 Kyoto University, (3 Kanazawa University, (4 Institute for Space-Earth Environmental Research, Nagoya University, (5 Kyushu Institute of Technology, (6 Institute for Space-Earth Environmental Research, Nagoya University, (7 Nagoya University, (8 Japan Aerospace Exploration Agency

It is known that isolated electrostatic potential exists in the Earth's magnetosphere, and is observed as pulse-like solitary waves by satellite electric field observations. Regarding such electrostatic solitary potentials, it has become clear that the properties of solitary waves in the inner magnetosphere observed by the Arase satellite differ significantly from those previously known. Solitary waves in the magnetotail, which have been studied using Geotail observations, are known to have no perpendicular component relative to the background magnetic field and to have a sheet-like potential structure [Matsumoto et al.,1994]. On the other hand, the waveforms in the inner magnetosphere are diverse and may have perpendicular components. Since the existing sheet-like structure is not suitable for the properties of these waveforms, the potential structure in inner magnetosphere is unclear.

In this study, we collected many solitary wave events from the observation result of WFC onboard the Arase satellite, and performed statistical analysis to elucidate the detailed properties of solitary waves in the inner magnetosphere. For event collection, we applied peak detection to long-term WFC electric field waveform data to extract numerous pulse-like solitary waves. We classified the obtained events based on waveform shape and examined correlations between these waveform shape and their observed locations, background magnetic field strength. This presentation shows the results of the analysis of such events and discusses the potential structure estimated from the results.

地球磁気圏において静電的な孤立ポテンシャルが存在し、衛星の電界観測によってパルス状の孤立波動として観測されることが知られている。このような静電孤立ポテンシャルについて、あらせ衛星で観測された内部磁気圏の孤立波の性質が、従来知られているものと大きく異なることが明らかになっている。Geotail 衛星の観測結果を用いて研究されてきた磁気圏尾部の孤立波は背景磁場に対して垂直な成分を持たず、シート型のポテンシャル構造をとることが知られている[Matsumoto et al.,1994]。一方で、内部磁気圏での波形形状は多様であり垂直成分を持つ場合もあることがわかっており、既存のシート型構造ではこのような波形を説明することができないため、内部磁気圏におけるポテンシャル構造は明らかでない。

本研究では、あらせ衛星に搭載されたプラズマ波動・電場観測機 (PWE) を構成する受信器の一つである電界波形観測 (WFC) の観測データから大量のイベントを収集し、内部磁気圏における詳細な孤立ポテンシャルの性質を解明すべく統計解析を行った。イベントの収集のため、長期間に渡る WFC の電界波形データに対してピーク検出を適用し、これによって多数のパルス状孤立波を抽出した。得られたイベントを背景磁場に対し平行/垂直な成分ごとに波形の形状を基準に分類し、それらが観測された位置や背景磁場強度等と各波形の間にみられる相関を調べた。本発表ではこのようなイベントについて解析を行った結果を示し、そこから推定されるポテンシャルの構造について議論する。

科学衛星あらせによって観測された広帯域静電ノイズ低周波成分の統計解析

#金武 剛史 $^{1)}$, 三宅 壮聡 $^{1)}$, 笠原 禎也 $^{2)}$ $^{(1)}$ 富山県立大学, $^{(2)}$ 金沢大学

Statistical analysis of low-frequency components of Broadband Electrostatic Noise observed by ARASE

#Tsuyoshi Kanetake¹⁾, Taketoshi MIYAKE¹⁾, Yoshiya KASAHARA²⁾
⁽¹Toyama Prefectural University, ⁽²Kanazawa University

Broadband Electrostatic Noise (BEN) is a plasma wave observed in the magnetosphere. This wave is observed as an electrostatic wave with a broad spectrum ranging from low-frequency mixed frequencies to electron plasma frequencies, and occurs in various regions of the magnetosphere, including the plasma sheet boundary layer. BEN is composed of two types of waves: low-frequency components and high-frequency components. It has been confirmed that the low-frequency components of BEN are waves with electric fields perpendicular to the magnetic field. The objective of this study is to perform statistical analysis of the low-frequency components of BEN based on observations from the scientific satellite Arase, and to clarify the detailed conditions for the generation of BEN's low-frequency components and their relationship with the surrounding plasma environment. In previous studies, waves considered to be the low-frequency component of BEN were extracted using machine learning. In this study, we will confirm the direction of the electric field relative to the magnetic field for waves considered to be the low-frequency component of BEN and analyze waves with a large vertical electric field component relative to the magnetic field using various plasma parameters such as observation location, magnetic field strength, and ion energy.

広帯域静電ノイズ(BEN: Broadband Electrostatic Noise)とは、磁気圏で観測されるプラズマ波動である。この波動は広帯域かつ低域混成周波数から電子プラズマ周波数に及ぶスペクトルを持つ静電波動として観測され、プラズマシート境界層をはじめ磁気圏の様々な領域で発生する。BENは低周波成分と高周波成分の2種類の波動によって構成されており、低周波成分は磁場に対して垂直方向に電場を持つ波動であることが確認されている。本研究の目的は、科学衛星あらせの観測結果からBENの低周波成分の統計解析を行い、BENの低周波成分の詳しい発生条件や周囲のプラズマ環境との関係などを解明することである。先行研究では、機械学習を用いたBENの低周波成分と考えられる波動の抽出が行われたため、本研究ではBENの低周波成分と考える波動に対して磁場に対する電場の方向を確認し、磁場に対して垂直な電場成分を多く持つ波動に対して、観測位置や磁場強度、イオンエネルギーなど様々なプラズマパラメータを用いて解析を行う

冷たいプラズマ中の波動の分散関係に対する背景磁場構造の影響についての局所標 構を用いた考察

#礒野 航 $^{1)}$, 吉川 顕正 $^{2)}$, 加藤 雄人 $^{1)}$, 熊本 篤志 $^{1)}$ (1 東北大学, $^{(2}$ 九州大学

Effect of the Background Magnetic-Field Geometry on the Dispersion Relation in Cold-Plasma Using a Local Field-Aligned Frame

#Ko ISONO¹⁾, Akimasa YOSHIKAWA²⁾, Yuto KATOH¹⁾, Atsushi KUMAMOTO¹⁾
⁽¹Tohoku University, ⁽²Kyushu University

The Earth's magnetosphere, structured by the terrestrial magnetic field and the solar wind, undergoes substantial variations driven by solar-wind dynamics. The spatial distribution and direction of the geomagnetic field are among the most important factors governing plasma phenomena observed near Earth. Characterizing and assessing the magnetic-field structure is therefore essential for understanding physics processes in magnetosphere.

We analytically investigate how inhomogeneities in the background magnetic field affect on the dispersion relation in a cold plasma based on our previous work of a local frame to quantify magnetic-field curvature and strength gradients, which enables us to evaluate magnetic-structure in arbitrary local regions (Yoshikawa, JpGU, 2023). Most previous studies of coldplasma waves either assume a spatially uniform magnetic field (e.g., Baumjohann, 1996) or rely on numerical calculations that discretely approximate inhomogeneous fields (e.g., Kimura, 1966). While the latter can reproduce spatial variation, they make it difficult to disentangle how individual geometric quantities of the background field—such as strength gradients, curvature, and torsion—contribute to the dispersion relation and propagation characteristics.

Using a local field-aligned frame, we derive and examine the dispersion relation including first-order gradients of the background field. We assume a wavenumber that is constant along a given field line to isolate the influence of the background geometry from effects due to wavenumber variation. Our analysis shows explicitly, at the level of the dispersion relation, that the background magnetic-field structure, especially the geometric term associated with field-line convergence, introduces an imaginary component in the wavenumber and thereby directly modulates the wave amplitude. We also find that torsion and curvature predominantly affect the amplitude to first order. In addition, we perform numerical calculations of plasma-wave propagation in locally measured magnetic fields to assess the applicability of the analytical framework and evaluate the effects of the inhomogeneity quantitatively.

地球磁場と太陽風の相互作用により形成される地球磁気圏は、太陽風の変動によって大きく変化する。地球磁場の強度 分布や方向は、地球周辺で見られるプラズマ現象の振る舞いを定める最も重要な要素の一つである。そのため、地球磁場 の構造を把握、評価することは地球周辺でのプラズマ現象を把握し、放射線帯やオーロラなどのジオスペース分野の研究 を進めるうえで非常に重要である。

本研究ではこれまでに、磁場の曲率や強度勾配を定量化するための局所標構を用いたシステム (Yoshikawa, JpGU, 2023) を構築し、任意の局所領域での磁場構造評価を可能とした。この枠組みを用い、冷たいプラズマ中の波動が、背景磁場の不均一性からどのような影響を受けるかを解析的に検討する。冷たいプラズマ波動に関する考察の多くは空間的に一様な磁場を仮定するか (e.g., Baumjohann, 1996)、あるいは不均一場を離散的に近似した数値計算 (e.g., Kimura, 1966) に依拠してきた。後者は波動の空間変化を再現できる一方、背景磁場の各幾何量(強度勾配・曲率・捩率など)が分散関係および伝搬特性に与える寄与を分離して理解することは難しい。

本研究では、局所標構を用いた手法によって背景磁場の一次の勾配までを考慮したプラズマ波動の分散関係について考察する。波動の波数は磁力線に沿って一定と置き、波数の変化の影響を除いた、背景磁場構造が分散関係に与える影響についての考察に焦点を当てる。その結果、背景磁場の構造、特に磁力線の密集に対応する幾何学的項が波数の虚数成分を生じさせ、波動の振幅に直接的な影響をもたらすことを明示した。また、他のねじれや曲率も主に波の振幅に影響を与えることを示した。さらに本発表では、実際に局所磁場におけるプラズマ波動の数値計算を試み解析結果と比較して、考察の妥当性を検討し、不均一性の影響を定量的に評価する。

木星探査機 Juno による観測結果に基づく木星磁気圏におけるインジェクション現象時に観測された電磁イオンサイクロトロン波動の事例解析

#野口 智史 $^{1)}$, 加藤 雄人 $^{1)}$, 熊本 篤志 $^{1)}$ 「「東北大・理・地球物理

A Case Study of EMIC Waves Observed During an Injection Event in Jupiter's Magnetosphere Based on Juno's Observation

#Tomofumi Noguchi¹⁾, Yuto Katoh¹⁾, Atsushi Kumamoto¹⁾

(1) Department of Geophysics, Graduate School of Science, Tohoku University

Unlike Earth's magnetosphere, the dynamics of Jupiter's giant magnetosphere are dominated by the planet's rapid rotation and its interaction with heavy ions supplied by moon Io. Plasma waves in this environment are a crucial subject of study for understanding energy transport and particle acceleration. This research focuses on a case in which Electromagnetic Ion Cyclotron (EMIC) waves were observed during an injection event in Jupiter's magnetosphere, where electrons and ions with a broad energy range from several keV to hundreds of keV are rapidly injected radially inward. The study is based on an analysis of data from the Juno spacecraft.

One excitation process for plasma waves like EMIC waves is temperature anisotropy in high-energy particles, where their temperature is predominantly perpendicular to the magnetic field lines. In Jupiter's magnetosphere, injection events are considered a primary mechanism for generating this anisotropy. It is thought that injections in the Jovian magnetosphere occur when high-energy particles are injected into the inner magnetosphere due to phenomena such as interchange instability (Mauk et al., 1999). Adiabatic heating associated with the inward radial transport during these injection events is expected to create strong temperature anisotropy in the velocity distribution of the high-energy particles. While recent studies have observed whistler-mode chorus waves caused by high-energy electrons with injection-induced temperature anisotropy in Jupiter's magnetosphere (Ma et al., 2024), there have been no reports of observational cases showing a clear association between particle injections and EMIC waves. Investigating whether injection-associated EMIC waves, which are frequently observed in Earth's magnetosphere, also occur at Jupiter is important for clarifying the details of particle acceleration processes in the Jovian magnetosphere and for exploring universal physical laws through comparison with Earth's magnetosphere.

This study aims to elucidate the details of Jupiter's magnetospheric dynamics and wave generation, as well as to confirm the contribution of wave-particle interactions and to make comparisons with Earth. For this purpose, we identified and investigated a case of the simultaneous occurrence of an injection event and EMIC waves using observational data from the Juno spacecraft. From observations by the Jovian Auroral Distributions Experiment (JADE) (McComas et al., 2017) around 05:00 UT on May 22, 2022, in the equatorial region at a distance of 15-20 Jovian radii (R_J) from the center of Jupiter, signs of an injection event were confirmed by a sharp increase in the energy flux of electrons and ions in the 0.1- several tens of keV range. Meanwhile, concurrent magnetic field observations by the Magnetometer (MAG) (Connerney et al., 2017) revealed significant magnetic field fluctuations.

A detailed analysis of these magnetic field fluctuations was conducted using Wavelet analysis and polarization analysis based on the Singular Value Decomposition (SVD) method (Santolik et al., 2003). The results confirmed a wave phenomenon with an intensity exceeding 10^2 nT²/Hz lasting for about 5 minutes. This wave exhibited left-hand polarization, quasi-parallel propagation, and a frequency below the local oxygen ion cyclotron frequency. Based on these wave characteristics, it is considered that the identified event captured EMIC waves generated in association with an injection event.

While there have been reports of EMIC waves in Jupiter's magnetosphere, such as those originating from pickup ions from the moon Io (Cao et al., 2025) and in the outer magnetosphere (90 R_J) (Yuan et al., 2024), the present study is the first report of EMIC waves associated with an injection event in the inner magnetosphere.

木星の巨大磁気圏のダイナミクスは、地球とは異なり、惑星本体の高速な自転と衛星イオから供給される重イオンとの相互作用に支配されている。この環境におけるプラズマ波動は、エネルギー輸送や粒子加速を理解する上で極めて重要な研究対象である。本研究では、木星磁気圏で発生する動径方向内側へ数 keV から数百 keV に及ぶ広いエネルギー帯の電子とイオンが急激に注入されるインジェクション現象において、電磁イオンサイクロトロン (EMIC) 波が観測された事例に着目し、探査機 Juno データに基づいて考察する。

EMIC 波のようなプラズマ波動の励起過程として、高エネルギー粒子の温度が磁力線垂直方向に卓越する温度異方性が挙げられる。木星磁気圏において、インジェクションはこの異方性を生成する主要なメカニズムの一つと考えられている。木星磁気圏におけるインジェクション現状は、交換型不安定性(Interchange Instability)などに伴って、磁気圏のより内側に高エネルギー粒子が注入されることで生じると考えられている(Mauk et al., 1999)。インジェクション現象に伴う動径方向内側への輸送に伴う断熱的な加熱により、高エネルギー粒子の速度分布には強い温度異方性が生じることが期待される。近年の研究では、木星磁気圏ではインジェクションによって温度異方性が卓越した高エネルギー電子に起因すホイッスラーモード・コーラス波が観測されているが(Ma et al., 2024)、一方で EMIC 波については、粒子注入との明

確な関連を示す観測事例の報告は未だない。地球磁気圏では多数の観測事例があるインジェクションに伴う EMIC 波が、木星磁気圏でも観測されるのか、という疑問を調査することは、木星磁気圏における粒子加速過程の詳細を明らかにするとともに、地球磁気圏との比較を通して普遍的な物理法則を探る上で重要である。

本研究は、木星磁気圏のダイナミクス、波動発生の詳細を明らかにすること、さらには波動粒子相互作用への寄与の考察や地球との比較を目的とし、インジェクションと EMIC 波の同時発生事例を Juno 探査機による観測データから同定して調査した。2022 年 5 月 22 日 5: 00 UT 前後における、木星中心からの距離が $15^{\circ}20$ 木星半径 (R_J) の赤道域付近における Jovian Auroral Distributions Experiment (JADE) (McComas et al., 2017) による観測結果から、0.1-数十 keV の電子とイオンのエネルギーフラックスが急増するインジェクション現象の兆候が確認された。さらに、これと同時刻における磁力計 (MAG) (Connerney et al., 2017) による観測では、顕著な磁場変動が観測された。

磁場変動に対して Wavelet 解析を行い、特異値分解 (SVD) 法に基づく偏波解析 (Santolik et al., 2003) を用いて詳細に分析した結果、強度が 10^2 nT 2 /Hz 以上の強度の波動現象が約 5 分間持続していることが確認された。この波動は、左回り偏波、準平行伝播、そして局所的な酸素イオンのサイクロトロン周波数より低い周波数という特徴を示した。得られた波動特性に基づいて、同定されたイベントはインジェクション現象にともなって発生した EMIC 波をとらえたものであると考えられる。

木星磁気圏における EMIC 波については、衛星イオからのピックアップイオンに由来する EMIC 波 (Cao et al., 2025) や外部磁気圏(90 R_J)における EMIC 波の報告例 (Yuan et al., 2024) があったが、内部磁気圏におけるインジェクション現象に伴う EMIC 波の報告としては初めての例となる。

#宮下 隼輔 $^{1)}$, 加藤 雄人 $^{1)}$, Ondřej Santolík $^{2)}$, Benjamin Grison $^{2)}$, 熊本 篤志 $^{1)}$ 東北大・理・地球物理、 $^{(2)}$ チェコ科学アカデミー大気物理学研究所

Statistical properties of the distribution of EMIC waves in the magnetosphere observed by the Cluster satellite in 2011-2022

#Miyashita Shunuske¹⁾, Katoh Yuto¹⁾, Santolík Ondřej²⁾, Grison Benjamin²⁾, Kumamoto Atsushi¹⁾
⁽¹⁾Department of Geophysics, Graduate School of Science, Tohoku University, ⁽²⁾Institute of Atmospheric Physics of the Czech Academy of Sciences, Prague, Czech Republic

Electromagnetic ion cyclotron (EMIC) waves are important for the loss of radiation belt electrons and ring current ions. After being excited by an instability driven by the temperature anisotropy followed by nonlinear wave-particle interactions occurring near the magnetic equator of the inner magnetosphere, EMIC waves propagate parallel along the magnetic field lines with left-handed polarization. As the waves propagate to higher latitudes, their wave normal angles with respect to the magnetic field increase. At latitudes where the wave frequency is the same as the crossover frequency, the polarization changes from left-handed to right-handed, called polarization reversal. After the polarization change to right-handed, EMIC wave cannot interact with radiation belt electrons. By utilizing this characteristic and investigating the location where polarization reversal occurred, it is possible to estimate the range in which EMIC waves can interact with radiation belt electrons.

Previous statistical studies of EMIC waves using Cluster data have been performed in the period from 2001 to 2010(Allen+2015,2016). We extend the analysis to the period from 2011 to 2022 to investigate the statistical properties especially polarization characteristics of EMIC waves in different solar cycles. The period from 2011 onwards corresponds to solar cycle 24, whose solar activities were weaker than those in solar cycle 23. Furthermore, since the Cluster's orbital coverage has changed since the earlier studies, extending the statistical analysis to the period of 2011-2022 is expected to yield new insights into EMIC wave characteristics under different solar activity levels and spatial coverage. The Cluster's polar orbit provides a unique advantage, enabling us to investigate EMIC wave properties at higher latitudes and throughout a wider range of L-shell.

In the present study, we show statistical distribution on the occurrence probability, spatial distribution, and polarization characteristics of EMIC waves in the magnetosphere observed by Cluster which cover the range of magnetic latitude up to 60 degrees and L-values up to 15. In particular, in order to investigate the relationship between magnetic latitude and polarization characteristics, the most frequent values and standard deviation of wave polarization derived by the SVD method were calculated. In this result, As latitude increases, a tendency toward right-handed polarization was observed, while no correlation was found in the standard deviation values. Furthermore, when the distribution was examined using L-values and MLT, left-handed polarization was observed even in high-latitude regions, with L-values exceeding 10. The data suggests that the plasma environment of the outer magnetosphere is reflected. This region has a lower concentration of heavy ions than the inner magnetosphere, but estimating the extent of left-handed polarization in the radiation belts still necessitates an analysis of its dependence on geomagnetic activity. This presentation will also address these points and report comprehensive analysis results of EMIC waves in the entire magnetosphere and radiation belt region.

地球磁気圏の EMIC 波: Arase 衛星による偏波解析を用いたイオン組成導出の試み #菊地 陸 ¹⁾, 笠羽 康正 ¹⁾, 松田 昇也 ²⁾, 笠原 禎也 ²⁾, 松岡 彩子 ³⁾, 土屋 史紀 ¹⁾, 佐藤 晋之祐 ¹⁾, 城 剛希 ¹⁾ (1 東北大学, ⁽² 金沢大学, ⁽³ 京都大学

EMIC Waves in the Magnetosphere: Attempts to Derive Ion Composition Using Polarization Analysis by the Arase Satellite

#Riku Kikuchi¹⁾, Yasumasa KASABA¹⁾, Shoya MATSUDA²⁾, Yoshiya KASAHARA²⁾, Ayako MATSUOKA³⁾, Fuminori TSUCHIYA¹⁾, Shinnosuke SATOH¹⁾, Koki TACHI¹⁾
⁽¹Tohoku University, ⁽²Kanazawa University, ⁽³Kyoto University)

Electromagnetic ion cyclotron (EMIC) waves are low-frequency, circularly polarized electromagnetic waves excited by anisotropic ion distributions. These waves exhibit frequency characteristics based on each ion's cyclotron frequency, while their frequencies and polarizations depend on the density of each ion species. Thus, if the wave is sufficiently strong and the signal-to-noise (S/N) ratio is high, it is potentially possible to estimate the ion composition of the surrounding plasma. A key phenomenon for this plasma diagnostic is mode conversion, where the wave polarization switches between R-mode (right-hand polarized) and L-mode (left-hand polarized). The boundary frequency of this conversion, known as the crossover frequency, contains crucial information on the ambient ion composition. Particle instruments onboard satellites often struggle to detect low-energy ions below 10-20 eV. Therefore, investigating EMIC waves enables the inference of ion species and their compositions, providing insights into magnetospheric dynamics.

Previous observations by the Akebono satellite and Radiation Belt Storm Probes (RBSP) have identified EMIC waves associated with various ion species, as well as mode conversion events that are useful for estimating ion composition [Matsuda et al., 2015; Miyoshi et al. 2019]. However, only one mode conversion event has been reported by the Arase satellite [Miyoshi et al., 2019, Fig.2], and ion compositions have not been extensively discussed. The inference of ion compositions from EMIC wave observations in planetary magnetospheres can also be applied to BepiColombo (arriving at Mercury in November 2026), Juno (having conducted close flybys at the Galilean satellites) [Satoh et al., in preparation], and JUICE (orbiting Jupiter from 2031), and the application to these missions has to be prepared.

This study aims to investigate EMIC waves more comprehensively using magnetic field data from the Arase satellite and determine the distribution and dynamics of cold ion compositions from the topside ionosphere to the plasmasphere. We focus particularly on low altitudes, where He⁺ and O⁺ are expected to be more abundant. We primarily use 1,024 Hz waveform data from Wave Form Capture (WFC) [Matsuda et al., 2018] (EMIC-Burst data: obtained intermittently from 2017 to October 2018, during periods when the triaxial magnetic field waveform data from the search coil were available) on PWE, and also the ambient magnetic field data from Magnetic Field Experiment (MGF) [Matsuoka et al., 2018] onboard the Arase satellite, which can observe EMIC waves at frequencies above several tens of Hz with high frequency resolution in regions including the topside ionosphere.

We first searched for "EMIC waves with sufficient S/N and broad frequency coverage over H⁺, He⁺, O⁺ cyclotron frequencies" in WFC EMIC-burst data. We then selected events near perigee (R<2.5Re) that exhibited sufficient intensity and mode conversion, allowing for the derivation of ion composition. For these events, we applied analysis methods previously used for Akebono and RBSP to estimate ion composition. Specifically, we performed polarization analysis with the singular value decomposition (SVD) method [Santolik et al., 2003] and identified the EMIC waves based on their polarization properties: polarization ellipticity, wave normal angle (WNA), which indicates the propagation direction, and planarity. Finally, we derived ion compositions by identifying cutoff and crossover frequencies, which provide information on the ambient ion population.

From March 2017 to October 2018, we identified approximately 100 EMIC mode conversion events, predominantly concentrated on the dayside (08-14 MLT). The derived ion composition ratios from these events confirm that the relative abundance of H⁺ decreases, while that of He⁺ increases, with decreasing altitude. This result is consistent with the International Reference Ionosphere (IRI) model and previous studies [Miyoshi et al. 2019], thereby indicating that ion compositions can be reliably inferred from Arase EMIC wave observations. As of August 2025, we are actively refining our analysis methods to obtain more precise ion composition ratios. Furthermore, we are attempting to extend our analysis period to after November 2018. We have already confirmed that, even with the constraint of a missing triaxial magnetic field component in the EMIC-burst data from this period, cutoff and crossover frequencies can still be identified from wave intensity and polarization information. We also plan to consider the use of data from the Hisaki space telescope to cross-validate our results, as it can be used to estimate exospheric neutral H, He, and O populations during the same period.

Electromagnetic ion cyclotron (EMIC) 波は、温度異方性のある各種イオンにより励起される円偏波を持つ低周波電磁波動である。各イオンのサイクロトロン周波数を基準とした周波数特性を示すが、各イオンの密度がその周波数や偏波特性に影響を与える。このため、波動が強く十分な S/N 比が得られる場合には、周辺プラズマのイオン組成を推定することが可能である。特に、波動の周波数特性が R モード(右旋円偏波)から L モード(左旋円偏波)、もしくは L モードから R モードに切り替わるモード変換イベントは、その境界周波数(crossover 周波数)が周囲のイオン組成比に関する情報を含むため、プラズマ診断に非常に有用である。粒子計測器では 10-20 eV を下回る低エネルギーイオンの定常的な観測が困難であるため、EMIC 波を用いたイオン種及びその組成の導出は、地球及び惑星の磁気圏・プラズマ圏におけるイオンの輸送ダイナミクスを紐解く手がかりになり得る。

これまでに、Akebono 衛星や Radiation Belt Storm Probes (RBSP) 衛星により、各種イオンの EMIC 波が観測され、イオン組成の推定に有益なモード変換イベントも報告されている [Matsuda et al., 2015; Miyoshi et al. 2019]。一方、Arase 衛星におけるモード変換イベントの観測事例は、Miyoshi et al. (2019) の Fig.2 に示される一例のみに留まっており、イオン組成に関する詳細な議論は行われていない。惑星磁気圏の EMIC 波とそれによるイオン組成及びその変動推定は、2026 年 11 月に水星到着予定の BepiColombo、木星を周回しガリレオ衛星におけるフライバイ観測を行った Juno [Satoh et al., in preparation]、2031 年から木星を周回する JUICE による磁場観測にも適用可能であるが、手法の最適化や精度向上の確立も同時に必要である。

本研究は、Arase 衛星の磁場波動データを用いて EMIC 波の広範な観測事例を調べ、電離圏のトップサイドからプラズマ圏における低温イオンの組成分布とその変動を見出すことを目的として着手された。特に、 He^+ 、 O^+ がより多く含まれる低高度で重点的に解析を進めている。本解析は、電離圏トップサイドを含む領域での数十 Hz 以上のEMIC 波を高い周波数分解能で観測可能な PWE WFC (Wave Form Capture) [Matsuda et al., 2018] による 1,024 Hz 波形データ(EMIC-Burst: 磁場 3 軸波形データが存在する 2017-2018 年 10 月の間欠的期間)、および MGF (Magnetic Field Experiment) [Matsuoka et al., 2018] による背景磁場情報を用いて進めた。

まず WFC EMIC バーストデータにおいて「S/N の良く、H⁺、He⁺、O⁺ のサイクロトロン周波数を跨ぐ広帯域の EMIC 波」を探索し、組成情報を導出し得る強度が十分大きくモード変換が見られる波を近地点近傍(R<2.5Re)でピックアップした。これらに Akebono・RBSP に対して行われてきた手法を適用してイオン組成の導出を行った。具体 的には、特異値分解 (Singular Value Decomposition; SVD) 法 [Santolik et al., 2003] 等を用いた偏波解析を行い、偏波度 (polarization ellipticity)、伝播方向を示す波数法線角 (Wave Normal Angle; WNA)、及び波の平面性 (planarity) を基礎に EMIC 波動を識別し、イオン組成情報を含む cutoff 周波数や crossover 周波数を同定してイオン組成の導出を行った。

2017 年 3 月-2018 年 10 月の期間では、これまでに約 100 の EMIC モード変換イベントを特定(特に日中側 08-14 MLT に集中して発生)している。これらの cutoff 周波数と crossover 周波数からイオン組成比を求めた結果、高度が低くなるにつれて \mathbf{H}^+ の割合が低くなり、 \mathbf{H}^+ の割合が高くなることを確認できた。これは IRI(International Reference Ionosphere)モデルや先行研究 [Miyoshi et al. 2019] の結果と整合しており、Arase 衛星の EMIC 観測量からイオン組成を導出可能であることを示すものである。2025 年 8 月現在、より高精度でイオン組成比を求めるための解析手法の改良を進めている。また、サーチコイル磁力計の一軸が欠損してしまう 2018 年 11 月以降への解析期間の延長も試みつつある。磁場 2 軸のデータから得られる波動強度・偏波情報から cutoff 周波数や crossover 周波数は同定でき、イオン組成の導出が可能であることを確認済である。なお、同時期の地球外圏における中性 $\mathbf{H} \cdot \mathbf{H} \cdot \mathbf{O}$ の量が極端紫外線望遠鏡衛星 Hisaki における $\mathbf{H} \cdot \mathbf{H} \cdot \mathbf{O}$ コロナ発光量から推定可能でもあり、その援用も今後検討する。

レイトレーシングを用いた多点同時観測 EMIC 波の伝搬特性解析

#梅澤 祐伊 $^{1)}$, 笠原 禎也 $^{1)}$, 松田 昇也 $^{1)}$, 太田 守 $^{2)}$ $^{(1)}$ 金沢大, $^{(2)}$ 富山高専

Study on the Propagation Characteristics of the EMIC Waves Observed at Multiple Points using ray tracing

#Yui Umezawa¹⁾, Yoshiya Kasahara¹⁾, Shoya Matsuda¹⁾, Mamoru Ota²⁾
⁽¹Kanazawa University, ⁽²NIT⁽KOSEN), Toyama College

The near-Earth space environment is strongly influenced by plasma waves and high-energy particles. Electromagnetic ion cyclotron (EMIC) waves play a key role in controlling the precipitation of high-energy ions and relativistic electrons in the inner magnetosphere. Furthermore, EMIC waves exhibit complex propagation characteristics such as reflection and cutoff, governed by dispersion relations that depend on the ion composition of the ambient plasma. Therefore, analyzing EMIC wave propagation provides valuable insights into the ion composition and spatial structure of the magnetospheric plasma.

In this study, we focus on the fine-structured EMIC wave event simultaneously observed on April 18, 2019, by Arase and RBSP-A and two ground-based stations at Gakona and Dawson (Matsuda et al., 2021). We analyze its propagation characteristics using the ray tracing method. Matsuda et al. (2021) have suggested that EMIC waves are spatially localised and may propagate

through ducts along magnetic field lines comparing the wave spectra measured at the locations of Arase and Van Allen Probes as well as ground stations. However, the specific shape of the ducts and the source regions of the EMIC waves have not been sufficiently examined in a manner consistent with all observational facts. In the present study, we conducted a series of ray tracing simulations by systematically varying the initial conditions (e.g., source location, frequency, and initial wave normal angle) as well as environmental parameters such as ion composition and duct geometry. We evaluated the relationships between these parameters and wave propagation characteristics, and attempted to identify the conditions under which simultaneous multi-point observations could be reproduced.

In this presentation, we will share the results of our analysis concerning the geomagnetic and plasma conditions that enable the observed multi-point detection of EMIC waves, and discuss how ion composition and duct structures influence EMIC wave propagation.

Reference

Matsuda et al., Geophysical Research Letters, doi:10.1029/2021GL096488, 2021.

地球周辺の宇宙環境は、プラズマ波動や高エネルギー粒子によって大きく左右される. なかでも電磁イオンサイクロトロン(EMIC)波は、地球内部磁気圏における高エネルギーイオンや相対論的電子の降下を制御する重要なプラズマ波動である. また、EMIC 波はプラズマ中のイオン組成に依存する分散関係に従い、反射やカットオフといった伝搬挙動を示すため、その伝搬解析は磁気圏のイオン組成や空間構造を推定する手がかりとなる.

本研究では Matsuda et al. (2021) により報告された 2019 年 4 月 18 日における 2 機の科学衛星(Arase 及び RBSP-A)と 2 つの地上局(Gakona 及び Dawson)による微細構造 EMIC 波の同時観測イベントを対象に、レイトレーシングを用いた伝搬特性解析を行う。Matsuda et al. (2021) は、両衛星のフットプリントと波動スペクトルの比較から、EMIC 波が空間的に局所的であり、磁力線に沿ったダクトを通じて伝搬している可能性が示唆されている。しかし、ダクトの具体的な形状やその周辺の環境条件については、すべての観測事実に整合する形での考察は十分に行われていない。よって本研究では、波動の初期条件(発生源の位置・周波数・初期伝搬角)やイオン組成・ダクト構造のパラメータを系統的に変化させながらレイトレーシングを実施し、伝搬特性と各種パラメータの関係性の評価、および多点同時観測を再現しうる条件の特定を試みた。

本講演では、対象 EMIC 波の多点同時観測を生じる地磁気・プラズマ環境条件についての解析結果を示し、イオン組成やダクト構造が EMIC 波の伝搬に及ぼす影響について議論する.

あらせ衛星を用いた高周波 EMIC の統計解析

#式守 隆人 $^{1)}$, 篠原 育 $^{2)}$, 浅村 和史 $^{2)}$, 三好 由純 $^{3)}$, 横田 勝一郎 $^{4)}$, 笠原 慧 $^{5)}$, 桂華 邦裕 $^{5)}$, 堀 智昭 $^{6)}$, 松岡 彩子 $^{7)}$, 寺本 万里子 $^{8)}$, 山本 和弘 $^{9)}$, 新堀 淳樹 $^{3)}$, 熊本 篤志 $^{10)}$, 土屋 史紀 $^{10)}$, Jun ChaeWoo $^{11)}$

 $^{(1)}$ 東大, $^{(2)}$ 宇宙航空研究開発機構, $^{(3)}$ 名古屋大学, $^{(4)}$ 大阪大学大学院, $^{(5)}$ 東京大学, $^{(6)}$ 名古屋大学・宇宙地球環境研究所, $^{(7)}$ 京都大学, $^{(8)}$ 九州工業大学, $^{(9)}$ 名古屋大学宇宙地球環境研究所, $^{(10)}$ 東北大学, $^{(11)}$ Nagoya University

Statistical Study of High-Frequency EMIC Waves with the Arase Satellite

#Takahito Shikimori¹⁾, Iku SHINOHARA²⁾, Kazushi ASAMURA²⁾, Yoshizumi MIYOSHI³⁾, Shoichiro YOKOTA⁴⁾, Satoshi KASAHARA⁵⁾, Kunihiro KEIKA⁵⁾, Tomoaki HORI⁶⁾, Ayako MATSUOKA⁷⁾, Mariko TERAMOTO⁸⁾, Kazuhiro YAMAMOTO⁹⁾, Atsuki SHINBORI³⁾, Atsushi KUMAMOTO¹⁰⁾, Fuminori TSUCHIZA¹⁰⁾, Chaewoo JUN¹¹⁾

⁽¹The University of Tokyo, ⁽²Japan Aerospace Exploration Agency, ⁽³Nagoya University, ⁽⁴Osaka University, ⁽⁵The University of Tokyo, ⁽⁶Institute for Space-Earth Environmental Research, Nagoya University, ⁽⁷Kyoto University, ⁽⁸Kyushu Institute of Technology, ⁽⁹Institute for Space-Earth Environmental Research, Nagoya University, ⁽¹⁰Tohoku University, ⁽¹¹Nagoya University)</sup>

HFEMIC waves are electromagnetic ion cyclotron (EMIC) waves with high frequency and a narrow bandwidth (Δ f \lesssim 0.1fcp, f <fcp). Previous case and statistical studies (Teng et al., 2019; Asamura et al., 2021; Min & Ma, 2024) have suggested that HFEMIC waves are likely driven by low-energy (\lesssim 100 eV) protons with temperature anisotropy (T \perp >T /). In particular, Asamura et al. (2021) analyzed simultaneous observations of HFEMIC waves and increases of low-energy proton fluxes from the Arase satellite. Using wave – particle interaction analysis, they showed that protons lost energy through the interaction, and this energy was

used to excite the waves.

Low-energy protons with temperature anisotropy (T \perp >T /) have been reported to be widely present in the inner magnetosphere (Wu et al., 2022), and they are considered the free energy source of HFEMIC waves. However, a statistical study using Van Allen Probes data (Teng et al., 2019) reported that HFEMIC waves occurred mainly in the morning and noon sectors, and no HFEMIC waves were reported on the nightside.

In this study, we extracted HFEMIC wave events from Arase satellite data and carried out a statistical analysis again, in order to confirm whether the excitation process of HFEMIC waves reported by Asamura et al. (2021) is general. Wave normal angles and polarization properties were considered in the event selection. As a result, HFEMIC waves were also found in the nightside region, where they had not been identified by the Van Allen Probes.

In this presentation, based on these findings, we discuss possible factors related to the occurrence of HFEMIC waves in the nightside region, such as the temperature anisotropy of low-energy protons, background electron density, the fpe/fcp ratio, and geomagnetic activity. We also compare our results with the statistical study of EMIC waves using Arase satellite data (Jun et al., 2023), to further improve our understanding of HFEMIC waves.

HFEMIC 波は、高周波で狭帯域(Δ f \lesssim 0.1fcp、f <fcp)の電磁イオンサイクロトロン(EMIC)波である。事例研究 および統計研究(Teng et al., 2019; Asamura et al., 2021; Min & Ma, 2024)により、HFEMIC 波は温度異方性(T \perp >T //)のある低エネルギー(\lesssim 100 eV)プロトンによって駆動される可能性が高いことが示されている。特に (Asamura et al., 2021) では、あらせ衛星によって取得された HFEMIC 波と低エネルギープロトンフラックス増加の同時観測データを解析し、波動・粒子相互作用解析手法を用いて、HFEMIC 波と相互作用するプロトンが実際にエネルギーを失い、そのエネルギーが波の励起に使われていることを明らかにした。

低エネルギーの温度異方性(T \bot >T /)のあるプロトンは内側磁気圏に広く存在することが報告されており(Wu et al., 2022)、HFEMIC 波の自由エネルギー源であると考えられている。しかし、Van Allen Probes の観測データを用いた (Teng et al., 2019) の統計研究では、HFEMIC 波の出現が MLT については主に朝側から昼側に限られており、夜側では報告されていない。

このような背景のもと、本研究では、最終的には HFEMIC の励起プロセスが Asamura et al. (2021) で示されたようなものが一般的であるかどうかを確認するために、あらせ衛星データを用いて HFEMIC 波イベントを新たに抽出し、再度統計研究を試みた。抽出には磁場に対する伝搬

方向や偏波特性を考慮した。解析の結果、Van Allen Probes では確認されなかった夜側領域においても HFEMIC 波の存在が明らかとなった。

本発表では、この発見を踏まえ、夜側領域に HFEMIC 波の出現に関係する要因として、励起源としての低エネルギープロトンの温度異方性、背景電子密度、fpe/fcp 比、地磁気活動度の影響について議論する。また、あらせ衛星を用いた EMIC 波の統計研究(Jun et al., 2023)とも比較を行い、HFEMIC 波に関する理解をさらに深める。

#Jun Chae-Woo¹⁾, 三好 由純 ¹⁾, 堀 智昭 ¹⁾, 山本 和弘 ¹⁾, KIM Khan-Hyuk²⁾, LEE Jun-Hyun³⁾, BORTNIK Jacob⁴⁾, 篠原 育 ⁵⁾, 浅村 和史 ⁵⁾, 寺本 万里子 ⁷⁾, 笠原 慧 ⁸⁾, 桂華 邦裕 ⁸⁾, 横田 勝一郎 ⁹⁾, 松田 昇也 ¹⁰⁾, 笠羽 康正 ¹¹⁾, 笠原 禎也 ¹⁰⁾, 松岡 彩子 ⁶⁾

(1 名古屋大学 宇宙地球環境研究所, ⁽²Kyung-Hee University, Suwon, Korea, ⁽³Korea Astronomy and Space Science Institute, Daejeon, Korea, ⁽⁴Atmospheric and Oceanic Sciences, University of California Los Angeles, Los Angeles, USA, ⁽⁵ 宇宙航空研究開発機構, ⁽⁶ 京都大学, ⁽⁷ 九州工業大学, ⁽⁸ 東京大学, ⁽⁹ 大阪大学, ⁽¹⁰ 金沢大学, ⁽¹¹ 東北大学

Discovery of hidden EMIC wave branches: Evidence of molecular and metallic ion contributions in the inner magnetosphere

#ChaeWoo Jun¹⁾, Yoshizumi MIYOSHI¹⁾, Tomoaki HORI¹⁾, Kazuhiro YAMAMOTO¹⁾, Khan-Hyuk KIM²⁾, Jun-Hyun LEE³⁾, Jacob BORTNIK⁴⁾, Iku SHINOHARA⁵⁾, Kazushi ASAMURA⁵⁾, Mariko TERAMOTO⁷⁾, Satoshi KASAHARA⁸⁾, Kunihiro KEIKA⁸⁾, Shoichiro YOKOTA⁹⁾, Shoya MATSUDA¹⁰⁾, Yasumasa KASABA¹¹⁾, Yoshiya KASAHARA¹⁰⁾, Ayako MATSUOKA⁶⁾

⁽¹Nagoya University, ⁽²Kyung-Hee University, Suwon, Korea, ⁽³Korea Astronomy and Space Science Institute, Daejeon, Korea, ⁽⁴Atmospheric and Oceanic Sciences, University of California Los Angeles, Los Angeles, USA, ⁽⁵Institute of Space and Astronautical Science, Japan Aerospace Exploration Agency, Sagamihara, Japan, ⁽⁶Kyoto University, Kyoto, Japan, ⁽⁷Kyushu Institute of Technology, Iizuka, Japan, ⁽⁸University of Tokyo, Tokyo, Japan, ⁽⁹Osaka University, Osaka, Japan, ⁽¹⁰Graduate School of Natural Science and Technology, Kanazawa University, Kanazawa, Japan, ⁽¹¹Graduate School of Science, Tohoku University, Sendai, Japan

The cold ion composition plays an important role in defining various wave branches in the dispersion relationship of electromagnetic ion cyclotron (EMIC) waves. EMIC waves are typically identified within three major wave branches: H-, He-, and O-band EMIC waves, which are associated with major ion species (H+, He+, and O+) in the Earth's magnetosphere. However, recent studies suggested that other ions (e.g., He++, N+, and O++) can contribute to creating additional wave branches depending on geomagnetic environments. Molecular ions can be supplied to the inner magnetosphere during the active solar period and/or high-speed solar wind conditions [Nagatani et al., 2024]. Sporadic E-regions or the lunar surface can be a candidate for supplying Fe+ in the inner magnetosphere [Lin et al., 2025]. While it is expected that molecular and metallic ion contributions have been hypothesized theoretically, their observational evidence has not been identified. From the point of view of observations, it is difficult to distinguish such low-frequency (LF) EMIC waves from typical ultralow-frequency (ULF) pulsations in the Pc 3-5 bands (2-100 mHz). In this study, we present the first satellite evidence of EMIC wave events observed below the gyrofrequencies of oxygen, molecular ions, and metallic ions observed by the Arase satellite. We investigated the characteristics of LF EMIC waves to discriminate from typical ULF waves. LF EMIC waves had left-handed and linear polarization sense with the field-aligned wave normal angles and non-zero Poynting vector in the ambient magnetic field direction, indicating similar wave properties as typical EMIC waves. We also found that LF EMIC waves used to be observed near the boundary between the tail lobes and the plasma sheet boundary layer (PSBL) on the nightside. They are also frequently detected on the dayside of the magnetosphere with a broad bandwidth. These waves sometimes show phase differences between the electric and magnetic fields of 45 or 135 degrees. If the observed waves can be categorized as EMIC waves, these LF events imply the presence of significant molecular and metallic ion populations in the inner magnetosphere. This finding contributes to the task of estimating the fraction of molecular and metallic ions in the inner magnetosphere using the dispersion relationship of EMIC waves. We discuss the underlying physical mechanism causing low-frequency EMIC waves and the possibility of LF EMIC wave-particle interactions, as well as the implications for cold ion compositions.

R006-P18

ポスター1:11/25 AM1/AM2 (9:15-12:35)

地球磁気圏における超低周波(ULF)波による低ハイブリッド波・ECH 波の変調

#李莉^{1,2)},大村善治²⁾

(1 中国地質大学(北京),(2 京都大学

Modulation of Lower Hybrid and ECH Waves by ULF Waves in the Earth's Magnetosphere

#Li Li^{1,2)}, Yoshiharu OMURA²⁾

(1 China University of Geosciences Beijing, (2 Kyoto University

ULF waves, with their characteristic periods ranging from a few seconds to several minutes, are known to interact with various plasma waves, including chorus wave and EMIC waves, which play a key role in particle acceleration and wave-particle interactions. In this study, we report for the first time the periodic modulation of lower hybrid waves by ULF waves, revealing a novel interaction that occurs near the troughs of ULF wave fields. At the same time, we observe the periodic excitation of ECH waves. The excitation and disappearance of these waves, confined to the troughs of the ULF waves, suggest a new mechanism of wave interaction. Additionally, the ULF waves are diagnosed as drift-mirror modes. These findings highlight the periodic coupling of ULF, lower hybrid, and ECH waves and provide new insights into their interaction dynamics in the magnetosphere.

科学衛星あらせによって観測された特徴的な低周波波動の解析

#完野 蒼雅 $^{1)}$, 三宅 壮聡 $^{1)}$, 笠原 禎也 $^{2)}$ $^{(1)}$ 富山県立大学, $^{(2)}$ 金沢大学

Analysis of characteristic low-frequency waves observed by the scientific satellite Arase

#Soga Shishino¹⁾, Taketoshi MIYAKE¹⁾, Yoshiya KASAHARA²⁾
⁽¹Toyama Prefectual University, ⁽²Kanazawa University

In this study, we apply machine learning to electric field spectrum images obtained by the electric field detector (EFD) mounted on the scientific satellite Arase to perform classification and analysis. First, we extracted and classified low-frequency waves from 1,987 spectrum images obtained between March 21, 2017, and August 31, 2022. As a result, 175 wave events showing relatively broad-band spectral structures were extracted, and k-means clustering and hierarchical clustering were applied using the duration, frequency band, and center frequency of each wave as features. This allowed us to exclude images without clear wave structures and classify the extracted waves into six types.

We analyzed the relationship between the classified wave events and the observation location (magnetic local time, L value), occurrence frequency, magnetic field strength, magnetic field disturbance, low-frequency hybridization frequency (LHR), and ion energy density. In particular, by comparing the frequency distribution of waves in each cluster with the ion composition and magnetic field strength, we evaluated the physical environment in which the waves are mainly excited and propagated.

本研究では、科学衛星あらせに搭載された電場観測器(EFD)によって取得された電場スペクトル画像に対して機械学習を適用し、分類と解析を行う。最初に、2017年3月21日から2022年8月31日までに得られた1,987個のスペクトル画像に対し、低周波波動の抽出と分類を行った。その結果、比較的広帯域なスペクトル構造を示す175個の波動イベントを抽出し、各波動の継続時間、周波数帯域、中心周波数を特徴量として、k-meansクラスタリグおよび階層型クラスタリングを適用した。これにより、明確な波動構造を有さない画像を除外し、抽出した波動を6種類に分類できた。

分類された波動イベントについて、観測位置(磁気地方時、L値)、出現頻度、磁場強度、磁場擾乱、低域混成周波数 (LHR)、およびイオンエネルギー密度との関係を解析した。特に、各クラスタにおける波動の周波数分布と、イオン組成や磁場強度との関連を比較することで、波動がどのような物理環境で主に励起・伝搬するかを評価した。

科学衛星あらせによって観測された狭帯域低周波波動の解析

#三浦 雅也 $^{1)}$, 三宅 壮聡 $^{2)}$, 笠原 禎也 $^{3)}$ $^{(1)}$ 富山県大院工, $^{(2)}$ 富山県立大学, $^{(3)}$ 金沢大学

Analysis of Narrowband Low-Frequency Waveforms Observed by the Scientific Satellite ARASE

#Masaya Miura¹⁾, Taketoshi MIYAKE²⁾, Yoshiya KASAHARA³⁾

(1 Graduate School of Engineering, Toyama Prefectual University, (2 Toyama Prefectural University, (3 Kanazawa University

In this study, we classify and analyze narrowband low-frequency waves observed by the Electric Field Detector (EFD) on-board the Arase scientific satellite. We identified 280 narrowband low-frequency waves and analyzed these waves. Is suggest that frequency variations of the narrowband low-frequency waves are influenced by the surrounding plasma environment. Next, we extended the observation period to March 21, 2017 - August 31, 2022, and applied machine learning at an hourly resolution with improved classification methods. We identified 3,876 narrowband low-frequency waves, and classified these waves into 10 distinct categories. We analyzed observation locations, magnetic field strength, and magnetic disturbances, and found that these narrowband low-frequency waves are frequently observed on the nightside of the Earth with strong magnetic field during geomagnetically quiet periods. We are going to analyze the relation these waves with ion cyclotron frequency, lower hybrid frequency and ion energy characteristics, and identify the conditions for generating narrowband low-frequency waves.

本研究では、科学衛星あらせに搭載された電場観測器 (EFD) によって観測された狭帯域なスペクトルを持つ低周波波動の分類および解析を行う。最初に R-CNN 法を用いて 2017 年 3 月 23 日~2019 年 11 月 22 日の期間において 24 時間ごとの EFD の観測データから狭帯域なスペクトルを持つ低周波波動を検出し、発生時間と周波数帯、中心周波数を取得した。取得したデータに k-means 法、取得した数値データに階層型クラスタリングを用いて 5 種類に分類した。分類した狭帯域低周波波動 280 個に対して解析を行ったところ狭帯域低周波波動の周波数変化が周囲のプラズマ環境から影響を受けていることが確認できた。しかし、狭帯域低周波波動のデータ数が少なかったため波動の種類を特定する特徴を見つけられなかった。そこで解析期間を 2017 年 3 月 21 日~2022 年 8 月 31 日までと拡大し、分類手法を改良して 1 時間単位で機械学習を適用した結果、3876 個の狭帯域低周波波動を検出した。検出した狭帯域低周波波動を R-CNN 法を用いて取得した数値データをもとに階層型クラスタリングで分類を行った結果、10 種類の特徴を持つ狭帯域低周波波動に分類することができた。これらのデータに対して波動の観測位置、磁場強度、磁場擾乱を調査した結果、狭帯域な特徴を持つ低周波波動は太陽と反対側で多く観測されていた。また、狭帯域な特徴を持つ低周波波動は磁場強度が高く、静穏な時に多く観測されることが分かった。今後さらに、波動の周波数とイオンサイクロトロン周波数や低域混成周波数などの特徴的な周波数との比較、イオンエネルギーとの相関について調査などを行い、狭帯域亭主は波動の発生条件を特定したい。

#Drastichova Kristyna¹⁾, Nemec Frantisek¹⁾, Shiokawa Kazuo²⁾, Martinez-Calderon Claudia²⁾, Manninen Jyrki³⁾, Raita Tero³⁾

⁽¹Faculty of Mathematics and Physics, Charles University, Prague, Czech Republic, ⁽²Institute for Space-Earth Environmental Research, Nagoya University, Nagoya, Japan, ⁽³Sodankylä Geophysical Observatory, Sodankylä, Finland

Power Line Harmonic Radiation Observed by the PWING Network

#Kristyna Drastichova¹⁾, Frantisek Nemec¹⁾, Kazuo Shiokawa²⁾, Claudia Martinez-Calderon²⁾, Jyrki Manninen³⁾, Tero Raita³⁾

⁽¹Faculty of Mathematics and Physics, Charles University, Prague, Czech Republic, ⁽²Faculty of Mathematics and Physics, Charles University, Prague, Czech Republic, ⁽³Faculty of Mathematics and Physics, Charles University, Prague, Czech Republic

We study Power Line Harmonic Radiation (PLHR), electromagnetic emissions from ground-based power systems. In particular, we focus on how geomagnetically induced currents (GICs), driven by rapid magnetic field variations during space weather events, influence the generation and intensity of PLHR. We show that during geomagnetically disturbed periods, when GIC levels increase significantly, PLHR intensities are enhanced, most notably at even harmonics. To quantify this effect, we use high-resolution wave data from the ground-based PWING stations, combined with local magnetometer measurements to characterize GIC strength and global geomagnetic indices for comparison. The results reveal how PLHR changes with geomagnetic conditions and what factors determine its intensity. PLHR properties are examined across different locations and local times; in addition, with propagation direction analysis applied to selected cases to assess source characteristics.

#河野 英昭 $^{1)}$, 行松 彰 $^{2)}$, 西谷 望 $^{3)}$, 田中 良昌 $^{4)}$, 堀 智昭 $^{5)}$ $^{(1}$ 九州大学, $^{(2)}$ 国立極地研究所、総合研究大学院大学, $^{(3)}$ 名古屋大学, $^{(4)}$ 国立極地研究所, $^{(5)}$ 名古屋大学・宇宙地球環境研究所

Two-dimensional distribution of the plasma density obtained by applying the DTFT to the FLR data from SuperDARN radars

#Hideaki KAWANO¹⁾, Akira Sessai YUKIMATU²⁾, Nozomu NISHITANI³⁾, Yoshimasa TANAKA⁴⁾, Tomoaki HORI⁵⁾
⁽¹Kyushu University, ⁽²National Institute of Polar Research, SOKENDAI, ⁽³Nagoya University, ⁽⁴National Institute of Polar Research, ⁽⁵Institute for Space-Earth Environmental Research, Nagoya University

Some of the fluctuations in the solar wind, including those causing sudden impulses (SI), propagate into the magnetosphere and excite eigen-oscillations of the magnetic field lines and the frozen-in plasma via the mechanism called field-line resonance (FLR). It is known that the gradient methods enable us to effectively extract FLR signals from observed data. From the identified FLR frequency, one can estimate the mass density of plasma along the magnetic field line because, in a simplified expression, 'heavier' field line oscillates more slowly.

We have been applying the gradient methods to the VLOS (Velocity along the Line of Sight) data of the SuperDARN radars. The radars emit azimuthally-collimated beams of radio waves in the HF range, and some of them are backscattered by the ionosphere, while some others are backscattered by the ground and sea surface. From the Doppler shift of backscattered signals, one can calculate VLOS.

Ionosphere-backscattered signals yield VLOS of the horizontally-moving ionospheric plasma (at mid- to low latitudes, VLOS also has a vertical component because the ambient magnetic field is tilted), while ground/sea-backscattered signals yield VLOS corresponding to the vertical motion of the ionospheric plasma because the length of the ray path of a beam can only be changed by the vertical motion of the ionosphere.

We have so far applied the gradient methods to VLOS for a few events after SI's, and identified an FLR event in which ionosphere-backscattered signals and sea surface-backscattered signals were simultaneously observed. The mass density was thereby estimated using both scatters. As a result, the latter was significantly smaller than the former in the nearby place. This significant difference could come from a fairly large frequency spacing of the FFT analysis due to the fairly small duration (30 min) of the event.

Thus, we have developed codes to apply the Discrete-Time Fourier Transform (DTFT) method to timeseries data in general. This method is designed to be applied to timeseries data with a constant sampling time. An advantage of this method is that it can calculate the Fourier Transform (FT) at any frequency (below the Nyquist frequency).

We have developed the DTFT codes and as a result of applying them to the above-stated ionosphere-backscattered signals and the sea surface-backscattered signals simultaneously observed at the radar, we judge that the DTFT generally provides smaller density differences between ionosphere-backscattered signals and sea surface-backscattered signals than the FFT. Based on this judgment, we will apply the DTFT to sea surface-backscattered signals simultaneously observed by a SuperDARN radar for different events, and obtain the two-dimensional (2D) distribution of the magnetospheric plasma density within its field of view. After that, we will combine densities obtained by a few radars simultaneously observing the same event, and obtain the larger-scale 2D density distribution. We will present the results with details at the meeting.

SuperDARN・地上磁力計・あらせ衛星による 1/4 波長磁力線共鳴振動の共役観測

#尾花 由紀 $^{1)}$, 西谷 望 $^{2)}$, 細川 敬祐 $^{3)}$, 堀 智昭 $^{4)}$, 寺本 万里子 $^{5)}$, 新堀 淳樹 $^{2)}$, 行松 彰 $^{6)}$, Waters Colin L. $^{7)}$, Sciffer Murray D. $^{7)}$, Lysak Robert L. $^{8)}$, Ponomarenko Pavlo V. $^{9)}$, Hussey Glenn $^{9)}$, 三好 由純 $^{2)}$, 松岡 彩子 $^{10)}$, 熊本 篤志 $^{11)}$, 土屋 史紀 $^{11)}$, 松田 昇也 $^{12)}$, 笠原 禎也 $^{12)}$, 篠原 育 $^{13)}$

 $^{(1)}$ 九大国際宇宙, $^{(2)}$ 名古屋大学, $^{(3)}$ 電気通信大学, $^{(4)}$ 名古屋大学・宇宙地球環境研究所, $^{(5)}$ 九州工業大学, $^{(6)}$ 情報・システム研究機構 国立極地研究所, $^{(7)}$ The University of Newcastle, $^{(8)}$ University of Minnesota, $^{(9)}$ University of Saskatchewan, $^{(10)}$ 京都大学, $^{(11)}$ 東北大学, $^{(12)}$ 金沢大学, $^{(13)}$ 宇宙航空研究開発機構 宇宙科学研究所

Quarter-Wave Resonances: Coordinated Observations by SuperDARN, Magnetometers, and Arase

#Yuki Obana¹⁾, Nozomu NISHITANI²⁾, Keisuke HOSOKAWA³⁾, Tomoaki HORI⁴⁾, Mariko TERAMOTO⁵⁾, Atsuki SHINBORI²⁾, Akira Sessai YUKIMATU⁶⁾, Colin L. Waters⁷⁾, Murray D. Sciffer⁷⁾, Robert L. Lysak⁸⁾, Pavlo V. Ponomarenko⁹⁾, Glenn Hussey⁹⁾, Yoshizumi MIYOSHI²⁾, Ayako MATSUOKA¹⁰⁾, Atsushi KUMAMOTO¹¹⁾, Fuminori TSUCHIYA¹¹⁾, Shoya MATSUDA¹²⁾, Yoshiya KASAHARA¹²⁾, Iku SHINOHARA¹³⁾

⁽¹International Research Center for Space and Planetary Environmental Science, Kyushu University, ⁽²Nagoya Unibersity, ⁽³The university of Electro-Communications, ⁽⁴Nagoya Unibersity, ⁽⁵Kyushu Institute of Technology, ⁽⁶National Institute of Polar Research, ⁽⁷The University of Newcastle, ⁽⁸University of Minnesota, ⁽⁹University of Saskatchewan, ⁽¹⁰Kyoto University, ⁽¹¹Tohoku University, ⁽¹²Kanazawa University, ⁽¹³Institute of Space and Astronautical Science

Between 00:00 and 02:00 UT on 23 November 2022, during exceptionally quiet geomagnetic conditions, a clear ultra-low frequency (ULF) wave in the Pc5 band (~2.4 mHz) was observed in the duskside subauroral region by two Canadian SuperDARN radars. The wave showed a periodic Doppler velocity signature resembling a "caterpillar" with northeastward (anti-sunward) propagation and an azimuthal wave number of ~12. Ground magnetometer data revealed latitude variations in amplitude and phase consistent with field line resonance (FLR), peaking near 66° magnetic latitude.

The Arase satellite, whose ionospheric footprint crossed the caterpillar wave region, detected toroidal oscillations in both electric and magnetic fields at magnetically conjugate locations in the inner magnetosphere. These oscillations showed strong coherence with ground observations. Importantly, the electric field led the magnetic field by ~45° in phase. This phase relationship suggests the wave included both a standing mode and a propagating component that carried energy toward the northern ionosphere.

Electron densities of ~21-25 cm^-3 at the satellite location were inferred from the upper hybrid resonance (UHR) frequency obtained by PWE/HFA. From this density, the resonance frequency of a fundamental half-wave mode was estimated to be ~3.9 mHz, higher than the observed frequency (~2.4 mHz). This difference suggests the observed wave may instead be a quarter-wave mode, which typically occurs at 1.5-1.7 times lower frequency than the half-wave.

Numerical simulations using a 2.5-dimensional dipole magnetosphere model also reproduce quarter-wave characteristics. Previous studies have shown that quarter waves are favored during quiet geomagnetic conditions and when ionospheric Pedersen conductance differs by a factor of five or more between hemispheres. Both conditions were satisfied in this event, supporting the quarter-wave interpretation.

R006-P24

ポスター1:11/25 AM1/AM2 (9:15-12:35)

#Kim Hyangpyo $^{1)}$, 塩川 和夫 $^{2)}$ $^{(1}$ IWF, $^{(2)}$ 名大宇地研

Recurrent Tailward Propagation of Auroral Arcs Driven by Kelvin-Helmholtz Instabilities

#Hyangpyo Kim¹⁾, Kazuo Shiokawa²⁾

⁽¹Space Research Institute, Austrian Academy of Sciences, ⁽²Institute for Space-Earth Environmental Research, Nagoya University

We report recurrent tailward-propagating auroral arcs associated with Kelvin-Helmholtz (KH) instabilities on January 2, 2011. During northward IMF, THEMIS satellites detected KH waves at the dawnside magnetopause boundary layer, downstream of the quasi-perpendicular shock. During the KH period, ground-based all-sky imager observations at Resolute Bay revealed auroral arcs detached from the poleward boundary of the auroral oval and propagating tailward. Concurrent DMSP satellite measurements identified multiple arcs on the dawnside and detected upward field-aligned currents with electron-only precipitation over the arcs, suggesting a solar wind origin. These combined observations demonstrate that KH instabilities play a key role in energy transfer between the solar wind, magnetosphere, and ionosphere.

#山川 智嗣 $^{1)}$, 高橋 主衛 $^{2)}$, 関 華奈子 $^{3)}$, 三好 由純 $^{4)}$, 山本 和弘 $^{5)}$, GKIOULIDOU Matina $^{2)}$, 松岡 彩子 $^{6)}$, 寺本 万里子 $^{7)}$, 浅村 和史 $^{8)}$, 土屋 史紀 $^{9)}$, 熊本 篤志 $^{9)}$, 笠原 禎也 $^{10)}$, 新堀 淳樹 $^{4)}$, 篠原 育 $^{8)}$ $^{(1)}$ 名古屋大学, $^{(2)}$ ジョンズホプキンス大学応用物理研究所, $^{(3)}$ 東京大学, $^{(4)}$ 名古屋大学, $^{(5)}$ 名古屋大学宇宙地球環境研究所,

(6 京都大学、(7 九州工業大学、(8 宇宙航空研究開発機構、(9 東北大学、(10 金沢大学

Non-uniform excitation of storm-time Pc5 ULF waves in the inner magnetosphere: Van Allen Probes and Arase observations

#Tomotsugu YAMAKAWA¹⁾, Kazue TAKAHASHI²⁾, Kanako SEKI³⁾, Yoshizumi MIYOSHI⁴⁾, Kazuhiro YAMAMOTO⁵⁾, Matina GKIOULIDOU²⁾, Ayako MATSUOKA⁶⁾, Mariko TERAMOTO⁷⁾, Kazushi ASAMURA⁸⁾, Fuminori TSUCHIYA⁹⁾, Atsushi KUMAMOTO⁹⁾, Yoshiya KASAHARA¹⁰⁾, Atsuki SHINBORI⁴⁾, Iku SHINOHARA⁸⁾

⁽¹ISEE, Nagoya University, ⁽²Johns Hopkins University Applied Physics Laboratory, ⁽³The University of Tokyo, ⁽⁴Nagoya University, ⁽⁵ISEE, Nagoya University, ⁽⁶Kyoto University, ⁽⁷Kyushu Institute of Technology, ⁽⁸ISAS, JAXA, ⁽⁹Tohoku University, ⁽¹⁰Kanazawa University)</sup>

Storm-time Pc5 ULF waves can be generated by the wave-particle interaction with ring current ions in the inner magnetosphere. Since Pc5 waves can drive the radial diffusion of radiation belt electrons, understanding the excitation of Pc5 waves is a key issues in the study of the inner magnetosphere. Southwood [1976] proposed that the drift-bounce resonance was a candidate excitation mechanism of ULF waves. However, where and how storm-time Pc5 waves are generated are still open to discussion. Recently, Yamakawa et al. [2025] investigated the excitation of Pc5 waves observed by GOES satellites based on the GEMSIS magnetosphere-ionosphere coupled model and simulation results qualitatively reproduced the observed Pc5 waves. Previous simulation studies have shown that wave properties such as wave frequency and azimuthal wave number are not uniform but different at different locations [Yamakawa et al., 2019; 2020]. The purpose of this study is to investigate what causes non-uniform excitation of storm-time Pc5 waves in the inner magnetosphere based on multi-spacecraft observations.

This study focuses on the magnetic storm on 27 February 2018. To investigate ULF waves excited by ring current ions, magnetic field and proton flux data of RBSP-A (EMFISIS and RBSPICE) and ERG (MGF and LEPi) were used. During the early recovery phase of the storm, poloidal Pc5 waves (2-4 mHz) were observed outside the plasmasphere simultaneously by RBSP-A and ERG. Results suggest that wave frequency is similar between the two spacecrafts. However, using the ion sounding technic, we find that the azimuthal wave numbers are different: -60 for ERG and -20 for RBSP-A (both westward propagation). The drift resonance condition is well satisfied for both spacecrafts and resonance energy is estimated to be 10-25 keV/q for ERG and 70-100 keV/q for RBSP-A. We consider that the difference of the azimuthal wave number is caused by the difference of resonance energy. We will also report on the instability condition of the excited ULF waves and future plans about the simulation of ULF waves during this storm.

あらせ衛星による中緯度磁気圏における kinetic Alfvén wave の観測研究

#齋藤 幸碩 $^{1)}$, Artemyev Anton $V^{(2)}$, 加藤 雄人 $^{(1)}$, 笠羽 康正 $^{(3)}$, 熊本 篤志 $^{(1)}$, 笠原 禎也 $^{(4)}$, 堀 智昭 $^{(5)}$, 松岡 彩子 $^{(6)}$, 寺本 万里子 $^{(7)}$, 山本 和弘 $^{(5)}$, 浅村 和史 $^{(8)}$, Wang Shiang-Yu $^{(9)}$, 風間 洋一 $^{(9)}$, Tam Sunny Wing-Yee $^{(10)}$, Jun Chae-Woo $^{(5)}$, 篠原 育 $^{(8)}$, 三好 由純 $^{(5)}$

⁽¹ 東北大学大学院理学研究科地球物理学専攻,⁽²Department of Earth, Planetary, and Space Sciences, University of California, Los Angeles,⁽³ 東北大学大学院理学研究科惑星プラズマ・大気研究センター,⁽⁴ 金沢大学学術メディア創成センター,⁽⁵ 名古屋大学宇宙地球環境研究所,⁽⁶ 京都大学大学院理学研究科附属地磁気世界資料解析センター,⁽⁷ 九州工業大学大学院工学研究院宇宙システム工学研究系,⁽⁸ 国立研究開発法人宇宙航空研究開発機構宇宙科学研究所,⁽⁹ 中央研究院天文及天文物理研究所,⁽¹⁰Institute of Space and Plasma Sciences, National Cheng Kung University

Observational study of kinetic Alfvén waves in the mid-latitude magnetosphere using the Arase satellite

#Koseki Saito¹⁾, Anton V. Artemyev²⁾, Yuto Katoh¹⁾, Yasumasa Kasaba³⁾, Atsushi Kumamoto¹⁾, Yoshiya Kasahara⁴⁾, Tomoaki Hori⁵⁾, Ayako Matsuoka⁶⁾, Mariko Teramoto⁷⁾, Kazuhiro Yamamoto⁵⁾, Kazushi Asamura⁸⁾, Shiang-Yu Wang⁹⁾, Yoichi Kazama⁹⁾, Sunny Wing-Yee Tam¹⁰⁾, Chae-Woo Jun⁵⁾, Iku Shinohara⁸⁾, Yoshizumi Miyoshi⁵⁾

⁽¹Department of Geophysics, Graduate School of Science, Tohoku University, ⁽²Department of Earth, Planetary, and Space Sciences, University of California, Los Angeles, ⁽³Planetary Plasma and Atmospheric Research Center, Graduate School of Science, Tohoku University, ⁽⁴Emerging Media Initiative, Kanazawa University, ⁽⁵Institute for Space – Earth Environmental Research, Nagoya University, ⁽⁶Data Analysis Center for Geomagnetism and Space Magnetism, Grad. Sch. Sci., Kyoto University, ⁽⁷Department of Space Systems Engineering, Faculty of Engineering, Kyushu Institute of Technology, ⁽⁸Institute of Space and Astronautical Science, Japan Aerospace Exploration Agency, ⁽⁹Institute of Astronomy and Astrophysics, Academia Sinica, ⁽¹⁰Institute of Space and Plasma Sciences, National Cheng Kung University

Kinetic Alfvén waves (KAWs) are electromagnetic waves with a perpendicular wavelength on the ion Larmor radius (ρ_i) scale. KAWs have a parallel electric field component (δ_{ij}), accelerating ions and electrons along a magnetic field line from several hundred eV to a few keV [e.g., Hasegawa, 1976]. KAWs are observed in various regions, such as the solar wind [e.g., Bale et al., 2005], the dayside magnetosphere [e.g., Gershman et al., 2017], the inner magnetosphere [e.g., Maynard et al., 1996], the nightside magnetotail [e.g., Chaston et al., 2012], and the plasma sheet boundary layer (PSBL) [e.g., Wygant et al., 2002].

In particular, the Polar satellite observed KAWs in the PSBL at altitudes of 4-6 R_E and reported parallel ion and electron beams of 1-2 keV, which were considered to be generated by the KAWs [Wygant et al., 2002]. However, the Polar observations had some limitations. For instance, the magnetometer had a 4 Hz Nyquist frequency, which prevented it from detecting higher-frequency components of kinetic Alfvén waves (KAWs). Additionally, particle instruments of Polar, which measured velocity distribution functions, operated with a 13-second cycle, making it challenging to resolve variations in the distribution on shorter timescales.

To overcome these observational limitations, this study utilizes high-resolution field and particle data from the Arase (ERG) satellite. We analyze an event from 22:25 to 23:25 UT on September 1, 2022, when Arase was at a magnetic latitude of 38 $^{\circ}$. This mid-latitude region is crucial for understanding the propagation of KAWs from their equatorial source region. The plasma parameters observed during this event were number density of $^{\circ}0.1~\rm cm^{-3}$, ion temperature of a few keV, electron temperature of several hundred eV, and a magnetic field strength of $^{\circ}270~\rm nT$. The ion plasma beta in this environment is comparable to the electron-to-ion mass ratio (β $_i \gtrsim m_e/m_i$), under which condition one can expect to observe KAWs. During this event, we identified an electric field enhancement at several Hz, which was associated with an enhancement of the electron energy flux from several hundred eV to several keV. Such observations are essential for understanding particle acceleration mechanisms, like the formation of several keV high-energy beams through nonlinear Landau resonance [Saito et al., 2025] and their connection to auroral processes.

To detect KAWs, we calculated the power spectral densities of the perpendicular electric (δ \mathbf{E}_{\perp}) and magnetic (δ \mathbf{B}_{\perp}) field components using the Morlet wavelet transform. We found that their amplitude ratio, $|\delta$ $\mathbf{E}_{\perp}|/|\delta$ $\mathbf{B}_{\perp}|$, in the several-Hz range is consistent with the KAW dispersion relation, which means that the electromagnetic field fluctuation can be the KAWs. During time intervals when this dispersion relation was satisfied, we also observed that the pitch angle distributions of protons and electrons were concentrated in the parallel (0°) and anti-parallel (180°) directions, suggesting parallel acceleration by KAWs. Furthermore, this event presents a good opportunity for conjugate observations with the THEMIS-A satellite located near the magnetic equator. In this presentation, we will report the results of these analyses and discuss the propagation and particle acceleration processes of KAWs.

Kinetic Alfvén wave (KAW) は、磁力線に垂直な波長がイオンラーマー半径 (ρ_i) と同程度のスケールを持つ電磁波動である。KAW は磁力線に平行な電場成分 (δ_{ij}) を持ち、この電場がイオンや電子を磁力線に沿って数百 eV から数 keV まで加速することが知られている [e.g., Hasegawa, 1976]。KAW は、太陽風 [e.g., Bale et al., 2005]、地球磁気圏の昼側 [e.g., Gershman et al., 2017]、内部磁気圏 [e.g., Maynard et al., 1996]、夜側磁気圏尾部 [e.g., Chaston et al., 2012]、プラズマシート境界層 (PSBL)[e.g., Wygant et al., 2002] など、様々な領域で観測される。

特に、Polar 衛星は高度 4 – 6 R_E の PSBL において KAW を観測し、それによって生成されたと考えられる 1 – 2 keV の平行イオン・電子ビームを報告した [Wygant et al., 2002]。しかし、Polar 衛星の観測には、磁力計のナイキスト周波数が 4 Hz であるため KAW の高周波成分を捉え切れない点や、粒子計測器の速度分布関数が 13 秒周期の算出であるため、それより短い時間スケールの変動を追跡できない点といった限界があった。

これらの観測的限界を克服するため、本研究では磁気圏衛星「あらせ」の高時間分解能な電磁場・粒子データを用いる。解析対象は 2022 年 9 月 1 日 22:25 – 23:25UT のイベントであり、この時あらせ衛星は磁気緯度 38 度に位置していた。このような中緯度帯は、磁気赤道付近で発生する KAW の伝播過程を理解する上で極めて重要である。観測時のプラズマは、数密度が $0.1~{\rm cm}^{-3}$ 程度、イオン温度が数 keV、電子温度が数百 eV、磁束密度が 270 nT 程度であった。この環境では、イオンプラズマベータ値が電子とイオンの質量比と同程度であり ($\beta_i \gtrsim m_e/m_i$)、KAW が観測され得る。本イベントでは、数 Hz の電場の増強と、それに関連した数百 eV から数 keV の電子エネルギーフラックスの増強が確認された。このような観測は、非線形ランダウ共鳴による高エネルギービームの形成 [Saito et al., 2025] や、オーロラ現象との関連を考える上で不可欠である。

観測される低周波電磁場擾乱が KAW であることを確認するために、Morlet wavelet 変換を用いて磁力線に垂直な電場成分 (δ \mathbf{E}_{\perp}) と磁場成分 (δ \mathbf{B}_{\perp}) のパワースペクトル密度を算出し、その比 ($|\delta$ $\mathbf{E}_{\perp}|/|\delta$ $\mathbf{B}_{\perp}|$) を求めた。その結果、数Hz 帯において比が KAW の分散関係と一致し、電磁場擾乱が KAW であることを確認した。また、この分散関係が確認された時間帯には、イオンと電子のピッチ角分布が磁力線に平行 (0°) または反平行 (180°) 方向に集中する様子が確認され、KAW による平行加速が示唆された。さらに、本イベントは磁気赤道付近に位置する THEMIS-A 衛星との共役観測の好機である。本発表では、これらの解析結果を総合し、KAW の伝播と粒子加速の過程について議論する。

#渡邉 智彦 $^{1)}$, 榊 剛志 $^{1)}$, 藤田 慶二 $^{2)}$ $^{(1)}$ 名大, $^{(2)}$ 核融合研

Gyrokinetic and reduced simulations of the feedback M-I coupling in dipole configuration

#Tomohiko Watanabe¹⁾, Tsuyoshi Sakaki¹⁾, Keiji Fujita²⁾
⁽¹Nagoya University, ⁽²NIFS

Feedback instability has been investigated as one of the possible mechanisms for explaining spontaneous growth of auroral arcs in the magnetosphere-ionosphere coupling system. Our previous simulation models employing the straight field-line geometry have demonstrated that the secondary growth of the Kelvin-Helmholtz instability leads to nonlinear deformation of arc structures and triggers transition to the Alfvenic turbulence. In the gyrokinetic simulation, we could further confirm parallel acceleration of auroral electrons in the dispersive Alfvenic turbulence.

Recently, we have extended our simulation model to a dipole geometry both for the reduced MHD and gyrokinetic cases. In the former, we have found convective growth of arcs and transition to turbulence followed by the auroral spreading in the latitudinal directions. The linear and nonlinear gyrokinetic simulations in the dipole field provide the first verification of the feedback instability in a kinetic system with the mirror force effect.

Comparison of the simulation results with the Reimei observation data is also in progress, and may be discussed at the meeting.

大規模 M-I 結合シミュレーションにおける MHD 系流速ヤコビアンの固有ベクトル 抽出可視化実験

#齊藤 慎之介 $^{1)}$, 吉川 顕正 $^{2)}$, 田中 高史 $^{3)}$

 $^{(1)}$ 九州大学 大学院理学府 地球惑星科学専攻, $^{(2)}$ 九州大学 理学研究院 地球惑星科学部門, $^{(3)}$ 九州大学 国際宇宙惑星環境研究センター

The visualization experiment for extracting eigenvalue of MHD system velocity Jacobian from large-scale M-I coupling simulation

#Shinnosuke Saito¹⁾, Akimasa YOSHIKAWA²⁾, Takashi TANAKA³⁾

⁽¹Department of Earth and Planetary Sciences, Guraduate School of Science, Kyushu university, ⁽²the Department of Earth and Planetary Sciences, Faculty of Science, Kyushu University, ⁽³the International Research Center for Space and Planetary Environmental Science, Kyushu University

he Earth's magnetosphere hosts diverse phenomena driven by solar wind interactions, yet many underlying mechanisms remain unresolved. To address this, we focus on Alfvén waves, fundamental MHD modes that transport information and energy along magnetic field lines. Alfvén waves can be categorized into shear Alfvén waves, oscillating perpendicular to the field and propagating along field lines, and magnetosonic waves, spreading within the magnetic plane. In the magnetosphere, they undergo mode conversion and resonance, contributing to auroral emissions, ionospheric current variations, and other phenomena observed by ground-based and satellite instruments. Thus, visualizing and analyzing Alfvén waves is crucial for understanding magnetospheric dynamics.

We employ the REProduce Plasma Universe (REPPU) code, a magnetosphere – ionosphere (M – I) coupled simulation developed by Prof. Takashi Tanaka at Kyushu University, to visualize Alfvén waves and examine their propagation. REPPU solves the MHD equations in the magnetosphere and the Hall – Pedersen current system in the ionosphere on a unique dodecahedral triangular mesh. The MHD calculations use a finite-volume scheme with TVD interpolation and Roe's method. A key point is that Roe's method inherently performs eigen-decomposition of the flux Jacobian, where the eigenvectors correspond to Alfvén wave modes. In this study, we extract these eigenvectors directly from the REPPU code and visualize them, enabling a direct analysis of Alfvén wave dynamics.

In this presentation, we validate the new visualization approach and demonstrate Alfvén wave propagation under southward IMF conditions as well as their response to high dynamic pressure IMF. These results provide new insights into energy transport and disturbance propagation in the magnetosphere, offering a pathway toward clarifying the generation mechanisms of geomagnetic activity mediated by Alfvén waves.

地球磁気圏では太陽風との相互作用により多様な現象が発生しているが、その詳細なメカニズムはいまだ未解明な点が多い。本研究は、これらの理解を深める手がかりとして Alfvén 波に注目する。Alfvén 波とは、磁場とプラズマの相互作用により生じる電磁流体波であり、磁場に沿って情報やエネルギーを伝搬する基本的な波動モードである。磁気圏においては、擾乱が生じた際にその情報が Alfvén 波として伝わり、磁力線に沿ったエネルギー輸送や他の波動モードとの相互作用を通じて多様な現象を引き起こす。特に Alfvén 波は、磁場に垂直方向に振動し磁力線に沿って伝搬する Shear Alfvén 波と、磁場面に広がる縦波の磁気音波(magnetosonic wave)に分けて理解される。地球磁気圏で発生した Alfvén 波は、モード変換や共鳴を通じてオーロラ発光や電離圏電流系の変動などを誘発している。したがって Alfvén 波の可視化と解析は、磁気圏での現象理解の鍵を握っている。

本研究では、M-I 結合系シミュレーションである REProduce Plasma Universe(REPPU)コードを用いて Alfvén 波の可視化を行い、その伝搬過程を解析することで磁気圏現象の発生メカニズム解明を目指す。REPPU コードは九州大学名誉教授の田中高史によって開発され、地磁気変動やオーロラ活動の詳細な再現に特化したモデルである。その特徴として、磁気圏領域では MHD 方程式を、電離圏領域では Hall・Pedersen 電流系を解き、さらに空間格子には 12 面体分割三角格子を採用している。MHD 計算は有限体積法に基づき、TVD 補間と Roe 法を用いたフラックス計算により行われる。特に Roe 法においては、保存方程式系を変数ベクトルと流速フラックスで記述し、そのフラックスを固有値分解することで得られる固有ベクトルが Alfvén 波モードに対応する。本研究では、この固有ベクトルをコード内部から抽出し、Alfvén 波を直接的に可視化することを試みた。

本発表では、まずこの手法によって得られた Alfvén 波の可視化結果の妥当性を検証する。さらに、南向き IMF 条件下での Alfvén 波の伝搬の様子、そして動圧の高い IMF 条件下における波動挙動についても紹介し、磁気圏現象の理解に向けた展望を示す。

夕方側における Pi2 地磁気脈動の空間分布特性の解析

#東根 侑加 $^{3)}$, 吉川 顕正 $^{1,2)}$, 魚住 禎司 $^{2)}$

 $^{(1)}$ 九州大学 大学院理学研究院 地球惑星科学部門, $^{(2)}$ 九州大学 国際宇宙天気科学・教育センター, $^{(3)}$ 九州大学理学部地球惑星科学科

Analysis of the Spatial Distribution Characteristics of Pi2 Geomagnetic Pulsations on the Dusk Side

#Yuka HIGASHINE³⁾, Akimasa YOSHIKAWA^{1,2)}, Teiji UOZUMI²⁾

⁽¹Department of Earth and Planetary Sciences, Faculty of Science, Kyushu University, ⁽²International Research Center for Space and Planetary Environmental Science, Kyushu University, ⁽³Department of Earth and Planetary Sciences, School of Science, Kyushu University

Pi2 geomagnetic pulsations are transient oscillations with periods of 40 - 150 seconds, observed globally at substorm onset, and mainly generated in the nightside magnetosphere. Investigating their spatial distribution and propagation characteristics is essential for understanding the magnetosphere – ionosphere (M – I) coupling system. The goal of this study is to clarify the global M – I coupling system at substorm onset by characterizing the spatiotemporal properties of Pi2.

In our previous studies, we analyzed data from the MAGDAS/CPMN network along the 210° meridian chain and the North – South America chain. These studies suggested that nightside Pi2 are associated with the Biot – Savart component of fast-mode waves and SCW oscillations, dayside Pi2 are related to ionospheric currents, and morning-side Pi2 are associated with the day – night boundary current. However, the generation mechanism and propagation process of dusk-side Pi2 remain poorly understood.

In this study, isolated substorm events occurring within three hours around the local E-layer sunset were selected from the 2011 MAGDAS/CPMN magnetometer dataset, and the spatial distribution of dusk-side Pi2 was analyzed. As a result, 40 events were identified, showing the following three characteristic features:

- (1) In the H component, the phase is delayed toward higher latitudes in the Southern Hemisphere, while in the D component, the phase reverses across the DAW region.
 - (2) At ZGN, the H component alone shows an earlier phase.
 - (3) A phase reversal is observed only at two high-latitude stations in the Northern Hemisphere.

This presentation describes the detailed analysis and discusses the propagation processes inferred from these characteristics.

Pi2 地磁気脈動は、主に夜側磁気圏に起源を持ち、サブストーム初動時に全球的に観測される周期 $40\sim150$ 秒の突発的な振動である。その空間分布や伝搬特性を明らかにすることは、磁気圏-電離圏結合系の理解において重要である。本研究の最終的な目的は、Pi2 の時空間特性を解明することで、サブストーム初動時における M-I 全球結合系の全体像を描き出すことである。

これまでの我々の研究では、MAGDAS/CPMN 磁場観測ネットワークの 210 度帯及び南北アメリカ帯で観測されたデータを用いて解析をしており、夜側 Pi2 は fast wave あるいは SCW 振動のビオ・サバール成分、昼側 Pi2 は電離圏電流、朝側 Pi2 は昼夜境界電流に起因することが示唆されていた。一方で、夕方側で観測される Pi2 の成因や伝搬過程については十分に理解されていない。

そこで本研究では MAGDAS/CPMN 磁場観測ネットワークの 2011 年のデータから E 層日没前後 3 時間に孤立型サブストームが発生しているデータを選定して、夕方側 Pi2 の空間的分布を解析した。その結果、40 イベントが選定され、以下の 3 つの特徴的な挙動が確認された。

- (1)H 成分で南半球の高緯度にかけて位相が遅れており、D 成分で DAW 付近を境に南北で位相が反転している。
- (2) H 成分で ZGN のみ位相が速い
- (3) 北半球高緯度 2 観測点のみで位相が反転している

本発表では、これらの解析結果の詳細と、それぞれの特徴から推定される伝搬過程についての考察を述べる。

あらせ衛星の観測による磁気嵐時における各種イオンの流出比の推定

#海江田 彪太 $^{1)}$, 横田 勝一郎 $^{1)}$, 寺田 健太郎 $^{1)}$, 笠原 慧 $^{2)}$, 桂華 邦裕 $^{2)}$, 堀 智昭 $^{3)}$, 三好 由純 $^{3)}$, 篠原 育 $^{4)}$ $^{(1)}$ 大阪大学, $^{(2)}$ 東京大学, $^{(3)}$ 名古屋大学・宇宙地球環境研究所, $^{(4)}$ 宇宙航空研究開発機構

Estimation of outflow ratios of various ions during magnetic storms based on Arase satellite observations

#Hyota KAIEDA¹), Shoichiro YOKOTA¹), Kentaro TERADA¹), Satoshi KASAHARA²), Kunihiro KEIKA²), Tomoaki HORI³), Yoshizumi MIYOSHI³), Iku SHINOHARA⁴)

(1The University of Osaka, (2University of Tokyo, (3ISEE, Nagoya University, (4ISAS/JAXA

Various studies have been conducted to elucidate the escape mechanism of the Earth's atmospheric ions. Heavy ions in the magnetosphere, such as O^+ , N^+ , and molecular ions (N_2^+, NO^+, O_2^+) , originate only from the ionosphere; therefore, observations of these ions may provide valuable information about atmospheric escape. Since the ionospheric N^+/O^+ ratio varies with altitude and latitude, simultaneous observations of N^+ and O^+ can yield information about the altitude and latitude dependence of their outflow processes. Therefore, it is important to observe N^+ and O^+ simultaneously. Because N^+ has a mass-to-charge ratio close to that of O^+ , it is thought that both ions follow almost the same outflow paths. However, the similarity of their mass-to-charge ratios makes it difficult to distinguish N^+ from O^+ in particle measurements made in space. Consequently, there are few studies that distinguish between O^+ and N^+ .

To estimate the outflow ratios of various ions from the Time-of-Flight (TOF) measurements of the Medium-energy particle experiments Ion Mass Spectrometer(MEP-i) onboard the Arase satellite, we utilized the simulation software "The Stopping and Range of Ions in Matter (SRIM)". By fitting the simulated TOF distributions to observational data, we were able to distinguish N^+ from O^+ . Using this method, we investigate the relative abundance of N^+ and O^+ outflows during magnetic storms and discuss their outflow processes and pathways.

地球大気イオンの流出メカニズムを解明するためにさまざまな研究が行われてきた。地球磁気圏内の O^+ 、 N^+ 、分子イオン $(N_2^+$ 、 NO^+ 、 O_2^+)などの重イオンは電離層のみから発生するため、これらのイオンを観測することで大気流出に関する情報が得られる可能性がある。電離層の N^+ / O^+ 比は高度と緯度によって変化するため、 N^+ と O^+ の観測から大気流出の高度と緯度に関する情報が得られる。そのため、 N^+ と O^+ を同時観測することは重要である。 N^+ は O^+ と 質量電荷比が近いためほとんど同じ流出経路をたどると考えられる。しかし、 N^+ と O^+ の質量電荷比が非常に近く、両者を分別するのが難しい。そのため、 O^+ と N^+ を区別している研究例は少ない。

我々は、あらせ衛星搭載の MEP-i(中間エネルギーイオン質量分析器)の TOF(Time of Flight) の観測結果から各種イオンの流出量比を推定するために、シミュレーションソフトウェア「The Stopping and Range of Ions in Matter(SRIM)」を利用した。これにより理論的に得られた TOF 分布を観測データにフィッティングすることで、観測データ中の N^+ と O^+ を分別しそれぞれの存在量を推定した。この手法を用いて、磁気嵐によって流出する N^+ と O^+ の存在比を調べ、それらの流出過程や経路について議論する。

#小池 春人 1), 山内 正敏 2), 田口 聡 1), ニルソン ハンス 2), ダンドゥラス ヤニス 3) $^{(1)}$ 京大理, $^{(2)}$ Swedish Institute of Space Physics, $^{(3)}$ Institut de Recherche en Astrophysique et Planétologie

Gradual and sudden energization of outflowing oxygen ions near the high-latitude magnetopause

#Haruto Koike¹⁾, Masatoshi Yamauchi²⁾, Satoshi Taguchi¹⁾, Hans Nilsson²⁾, Iannis Dandouras³⁾
⁽¹Graduate School of Science, Kyoto University, ⁽²Swedish Institute of Space Physics, ⁽³Institut de Recherche en Astrophysique et Planétologie

Among the oxygen ions originating from the ionospheric cusp, those with relatively higher energies can access the high-altitude cusp (above several Earth radii) and subsequently escape into the high-latitude magnetosheath along open field lines. Although escaping oxygen ions into the magnetosheath have been reported in many observations, their dynamics near the high-latitude magnetopause remain poorly understood. Using data from the Cluster Ion Spectrometry, we analyzed more than 40 events in which field-aligned beams of oxygen ions were observed near the high-latitude boundaries. In most events, the beam energy is several hundred eV in the lobe/mantle region and increases to several keV, sometimes exceeding 20 keV at the boundary. We identified two types of energy change in the energy-time spectrograms: gradual increases and sudden increases. The gradual increase may be attributed to cyclotron resonance and the centrifugal acceleration, which operate over timescales much longer than a gyroperiod, whereas the sudden increase may be caused by non-adiabatic acceleration due to sharp spatial gradients in the convection electric field, which operates on timescales comparable to a gyroperiod, possibly associated with dayside magnetopause reconnection. We present statistical results on the occurrence of these two types of energy change, and discuss their occurrence in relation to the background magnetic field structure and solar wind conditions.

#今城 峻 $^{1)}$, 三好 由純 $^{2)}$, 笠原 慧 $^{3)}$, 横田 勝一郎 $^{4)}$, 松岡 彩子 $^{5)}$, 桂華 邦裕 $^{3)}$, 堀 智昭 $^{6)}$, 篠原 育 $^{7)}$, 塩川 和夫 $^{2)}$, 山本 和 弘 $^{8)}$, 寺本 万里子 $^{9)}$

 $^{(1)}$ 京大地磁気センター, $^{(2)}$ 名古屋大学, $^{(3)}$ 東京大学, $^{(4)}$ 大阪大学大学院, $^{(5)}$ 京都大学, $^{(6)}$ 名古屋大学・宇宙地球環境研究所, $^{(7)}$ 宇宙航空研究開発機構, $^{(8)}$ 名古屋大学宇宙地球環境研究所, $^{(9)}$ 九州工業大学

First evidence of field line curvature scattering effect on heavy ion species: property of isotropic distribution boundaries

#Shun IMAJO¹⁾, Yoshizumi MIYOSHI²⁾, Satoshi KASAHARA³⁾, Shoichiro YOKOTA⁴⁾, Ayako MATSUOKA⁵⁾, Kunihiro KEIKA³⁾, Tomoaki HORI⁶⁾, Iku SHINOHARA⁷⁾, Kazuo SHIOKAWA²⁾, Kazuhiro YAMAMOTO⁸⁾, Mariko TERAMOTO⁹⁾

⁽¹Kyoto University, ⁽²Nagoya University, ⁽³University of Tokyo, ⁽⁴Osaka University, ⁽⁵Kyoto University, ⁽⁶Nagoya University, ⁽⁷JAXA, ⁽⁸Nagoya University, ⁽⁹Kyushu Institute of Technology

This study provides the first observational evidence of the field line curvature (FLC) scattering effect on heavy ion species (He+, He++, and O+) in the inner magnetosphere. FLC scattering theory predicts that, for a given energy per charge, ions with a higher mass-per-charge ratio have larger gyroradii and will thus become isotropic on more dipolar magnetic field lines closer to Earth. To verify this prediction, we used Arase satellite data to determine the L-shell of the isotropic distribution boundary (IDB) for each ion species and compared their locations relative to the proton IDB. We found that the observed order of the IDBs (O+, He+, He++, H+ from lowest to highest L-shell) was consistent with FLC scattering predictions, particularly under specific conditions: high proton IDB L-shells (L >7), higher energies (80 – 180 keV/q), and in the postmidnight sector. However, the order deviates from theory at lower L-shells, lower energies, and premidnight, suggesting that other isotropization processes may become dominant in these conditions. These results indicate that FLC scattering is an important mechanism for the loss of energetic heavy ions from the outer ring current region via isotropization and subsequent precipitation into the atmosphere.

ダブルプローブ法で観測されたスプリアス電場の推定: あらせと GEOTAIL の比較

#中川 朋子 $^{1)}$, 今野 翼 $^{1)}$, 堀 智昭 $^{2)}$, 笠羽 康正 $^{3)}$, 松田 昇也 $^{4)}$, 笠原 禎也 $^{4)}$, 土屋 史紀 $^{3)}$, 熊本 篤志 $^{3)}$, 新堀 淳樹 $^{2)}$, 松岡 彩子 $^{5)}$, 篠原 育 $^{6)}$, 齋藤 義文 $^{6)}$, 三好 由純 $^{2)}$

(1 東北工大, (2 名古屋大学・宇宙地球環境研究所, (3 東北大学, (4 金沢大学, (5 京都大学, (6 宇宙航空研究開発機構

Estimation of spurious sunward electric field observed by double probes onboard Arase and Geotail

#Tomoko Nakagawa¹⁾, Tsubasa Konno¹⁾, Tomoaki HORI²⁾, Yasumasa KASABA³⁾, Shoya MATSUDA⁴⁾, Yoshiya KASAHARA⁴⁾, Fuminori TSUCHIYA³⁾, Atsushi KUMAMOTO³⁾, Atsuki SHINBORI²⁾, Ayako MATSUOKA⁵⁾, Iku SHINOHARA⁶⁾, Yoshifumi SAITO⁶⁾, Yoshizumi MIYOSHI²⁾

⁽¹Tohoku Institute of Technology, ⁽²ISEE, Nagoya University, ⁽³Tohoku University, ⁽⁴Kanazawa University, ⁽⁵Kyoto University, ⁽⁶JAXA/ISAS

In a tenuous plasma, electric field observations using the double probe technique suffer from spurious sunward electric field arising from photo-electron emissions from spacecraft. An attempt was made to estimate the spurious electric field component assuming that 1) an observed electric field is a sum of natural and spurious fields, 2) the natural electric field is perpendicular to the background magnetic field, and 3) the spurious electric field points the sun. A sunward component of the spurious electric field in the spin plane can be calculated for selected cases in which the background magnetic field is parallel to the spin plane. The spurious electric field components estimated from Arase PWE/EFD data exhibited a relationship with ambient electron density obtained by Arase PWE/HFA.

The spurious electric field arising from the asymmetric photoemission should be more pronounced for spacecraft such as GEOTAIL or Mio, whose spin axes are nearly perpendicular to the sun-spacecraft direction. Estimation of the spurious electric field in the GEOTAIL electric field observation was carried out by using EFD and MGF data from January 1, 1994 to February 28, 1994 in ISAS/ Data Archives and Transmission System (DARTS). The result was investigated with the spacecraft potential observed by EFD and the plasma density observed by LEP also opened in DARTS. Differently from Arase cases, the spurious electric field of GEOTAIL observation decreased in low density plasma (less than 10 cm⁻³) due to high spacecraft potential.

磁気圏電場の観測は、太陽風に対する磁気圏のダイナミックな反応を知るうえで重要である。人工衛星からの電場観測に最もよく使われるのは2つのプローブ間の電位差を距離で割って電場を求めるダブルプローブ法であるが、これにより検出される電場には、衛星からの光電子放出に由来する擬似的な太陽向き成分が含まれてしまうことが多い。この影響を除いた解析を行うため、擬似電場の推定が必要である。

これまで、あらせ衛星搭載の PWE/EFD による電場観測を用いて、次のような方法で光電子由来の擬似電場の推定を行ってきた。観測された電場を自然電場と擬似電場の和と考え、自然電場は外部磁場に直交し、擬似電場は太陽方向を向くと仮定すると、観測電場と外部磁場の内積は擬似電場によるものと考えることができる。電場は衛星のスピン面内 2成分のみ観測されているが、外部磁場がスピン面に平行な場合を選べば擬似電場のスピン面内太陽方向の成分を算出することができる。こうして得られた擬似電場成分は-5~15mV/m の大きさで、衛星電位 0-5V の範囲では衛星電位につれて疑似電場も大きくなる傾向があった。電子密度 100cm⁻³以上では擬似電場は消え、それ以下では擬似電場と電子密度の対数との間に線形の関係が見られることがあった。この関係から、電子密度を介して擬似電場を推定できる可能性が示された。

あらせ衛星のスピン軸は太陽方向から 15 度程度であったのに対し、GEOAIL 衛星のスピン軸は太陽方向に対し垂直に近いため、擬似電場の影響がより大きいと考えられる。そこで、今般、GEOTAIL 衛星の電場観測について、同様の擬似電場推定を行った。使用したのは Data Archives and Transmission System (DARTS) で公開されている 1994 年 1-2 月の電場 (EFD)、磁場 (MGF) である。その結果を低エネルギー粒子 LEP によるプラズマ(イオン)密度と合わせて解析した。擬似電場の強さはおおむね 0-10mV/m であったが、あらせ衛星とは異なり、プラズマ密度 10 cm<sup>-3</br>
《以下では擬似電場が減少していくことが分かった。これは低密度のために衛星電位が数十 V に上昇し、衛星電位から逃走できる光電子が極めて少なくなり、日照側プローブへの光電子の影響が小さくなったためと考えられる。擬似電場成分があらせ衛星の推定より小さいのはアンテナ長(50m)があらせの場合 (15m) より大きいためと考えられる。

機械学習モデルを用いた内部磁気圏における UHR 周波数推定の精度向上

#佐渡 匠 $^{1)}$, 松田 昇也 $^{1)}$, 笠原 禎也 $^{1)}$

A Machine Learning Approach for Improving UHR Frequency Determination in the Inner Magnetosphere

#Takumi Sado¹⁾, Shoya Matsuda¹⁾, Yoshiya Kasahara¹⁾
⁽¹Kanazawa University

Electron density is one of the important properties of space plasma, especially for understanding the wave-particle interactions in the inner magnetosphere. The upper hybrid resonance (UHR) frequency is commonly used as a proxy of the local electron number density, since the UHR frequency is a function of electron number density and local electron cyclotron frequency. In order to determine the UHR frequencies from electric field spectra, several semi-automatic identification techniques have been developed. For example, Kumamoto et al. (2018) proposed a hybrid approach by combining an algorithm and visual inspection to determine the UHR frequencies measured by the High-Frequency Analyzer (HFA) and the Onboard Frequency Analyzer (OFA) of the Plasma Wave Experiment (PWE) aboard Arase. However, these methods require significant human effort and their reproducibility remains limited in cases where identification is challenging. In this study, we developed and evaluated an automatic UHR frequency detection model based on a convolutional neural network (CNN) model. To improve the accuracy of the UHR frequency determination, we included the additional machine learning inputs (e.g., local electron cyclotron frequency, McIlwain-L value, magnetic local time, magnetic latitude, geomagnetic activity indices, and spacecraft potential). Hasegawa et al. (2019) used the orbital information and geomagnetic indices and evaluate the average of the mean absolute error (MAE) of the determined UHR frequencies over the entire dataset. On the other hand, our study evaluated regional and geomagnetic conditional dependence of the determined UHR frequencies by the CNN model. We found that the additional inputs improve the accuracy of the UHR frequency determination in a specific magnetic local time region.

#風間 洋一 $^{1)}$, Jun ChaeWoo²⁾, 堀 智昭 $^{3)}$, 三好 由純 $^{4)}$, 浅村 和史 $^{5)}$, 笠原 慧 $^{6)}$, 横田 勝一郎 $^{7)}$, Wang Bo-Jhou¹⁾, Wang Shiang-Yu¹⁾, Tam Sunny⁸⁾, Chang Tzu-Fang⁸⁾, 桂華 邦裕 $^{6)}$, 松岡 彩子 $^{9)}$, 寺本 万里子 $^{10)}$, 山本 和弘 $^{11)}$, 篠原 育 $^{5)}$ (1 ASIAA, $^{(2)}$ N a g o y a U n i v e r s i t y, $^{(3)}$ 名古屋大学・宇宙地球環境研究所, $^{(4)}$ 名古屋大学, $^{(5)}$ 宇宙航空研究開発機構, $^{(6)}$ 東京大学, $^{(7)}$ 大阪大学大学院, $^{(8)}$ Institute of Space and Plasma Sciences, National Cheng Kung University, Tainan, Taiwan, $^{(9)}$ 京都大学, $^{(10)}$ 九州工業大学, $^{(11)}$ 名古屋大学宇宙地球環境研究所

Recent updates of Level-2/-3 datasets of the LEPe instrument on the Arase satellite

#Yoichi Kazama¹⁾, Chaewoo JUN²⁾, Tomoaki HORI³⁾, Yoshizumi MIYOSHI⁴⁾, Kazushi ASAMURA⁵⁾, Satoshi KASAHARA⁶⁾, Shoichiro YOKOTA⁷⁾, Bo-Jhou Wang¹⁾, Shiang-Yu Wang¹⁾, Sunny Tam⁸⁾, Tzu-Fang Chang⁸⁾, Kunihiro KEIKA⁶⁾, Ayako MATSUOKA⁹⁾, Mariko TERAMOTO¹⁰⁾, Kazuhiro YAMAMOTO¹¹⁾, Iku SHINOHARA⁵⁾
(¹Academia Sinica Institute of Astronomy and Astrophysics, (²Nagoya University, (³Nagoya University, (⁴Nagoya University, (⁵ISAS/JAXA, (⁶University of Tokyo, (⁷Osaka University, (⁸Institute of Space and Plasma Sciences, National Cheng Kung University, Tainan, Taiwan, (⁹Kyoto University, (¹⁰Graduate School of Engineering, Kyushu Institute of Technology, (¹¹Nagoya University

We present recent updates of the datasets of the Low-Energy Particle Experiments - Electron Analyzer (LEPe) onboard the Arase satellite. Calibration for LEPe data requires evaluating the effects of background radiation and estimating the absolute sensitivity of the detector channels. Accounting for such factors, our calibration method consists of the following steps: (1) evaluation of sensitivity differences between the background channel and the electron channels, (2) relative sensitivity correction among the electron channels, and (3) estimation of the absolute quantum efficiency of the micro-channel plates (MCPs). In each calibration step, the data process is modeled using parameters to incorporate temperature dependence and time variation of detector properties. On March 1, 2023, the MCP voltage was increased to enhance electron detection sensitivity. In response to the voltage increase, the calibration parameters have recently been updated for measurement data after the voltage change operation. The newly calibrated data with versions "05" and "06" are going to be released shortly. Alongside the update of the dataset, we also refined data structure of LEPe Level-2 and Level-3 datasets in Common Data Format (CDF) for more consistent naming of variables, better index ordering, and also excluding rarely-used packet data, to improve data usability. In this presentation, we will introduce the updated datasets, discuss MCP detector degradation, and highlight the improvements made to the new data structure.

サブストーム時の放射線帯・プラズマシート遷移領域における電子の位相空間密度 の時空間変動

#太田 悠輝 $^{1)}$, 海老原 祐輔 $^{1)}$, 田中 高史 $^{2)}$ $^{(1)}$ 京都大学生存圏研究所, $^{(2)}$ 九州大学

Spatio-temporal evolution of electron phase space density in the radiation beltplasma sheet transition region during substorm

#Yuki OTA¹⁾, Yusuke EBIHARA¹⁾, Takashi TANAKA²⁾

(1 Kyoto University, Research Institute for Sustainable Humanosphere, (2 KYUSYU UNIVERSITY

For the rebuilding of radiation belts, two theories, the internal acceleration theory and the external supply theory, have been proposed as mechanisms, and in both theories, the phase space density (PSD) of electrons in the transition region between the radiation belt and the plasma sheet is important. To understand the fluctuations in the PSD of electrons, it is necessary to track a large number of electron orbits. However, in the transition region between the radiation belt and the plasma sheet, the curvature radius of the magnetic field lines is close to the cyclotron radius, so the bounce-averaging approximation or the gyrocenter approximation may not always be applicable. To track electron trajectories, it is necessary to solve the equations of motion sequentially, but the characteristic timescale of large-scale geomagnetic disturbances such as substorms (100 - 1000 seconds) is long compared to the cyclotron period (0.1 milliseconds), making this computationally challenging. Furthermore, since the global magnetohydrodynamic (MHD) simulation REPPU uses an unstructured grid, complex interpolation calculations are required to obtain the magnetic and electric fields at arbitrary positions and times. Therefore, we significantly reduced the time required for interpolation calculations by pre-assigning the fields to a simple orthogonal coordinate grid. In this study, we focused on the time period when magnetic dipolarization associated with substorms occurred, placed test particles on concentric circles at the magnetic equatorial plane and a geocentric distance of 7 RE, and traced them backward in time. Assuming a distribution function at the simulation boundary, we reconstructed the PSD using the phase space mapping method. As a result, we confirmed that the PSD of electrons with energies below 60 keV increased in a relatively wide region on the night side, and that the PSD of electrons with specific energies about 100 keV increased selectively in a narrow region around midnight. Upon examining the acceleration process along the electron trajectory, we found that the first adiabatic invariant is generally conserved from the far side of the plasma sheet to 7 RE. but since the trajectory depends on the gyro phase, the gyro-center approximation cannot be applied, and it is possible that two different types of acceleration are occurring. We will examine the spatio-temporal evolution in the PSD of electrons associated with substorms from the perspective of their dependence on energy, pitch angle, and gyro phase, and discuss the details.

放射線帯の再生機構として内部加速説と外部供給説が考えられているが、その双方において放射線帯・プラズマシート 遷移領域における電子の位相空間密度は重要である。電子の位相空間密度の変動を理解するためには非常に多くの電子 の軌道を追跡する必要があるが、放射線帯・プラズマシート遷移領域では磁力線の曲率半径がサイクロトロン半径に近 く、バウンス平均近似や旋回中心近似をいつも適用できるとは限らない。電子の軌道を追跡するためには運動方程式を 逐次的に解く必要があるが、0.1 ミリ秒オーダーのサイクロトロン周期に対し、サブストームなど磁気圏大規模変動の特 徴時間スケール(100~1000 秒オーダー)は長く、計算時間の観点から困難である。また、グローバル電磁流体(MHD) シミュレーション REPPU は非構造格子を用いているため、任意の位置・時刻における磁場と電場を取得するためには複 雑な内挿計算が必要である。そこで、単純な直交座標格子に予め場を割り当てることで内挿計算にかかる時間を大幅に短 縮した。本研究では、サブストームに伴う磁気双極子化がおきた時間帯に着目し、磁気赤道面かつ地心距離7RE の同心 円上にテスト粒子を配置し、時間について逆方向に追跡した。シミュレーション境界における分布関数を仮定し、位相空 間写像法を用いて位相空間密度の再構築を行った。その結果、双極子化に伴い、夜側の比較的広い領域で 60 keV 以下の エネルギーを持つ電子の位相空間密度が増加すること、真夜中付近の狭い領域では 100 keV 帯の特定のエネルギーを持 つ電子の位相空間密度が選択的に増加することを確認した。この電子の軌道に沿って加速過程を精査したところ、プラズ マシート遠方から 7 RE に到達するまでの間、第一断熱不変量は概ね保存されているが、軌道はジャイロ位相に依存する ため、旋回中心近似は適用できないことや、二つの異なるタイプの加速を受けている可能性があることが分かった。サブ ストームに伴って変動する電子の位相空間密度の時空間変化について、エネルギー、ピッチ角、ジャイロ位相に対する依 存性の観点から精査し、その詳細を議論する。

#篠原 育 1), 三谷 烈史 1), 東尾 奈々 2), 笠原 慧 3), 横田 勝一郎 4), 桂華 邦裕 3), 山本 和弘 5), 堀 智昭 6), 浅村 和史 1), 三好 由純 7), 風間 洋一 8), Wang Shiang-Yu 8), Tam Sunny 9), Jun ChaeWoo 10), 松岡 彩子 11), 寺本 万里子 12) $^{(1}$ JAXA, $^{(2}$ JAXA, $^{(3)}$ 東京大学, $^{(4)}$ 大阪大学, $^{(5)}$ 名古屋大学, $^{(6)}$ 名古屋大学, $^{(6)}$ 名古屋大学, $^{(8)}$ 名古屋大学, $^{(8)}$ 名以, $^{(9)}$ 00、名古屋大学, $^{(11)}$ 京都大学, $^{(12)}$ 九州工業大学

MeV electrons observed at near-Earth plasma sheet boundary

#Iku Shinohara¹⁾, Takefumi MITANI¹⁾, Nana Higashio²⁾, Satoshi KASAHARA³⁾, Shoʻchiro YOKOTA⁴⁾, Kunihiro KEIKA³⁾, Kazuhiro YAMAMOTO⁵⁾, Tomoaki HORI⁶⁾, Kazushi ASAMURA¹⁾, Yoshizumi MIYOSHI⁷⁾, Yoichi KAZAMA⁸⁾, Shiang-Yu Wang⁸⁾, Sunny Tam⁹⁾, Chaewoo JUN¹⁰⁾, Ayako MATSUOKA¹¹⁾, Mariko TERAMOTO¹²⁾
(1JAXA, (2JAXA, (3University of Tokyo, (4Osaka University, (5Nagoya University, (6Nagoya University, (7Nagoya University, (8ASIAA, (9NCKU, (10Nagoya University, (11Kyoto University, (12Kyushu Institute of Technology

We have reported that energetic electron bursts over 300 keV up to MeV occur at the plasma sheet boundary. In this study, using an 8-year dataset of Arase (ERG) observations of electron burst events, we try to address where the energetic electron bursts at higher latitudes come from and their acceleration process. The pitch angle distribution of 100-200 keV electrons typically shows an enhancement in parallel flux, which is consistent with common observations in the plasma sheet boundary layer. However, the higher energy portion of the energetic electron bursts exhibits a perpendicular flux enhancement, resembling typical dispersion-less injection events. The magnetic field line model suggests that the Arase satellite was located in a transition region between dipole-like and tail-like fields. This leads to the interpretation that the higher-energy electron bursts may result from electron acceleration in the downstream region of the magnetotail reconnection site. We will present the statistical features of these electron burst events in the near-Earth plasma sheet boundary layer, discuss the origin of MeV electrons based on particle dynamics, and compare their distribution functions with those observed in the magnetotail.

リオメータを用いたサブストーム発生前後の高エネルギー電子降下特性の研究

#大山 礼華 $^{1)}$, 細川 敬祐 $^{1)}$, 大山 伸一郎 $^{2,3,4)}$, 田中 良昌 $^{3)}$ $^{(1)}$ 電気通信大学、 $^{(2)}$ 名古屋大学宇宙地球環境研究所、 $^{(3)}$ 国立極地研究所、 $^{(4)}$ オウル大学

Characteristics of high-energy electron precipitation before and after substorm using riometer

#Ayaka OOYAMA¹⁾, Keisuke HOSOKAWA¹⁾, Shin-ichiro OYAMA^{2,3,4)}, Yoshimasa TANAKA³⁾
⁽¹The University of Electro-Communications, ⁽²Institute for Space-Earth Environmental Research, ⁽³National Institute of Polar Research, ⁽⁴University of Oulu

It is well known that, immediately after substorm onsets, highly energetic electrons precipitate from the magnetosphere into the ionospheric D region (60 – 90 km altitude), causing low-altitude ionization. Ionization in the D region, which is the low-altitude part of the ionosphere, is detected as "absorption spikes" in cosmic noise absorption (CNA) using a riometer. In previous studies, riometer operating at a single frequency was used, which limited the ability to estimate the energy range of precipitating electrons based on the observed frequency dependence of CNA and conduct comprehensive statistical analyses. In this study, we examined frequency dependence and statistical properties of CNA variations using a spectral (i.e., multi-frequency) riometer (20 – 55 MHz) in Kilpisjärvi, Finland (KIL; 69.07N, 20.75E). Using a substorm list by Forsyth et al. (2015), we identified 4,506 substorms over two years from 2023 to 2024. To investigate the typical pattern of electron precipitation, Superposed Epoch Analysis (SEA) was applied to characterize variations in CNA around substorm onsets, with the zero epoch-time is set to the substorm onset.

The SEA results reveal a slight decrease (about 0.03 dB) in CNA approximately 20 min before onset, suggesting a temporal reduction in electron precipitation before onset. This behavior during the growth phase may be a precursor of substorm onset (or substorm-related ionization) in the CNA data. Additionally, SEA with MLT sorting showed propagation of CNA enhancements from midnight to eastward at 30 MHz, indicating eastward drift of high-energy electrons in the magnetosphere. The estimated zonal propagation speed at ionospheric altitudes was estimated to be approximately 4.65 km/s during the initial phase. However, all the events we used include cases where other substorms occurred before and after, so we cannot rule out the possibility that the observations were affected by multiple overlapping events. To investigate this trend in more detail, we analyzed 1,693 isolated-substorms (no other substorm within \pm 3 hours) at 30 MHz. In the SEA with the isolated-substorms, eastward propagation was more clearly identified, with a slower eastward speed of approximately 2.35 km/s, indicating that isolated substorms produce cleaner CNA features. From the derived propagation speeds, it was found that electrons precipitating into the D region after substorm onset propagate eastward at speeds of a few kilometers per second, rather than westward. The propagation eastward is attributed to the grad-B drift in the magnetospheric equatorial plane. It should be noted that the propagation velocity includes the Earth's rotational velocity. For a given observation site at latitude θ , the rotational velocity is expressed as v =(2 π Re cos θ)/(24 \times 3600) where Re is the Earth's radius. At Kilpisjärvi, this value is approximately 0.16 km/s. Since the rotational velocity varies with latitude, it depends on the location of observation.

In the presentation, we will discuss how the substorm-related CNA varies based on substorm size, season, event isolation, and the magnetic latitude of the riometer location.

サブストームオンセットの直後に、磁気圏からの高エネルギー電子が電離圏 D 領域(高度 60-90~km)に降下し、電離を引き起こすことが知られている。電離圏の中でも低高度である D 領域での電離は、リオメータによって観測される銀河電波雑音吸収(Cosmic Noise Absorption: CNA)の急増として現れ、「absorption spike」と呼ばれる。従来の研究では、主に単一周波数のリオメータが用いられており、観測された CNA の周波数依存性に基づいて、降下電子のエネルギー帯域を推定することや、その統計的な解析には限界があった。そこで本研究では、20-55~MHz の帯域を同時に観測可能な多周波数リオメータと、サブストームオンセットリスト(Forsyth et al., 2015)を組み合わせて用いることで、サブストーム前後における高エネルギー電子降下の周波数依存性および統計的性質を明らかにすることを目的とする。使用データは、フィンランド・キルピスヤルビ(69.07~N, 20.75~E)に設置されているリオメータによって 2022~E~E 10 月から取得された CNA データで、2023-2024~E 6 4506 件のオンセットに対して Superposed Epoch Analysis(SEA)を実施した。これにより、CNA の平均的時間変化から電子降下の特性解明を明らかにすることができる。

Superposed Epoch Analysis(SEA)解析の結果、サブストームオンセットの約20分前からオンセットまでの時間帯に、CNAのわずかな減少(約0.03 dB)が見られることが明らかとなった。これは、オンセット直前において電子降下量が一時的に減少している可能性を示唆するものであり、低高度電離の「予兆」として観測されている可能性を示唆する。さらに、サブストームオンセット位置とリオメータ観測点との相対的な位置関係を考慮し、オンセットの磁気地方時(MLT)に基づいてデータを分類、観測周波数30 MHzで SEA を実施した。その結果、CNAの急増が朝方方向に伝搬していく様子が確認され、CNAの増大をつくりだす高エネルギー電子が磁気圏において東向きへ伝搬していることが示唆された。初期応答における伝搬速度を計算したところ、およそ4.65 km/sの速度で東方向に伝搬していることが明らかになった。ただし、使用した全イベントには、前後に他のサブストームが存在する場合も含まれており、複数イベントの影響が重

なって観測されている可能性も否定できない。そこでこの傾向の純粋性を検証するため、前後 3 時間に他のサブストームが存在しない孤立型サブストームのみを抽出し、30 MHz で同様に SEA を実施した。その結果、対象イベント数は 1,693 件に減少したが、電子降下の東方向への伝搬傾向がより明瞭に確認された。この場合の伝搬速度は約 2.35 km/s であった。これら伝搬速度の導出から、サブストーム発生後、電離圏 D 層に降下した電子は西向きではなく東向きに数 km/s 程度で伝搬することが分かった。東向きに伝搬が起こる理由として、磁気圏赤道面での電子の磁場勾配 (grad B) ドリフトによるものだと考えられる。なお、伝搬速度には地球の自転速度が包含されている。観測地点の緯度 θ に対応して自転速度 θ に対応して自転速度 θ に対応して自転速度 θ に対応して自転速度によって変化するため観測地点に依存する。

発表では、サブストームの規模別、季節別、孤立型イベントのような条件別に実施した解析結果やリオメータ観測箇所を変えた場合の解析結果についても詳細に報告する予定である。これらの解析を通じて、サブストームに伴う高エネルギー電子の降下過程とその電離圏応答について議論を行う。

#Varghese Manu¹⁾, SHIOKAWA Kazuo²⁾, Zhang Qing-He¹⁾, N Balan^{1,2)}, Raj Jijin K¹⁾, P R Shreedevi²⁾
⁽¹NSSC, 中国科学院, ⁽²Nagoya University

Understanding the Magnetosphere-ionosphere coupling during two low latitude auroras on 28 February 2023 and 24 April 2023

#Manu Varghese¹⁾, Kazuo SHIOKAWA²⁾, Qing-He Zhang¹⁾, Balan N^{1,2)}, Jijin K Raj¹⁾, Shreedevi P R²⁾
⁽¹⁾National Space Science Center, Chinese Academy of Sciences, Beijing, China, ⁽²⁾Nagoya University

Low latitude auroras are seen during large geomagnetic disturbances when precipitation of electrons from the inner magnetosphere occur. Stable Auroral Red (SAR) arcs formed from the overlap region between outer plasmasphere electrons and ring current ions contribute to the 630 nm (red) emission in the equatorward edge of the auroral oval. Broadband flux of low energy electrons from the inner magnetosphere causes red-green auroras at low latitudes. However, the red emissions alone are usually seen because the green emissions are hidden below the horizon. Recent observations of the low latitude auroras at Rikubetsu (magnetic latitude, 34.70 N) in Japan in the rising phase of solar cycle 25 have shown unusual red-green aurora of comparable intensity. Two such events occurred during the geomagnetic storms on 28 February 2023 and 24 April 2023 (F10.7 = 157.9 and 135.5, SymHMin = -161 nT and -233 nT). In this paper, we study the magnetosphere-ionosphere coupling during these events by modelling the plasmapause location using OBM03 model and ring current particle populations using BATSRUS+RAM-SCB model to understand the causative physical mechanisms.

高空間分解能カメラを用いたディフューズオーロラ微細構造の観測: 二次的な不安 定性による構造形成

#佐野 友祐 $^{1)}$, 細川 敬祐 $^{1)}$, Winn Wandal $^{1)}$, 大山 伸一郎 $^{2)}$, 三好 由純 $^{2)}$, 小川 泰信 $^{3)}$, 田中 良昌 $^{3)}$ (1 電気通信大学, $^{(2)}$ 名古屋大学宇宙地球環境研究所, $^{(3)}$ 国立極地研究所

Observation of Fine Structures in Diffuse Aurora with a High-Spatial-Resolution Camera: Manifestation of Secondary Instabilities

#Yusuke SANO¹⁾, Keisuke HOSOKAWA¹⁾, Wandal WINN¹⁾, Shin-ichiro OYAMA²⁾, Yoshizumi MIYOSHI²⁾, Yasunobu OGAWA³⁾, Yoshimasa TANAKA³⁾

⁽¹University of Electro-Communications, ⁽²Institute for Space and Earth Environmental Research, Nagoya University, ⁽³National Institute of Polar Research

Diffuse auroras including pulsating auroras are frequently observed in the morning sector during the recovery phase of auroral substorms. They are often distributed in a wide area and last for several hours. These auroras sometimes patchy spatial structures, but the processes responsible for their formation remain unclear. Electron Multiplying Charge Coupled Device (EMCCD) cameras have been widely used to study pulsating auroras. Their electron-multiplying mechanism enables high signal-to-noise ratio observations even for faint emissions at high temporal resolution. However, the limited number of pixels and narrow dynamic range of EMCCD cameras restrict detailed analyses of spatial brightness distributions, contrast, and small-scale features. To overcome these limitations, we used a quantitative Complementary Metal Oxide Semiconductor (qCMOS) camera with high spatial resolution and wide dynamic range. The qCMOS system provides a spatial resolution of 0.1 km near zenith and preserves brightness contrasts without saturation. This capability allows us to visualize fine structures inside diffuse auroras and along patch boundaries in detail. The images were calibrated using star maps and mapped onto the geographic coordinates, enabling us to combine multiple fields of view and quantify the spatial scale and drift velocity of auroral structures with high accuracy.

We analyzed patchy diffuse auroras observed by the qCMOS camera at Skibotn, Norway (69.35N, 20.36E), during 04 – 05 UT on February 2, 2025. During this interval, finger-like structures were identified along the outer boundary of diffuse auroras. A wavy boundary with a wavelength of 10 – 25 km appeared on the southwestern edge of an eastward-drifting patch (100 – 150 m/s). These undulations developed into finger-like forms with phase speeds of 120 – 250 m/s. The observed scales, drift velocity, and timing of appearance were consistent with the structures attributed to pressure-driven instability reported by Shiokawa et al. (2010), suggesting that instability was involved in their formation. In addition, we identified smaller-scale wavy patterns on the side of one finger-like structure, which had been difficult to resolve with the spatial resolution of previous observations. This feature had a wavelength of 3 – 5 km and appeared on the northwestern side of a bright finger. It propagated northeastward along the boundary as the finger developed. This behavior suggests that velocity shear associated with the nonlinear development of pressure-driven instability excited a secondary Kelvin – Helmholtz instability (KHI). Thus, observational evidence directly suggesting a transition from pressure-driven instability to KHI in diffuse auroras has been scarce, and this study provides one of the first cases that clearly captured this process. We will discuss the generation and evolution of these auroral fine structures as a possible transition from pressure-driven instability to KHI.

サブストームの回復相では、朝側のローカルタイムにおいて、脈動オーロラを含むディフューズオーロラが、広い範囲で、かつ長時間にわたって観測される。これらのディフューズオーロラはパッチ状の空間構造を示すことが知られているが、これらのパッチ構造がどのように形成されるのかについては、未だに統一的な理解が得られていない。パッチ状ディフューズオーロラの観測には、これまで様々な機器が用いられてきたが、中でも Electron Multiplying Charge Coupled Device (EMCCD) カメラは、電子倍増機構により微弱な発光の高時間分解能観測において高い S/N 比の観測を実現してきた。一方で、画素数やダイナミックレンジに制限があるため、オーロラの輝度空間分布やコントラストの保持、微細構造の抽出には限界があった。本研究では、そうした制約を乗り越え、従来では見逃されていた可能性のあるディフューズオーロラの微細構造を検出するために、高空間分解能かつ広ダイナミックレンジ性能を有する quantitative Complementary Metal Oxide Semiconductor (qCMOS) カメラを用いた観測を行った。これにより、解像度の大幅な向上(天頂付近で 0.1 km の空間分解能)に加え、輝度の差を潰すことなく明瞭なコントラストを保持することが可能となり、ディフューズオーロラ内部の微細構造やパッチの境界を詳細に可視化することが期待できる。また、観測データに対しては、スターマップを用いた視野較正および地理座標系へのマッピング処理を行い、複数地点の観測視野を統合することによって、オーロラの空間スケールや移動速度の高精度な定量化を可能にした。

本研究では、2025 年 2 月 2 日の 04 - 05 UT の時間帯に、ノルウェーの Skibotn (69.35N, 20.36E) に設置された qCMOS カメラによって観測されたパッチ状ディフューズオーロラに着目して解析を行った。この時間帯の複数のタイミングで、ディフューズオーロラの外縁部に指状の微細構造が形成されている様子が確認できた。 東向きに 100 - 150 m/s でドリフトするパッチの南西側の外縁部に出現した波長 10 - 25 km の波状の境界が、120 - 250 m/s の速さで振幅を発

達させながら伝搬することで指状構造が形成された.この指状構造は,Shiokawa et al. (2010) によって報告された圧力駆動型不安定性 (Pressure Driven Instability) に起因して発生する微細構造と,現象の空間スケールやドリフト速度,出現したタイミングなどの条件が一致していたことから,その形成に圧力駆動型不安定性が関与している可能性が高いと考えられる.さらに,ある指状構造の側面には,従来の観測の空間分解能では捉えることが困難であった,より細かいスケールの波状パターンが形成されていることも明らかになった.明るい指状構造の北西側の側面に波長 3-5 km の空間スケールを持って現れたこの微細構造は,指状構造の発達に伴い,境界に沿うように北東方向に移動した.これは,圧力駆動型不安定性の非線形発展に伴いパッチの境界に速度シアーが生じ,二次的なケルビンヘルムホルツ不安定性 (Kelvin – Helmholtz instability: KHI) による波状構造が励起されている可能性を示唆するものである.このように,ディフューズオーロラにおいて圧力駆動型不安定性から KHI への移行を直接示唆する観測例はこれまで報告が少なく,本研究がその過程を具体的に捉えた初めての事例の一つである.発表では,この移行過程を示唆するオーロラの微細構造に注目し,その形成過程や発展メカニズムについて議論する.

高空間分解能カメラを用いたオーロラビーズ発生過程の可視化: 複数事例の解析

#秋元 咲那 $^{1)}$, 細川 敬祐 $^{1)}$, 大山 伸一郎 $^{2)}$, 小川 泰信 $^{3)}$, 三好 由純 $^{2)}$, 田中 良昌 $^{3)}$ $^{(1)}$ 電気通信大学、 $^{(2)}$ 名古屋大学宇宙地球環境研究所、 $^{(3)}$ 国立極地研究所

Fine-scale visualization of initial development of auroral beads: Multi-event analysis using a high-spatial-resolution camera

#Sana AKIMOTO¹⁾, Keisuke HOSOKAWA¹⁾, Shin-ichiro OYAMA²⁾, Yasunobu OGAWA³⁾, Yoshizumi MIYOSHI²⁾, Yoshimasa TANAKA³⁾

⁽¹The University of Electro-Communications, ⁽²Institute for Space and Earth Environmental Research, Nagoya University, ⁽³National Institute of Polar Research

During the early stage of the expansion phase of substorms, discrete auroras with enhanced optical luminosity are seen to fill the entire sky, which is called auroral breakup. This study focuses on a phenomenon called "auroral beads," which have attracted attention as a precursor of auroral breakup. Auroral beads are bead-like spatial structure of auroras that appear immediately before the auroral breakup. Beads have a spatial scale of several kilometers to several tens of kilometers, grow while propagating in the longitudinal direction, and eventually form large vortical structures. Based on its magnetic conjugacy and the exponential time evolution of luminosity, plasma instability in the magnetotail is thought to be involved in their formation. However, the specific mechanism has not yet been identified. Previous studies often used all-sky cameras with a low spatial resolution, which were not sufficient to capture the site of formation or the initial development of auroral beads at the ionospheric altitude. Further high-resolution observations in the ionosphere may reveal the spatiotemporal characteristics of bead structures, and help to understand how plasma instabilities in the magnetotail are projected onto the ionosphere. Thus, by utilizing the new qCMOS camera with a relatively narrower field-of-view, more detailed observations will be possible.

This study analyzes three cases of auroral beads using the qCMOS camera, in Skibotn, Norway (69.35N, 20.36E), which has a higher spatial resolution than conventional all-sky cameras. We analyzed three events respectively appeared on November 10, 2023, December 21, 2024, and December 24, 2024. As for the geomagnetic activity, substorm-induced variations of the geomagnetic X component (negative bays) were detected at Kilpisjärvi with amplitudes of about 200 nT, 300 nT, and 250 nT, respectively, and increases in the AE index of about 200 nT, 500 nT, and 600 nT were observed, suggesting that these beads events were observed in association with small to moderate substorm activities. The camera is equipped with a lens with a field of view of about 70 degrees and a BG3 filter to measure only the prompt emissions. The qCMOS camera has a spatial resolution of 1024 x 576 pixels and a temporal resolution of 20 FPS, enabling high-speed imaging of aurora with approximately 0.1 km spatial resolution near the center of the field of view. This allows us to detect smaller auroral beads at earlier stages of their development, which has been difficult to observe with conventional EMCCD cameras (256 x 256 pixels). These observations provide important dataset for understanding the generation mechanisms of beads in the magnetotail by monitoring auroral development at ionospheric altitudes.

To clarify the spatiotemporal evolution of auroral bead structures, we analyzed three events in which auroral beads were clearly observed within the narrow field-of-view of the qCMOS camera. The images were mapped and flat-fielded to geographic coordinates, and we analyzed the north-south and east-west keograms, continuous auroral images, and the temporal variation of the brightness and wavenumber in the regions containing the beads. In the case of the event on November 10, 2023, we found that wave-like structures with scales less than ~10 km propagating eastward were visible in the background-subtracted images starting approximately five minutes before the auroral bead structures became prominent. During this pre-bead period, the east-west wavenumber was observed to decrease, and a two-stage growth in brightness was identified. These wave-like structures may correspond to the seed perturbations for the instability that drives the formation of auroral beads. In the event on December 21, 2024, we observed that a bead-like structure initially developed, temporarily faded, and then reformed, indicating a more dynamic development process. In the event on 24 December 2024, the camera captured motion of an auroral arc and subsequent rapid development into clearer bead-like structures. Among the three events, the beads appeared at different locations within the field of view (to the north, near zenith, and to the south) suggesting that the apparent spatial characteristics of auroral beads may vary depending on the viewing angle. In the presentation, we will show the temporal evolution of these three auroral bead events and discuss the time development of propagation speed and wavenumber.

サブストームの爆発相では、輝度が高いディスクリートオーロラが全天を埋め尽くすように見られ、これをオーロラブレイクアップと呼ぶ。本研究では、オーロラブレイクアップの前兆として注目されている「オーロラビーズ」と呼ばれる現象に着目する。オーロラビーズは、オーロラブレイクアップ前に現れる微小なビーズ状のオーロラで、数 km から数十km の空間スケールを持ち、東西に伝搬しながら成長し、最終的には大きな渦構造を形成するという特徴を持つ。南北半球での磁気共役性や、輝度が指数関数的に時間発展する様子から、磁気圏尾部のプラズマ不安定性がその生成に関与していると考えられるが、その具体的なメカニズムの特定には至っていない。これは、従来研究の多くが空間解像度の低い全

天カメラを用いていたため、電離圏高度におけるオーロラビーズの形成場所や初期発達過程を十分に捉えることができなかったためである。今後、高空間分解能による電離圏での観測から、ビーズ構造の時空間的な特徴を明らかにすることは、磁気圏尾部でのプラズマ不安定性がどのように電離圏に投影されるかを理解する端緒となり得る。しかし、このような問題意識に基づいて、本研究では、新しく稼働を開始した広視野レンズを用いた qCMOS カメラによる観測を活用することで、オーロラビーズの高時空間分解能観測を行った。

本研究では、従来の全天カメラよりも空間解像度の高い qCMOS カメラを用いて、オーロラビーズの複数の事例の解析を行った。 qCMOS カメラはノルウェーの Skibotn (69.35N, 20.36E) に設置されており、解析は 2023 年 11 月 10 日, 2024年 12 月 21 日, 2024年 12 月 24 日の 3 例のデータに対して実施した。カメラの設置場所の近傍であるキルピスヤルビにおけるこれら 3 例に伴う地磁気活動は、サブストームによる地磁気 X 成分の変動(negative bay)が約 200 nT, 300 nT, 250 nT 程度の振幅で観測され、AE 指数の増大も 200 nT, 500 nT, 600 nT 程度であったことから、小規模から中規模のサブストームに繋がるオーロラビーズを捉えていたと考えられる。カメラには、視野角 70° 程度の広視野レンズと即時発光のオーロラ光のみを透過する BG3 フィルターが装着されている。本研究で用いる qCMOS カメラは空間分解能 0.1 km を有し、従来は検出困難であったより小さな初期段階のオーロラビーズを捉えることを可能にする。取得される画像の画素数は 1024×576 ピクセルであり、従来の EMCCD カメラと比較して約 8 倍の空間解像度を持つ。 20 FPS の高時間分解能により、先行研究と同等かより小さい 10 km 以下のビーズ構造とその挙動をより鮮明に捉えることができた。これらの特性は、電離圏高度でのビーズの発現を詳細に観測することで磁気圏尾部での生成メカニズム解明へとつながる重要な観測情報を与えることが期待される。

qCMOS カメラの視野内でビーズが鮮明に観測された 3 例の画像に対して、地理座標へのマッピングとフラットフィールディングを行い、南北・東西ケオグラム、オーロラビーズの連続画像、オーロラビーズを含む領域の輝度、波数の時間変化を解析した。 2023 年 11 月 10 日事例では、オーロラビーズの構造が顕在化する 5 分程度前から、背景成分を引いた画像において東へ伝搬する 波長 10 km 程度の小スケールの波状構造が見えていることが明らかになった。 この時間帯において、波数の減少と輝度の増大に二段階の成長性が見られた。 この波状構造は、オーロラビーズの駆動源となる不安定性の種に対応している可能性がある。 また、 2024 年 12 月 21 日の観測例に関しては、ビーズのような構造ができ始めてから一度収まり、再び東西アークが構造化してビーズができるような振る舞いが見られた。 2024 年 12 月 24 日の例では、オーロラアークが移動したあとに、明瞭なビーズ構造が急激に形成されるところが捉えられた。 これら 3 つの例では、ビーズがカメラの視野に対して北側、 天頂角付近、 南側に存在しており、 視野角によってビーズの空間構造の見え方が異なる可能性があることも分かった。 発表では、 これらの 3 つのオーロラビーズの時間発展を示し、 伝搬速度や波数の時間発展から、 ビーズの形成過程についての議論を行う。

EISCAT_3D レーダーを用いた降下電子エネルギースペクトルの水平分布の推定 #吹澤 瑞貴 $^{1,2)}$, 小川 泰信 $^{1,2,3)}$, 田中 良昌 $^{1,2,3)}$

⁽¹ 国立極地研究所、⁽²⁾ 総合研究大学院大学、⁽³⁾ データサイエンス共同利用基盤施設 極域環境データサイエンスセンター

Estimation of the horizontal distribution of the precipitating electron energy spectrum using EISCAT_3D radar

#Mizuki Fukizawa^{1,2)}, Yasunobu OGAWA^{1,2,3)}, Yoshimasa TANAKA^{1,2,3)}

(1) National Institute of Polar Research, (2) The Graduate University for Advanced Studies, SOKENDAI, (3) Polar Environment Data Science Center, ROIS-DS

The CARD method estimates the energy spectrum of precipitating electron flux from the E-region electron density height distribution obtained by the European Incoherent Scatter (EISCAT) radar. This method was developed in 1989 and has been widely used. However, the conventional EISCAT radar is practically a unidirectional instrument using a large aperture antenna. It can only estimate the spectrum at a single point along the magnetic zenith. In contrast, the EISCAT_3D radar will be able to observe the ionosphere in three dimensions using a phased-array antenna. The aim of this study is to develop a method to estimate the horizontal two-dimensional distribution of the precipitating electron energy spectrum from the threedimensional electron density distribution obtained by the EISCAT_3D radar.

First, we prepared a typical electron energy spectrum, which is often observed in a discrete aurora, as the true model. The energy distribution was defined as a combination of a Gaussian distribution with a characteristic energy of 5 keV and a onesided power-law component. The power-law slopes were 1 on the low-energy side and 3 on the high-energy side. The spatial distribution of the total energy flux was assumed to follow a Gaussian distribution. It had a peak of 40 mW/m², a uniform offset of 10 mW/m², and a full width at half maximum of 47 km in the north – south direction. In the east – west direction, the center of this north - south Gaussian was set to meander with a sinusoidal amplitude of 20 km and a wavelength of 200 km. From this true-value spectrum, a three-dimensional (3D) electron density distribution was created. This was done by solving the electron density continuity equation under the steady-state assumption. Models for the ionization rate, neutral atmosphere, and effective recombination coefficient were adopted from previous studies.

For estimating the precipitating electron spectrum, the electron density height profile along the magnetic field lines was required. Therefore, we used the coordinate system (x, y, z) = (East, North, Magnetic Zenith). The prepared 3D data were then sampled according to the 27-beam configuration planned for the EISCAT_3D Common Programme. Finally, observation noise was added to generate synthetic data. The electron density values at 27 beam points in each altitude plane were spatially interpolated. This interpolation was used to construct the electron density height profile along the magnetic field line at each grid point.

When the least-squares estimation, as in the conventional CARD method, was applied to the 3D observation data, the total energy flux was reproduced with an accuracy better than 5 mW/m², and the average energy with an accuracy better than 2 keV. This result held within a region of \pm 25 km east – west and \pm 50 km north – south around the magnetic zenith. However, some oscillations remained in the estimated energy distribution. To address this, reconstruction was performed using maximum a posteriori estimation. In this approach, two smoothness priors were imposed: (i) the second-order derivative in the energy direction and (ii) the spatial second-order derivative between adjacent grids. As a result, the oscillations were suppressed, and the 5 keV peak was more clearly resolved compared with the least-squares method. Nevertheless, oscillations at high energies were not fully eliminated, and further improvements to the design of the prior distribution are planned in future works.

欧州非干渉散乱(EISCAT)レーダーから得られる E 領域電子密度高度分布から最小二乗法により降下電子フラックス のエネルギースペクトルを推定する CARD 法 が開発され、広く用いられてきた。しかし、従来の EISCAT レーダーは大 口径アンテナを使用しており実質的に単一方向観測であるため、磁気天頂一点でのスペクトル推定にとどまる。一方で、 近年観測開始予定の EISCAT_3D レーダー は位相配列式アンテナにより電離圏の 3 次元観測が可能となる。そこで本研 究は、EISCAT_3D レーダー により得られる電子密度の 3 次元分布から降下電子フラックスのエネルギースペクトル水平 面内2次元分布を推定する手法の開発を目的とする。

まず、真値モデルとしてディスクリート・オーロラを想定し、エネルギー分布は特性エネルギー5keVのガウス分布 に、低エネルギー側および高エネルギー側へそれぞれ傾き1と3の片側パワー則成分を加えた合成分布とした。全エネ ルギーフラックスの空間分布は、ピーク $40~\mathrm{mW/m^2}$ 、南北方向の半値全幅 $47~\mathrm{km}$ のガウス分布とし、さらに一様なオフ セット 10 mW/m² を加えた。東西方向には、この南北方向のガウス分布の中心位置が振幅 20 km、波長 200 km の正弦 で蛇行するように設定した。この真値スペクトルから、先行研究に基づく電離率・中性大気・実効再結合係数のモデルを 用い、定常状態を仮定した電子密度の連続の式を解くことで電子密度の3次元分布を作成した。さらに、EISCAT.3Dの Common Programme で予定される 27 本ビーム配置に合わせてサンプリングし、観測ノイズを付与して擬似観測データ を生成した。降下電子スペクトル推定には磁力線に沿った電子密度高度分布が必要であるため、座標系 (x, y, z) = (東, 北, 磁気天頂)を用い、各高度面で27本のビーム点での電子密度データを空間補間して、磁力線方向の電子密度高度プロファイルを格子点ごとに構成した。

このようにして用意した擬似的な電子密度の 3 次元観測データに対して、従来の CARD 法と同様に最小二乗推定を適用したところ、磁気天頂近傍で東西 \pm 25 km、南北 \pm 50 km の範囲において、全エネルギーフラックスは 5 mW/m² 未満、平均エネルギーは 2 keV 未満の精度で再現できた。一方で、推定されたエネルギー分布には振動が残存した。そこで、最大事後確率推定に基づき、(i)エネルギー方向の 2 階微分と(ii)隣接格子間の空間 2 階微分を滑らかさ事前として課すことで再構成を行った。その結果、最小二乗法に比べて振動が抑制され、5 keV のピークが明瞭化した。ただし、高エネルギー側の振動は完全には除去することができておらず、今後の課題として事前分布の設計をさらに工夫する予定である。

Geotail 衛星による Auroral Kilometric Radiation の長期統計解析:自動検出技術の 適用

#山中 陽斗 $^{1)}$, 笠羽 康正 $^{1)}$, 栗田 怜 $^{2)}$, 小嶋 浩嗣 $^{2)}$, 土屋 史紀 $^{1)}$, 三澤 浩昭 $^{1)}$ (1 東北大学, $^{(2)}$ 京都大学

Long-term Statistical Analysis of Auroral Kilometric Radiation Observed by Geotail: Applied Automated Detection Technique

#Haruto Yamanaka¹⁾, Yasumasa KASABA¹⁾, Satoshi KURITA²⁾, Hirotsugu KOJIMA²⁾, Fuminori TSUCHIYA¹⁾, Hiroaki MISAWA¹⁾

(1Tohoku University, (2Kyoto University

Auroral Kilometric Radiation (AKR) is the most intense radio emission from the Earth. It is generated by precipitating energetic electrons along auroral field lines by electron cyclotron resonance. Its intensity correlates with the field-aligned current density, while its frequency is related to the source altitude through the local electron cyclotron frequency. Consequently, AKR provides a valuable diagnostic of both the auroral electron precipitations and their acceleration altitude. The objective of this study is to investigate these statistical characteristics, including their dependence on solar activity.

We performed a long-term statistical analysis of AKR, covering nearly three decades (September 1992 – June 2022) using the Plasma Wave Instrument (PWI) onboard the Geotail satellite. This dataset enables us to investigate AKR occurrence and characteristics over 3 solar cycles.

Since Solar type-III bursts also overlap the AKR frequency range (from several 10s kHz up to 500 – 600 kHz), their automatic removal is essential for robust statistics. In previous studies by the Wind spacecraft, a method using 3-second standard deviations of the spin-axis antenna (Waters et al., 2021) and its extension with the criteria combining frequency and temporal continuity (Fogg et al., 2022).

We modified those methods and applied the long-term dataset of high-quality measurements from the Geotail Plasma Wave Instrument (PWI) Sweep Frequency Analyzer (SFA), covering nearly 30 years from September 1992 to June 2022. Compared with Wind, Geotail needs two major challenges. (1) It lacks a spin-axis antenna, so the angle between the antenna and the radio wave direction varies with the spin (period: "3 second), producing artificial spin modulations which Wind spin-antenna data does not have. (2) The SFA Band-5 (100-800~kHz), the most suitable for AKR, requires 8 seconds for one frequency sweep, so it limits the ability to get short-term fluctuations used in Wind. In order to overcome these issues, we identified AKR with following three criteria: (A) Larger time variability: To mitigate spin-induced fluctuations, we deleted the spin modulation by averaging a longer averaging window (168~s: three 8-s cycles and 8 spin periods), and picked up AKR with a threshold based on the standard deviation of time variations (e.g., $4.65 \times 10^{-3}~\text{W/m}^2/\text{Hz}$). (B) Larger frequency variability: Since AKR shows stronger frequency fluctuations than solar type-III bursts, we set an additional threshold on the standard deviation across frequency (e.g., $2.65 \times 10^{-3}~\text{W/m}^2/\text{Hz}$, 32 channels, 175~kHz). © Larger temporal continuity: To exclude short-lived type-III bursts, we require events to satisfy a wide frequency wave (e.g., 30 channels, 160~kHz) with the continuity of 528 seconds (allowing short gaps of up to 168~seconds). By combining these criteria, contamination from solar type-III bursts was substantially reduced.

Next, we applied a distance correction (normalized to 30 Re, assuming an r² decay) and start the investigation how the factors controlling AKR appearance and strength are affected with solar activity. The analysis covers the full 30-year Geotail mission period (1992 – 2022). We started the solar maximum (2000 and 2014) and the solar minimum (1996 and 2009), to examine correlations with the solar cycle. Our preliminary analysis yields the following results. (1) AKR occurrence frequency (time fraction of AKRs above a threshold intensity) tends to increase during periods of low solar activity. (2) AKR intensity (frequency-integrated power) does not show a simple or strong correlation with solar activity.

Solar activity can affect AKR through ionospheric conductivity and magnetospheric activity. For examples, it is known that the appearance, strength, and frequency range of AKR show diurnal and seasonal variations associated with the angle of the magnetic axis relative to the Sun (Morioka et al., 2013). These variations are thought to arise from changes in ionospheric conductivity and the configuration of the magnetosphere, and clarifying their relationship with solar activity may provide further insights into these processes. Moreover, frequency variations in AKR could shed light on the dependence of auroral electron acceleration altitudes—linked to magnetosphere – ionosphere coupling—on.

Our analysis will address the dependence of AKR intensity and occurrence frequency in (i) the entire frequency range (78.125 – 625 kHz), (ii) the high-altitude region (low-frequency range, \leq 200 kHz), and (iii) the low-altitude region (high-frequency band around 500 kHz), with the following three factors: (A) Geomagnetic indices: AKR intensity and occurrence can correlate with AE, Kp, and Dst, and their respective influences will be examined separately. (B) Local time dependence: Since AKR is more observed on the nightside, so the local time effect will be distinguished. © Magnetic latitude dependence: AKR is emitted above both polar region and is more readily observed at high latitudes (|MLAT| \geq 20°). Near the magnetic equator, propagation shadow can also occur near the Earth.

In this presentation, we will report on these initial results.

Auroral Kilometric Radiation (AKR) は、地球が放つ最強の電波放射である。オーロラ磁力線上の高エネルギー電子がサイクロトロン共鳴を起こすことで放射される。強度は沿磁力線電流量、周波数は放射高度(電波源のサイクロトロン周波数)と相関しうるため、オーロラ電子の全体量と加速高度の良い指標となる。本研究の目的は、太陽活動からの影響を含めたこれらの統計的な特徴を明らかにすることである。

AKR の発生周波数帯(〜数十 kHz 〜 500-600 kHz)には Solar type-III burst も重畳するため、Wind 衛星(1994〜)を用いた先行研究では、スピン軸平行アンテナの 3-sec 変動標準偏差を閾値とする AKR の自動検出(Waters et al., 2021)や、周波数・時間連続性を組み合わせた拡張(Fogg et al., 2022)が提案されている。

我々は、この手法を改良し、1992 年 9 月から 2022 年 6 月の約 30 年間に及ぶ Geotail 衛星 Plasma Wave Instrument (PWI) の良質なデータから AKR を自動検出した。PWI Sweep Frequency Analyzer (SFA) データへ自動検出手法を適用する際、Wind 衛星と比べて Geotail 衛星は以下の問題を有する。(1) スピン軸平行アンテナが存在しない。衛星スピン(周期: 3-sec)によって電場アンテナと電波到来方向の角度が変動し、スピン位相に起因する変動が重畳する。(2) AKR 観測に最も適する SFA Band-5 (100-800kHz) は、周波数方向のスイープに 8-sec かかる。このため、同一周波数におけるデータ取得周期は 8-sec で、より短時間の変動を捉えられない。このため、我々は以下の 3 つの方法を混合して AKR を識別した。(A) 時間方向の変動が大きい: スピンに伴う強度変動の影響を抑制するため、24-sec 平均(8-sec 周期のデータ 3 つ分、3-sec 周期のスピン 8 回分)をとり、その時間変動の標準偏差を閾値とした(例:4.65 × 10 ^-3 W/m^2/Hz、+-3 回分 = 168-sec)。(B) 周波数方向の変動が大きい: AKR は Solar type-III burst より周波数変動が大きいため、この標準偏差も閾値(例:2.65 × 10 ^-3 W/m^2/Hz、 32 チャンネル(~175kHz)幅)とした。(C)継続時間が長い:より短時間の Solar type-III burst を除外するため、一定の周波数ビン充填数を連続して満たしていること(例:30 チャンネル(~160 kHz)幅で 24-sec x 22 ≈ 528-sec 連続。最大 24-sec x 7 ≈ 168-sec のギャップ許容)を閾値とした。これらを組み合わせることで、Solar type-III の混入を低減し、AKR の検出精度を高めた。

この手法に基づいて検出した AKR に距離補正を加えたうえで(地球距離:30 Re 基準、r² 減衰を想定)、AKR の頻度や強度に影響を与えうる要素が太陽活動度に対してどう変化しうるか、評価を進めている。解析対象期間は Geotail の全運用期間である 1992 年~2022 年の 30 年間である。まずは太陽活動が極大であった 2000 年と 2014 年、極小であった 1996 年と 2009 年に注目して解析している。太陽活動度への依存性については、暫定的に以下の解析結果を得ている。(1)AKR の頻度(一定強度以上の AKR の観測時間):太陽活動度が低い時期ほど高まる傾向が見られる。(2)AKR の強度(周波数積分):太陽活動度との間の単純な相関は必ずしも強くはない。

太陽活動度は、電離圏伝導度や磁気圏活動度を介して AKR に影響を与えうる。その例として、AKR の頻度・強度・周波数範囲は、磁軸が地球と太陽を結ぶ線と成す角の変動に伴って日変動・季節変動を示すことが知られている(Morioka et al., 2013)。原因として、電離圏伝導度や磁気圏形状の変動が示唆されており、太陽活動度との関係の解明はこの解明につながる。AKR の周波数変動は M-I 結合に起因するオーロラ電子加速域高度の情報を与えるため、その太陽活動度からの影響も解明しうる。

解析は(i)全域(全周波数域:78.125-625kHz)、(ii)高高度域(低周波域: \sim 200kHz)、(iii)低高度域(高周波域:500kHz 帯) それぞれの強度・頻度について、以下への依存性を考慮しつつ進めている。

- (A)地磁気指数との関係: AKR の強度・頻度は AE、Kp および Dst 指数と相関しうるため、これらの影響を分離する。
 - (B) ローカルタイム依存性: AKR は夜側でより顕著に観測されるため、この影響を分離する。
- (C)磁気緯度依存性: AKR は両極から放射されるため~ \pm 20°以上の高緯度でより観測されやすい。磁気赤道域では地球に近いと伝播遮蔽も起きるため、その影響も考慮を要する。

本講演では、これらの初期結果について報告する。

ポーラーレインオーロラの発生周期性と太陽活動との関係

#西澤 睦樹 ¹⁾, 細川 敬祐 ¹⁾, Paxton Larry²⁾, Zhang Yongliang²⁾ (¹ 電気通信大学, ⁽² ジョンズ・ホプキンズ大学

Retitive occurence of Polar Rain Aurora Across the Solar Cycle

#MUTSUKI NISHIZAWA¹⁾, Keisuke HOSOKAWA¹⁾, Larry Paxton²⁾, Yongliang Zhang²⁾
⁽¹University of Electro-Communications, ⁽²The Johns Hopkins University Applied Physics Laboratory

Auroras are luminous phenomena that occur when charged particles precipitate into the upper atmosphere (altitude ~100 – 300 km) along the magnetic field lines, where they excite and subsequently de-excite atmospheric oxygen atoms and nitrogen molecules, emitting light. The electrons responsible for auroras do not always come directly from the Sun but are often accelerated in the Earth's magnetotail (plasma sheet). These electrons precipitate into the polar region along closed magnetic field lines, forming a ring-shaped auroral oval centered on the magnetic pole. As a result, during moderately disturbed conditions(i.e., during southward IMF conditions), auroras are absent in the polar cap region. However, on December 25, 2022, during an interval of exceptionally low solar wind density (~0.5 cm⁻³ or lower), a large auroral structure covering the entire polar region was observed (Hosokawa et al., 2024). The unique physical mechanism responsible for this phenomenon was suggested to be polar rain precipitation, generated by a direct influx of solar wind electrons into the polar ionosphere. This type of aurora is observed near the geomagnetic poles and is called polar rain aurora (PRA; Zhang et al., 2007). Highenergy (~keV) electrons in the solar wind, known as "Strahl," directly precipitate along open magnetic field lines, producing spatially uniform emissions in the polar cap. Under typical solar wind conditions, for example southward IMF conditions, auroras do not appear in the polar cap. PRA becomes evident only when the solar wind density is exceptionally low and the Interplanetary Magnetic Field (IMF) is directly connected to the Earth's magnetic field. Because PRA is an extremely rare phenomenon, with fewer than ten reported cases, it has not been widely recognized as a major auroral category.

To investigate the characteristics and origin of this unique aurora, we conducted a long-term statistical analysis using SSUSI data from the DMSP F16, F17, and F18 satellites. The study covers the period from 2005 to 2023. We analyzed transpolar auroral images obtained in the Lyman-Birge-Hopfield short-wavelength channel (140 - 150 nm) through line-scanning observations in imaging mode. The DMSP satellites operate in a Sun-synchronous polar orbit at an altitude of ~850 km, completing a full orbit in ~97 minutes. During the analysis period, at least two of the three DMSP satellites were operational simultaneously, allowing us to obtain large-scale images of auroras in the polar cap at ~50-minute intervals. From the dataset, we identified PRA events and then examined their occurrence frequency, hemispheric distribution, and corresponding solar wind plasma and IMF conditions using NASA's OMNIWeb database. As a result, we detected 14 PRA events over the past two decades, ranging from weak, localized occurrences to strong events covering the entire polar cap. Furthermore, for the first time, we identified a repetitive occurrence of PRA with a cycle of ~25 - 30 days. PRA events were particularly concentrated during periods of significantly reduced solar wind density, and their ~27-day recurrence pattern suggests a potential relationship with Corotating Interaction Regions (CIR). When categorized by solar cycle, we found that during the solar maximum transition of Cycle 25, intense PRA events occurred frequently, whereas only two weak events were detected in Cycle 24. This suggests that PRA occurrence frequency is influenced by the overall strength of solar activity. For Cycle 23, we did not check day-by-day coverage for the entire period; however, previous studies have reported PRA cases within this cycle that also exhibited similar periodicity (e.g., two cases reported by Foster et al. (1976) showed the same ~27-day periodicity). Nevertheless, not every ~27-day recurrence was accompanied by a PRA event; in some cases, it appeared only after skipping one or two ~27-day cycles. This suggests that, even under similar solar wind conditions, additional factors beyond low-density conditions are required for PRA to occur. Future work will include a full day-by-day survey of Cycle 23 to clarify its relationship with solar activity.

2023-2024年で観測された南極昭和基地における準共回転オーロラの出現特性

#佐藤 薫野 $^{1)}$, 田中 良昌 $^{2)}$, 片岡 龍峰 $^{2,3,4)}$, 西山 尚典 $^{2)}$, 小川 泰信 $^{4)}$ $^{(1)}$ 総研大, $^{(2)}$ 国立極地研究所, $^{(3)}$ 沖縄科学技術大学院大学, $^{(4)}$ 情報・システム研究機構

Occurrence Characteristics of Quasi-Co-rotating Auroras Observed at Syowa Station, Antarctica, during 2023 – 2024

#Yukino Sato¹⁾, Yoshimasa TANAKA²⁾, Ryuho KATAOKA^{2,3,4)}, Takanori NISHIYAMA²⁾, Yasunobu OGAWA⁴⁾
⁽¹⁾The Graduate University for Advanced Studies, ⁽²⁾National Institute of Polar Research, ⁽³⁾Okinawa Institute of Science and Technology, ⁽⁴⁾Research Organization of Information and Systems

Auroras with unusual stationary patches were first reported at Poker Flat Research Range (PFRR), Alaska, in October 2000, and were named the "Evening Corotating Patch (ECP) aurora" [Kubota et al., 2003]. Subsequently, Toyoshima (2003) identified 44 similar events and named them "Quasi-Corotating (QC) aurora." Due to geographical restrictions, previous studies have been scarce, and the statistical characteristics are poorly understood.

We present a statistical analysis of QC auroras using data from a monochromatic 391.4 nm all-sky camera at Syowa Station, Antarctica (2023 - 2024). We identified 23 events that occurred in the evening sector (until 20 MLT) and retained their shape and position for more than 20 minutes. Their occurrence peaked around 15 MLT, earlier than previously reported, and most events occurred under quiet conditions (Kp = 1 - 3), consistent with Toyoshima (2003). In September 2025, we will install a multi-wavelength all-sky camera at PFRR, Alaska. In this presentation, we report the Syowa results and outline the new system.

2000 年 10 月にアラスカ・Poker Flat Research Range (PFRR) で、夕方セクターにほぼ同じ形状を維持しながら長時間 視野内に留まり続けるパッチ状オーロラが報告され、Evening Co-rotating Patch (ECP) aurora と名付けられた [Kubota et al., 2003]。ECP aurora はオーロラオーバルの赤道側(L=5~8)に位置し、主に OI 557.7 nm および N2+ 427.8 nm で観 測され、数 keV~10 keV 程度の降下電子が起源とされる。その後、豊島(2003)は類似事例を 44 件報告し、厳密には共 回転せずに漂う特徴から「準共回転オーロラ(QC aurora)」と名付けた。しかし、地理的制約や QC aurora の微弱な発光のため事例数は限られ、統計的理解は不足している。

本研究では、昭和基地に設置された 391.4 nm 全天カメラ(2023 – 2024)より、23 例を抽出し、発生時刻分布を解析した。抽出条件は、夕方セクター(観測開始から 20 MLT まで)、20 分以上、ほぼ形が変わらず、動いていない場合とした。昭和基地は、磁気地方時(MLT)が地方時に比べて約 3 時間遅いため、より早い MLT のオーロラが観測できるという利点がある。その結果、QC aurora は 15 MLT 付近にピークを持ち、豊島(2003)より早い時間帯に出現することを発見した。多くは Kp=1-3 の地磁気静穏時に発生し、豊島(2003)の結果とも一致する。今後は降下粒子メカニズムの解明を進めるとともに、2025 年 9 月よりアラスカで新たに多波長全天カメラを設置し、QC aurora の観測を開始する予定である。本発表では、昭和基地で得られた QC aurora のデータ解析結果と、アラスカでの観測システムの概要についても報告する。

参考論文

記載した参考論文を追加する。

- [1] Kubota, M., et al. (2003), Evening co-rotating patches: A new type of aurora observed by high sensitivity all-sky cameras in Alaska, Geophys. Res. Lett., 30(12), 1612. https://doi.org/10.1029/2002GL016652
- [2] Toyoshima, S. (2003), Characteristics of Quasi-corotating Aurora and Remote Sensing of Magnetospheric Dynamics. Master Thesis, Department of Geophysics, Tohoku University, Japan

#桂華 邦裕 $^{1)}$, 川口 智也 $^{2)}$, 今城 峻 $^{3)}$ $^{(1)}$ 東大・理, $^{(2)}$ 東京大学地震研究所, $^{(3)}$ 京都大学大学院理学研究科附属地磁気世界資料解析センター

Spatiotemporal Evolution of the Storm-Time Ring Current Inferred from Low-Latitude Geomagnetic Observations

#Kunihiro Keika¹⁾, Tomoya KAWAGUCHI²⁾, Shun IMAJO³⁾

⁽¹Graduate School of Science, The University of Tokyo, ⁽²Earthquake Research Institute, The University of Tokyo, ⁽³Graduate School of Science, Kyoto University

The spatiotemporal evolution of the ring current during geomagnetic storms is fundamental to understanding the magnetospheric current system and overall magnetospheric dynamics. Previous studies have examined the ring current intensity and its magnetic local time (MLT) asymmetry mainly through geomagnetic indices such as SYM-H/ASY-H and SMR. In this study, we use geomagnetic field data from a dense global network of low-latitude observatories ($|MLAT| = 10 - 30^{\circ}$) to investigate the temporal development of the storm-time partial ring current. We focus on two superstorms that occurred in 2024 and compare their features with those of other intense and moderate storms.

The analysis is based on geomagnetic data from 14 low-latitude INTERMAGNET observatories. From the horizontal component, we subtract the quiet-time baseline and the diurnal variation (Sq). Using the residuals, we construct UT – MLT maps binned at 3 h in UT and 2 h in MLT. These maps are then processed with harmonic fitting in the MLT direction.

Our results show that the partial ring current initially expands from midnight (00 MLT) toward the noon – dusk sector (12 – 18 MLT) during the main phase, followed by a shift toward noon (12 MLT) in the early recovery phase. This progression likely reflects plasma injection from the midnight sector, subsequent westward drift of energetic ions, and eventual escape through the dayside magnetopause. The observed spatiotemporal evolution indicates that open drift paths of ring current ions persist even during the recovery phase. We further compare the characteristics of superstorms with those of intense storms (SYM-H minima between – 100 and – 200 nT) and moderate storms (SYM-H minima > – 100 nT) to clarify similarities and differences in ring current ion dynamics and the associated partial ring current system.

#桑原 正輝 $^{1)}$, 吉岡 和夫 $^{2)}$, 村上 豪 $^{3)}$, 吉川 一朗 $^{4)}$ $^{(1)}$ 立教大学, $^{(2)}$ 東京大学, $^{(3)}$ 宇宙航空研究開発機構, $^{(4)}$ 東京大学大学院

Observation of the Earth's Plasmasphere in Extreme Ultraviolet by PHOENIX onboard EQUULEUS

#Masaki KUWABARA¹⁾, Kazuo YOSHIOKA²⁾, Go MURAKAMI³⁾, Ichiro YOSHIKAWA⁴⁾
⁽¹Rikkyo University, ⁽²The University of Tokyo, ⁽³Japan Aerospace Exploration Agency, ⁽⁴The University of Tokyo

The Plasmaspheric Helium ion Observation by Enhanced New Imager in eXtreme ultraviolet (PHOENIX) onboard the 6U CubeSat EQUULEUS is a compact extreme ultraviolet telescope optimized for the He II 30.4 nm emission line, which originates from resonant scattering of solar radiation by plasmaspheric He ion. The Earth's plasmasphere is a torus-shaped region of cold plasma surrounding the Earth, whose dynamics are strongly influenced by geomagnetic disturbances. Imaging the plasmasphere in EUV provides a direct method to study its global structure and temporal evolution.

PHOENIX, despite its small size, consists of a multilayer-coated mirror, a metallic thin filter, and a photon-counting detector, achieving an angular resolution better than 0.19 degree and a temporal resolution shorter than 1.5 hr. In May 2023, during EQUULEUS's cruise to the Earth – Moon Lagrange point 2, PHOENIX successfully obtained global meridian-view images of the plasmasphere. The results clearly revealed plasma density structures aligned with dipole-shaped geomagnetic field lines and captured the shrinkage of the plasmasphere associated with a geomagnetic disturbance on May 6. These achievements represent the first global imaging of the plasmasphere using an ultra-small instrument, highlighting the potential of nano-spacecraft to perform advanced space plasma observations.

In addition to these imaging results, ongoing work applies the Minimum L Algorithm to map the plasmapause position onto the geomagnetic equatorial plane based on line-of-sight brightness profiles. Preliminary analysis also indicates an inward motion of the plasmapause during the same disturbance event, demonstrating that the mapping technique can reproduce and quantify the plasmaspheric erosion observed in the images. This presentation will show both the established imaging results and the ongoing efforts toward quantitative plasmapause mapping, highlighting the expanding scientific potential of PHOENIX for future planetary and magnetospheric exploration.

人工衛星観測データの大量統計解析による、赤道面上磁気圏境界の磁気圏サブストームに伴う変形の時間・空間・太陽風依存性の解明

#中村 涼太 ¹⁾, 河野 英昭 ²⁾
⁽¹ 九大, ⁽² 九州大学

Statistical Analysis of Substorm-Associated Deformations of the Equatorial Tail Magnetopause Observed by Satellites

#Ryota Nakamura¹⁾, Hideaki KAWANO²⁾
⁽¹Kyushu University, ⁽²Kyushu University)

Substorms are typically categorized into three phases: the growth phase, the expansion phase, and the recovery phase. During the growth phase, southward interplanetary magnetic fields (IMF) arriving from the Sun become anti-parallel to the geomagnetic field at the dayside magnetopause, triggering magnetic reconnection. The reconnected field lines are carried by the solar wind into the magnetotail, where they accumulate. In the expansion phase, a Near-Earth Neutral Line (NENL) forms around 20 – 30 Re in the magnetotail. Magnetic reconnection at the NENL generates high-speed plasma flows directed both earthward and tailward. During the recovery phase, the IMF turns northward, leading to a gradual restoration of the magnetospheric configuration.

This study aims to investigate the deformation of the magnetotail magnetopause associated with substorms by analyzing satellite data near the magnetic equatorial plane. Previous studies have identified two types of transient events: the Temporary Out-going Event, where the GEOTAIL satellite briefly exits the magnetosphere and re-enters [Kawano et al., 2000], and the Temporary Getting-In Event, where the satellite briefly enters the magnetosphere from the outside and exits again [Shirotani, Master's Thesis, 2017]. These events are believed to be associated with substorms: the former with the equatorial tail-plasma flow toward the NENL to compensate the decrease in the plasma density near the NENL due to high-speed plasma flows during the expansion phase, and the latter with magnetic flux accumulation during the growth phase.

A preceding study (Tsukamoto, Undergraduate Thesis, 2022) analyzed approximately nine years of data from the GEO-TAIL and WIND satellites, along with the AU/AL indices provided by the World Data Center for Geomagnetism, Kyoto University. By relaxing the event selection criteria from Shirotani's study, Tsukamoto increased the number of identified events and found that the time difference between the substorm onset and the start of the Temporary Out-going Event tends to increase with distance from X = -30 Re in the GTL_X coordinate. However, the number of analyzed events was still insufficient in terms of the statistical significance of this feature.

In this study, we aim to improve upon previous results and discover new insights by incorporating additional data from the THEMIS satellites to increase the number of events. In this presentation, we will report on the analysis of all the events consisting of the events newly identified in the THEMIS data and the above-stated GEOTAIL events.

サブストームは成長相、爆発相、回復相の3つに分けられる。成長相においては、地球の昼側で太陽方向からやってくる南向き惑星間空間磁場がマグネットポーズ内の磁気圏磁場との間で反平行になり、磁気リコネクションが発生する。リコネクションでできた磁力線は太陽風により磁気圏尾部へと流されて堆積していく。爆発相においては、磁気圏尾部20~30Re 付近に NENL が形成される。NENL では反平行の磁力線がリコネクションを起こし、地球方向と反地球方向へプラズマの高速フローが発生する。回復相で太陽からやってくる惑星間空間磁場が北向きになることで磁力線の蓄積は徐々に回復し、元に戻る。本研究では、磁気赤道面付近の人工衛星データの解析により、サブストームに伴った磁気圏尾部マグネトポーズの変形の様相を調べることを目標としている。

これまでの研究により、磁気赤道面付近の GEOTAIL 衛星が磁気圏内から短期間で磁気圏外に出て、再び磁気圏に戻る Temporary Out-going Event[Kawano et al.2000] と、磁気圏外から短期間で磁気圏内に入り、再び磁気圏外に出る Temporary getting-In Event[城谷修論 2017] について、サブストームと対応のある場合に前者は爆発相でプラズマの高速フローが発生して NENL 近傍のプラズマが希薄化したのを埋め合わせる為に NENL と磁気圏境界面の間の赤道面上領域でプラズマが NENL に吸引される影響する影響、後者は成長相で磁力線が磁気圏尾部に蓄積することにより発生すると考察されてきた。

先行研究(塚本卒論 2022)では、GEOTAIL 衛星、WIND 衛星による観測データと京都大学大学院理学研究科附属地磁気世界資料解析センターより公開されている AU/AL データを用いて約9年間分のデータ解析が行われた。塚本卒論では城谷修論のイベント選定条件を緩和してイベント数を増やすことで、サブストームオンセットから Temporary Out-going Event 開始時刻までの時間差と GTL $_$ X について、X=-30Re 付近を中心に離れると時間差が大きくなる関係が見られた。しかし、解析されたイベント数は十分ではないため、本研究では、新たに THEMIS 衛星のデータを解析してイベント数を増やすことで、先行研究で得られた結果の向上を目指すと共に、新たな発見を目標とした。本発表では、THEMIS 衛星からのイベントと先行研究のイベントを合わせた解析結果について述べる。

あらせ衛星の地球近傍磁場データを用いた南大西洋異常帯の西方移動の観測

#久田 大生 $^{1)}$, 寺本 万里子 $^{2)}$, 松岡 彩子 $^{3)}$, 山本 和弘 $^{4)}$, 三好 由純 $^{5)}$, 篠原 育 $^{6)}$, 北村 健太郎 $^{2)}$ $^{(1)}$ 九工大, $^{(2)}$ 九州工業大学, $^{(3)}$ 京都大学, $^{(4)}$ 名古屋大学宇宙地球環境研究所, $^{(5)}$ 名古屋大学, $^{(6)}$ 宇宙航空研究開発機構

Observation of the west-shift of the South Atlantic Anomaly with using geomagnetic data from MGF on board the Arase Satellite

#Taiki Hisada $^{1)}$, Mariko TERAMOTO $^{2)}$, Ayako MATSUOKA $^{3)}$, Kazuhiro YAMAMOTO $^{4)}$, Yoshizumi MIYOSHI $^{5)}$, Iku SHINOHARA $^{6)}$, Kentaro KITAMURA $^{2)}$

⁽¹Kyushu Institute of Technology, ⁽²Kyushu Institute of Technology, ⁽³Kyoto University, ⁽⁴Institute for Space-Earth Environmental Research ⁽¹ISEE), Nagoya University, ⁽⁵Nagoya University, ⁽⁶Japan Aerospace Exploration Agency/Institute of Space and Astronautical Science

There is an area called "South Atlantic Anomaly: SAA" above Brazil where the geomagnetic field is weaker than surrounding area and a lot of high energy particle fall in this area. When the spacecraft approaches SAA, some breakdowns may occur due to high energy particles falling from radiation belt. Also, it is known that SAA is moving particularly to the west and the amount of change is approximately 0.2 degrees per year [Jones et.al., 2016]. Therefore, when we operate spacecrafts, it is important to check the position of the SAA and make some measures such as avoiding that area.

In this research, we investigate geomagnetic field at altitudes below 2,000 km by using some data in near Earth obtained by Magnetic Field Experiment (MGF) which is scientific magnetometer onboard the ARASE satellite [Matsuoka et.al., 2018]. We examined spatial distribution by calculating the difference between the magnetic field observed by MGF and the International Geomagnetic Reference Field (IGRF) 14 model every year from 2017 to 2024. By conducting differential analysis with IGRF model, we can extract local and annual geomagnetic field fluctuations obtained from satellite observations based on the main geomagnetic field originating from the inside of the Earth. This method enables quantitative tracking of phenomena such as the westward shift and expansion of the SAA. From 2017 to 2022, particularly at altitudes of 800 km, we confirmed that the weak magnetic field region observed above Brazil was moving westward and that the difference region was expanding.

The weak geomagnetic field region has been observed in detail by the Swarm satellites, orbiting at altitudes of 450km [Finlay et al., 2020]. On the other hand, Arase Satellite has been covering the medium altitude region including 460~1000km. Thus, we can reveal the spatial extension and annual changes of the SAA in this region.

ブラジル上空に存在する地磁気が周囲より弱い領域である南大西洋異常帯 (South Atlantic Anomaly: SAA) では放射線帯からより多くの高エネルギー粒子が降り込みやすくなっており、宇宙機がこの領域に接近すると放射線帯から飛来した粒子が宇宙機に降り込み、誤作動や故障などの原因となる。また、SAA の位置は常に一定ではなく、特に西側方向に大きく移動していることが明らかとなっており、その変化量は年間で 0.2°程度とされている [Jones et.al., 2016]。そのため、宇宙機を運用するときは SAA の位置を把握したうえで SAA 周辺を通過しない軌道にするなどの対策を講じることが重要となる。

本研究ではあらせ衛星に搭載された科学観測用磁力計 Magnetic Field Experiment(MGF) [Matsuoka et.al., 2018] が地球近傍で取得した磁場データを用いて、高度 2000km 以下における地磁気の調査を行った。2017 年から 2024 年までの磁場データを 1 年ごとに区切り、MGF が観測した磁場と International Geomagnetic Reference Field(IGRF)14 モデルとの差分を取り空間分布について調べた。IGRF との差分解析を行うことで、地球内部起源の主磁場を基準に、衛星観測によって得られる局所的かつ経年的な磁場変動を抽出できる。この手法により、SAA の西方移動や広がりといった現象を定量的に追跡することが可能となる。2017 年から 2022 年にかけて特に高度 800km 付近においてブラジル上空にみられた弱磁場領域が西側に移動していること、差分領域が拡大している様子が確認できた。

弱磁場領域そのものは、高度約 450 km を周回する Swarm 衛星によって詳細に観測されてきた [Finlay et al., 2020]。一方、あらせ衛星は 460~1000 km を含む中高度域を長期間にわたってカバーしており、この領域における SAA の空間的広がりや経年的な変化を明らかにすることができる。

AMPERE データを用いた高緯度フィールドアライン電流のクラスタリング解析と 代表構造の抽出

#池元 大 ¹⁾, 吉川 顕正 ²⁾
⁽¹ 九大院理・地球惑星, ⁽² 九大・理

Clustering Analysis and Extraction of Representative Field-Aligned Current Patterns Using AMPERE Data

#Dai Ikemoto¹⁾, Akimasa Yoshikawa²⁾

(1 Graduate School of Science, Kyushu University, (2 Faculty of Science, Kyushu University

Field-Aligned Currents (FACs), which connect the Earth's magnetosphere and ionosphere, form large-scale current systems in response to solar wind variability and play a crucial role in understanding the magnetosphere – ionosphere (M-I) coupling process. In particular, the spatial distribution and temporal evolution of high-latitude FACs are essential for understanding magnetospheric dynamics and for space weather forecasting. However, traditional statistical models and empirical reconstructions (e.g., Weimer, 2001) are based on averaged FAC structures and are limited in their ability to capture the diversity of observed current patterns and nonlinear state transitions.

Recently, Kunduri et al. (2020) demonstrated that deep learning models can be used to predict future distributions of FACs by treating AMPERE FAC maps as time-series image data. Their results suggest that FAC structures tend to evolve in temporally and spatially ordered patterns, which indicates the potential usefulness of unsupervised machine learning approaches for extracting typical current structures and classifying dynamic states.

In this study, we apply principal component analysis (PCA) and k-means clustering to global FAC maps obtained every 10 minutes from the AMPERE (Active Magnetosphere and Planetary Electrodynamics Response Experiment) project using the Iridium satellite constellation. The objective is to extract representative spatial patterns of high-latitude FACs in a data-driven manner. We are currently conducting data preprocessing and initial clustering analysis, and the results will be presented at the conference.

地球磁気圏と電離圏を結ぶ沿磁力線電流(Field-Aligned Currents, FACs)は、太陽風の変動に応答して大規模に形成される電流系であり、磁気圏―電離圏結合過程の理解において重要な役割を果たす。特に高緯度電離圏における FAC の空間分布や時間発展の特徴は、宇宙天気予報や磁気圏状態の把握にとって不可欠である。しかし、従来の統計モデルや経験的再現(例:Weimer, 2001)は FAC の平均構造に基づいており、観測に見られる多様な電流分布や非線形な状態遷移を十分に捉えるには限界があった。

近年、Kunduri et al. (2020) は、AMPERE の FAC マップを深層学習モデルに入力することで、FAC の将来的な空間分布を予測可能であることを示した。この成果は、FAC 構造が時空間的に一定の秩序やパターンに従って遷移することを示唆しており、教師なし機械学習によるパターン分類や代表構造の抽出にも有効性を示唆するものである。

本研究では、Iridium 通信衛星群によって取得された AMPERE(Active Magnetosphere and Planetary Electrodynamics Response Experiment)の 10 分間隔・全球 FAC マップに対して、主成分分析(PCA)および k-means クラスタリングを適用することで、高緯度 FAC 構造の代表的な空間パターンをデータ駆動的に抽出することを目的とする。現在、データの前処理および初期的なクラスタリング解析を進めており、その結果については学会にて報告する予定である。

磁気圏3次元グローバル電磁流体シミュレーションに基づく超低温矮星のオーロラ 電流の推定

#原 亮太 $^{1)}$, 木村 智樹 $^{1)}$, 深沢 圭一郎 $^{2)}$, アサ サティアグラハ $^{1)}$, 藤井 友香 $^{3)}$, 垰 千尋 $^{4)}$ (1 東京理科大, $^{(2)}$ 総合地球環境学研究所, $^{(3)}$ 国立天文台, $^{(4)}$ 情報通信研究機構

Estimation of Auroral Currents in Ultracool Dwarfs Based on 3D Global Magnetohydrodynamic Simulations

#Ryota HARA¹⁾, Tomoki KIMURA¹⁾, Keiichiro FUKAZAWA²⁾, Satyagraha ASA¹⁾, Yuka FUJII³⁾, Chihiro TAO⁴⁾
⁽¹Tokyo University of Science, ⁽²Research Institute for Humanity and Nature, ⁽³National Astronomical Observatory of Japan, ⁽⁴National Institute of Information and Communications Technology

Auroral emissions occur when charged particles surrounding an astronomical body are accelerated along magnetic field lines by energy input from the stellar winds, planetary rotation, or intrinsic magnetic fields, and subsequently collide with the atmosphere. The detection of auroral emissions thus serves as a key indicator of the presence of both magnetic fields and atmospheres. If auroral emissions are detected from exoplanets, they would provide direct evidence of magnetic fields and atmospheres, significantly contributing to the assessment of planetary habitability. Auroral radio emissions exhibit circular polarization (Wu & Lee, 1979), allowing them to be distinguished from other astrophysical radio sources, such as stellar radio bursts, which are typically weakly polarized. To prioritize observational targets among the many known exoplanets, researchers have employed theoretical and numerical estimations of auroral radio power using models such as the magnetosphere-ionosphere (M-I) coupling framework (Nichols & Milan, 2016) and global 3D MHD simulations (Turnpenney et al., 2020). These studies suggest that the typical auroral radio power of hot Jupiters is approximately 10^{15} W. Nevertheless, only one marginal detection of auroral radio emission from an exoplanet has been reported to date (Turner et al., 2021), which requires further model validation and refinement with the observation data.

In this context, ultracool dwarfs (UCDs) have recently attracted attention as promising analogs for testing auroral models relevant to exoplanets. Several UCDs with rapid rotation (periods of a few hours) and strong surface magnetic fields (several kilogausses) have exhibited intense, highly circularly polarized radio bursts, which are likely the auroral radio emissions (e.g., Hallinan et al., 2006). Nichols et al. (2012) and Turnpenney et al. (2017) extended their magnetosphere-ionosphere (M-I) coupling models originally developed for Jupiter and Saturn (e.g., Hill, 1979) to UCD's auroral processes using input parameters of UCD's typical environment. While these studies successfully reproduced observed radio power levels, some of the input parameters, including plasma angular velocity profiles and mass loading rates, remain largely uncharacterized, which introduced considerable uncertainty in the obtained auroral radio power.

Here, we conduct a three-dimensional global MHD simulation (Fukazawa et al., 2005) for UCDs that utilizes only well-constrained parameters, leading to a reduction of model uncertainty. This approach minimizes assumptions and enables a more self-consistent modeling of magnetospheric dynamics. Based on this simulation, we derived the auroral current and estimated the auroral radio power as a function of ionospheric Pedersen conductance. For example, the total auroral current of the UCD LSR J1835+3259 was estimated to be $^{\sim}1\times10^{10}$ A in our simulation. By comparing our results with VLA observations of LSR J1835+3259 (Hallinan et al., 2008), we inferred that a Pedersen conductance of approximately 1 – 10 mho is required to reproduce the observed radio power ($^{\sim}10^{15}$ - 10^{16} W). This estimate is consistent with another independent estimation from the M-I coupling model (0.1-10 mho) presented by Satyagraha et al. (SGEPSS 2024). These results suggest the validation of our model. In future work, we aim to extend this methodology to hot Jupiters and Earth-like exoplanets to further validate our model and support future observational strategies. Here, we present the current status of our study.

オーロラは、天体周囲の宇宙空間に存在する荷電粒子が、恒星風や惑星の自転・固有磁場からエネルギーを得て磁力線に沿って加速され、大気に衝突することで起こる現象である。オーロラは、天体に磁場と大気が存在することを示す重要な指標となる。系外惑星からオーロラ放射が検出されれば、磁場と大気の存在を示す直接的な証拠となり、生命居住可能性の評価に大きく貢献する。オーロラ由来の電波放射は円偏波を示すため (Wu & Lee, 1979)、円偏波しにくい恒星電波など他の電波源と区別できる。数ある系外惑星の中から観測候補天体を絞り込むには、理論モデル・数値シミュレーションによる系外惑星オーロラ電波の放射パワー等の推定が必要である。先行研究よって、系外惑星向けに磁気圏-電離圏 (M-I) 結合モデリング (Nichols and Milan, 2016) や 3 次元グローバル電磁流体力学 (MHD) シミュレーション (Turnpenny et al., 2020) が行われ、Hot Jupiter のオーロラ電波放射パワーは典型的には約 10^{15} W と見積もられた。この推定値は観測で検証されるべきであるが、現在までの系外惑星からのオーロラ電波の検出報告は 1 例(Turner et al., 2021)のみであり、検証が進んでいない。

系外惑星オーロラモデルの検証対象として、超低温矮星(Ultracool Dwarf; UCD)が注目されている。 UCD の中でも、

自転周期が数時間程度と極めて短く、磁場強度が数 kG に達する強磁場天体では、円偏光度の高い $^{-10^{16}}$ W の強力なオーロラ電波と思われる放射が複数報告されている(例:Hallinan et al., 2006)。Nichols et al. (2012) および Turnpenny et al. (2017) は、木星や土星などの回転磁化惑星向けの M-I 結合モデル(Hill, 1979)を応用し、UCD のパラメータでオーロラ過程を模擬した。その結果、観測値に匹敵するオーロラ電波放射パワーが再現された。しかし、UCD の周囲のプラズマ環境は未探査のため、モデルでは磁気圏プラズマの回転角速度やマスローディングレートなど、多くの未確定パラメータを仮定しており、得られた結果には恣意性や大きな不定性が含まれている。

そこで本研究では、不定性の小さなパラメータのみを採用し、3次元グローバル MHD モデル (Fukazawa et al., 2005) で、UCD の磁気圏及びオーロラ過程を客観的に模擬した。本研究のモデルでは、先行研究のモデルに比べて仮定すべきパラメータが少なく、各物理量がシミュレーション内で自己無撞着に決定することができる。UCD の 1 つである LSRJ1835+3259 の磁気圏を模擬した結果、電波放射に関連するオーロラ電流の総量は $^{-1}$ × $^{-10^{10}}$ A と推定された。この電流総量の推定値から、オーロラ電波放射のパワー を電離圏の電気伝導度の関数として導出した。VLA による LSRJ1835+3259 の観測値 (Hallinan et al., 2008) と比較した結果、観測されたオーロラ電波のパワー($^{-15}$ - $^{-10^{16}}$ W)を再現するために必要な電離圏の伝導度は、 $^{-10}$ mho であると推定された。この値は Satyagraha et al. (SGEPSS 2024) による UCD の M-I 結合モデルにおいて、本研究と独立に制約された電離圏伝導度 (0.1-10 mho) と矛盾しない。従って、本研究の MHD モデルは UCD のオーロラ過程を説明する妥当なモデルである可能性が高い。 今後は本研究で構築したモデルを Hot Jupiter や地球型系外惑星にも応用し、モデルの検証や系外惑星探査を行う予定である。本発表では現状について報告する。

R006-P52

ポスター1:11/25 AM1/AM2 (9:15-12:35)

#中溝 葵 $^{1)}$, 吉川 顕正 $^{2)}$, 中田 裕之 $^{3)}$, 深沢 圭一郎 $^{4)}$, 田中 高史 $^{2)}$ $^{(1)}$ 情報通信研究機構, $^{(2)}$ 九州大学, $^{(3)}$ 千葉大学, $^{(4)}$ 総合地球環境学研究所

Large-scale FAC pattern and SW-M-I coupling 2

#Aoi Nakamizo¹⁾, Akimasa YOSHIKAWA²⁾, Hiroyuki NAKATA³⁾, Keiichiro FUKAZAWA⁴⁾, Takashi TANAKA²⁾
⁽¹National Institute of Information and Communications Technology ⁽NICT), ⁽²Kyushu University, ⁽³Chiba University, ⁽⁴Research Institute for Humanity and Nature ⁽RIHN)

The motivation for this study arises from a question: While it is observationally known that the Field-Aligned Current (FAC) patterns change depending on factors such as the IMF orientation, can they also be influenced by ionospheric conductance? Here note that we are targeting the FAC pattern, not the electric potential pattern for which we have reported on various types of deformation and its causes in our past research.

Since FAC is driven by the SW-M-I dynamics, we investigate this issue using a global MHD model. We performed the simulations with various combinations of conductance distributions and IMF orientations:

- (1) Uniform conductance distribution
- (2) Distribution including only the increase due to solar illumination
- (3) Distribution including an increase in the auroral zone

IMF-By values were considered as zero, positive, and negative.

As an initial result, we found that when there is auroral enhancement in the conductance distribution, the FAC patterns exhibit dawn-dusk asymmetry. We will show further details, including other results and discussions related to SW-M-I coupling.

R006-P53

ポスター1:11/25 AM1/AM2 (9:15-12:35)

水星磁気圏内部における太陽風イオンダイナミクスの3次元シミュレーション解析

#高村 彪丸 ¹⁾, 臼井 英之 ¹⁾, 三宅 洋平 ¹⁾, 松本 正晴 ²⁾

(1 神戸大学大学院システム情報学研究科, (2 福島大学情報基盤センター

Hybrid particle simulation for ions dynamics in Mercury's inner magnetosphere

#Toramaru TAKAMURA¹⁾, Hideyuki USUI¹⁾, Yohei MIYAKE¹⁾, Masaharu MATSUMOTO²⁾

(1) Kobe University Graduate School of System Informatics, (2) Information Technology Center, Fukushima University

Mercury, like Earth, has an intrinsic magnetic field. However, because it is the innermost planet of the Solar System and its magnetic field is weak, it responds sensitively to solar wind fluctuations, creating a unique magnetospheric environment with characteristics similar to but distinct from Earth's magnetosphere. Due to the harsh environment, past in situ observations have been limited to Mariner 10 and MESSENGER. Much remains unknown about the plasma environment of Mercury's magnetosphere, particularly its internal current structure and associated particle dynamics. The ongoing BepiColombo international mission is expected to provide more detailed observational data, and advance prediction of the physical picture through simulation studies is crucial. In this study, we employ a three-dimensional hybrid code, which treats ions as particles and electrons as fluids, focusing particularly on the solar wind condition during the BepiColombo flyby. In addition to plasma structures derived from the hybrid runs, we also track ion trajectories using test particle simulations using electromagnetic field data obtained from the hybrid simulations and analyze their dynamics in detail.

水星は、地球と同様に固有磁場を持つ惑星であるが、太陽系惑星の中で太陽に最も近く、その磁場が弱いことから、太陽風の変動に対して敏感に応答し、地球磁気圏と似通りつつも異なる特徴を持つユニークな磁気圏環境を形成する。過酷な環境下であるため、過去の探査機観測はマリナー 10 号と MESSENGER に限られており、水星磁気圏のプラズマ環境、特に内部の電流構造やそれに関連する粒子ダイナミクスには未解明な点が多い。現在進行中の BepiColombo 探査計画では、より詳細な観測データが得られることが期待されており、シミュレーション研究による物理描像の事前予測は極めて重要である。本研究では、シミュレーションツールとしてイオンを粒子、電子を流体として扱う 3 次元ハイブリッドコードを使用し、特に BepiColombo 計画におけるフライバイ時の太陽風ケースについて着目した。得られた磁気圏構造の他、ハイブリッドシミュレーションで得られた電磁場データを用いたテスト粒子シミュレーションによってイオンの軌道を追跡し、そのダイナミクスを詳細に解析、結果を議論する。

北向き IMF における太陽風磁気圏系での磁力線トポロジーとプラズマの相互作用 (2)

#藤田 茂 $^{1)}$, 渡辺 正和 $^{2)}$, 田中 高史 $^{2)}$, 蔡 東生 $^{3)}$ $^{(1)}$ 統数研, $^{(2)}$ 九州大学, $^{(3)}$ 筑波大学

Interaction between topology and plasma dynamics of the solar wind-magnetosphere system in the northward IMF conditions (2)

#Shigeru Fujita¹⁾, Masakazu WATANABE²⁾, Takashi TANAKA²⁾, Dongsheng CAI³⁾
⁽¹Institute of Statistical Matheematics, ⁽²Kyushu University, ⁽³University of Tsukuba

Fujita et al. [2025] discussed the quasi-steady magnetic field structure of the solar wind-magnetosphere system under northward IMF conditions. Their discussion was framed from the perspective of the interaction between magnetic topology and plasma dynamics. In addition, they demonstrated that the vacuum magnetic field, which is produced by the superposition of the Earth's dipole field and the IMF, preserves the fundamental topological form of the solar wind-magnetosphere system. This topology provides the fundamental magnetic field structure necessary for magnetic reconnection between the IMF and the Earth's magnetic field. They further pointed out that the vacuum magnetic field represents the ground state of the system. Based on this finding, they argued that the quasi-steady magnetic field structure is determined by the balance between two forces: the deformation force exerted by plasma and the restoring force that tends to return the field to its ground state. Furthermore, the magnetic reconnection process is inherently built into this magnetic structure. From this viewpoint, the process of magnetic reconnection is naturally incorporated into the overall description.

We apply the above theory to a detailed poster discussion of the magnetic field structure and plasma distribution in the solar wind-magnetosphere system under northward IMF conditions. The topics we will address include:

- (1) the relationship between the magnetic field structure and plasma distribution in the tail, and the resulting plasma flow;
- (2) the contribution of topology to the generation of plasma sheets and the flow path of the electromagnetic energy carried by them;
 - (3) the current distribution leading to a magnetic field structure deformed from the vacuum magnetic field.

References

Fujita, et al. (2025), Fundamental physical processes of the steady solar wind-magnetosphere system in the northward IMF condition, submitted to EPS.

惑星間空間磁場北向き時の磁気圏尾部に現れる閉磁束と惑星間空間磁束の鎖交

#渡辺 正和 $^{1)}$, 田中 高史 $^{2)}$, 蔡 東生 $^{3)}$, 藤田 茂 $^{4)}$ $^{(1)}$ 九州大学, $^{(2)}$ 九州大学, $^{(3)}$ 名古屋商科大学, $^{(4)}$ 情報・システム研究機構

Interlinkage of closed and interplanetary magnetic flux in the magnetotail during northward interplanetary magnetic field periods

#Masakazu WATANABE¹⁾, Takashi TANAKA²⁾, Dongsheng CAI³⁾, Shigeru FUJITA⁴⁾
⁽¹Kyushu University, ⁽²Kyushu University, ⁽³Nagoya University of Commerce and Business, ⁽⁴Research Organization of Information and Systems

In global magnetohydrodynamic simulations for northward interplanetary magnetic field (IMF), interlinkage of closed and interplanetary magnetic flux sometimes appears in the magnetotail. This indicates that the basic 2-null, 2-separator structure of the magnetosphere is broken, at least locally. Due to numerical errors etc., however, the location of the new nulls that are breaking down the 2-null, 2-separator structure has long been a mystery. We here propose a model in which the new nulls appear near the two original nulls that constitute the 2-null, 2-separator structure. That is, the original magnetic null (one in each hemisphere) multiplexes to form a null cluster (null region), and the magnetic flux interlinkage is formed within the null region. The simplest magnetic topology of the clustering is a 4-null, 4-separator structure, with two nulls in each hemisphere and four separators connecting them. If we trace the reconnection sequence expected in the 4-null, 4-separator structure from the simulation results, the formation process of the magnetic flux interlinkage is obtained in a natural way. The key reconnection is IMF-lobe reconnection that occurs simultaneously in both hemispheres (the so-called dual lobe reconnection, DLR). In the 2-null, 2-separator structure, IMF-lobe reconnection normally occurs independently in the northern hemisphere and in the southern hemisphere (or in the dawn hemisphere and in the dusk hemisphere), forming independent magnetic flux circulations. The DLR mixes the two magnetic flux circulations; therefore, a steady magnetic flux circulation is no longer maintained.

惑星間空間磁場(interplanetary magnetic field, IMF)北向き時のグローバル磁気流体シミュレーションでは、磁気圏尾部に鎖交する閉磁力線と惑星間空間磁力線が現れることがある。これは磁気圏の基本構造である 2-null, 2-separator 構造が、少なくとも局所的には壊れていることを意味する。しかし数値誤差などの影響もあり、2-null, 2-separator 構造を壊す新たな零点がどこにあるのか長らく謎であった。このたび我々は、新たな零点は元々の 2-null, 2-separator 構造を形成する 2 つの零点近傍に出来るとするモデルを提案する。すなわち、元々南北半球に 1 個ずつある零点が、複数個の零点から成る零点クラスタ(零領域)を形成し、零領域の内部で鎖交する磁力線が形成される。その最も簡単な磁場トポロジー構造は、南北半球にそれぞれ 2 個ずつ零点が存在する 4-null, 4-separator 構造である。シミュレーション結果から予想されるリコネクションの時系列をこの 4-null, 4-separator 構造で追跡すると、自然な流れで鎖交磁力線が形成される。特に鍵となるリコネクションは、南北同時に起こる IMF-lobe リコネクション(いわゆる dual lobe reconnection, DLR)である。2-null, 2-separator 構造では、通常 IMF-lobe リコネクションは南北(あるいは朝夕)独立に起こり、それぞれに独立な磁束循環を形成する。DLR は 2 つの磁束循環を混合させるため、定常な磁束循環は維持できなくなる。

#坂野井 健 $^{1)}$, 吉川 一朗 $^{2)}$, 石井 智士 $^{3)}$, 吹澤 瑞貴 $^{4)}$, 西山 尚典 $^{4)}$, 山崎 敦 $^{5)}$, 浅村 和史 $^{5)}$, 三好 由純 $^{6)}$ $^{(1)}$ 東北大学理, $^{(2)}$ 東京大学大学院, $^{(3)}$ 立教大学, $^{(4)}$ 国立極地研究所, $^{(5)}$ 宇宙航空研究開発機構, $^{(6)}$ 名古屋大学

Design and development of visible and far ultraviolet auroral imagers for the future satellite mission FACTORS

#Takeshi Sakanoi¹⁾, Ichiro YOSHIKAWA²⁾, Satoshi ISHII³⁾, Mizuki FUKIZAWA⁴⁾, Takanori NISHIYAMA⁴⁾, Atsushi YAMAZAKI⁵⁾, Kazushi ASAMURA⁵⁾, Yoshizumi MIYOSHI⁶⁾

⁽¹Graduate School of Science, Tohoku University, ⁽²The University of Tokyo, ⁽³Rikkyo University, ⁽⁴NIPR, ⁽⁵ISAS/JAXA, ⁽⁶Nagoya University

We report the recent status of design and development of auroral imagers at visible and far-ultraviolet (FUV) wavelengths for the future satellite mission FACTORS. In addition, we also concern the science objectives with these imagers. FACTORS stands for Frontiers of Formation, Acceleration, Coupling, and Transport Mechanisms Observed by the Outer Space Research System, which will be proposed as a next generation polar orbiting formation flight multi-satellite mission. Major scientific targets are: 1) energy transport in the magnetosphere-ionosphere (MI) coupling system and their relationship to small-scale auroral phenomena, 2) particle transport in the MI system by ion outflow, and. Observation of small-scale plasma parameters and simultaneous auroral imaging data obtained with multi-satellite measurements in the altitude range from ~300 km to ~3500 km enable us to understand dynamical spatial and time variations in the MI coupling system, such as an Alfvenic wave acceleration and small-scale discrete aurora. Field-aligned current, particle distribution function, and Poynting flux obtained with FACTORS are the key parameters to reveal small-scale aurora.

We are designing and developing visible and FUV imagers for this mission. To observe dynamical morphology of small-scale aurora, both visible and FUV images are required to have high-spatial and high-time resolution capability. For the visible camera, called VISAI, we require the spatial resolution of ~1km x1km at apogee (~3500km altitude) with a time resolution of ~1 to 10 frame/sec and the sufficient sensitivity for auroral intensity of ~1 kR. Target auroral emission should be permitted lines for the high-time resolution imaging, and N2 1PG (670nm) or N2+ 1NG (391 or 428nm) is candidate. We have established high-spatial and high-time resolution auroral imaging measurement with MAC on the Reimei satellite and AIC on the LAMP rocket. We require the capability of VISAI to achieve the field- of-view (FOV) of 8deg x 8deg which mapped area on the auroral emission layer is ~500km x 500km with the spatial resolution of ~1.5km x 1.5km when the satellite is at the apogee. We carried out the optical design of objective lens (f=120mm, F/1.5). We are selecting an appropriate CMOS sensor to satisfy the required FOV and spatial resolution.

We developed the engineering model (EM) of VISAI with a candidate CMOS detector (Caeleste, ELFIS2), a commercial objective lens (Tholab, f=200mm, F/8.3), and an interference filter 620nm with the bandwidth (FWHM) of 3nm. We calibrated the sensitivity of VISAI-EM using the integrated sphere in NIPR on Jan. 7, 2025. By changing the intensity of integrated sphere from 1kR/nm to 100kR/nm (at 630nm), we captured 100 images for each exposure time (1s, 0.1s, 0.01s). We also measured dark frame by turning off the lamp of integrated sphere. Using these data, we determined the read noise of 21 count r.m.s., dark noise in a room temperature of 1000 count/s/pix with the A/D conversion unit of 0.259 el/count, which is consistent with the specification of the Caeleste ELFIS2 CMOS. We estimated the counts for the case of VISAS by converting the counts using the lens parameters between the EM lens and FACTORS lens including pixel binning. We finally examined the SNR of auroral image including the read noise, dark noise, and photon shot noise, and validated that SNR of ~20 with a 0.1 s exposure time for 1kR auroral intensity.

Concerning the FUV imager, called FUVI, we are discussing to observe only OI 135.6nm aurora or both of OI 130.4nm and 135.6nm. We designed the FOV of FUVI of 14deg x 14deg, which is wider FOV of VISAI. The advantage of FUVI is the capability of FUV auroral observation in a sunlit condition. To avoid the solar contamination in the visible range, we adopt the image intensifier (II) with MCP as a 2D array detector. We fabricated the candidate II without coating of the photocathode (i.e., bare MCP) for FUVI. Using this II, we developed the engineering model (EM) of FUVI, and going to test it with UV light in FY2025 to check the performance of bare II. In addition, we will investigate the coating material of photocathode (e.g., CsI) to gain signal-to-noise ratio obtaining better sensitivity of FUV aurora and sufficient suppression of solar visible contamination. We will procure the II with coating, and make testing or the capability to compare with the bare II.

デジタル方式フラックスゲート磁力計開発のための入出力周波数特性の評価

#田中 颯 1), 松岡 彩子 2)

(1 京都大学 理学研究科 地球惑星科学専攻, (2 京都大学 理学研究科 地磁気世界資料解析センター

Evaluation of input-output frequency characteristics for digital-type fluxgate magnetometer

#Hayato Tanaka¹⁾, Ayako Matsuoka²⁾

⁽¹Division of Earth and Planetary Sciences, Graduate School of Science, Kyoto University, ⁽²Data Analysis Center for Geomagnetism and Space Magnetism, Kyoto University

Recently the target of space exploration is expanded to the wider area in the solar system. As a result, observation instruments of wider variety are installed on a single spacecraft and the technology for the in-situ observation has been developed to design the feasible spacecraft. Digital-type fluxgate magnetometer, which is small and power-saving compared with the conventional analog-type, is more suitable for the future exploration by spacecraft, on which more various and smaller observation instruments would be installed. Meanwhile the devices and materials used for instruments on spacecraft require a high degree of reliability and must be tolerant of the severe space environment, e.g., high and low temperatures and radiation. The reliability and environment tolerance strictly restrict the available device, material and design of the instruments. A Field Programmable Gate Array (FPGA), a digital logical processor, is used for the most processing of the pickup signal from the sensor of the digital-type fluxgate magnetometer. The goal of this research is to develop the processing in the FPGA of a digital-type magnetometer with improved performance over conventional one while overcoming these limitations.

This study and development are based on the design of a digital-type fluxgate magnetometer developed for the SS-520-3 sounding rocket experiment. Since the output data from the magnetometer to the magnetic-field input depend on the frequency of the magnetic field time variation, the frequency characteristics of the response of the magnetometer should be evaluated with high accuracy. We numerically simulated and modeled the frequency characteristics and derived the overall transfer function of the digital-type fluxgate magnetometer. When the frequency response of the model was compared with the actual breadboard device designed similarly to the digital-type fluxgate magnetometer installed on the SS-520-3 sounding rocket, differences were identified. These differences are supposed to be caused by the disagreement of characteristics of the modulation process of the signal, particularly a phase detection unit. The fluxgate magnetometer modulates the AC pickup voltages into DC signals corresponding to their amplitude. In the numerical model, the phase detection unit's computations, performed in the FPGA, may not be exactly simulated by the model due to the shortage of accuracy in the numerical expression of the frequency characteristics of the modulation operations. Therefore, to conduct a more detailed comparison between the actual device and the model concerning the FPGA's operations, we established a new evaluation method. This method involves generating a simulated pickup signal within the FPGA and extracting the phase detection output. This allows us to obtain the frequency characteristics of the phase detection unit in isolation, enabling us to compare and revise the frequency characteristics of the model and the actual device for just the phase detection unit. By modifying the model based on this comparison, we aim to achieve better agreement between the frequency characteristics of the model and the actual device.

In this presentation, we will show this new evaluation method for a more detailed investigation of the frequency characteristics of the FPGA-based phase detection unit and discuss its results. Furthermore, we will discuss the suitable scheme to define the FPGA parameter design to enhance the performance of digital-type fluxgate magnetometers.

近年の探査技術の向上により、太陽系における直接探査の領域や対象が広がりつつある。これに伴い、一つの宇宙機に多種多様な観測機器を搭載する傾向にある。小型化・省電力化したデジタルフラックスゲート磁力計は、観測機器の増加、小型化の進む近年の宇宙機での観測に適している。しかし、宇宙機に搭載する機器で使用する部品には高度な信頼性が要求され、また熱や放射線等の過酷な宇宙環境に耐える必要があることから、設計は制約を受ける。デジタル方式のフラックスゲート磁力計では、デジタル演算素子の Field Programmable Gate Array (FPGA) でピックアップ信号の処理の大半を行う。この制約を克服しつつ、従来よりも性能を向上させたデジタル方式の磁力計における FPGA 演算を開発することが本研究の最終的な目標である。

本研究では観測ロケット SS-520-3 号機に搭載されたデジタル方式フラックスゲート磁力計の設計をベースに検討と開発を行う。磁場の入力に対する磁力計の出力の振幅や時間遅れは磁場変動の周波数に依存するため、入力信号に対する出力信号の応答の周波数特性を精度よく評価することが求められる。そこで磁力計の伝達関数を計算機でシミュレーションして求め、周波数特性をモデル化した。そしてこの周波数特性モデルを SS-520-3 号機搭載デジタル方式フラックス

ゲート磁力計と同じ設計を持つ試験機の周波数特性と比較したところ、モデルと実機の周波数特性には差異があった。この差異の要因として考えられるのが信号を変調している部分、特に位相検波部である。フラックスゲート磁力計の位相検波部では、交流のピックアップ電圧を、その振幅に対応する直流の信号に変調している。位相検波部は FPGA の内部で計算しているが、モデルでは信号を変調する演算の周波数特性が厳密な正確さで数式化できていないことが差異の原因であると考えられる。そこで、FPGA での演算について、より詳細な実機とモデルの比較を行うために新たな評価方法を考案した。この評価方法では FPGA の内部でピックアップ信号を模擬した信号を生成して、位相検波の出力を取り出す。これにより位相検波部単体の周波数特性が得られ、位相検波部に限定した周波数特性をモデルと実機の間で比較することができる。この評価方法によりモデルを修正することで、モデルと実機の周波数特性の一致をはかる。

今回の発表においては FPGA による位相検波部の周波数特性をより詳細に検討するため新たに構築した評価方法を提示し、その結果を考察する。また、デジタル方式フラックスゲート磁力計の性能を向上させるための、FPGA コーディングにおけるパラメータ設計を検討する。

フローティング電源プリアンプを用いた宇宙プラズマ電界観測システムの開発

#田中 恵太 ¹⁾, 栗田 怜 ²⁾, 小嶋 浩嗣 ²⁾

(1 京都大学大学院工学研究科, (2 京都大学生存圈研究所

Development of an electric field measurement system in space plasmas using a preamplifier based on a floating power supply

#Keita TANAKA¹⁾, Satoshi KURITA²⁾, Hirotsugu KOJIMA²⁾

(1 Graduate School of Engineering, Kyoto University, (2 RISH, Kyoto University

In the observation of electric fields in space plasma, electric field detectors must cover a wide frequency range, from DC to 10 MHz, with high sensitivity. Because plasma is a dispersive medium, the impedance of electric field sensors is a function of frequency, and impedance matching between the sensor and preamplifier is impossible. An extremely high input impedance is required for the preamplifier to improve observation sensitivity. Additionally, electric field sensors exhibit complex features in measuring DC electric fields, influenced by the electrostatic potentials of the sensors and spacecraft charging.

The Japanese conventional design for preamplifiers features two independent units, each dedicated to DC or AC measurement, respectively. However, this structure leads to an impedance drop due to the interaction of the input impedances of two amplifiers, which declines sensitivity, especially in DC measurements.

On the other hand, European and U.S. missions have used floating power supply preamplifiers that automatically follow the DC voltage of the sensor by supplying power to the preamplifier at a potential independent from the satellite with an isolated DC/DC converter, and by using the output potential of the preamplifier as the potential reference of the converter. The input impedance in this method is theoretically infinite.

In this study, we propose a floating power supply preamplifier utilizing a bootstrapping power supply consisting of transistors, rather than isolated DC/DC converters, which are commonly used in conventional floating power preamplifiers. This is intended to operate in the same way as a European or U.S. floating power supply preamplifier, generating a constant current from the satellite's internal high-voltage power supply to create a floating potential independent of the satellite's potential, and using the preamplifier's output as the reference for the floating potential. This device does not need a DC/DC converter in the floating power supply, thereby eliminating the effect of switching noise on the observation results, which was a problem with the European and American types. Moreover, since the floating power supply system uses only one preamplifier, it can prevent sensitivity degradation in DC measurements, which was a problem with conventional Japanese satellites.

Through performance evaluations, we have confirmed that this design has a good DC response and linearity within \pm 98.5 V, a flat frequency response up to approximately 3 MHz, and a low noise level comparable to that of the Arase satellite in operation.

In this presentation, we will show the outline and details of the new preamplifier under development, as well as the results of the performance evaluation of the test circuit.

宇宙プラズマ中における電界計測では、直流電場から広帯域の交流電場までを高感度に計測する必要がある。ここで、プラズマは分散性媒質であるため計測装置の電界センサーのインピーダンスが周波数の関数となり、センサーとプリアンプの間のインピーダンス整合をとることが難しい。このため、計測感度向上には、プリアンプの入力インピーダンスを極めて高くすることが求められる。また、特に直流電場の計測では、衛星やセンサーそのものの帯電が影響する複雑な系となり、正確な計測を行うには、センサーの電位制御などが重要となる。

過去の日本の観測衛星では、直流計測と交流計測のダイナミックレンジの違いから、交流計測用と直流計測用のプリアンプを並列してセンサーに接続する形式となっていた。しかし、この構造は、2台のプリアンプの入力インピーダンスの干渉にから、特に直流計測側で、入力インピーダンスの低下を起こし、計測感度の低下を招いていた。また、プリアンプが2台であるため、重量・サイズ・電力において多くのリソースが必要となっていた。

一方で、欧米の観測衛星では、絶縁型 DC/DC コンバータを用いたフローティング電源プリアンプが利用されてきた。これは、絶縁型 DC/DC コンバータにより、衛星から独立した電位で電力供給をプリアンプに行い、かつ、その電位基準をプリアンプの出力とすることで、電界センサーの直流電位に電力供給電位が自動追従するという方式である。この方式では、プリアンプを1つとできるため、インピーダンス低下を起こさず、更に、これを衛星からブームを用いて離れた位置に置くことで、更に高感度の計測が期待できる。

本研究では、一般にフローシング具電源で用いられている絶縁型 DC/DC コンバータではなくトランジスタを用いたブートストラップ手法を利用したフローティング電源プリアンプを提案し、性能評価を行った。この方式では、衛星内部の高圧電源から定電流を作り、この電流を用いて衛星電位と独立な定電圧を発生させ、この定電圧の電位基準をプリアンプの出力電位とする。さらに、この電位をもとに高圧電源よりプリアンプへの電力供給を行うことで、欧米型のフローティング電源プリアンプと同様の動作を意図している。この工夫により、フローティング電源における DC/DC コンバータが不要となるため、欧米型の問題点であったスイッチングノイズによる観測結果への影響を無くすことができる。また、フローティング電源方式でありプリアンプは1つであることから、従来の日本の衛星の問題点であった直流計測にお

ける感度低下も防ぐことが可能である。性能評価では、 \pm 98.5 V の間での直流応答と良好な線形性、おおよそ 3 MHz までの帯域でのフラットな周波数特性、現在運用中の「あらせ」衛星と同程度のノイズレベルであることが確認できている。本発表では、開発中の新型プリアンプについて、その概要と詳細、試験回路の性能評価の結果について報告する。

CubeSat に搭載可能な超小型・省電力なプラズマ波動受信器の開発

#頭師 孝拓 $^{1)}$, 山本 康輔 $^{2)}$, 小嶋 浩嗣 $^{3)}$ $^{(1)}$ 奈良高専, $^{(2)}$ 金沢大学, $^{(3)}$ 京都大学

Development of a Compact and Low-Power Plasma Wave Receiver Compatible with CubeSat Platforms

#Takahiro Zushi¹⁾, Kosuke YAMAMOTO²⁾, Hirotsugu KOJIMA³⁾
⁽¹National Institute of Technology, Nara College, ⁽²Kanazawa University, ⁽³Kyoto University)</sup>

In recent years, the use of CubeSats has gained significant momentum. However, due to the extremely limited resources available on CubeSats, scientific applications have been restricted to basic observational missions. On the other hand, the use of CubeSats in scientific observation offers significant advantages for mission cost reduction and the realization of multi-point simultaneous observation missions. In this study, we develop an extremely compact and low-power plasma wave instrument suitable for using in CubeSats.

To achieve miniaturization, we developed the analog circuitry for the plasma wave instrument as an Application-Specific Integrated Circuit (ASIC). The IC includes a band-limited filter, main amplifier, and anti-aliasing filter. We successfully implemented circuitry for six electromagnetic field channels within a 5 mm \times 5 mm chip. For further miniaturization and power reduction, we selected the low-power RP2350 processor for the digital components. The processor controls the six-channel analog-to-digital converters and performs Fast Fourier Transforms. Additionally, the analog circuitry was designed to allow adjustable bandwidth, dividing the entire observation bandwidth into three bands. The receiver performs FFTs on each band to calculate the frequency spectrum across the entire bandwidth. This approach enables significantly reduces the time spent in high sampling rate A/D conversion and decreasing power consumption.

In the presentation, we will shows the detailed design of the ASIC and the instrument, along with performance evaluation results of the breadboard model.

近年、CubeSat と呼ばれる $10 \text{ cm} \times 10 \text{ cm} \times 10 \text{ cm}$ を基準サイズとした衛星の利用が盛んになっている。しかしながら、衛星で利用可能なリソースが極めて限られることから、理学目的での利用は限定的な観測にとどまっている。一方で、理学観測における CubeSat の利用が可能となれば、低コストでのミッションの実現や、多点同時観測ミッションの実現など、大きな利点がある。そこで本研究では、CubeSat に搭載可能な超小型かつ省電力なプラズマ波動受信器の開発を行う。

小型化のため、プラズマ波動受信器に必要となるアナログ回路を特定用途向け集積回路として開発した。集積回路には 帯域制限フィルタ、メインアンプ、アンチエイリアシングフィルタを搭載し、電磁界 6ch 分の回路を 5~mm x 5~mm の チップ内に実現することができた。小型化および省電力化のため、受信器のディジタル部には省電力プロセッサである RP2350 を使用した。プロセッサでは 6ch 分の A/D コンバーターの制御および FFT を実行している。さらに、アナログ 回路において帯域を変更可能とし、観測帯域全体を 3~0に分け、それぞれの波形について FFT を実行することで観測帯域全体の周波数スペクトルを計算している。これにより、高いサンプリング周波数で A/D 変換している時間を大幅に短くし、受信器の消費電力を減らすことに成功した。

発表においては、専用集積回路および受信器全体の詳細な設計と、作成したブレッドボードモデルにおける性能評価の 結果を示す。

次期気象衛星ひまわり 10 号搭載用電子線計測装置 (RMS-e) の開発

#滑川 拓 $^{1)}$, 坂口 歌織 $^{1)}$, 大辻 賢一 $^{1)}$, パク インチュン $^{1)}$, 齊藤 慎司 $^{1)}$, 三谷 烈史 $^{2)}$ $^{(1)}$ 情報通信研究機構, $^{(2)}$ 宇宙航空研究開発機構

Development of Radiation Monitor for Space weather measuring Electrons (RMS-e) for Himawari-10

#Taku Namekawa¹⁾, Kaori SAKAGUCHI¹⁾, Kenichi Otsuji¹⁾, Inchun Park¹⁾, Shinji SAITO¹⁾, Takefumi MITANI²⁾
⁽¹⁾National Institute of Information and Communications Technology, ⁽²⁾JAXA

Radiation Monitor for Space weather measuring Electrons (RMS-e) is an electron detector that will be installed on the next geostationary meteorological satellite Himawari-10 to provide continuous observations of high-energy electrons in the geostationary satellite orbit over Japan. Current space weather forecasting in Japan is based on observations from the GOES satellites, which have different conditions from the space environment around the geostationary satellite orbits over Japan. RMS-e will provide continuous observations of energetic electrons in geostationary satellite orbits over Japan, which are critical for improving the accuracy of space weather forecasts in Japan.

RMS-e consists of two sets of stacked solid-state detectors (SSDs) made of silicon semiconductors called RMS-e lo and RMS-e hi. RMS-e lo and RMS-e hi are designed to measure electrons with energies in the range of 50 keV to 1300 keV and 0.8 to 6 MeV, respectively. The energy resolution of RMS-e lo is 26% for 50 keV electrons and that of RMS-e hi is 15.8% for 1 MeV electrons based on the results of electron irradiation tests performed on the engineering model (EM) of RMS-e up to last year. An improvement in energy resolution is confirmed based on the results of electron irradiation tests performed on RMS-e EM this year after implementing noise reduction measures. Qualitative confirmation of the effect of the collimator, which determines the field of view of RMS-e lo and RMS-e hi, has also been completed based on the results of electron irradiation tests.

We are currently developing a proto-flight model (PFM) of RMS-e with the aim of supplying observation data in 2029. In this presentation, we report on the development status of RMS-e and the results of the irradiation tests conducted on RMS-e EM.

RMS-e(Radiation Monitor for Space weather measuring Electrons)は、次期静止気象衛星ひまわり 10 号に搭載される予定の、日本上空の静止衛星軌道における高エネルギー電子の定常観測を行うことを目的として開発が行われている宇宙用高エネルギー電子計測装置である。現在の日本における宇宙天気予報は GOES 衛星の観測に基づいて行われており、日本上空の静止衛星軌道周辺の宇宙環境とは異なる条件のものとなっている。RMS-e による日本上空の静止衛星軌道における高エネルギー電子の定常観測の実現は、日本における宇宙天気予報を高精度化するために極めて重要である。

RMS-e は RMS-e lo、RMS-e hi と呼称される 2 つの積層シリコン半導体(SSD)センサーで構成されている。RMS-e lo、RMS-e hi はそれぞれ 50-1300 keV と 0.8-6 MeV の電子を観測することを目的として設計されている。昨年度までに 実施した RMS-e のエンジニアリングモデル (EM) に対する電子線照射試験の結果では、RMS-e lo/hi のエネルギー分解 能は 50keV 電子に対して 26%、1MeV 電子に対して 15.8% である。今年度、雑音低減策を講じたうえで、再度 RMS-e EM に対して電子線照射試験を実施したところ、エネルギー分解能の向上が確認された。また、RMS-e lo と RMS-e hi の 視野を決めるコリメーターの効果についても電子線照射試験の結果から、定性的な確認が完了している。

現在、我々は 2029 年の RMS の運用開始と観測データ供給を目指し、RMS-e のプロトフライトモデル (PFM) の開発を進めている。本発表では RMS-e の開発状況と、RMS-e EM に対して実施された照射試験の結果について報告する。

プラズマ粒子観測器向け汎用高速アナログフロントエンド ASIC の開発

#高橋 士門 $^{1)}$, 浅村 和史 $^{2)}$, 頭師 孝拓 $^{3)}$, 栗田 怜 $^{1)}$, 横田 勝一郎 $^{4)}$, 小嶋 浩嗣 $^{1)}$ $^{(1)}$ 京都大学, $^{(2)}$ 宇宙航空研究開発機構, $^{(3)}$ 奈良工業高等専門学校, $^{(4)}$ 大阪大学大学院

Development of a General-Purpose High-Speed Analog Front-End ASIC for Plasma Particle Instruments on board Satellites

 $\#Shimon\ TAKAHASHI^1$, Kazushi ASAMURA 2), Takahiro ZUSHI 3), Satoshi KURITA 1), Shoichiro YOKOTA 4), Hirotsugu KOJIMA 1)

⁽¹Kyoto University, ⁽²Japan Aerospace Exploration Agency, ⁽³National Institute of Technology, Nara College, ⁽⁴Osaka University

Simultaneous, multi-point measurements by multiple satellites are indispensable for the detailed observation of spatially non-uniform space plasma. However, the substantial resources required for multi-satellite missions have limited their implementation. Therefore, instrument miniaturization is a critical challenge to expanding opportunities for such multi-point observations. An effective solution is to implement the instrument electronics using Application-Specific Integrated Circuits (ASICs). We have been developing a high-speed preamplifier ASIC for a Time-of-Flight (TOF) type ion energy-mass spectrometer. This ASIC amplifies weak current pulses from the sensor and provides a Low-Voltage Differential Signaling (LVDS) output. Ion beam irradiation experiments have confirmed that this preamplifier has sufficient time resolution for the TOF-type analyzers. This study aims to evolve this preamplifier into a general-purpose, high-speed analog front-end ASIC applicable not only to ion energy-mass spectrometers but also to a wide range of particle instruments, such as electron analyzers, by incorporating a signal-counting function. To achieve this, we have newly designed a counter circuit, an on-chip reference voltage/current source for internal bias generation, and a Digital-to-Analog Converter (DAC) for generating an adjustable threshold voltage to discriminate signals from noise and tune the preamplifier sensitivity. In this presentation, we will report on the performance evaluation of a prototype chip integrating these new circuits.

空間的に非一様性が強い宇宙プラズマの詳細な観測においては、複数衛星による同時多点観測が不可欠である。しかし、複数衛星ミッションは非常に多くのリソースを要求するため、その実施例は限られてきた。したがって、同時多点観測の機会を拡充する上で、観測器の小型化は極めて重要な課題となる。この課題を解決する有効な手段が、観測器の電子回路部を特定用途向け集積回路 (ASIC) によって実装することである。我々はこれまで、飛行時間 (TOF) 型イオンエネルギー質量分析器用として、センサからの微弱な電流パルスを増幅し、低電圧差動信号 (LVDS) として出力する高速プリアンプ ASIC の開発を進めてきた。この高速プリアンプはイオン質量分析器を用いたイオンビーム照射実験により、飛行時間分析を行う上で十分な時間分解能を持つことが確認されている。本研究の目的は、この高速プリアンプ ASIC に粒子計数機能を追加することによって、イオンエネルギー質量分析器のみならず、電子観測器など多様な粒子観測に適用可能な汎用高速アナログフロントエンド ASIC へと発展させることである。その実現に向けて、カウンタ回路に加え、バイアスを内部生成する参照電圧・電流源回路、および信号とノイズを識別しプリアンプ感度を調整する閾値電圧を生成するDAC 回路を新たに設計した。本発表では、これら新規回路を統合した試作チップの性能評価結果について報告する。

位置検出器型の半導体検出器を用いた高エネルギー電子分析器の高感度化 #三谷 烈史 1)

(1JAXA

Concept design of high-sensitive high-energy electron analyzer using position sensitive semiconductor detectors

#Takefumi Mitani¹⁾

(1 Japan Aerospace Exploration Agency

To understand the underlying mechanisms of high-energy electron generation and loss in the Earth and planetary magneto-sphere, we are developing a compact and highly sensitive high-energy electron analyzer. The ERG (Arase) satellite, launched in 2016, is equipped with the high-energy electron analyzer (HEP), that uses silicon strip detectors to detect electrons that have passed through a pinhole. These detectors consist of segmented electrodes that divide the silicon detector into multiple channels. Each channel outputs a signal when hit by an electron, and these signals are processed using a custom-designed IC (ASIC) to measure the position and energy of the incident electrons.

However, this design has a significant constraint: the processing speed of the measurement system. The ASICs used in ERG/HEP process all channels simultaneously after receiving a signal from one electrode, which takes around 100 microseconds per energy measurement, making it difficult to measure high counting rates. Due to this constraint, we had no choice but to design a smaller opening and detector in order to reduce the number of incoming particles.

To fundamentally improve this design, our research aims to develop an ASIC that can read out multiple channels independently in parallel. The envisioned ASIC will have a lower energy resolution compared to the ASIC in ERG/HEP but still provide sufficient performance for electron measurements. Moreover, each channel will be able to process signals independently, which is a significant departure from previous designs. For example, with one silicon semiconductor detector, we would need to process signals at 8 MHz without any parallel processing. However, by dividing the electrodes into 64 segments and processing them in parallel, we can reduce the processing rate to around 125 kHz per channel.

This presentation will outline the concept design of an high-energy electron analyzer using our envisioned ASIC and present future development plans.

地球・惑星磁気圏での高エネルギー電子の生成・消失メカニズムに通底する素過程の理解を進めるために、小型・高感度の高エネルギー電子分析器の開発を始めている。2016 年 12 月に打ち上げられたジオスペース探査衛星 ERG(「あらせ」)に搭載した高エネルギー電子分析器においては、電子の入射方向とエネルギーを検出するために、ピンホールを通過した電子の検出部として半導体検出器の電極を分割した「シリコンストリップ検出器」を用い、それぞれの電極からの信号を読み出すために特定用途向け IC(ASIC)を利用することにより、入射電子が半導体検出器と反応した位置とそこで落とすエネルギーを計測した。この際に、設計の大きな制約となったのが計測系の処理速度である。これに用いたASIC は、半導体検出器の電極のどれか 1 つに信号が入力されると全てのチャンネルを同時に処理し、1 回のエネルギー計測に 100 マイクロ秒程度を要し、高計数率には向かなかった。この計測系の制約のために、開口部のサイズや検出器サイズを小さくし、入射してくる粒子の数を減らす設計とせざるを得ず、結果として、分析器の感度指標である幾何学的因子(G-factor)を小さくせざるを得なかった。

本研究ではこれを抜本的に改善するために、複数チャンネルを独立・並列に読み出すことを実現する ASIC を利用することとした。現在想定している ASIC では、ERG に用いた ASIC の方式に比べ、エネルギー分解能は落ちるものの電子計測には十分な性能を実現しうる。さらに、各チャンネルを独立に読み出せる点がこれまでと決定的に違う。例えば、1枚のシリコン半導体検出器であれば 8 MHz で信号を処理しなくてはならないところ、電極を 64 分割しそれぞれを独立・並列に処理すれば、処理すべき計数率も 1/64 の 125 kHz 程度まで下げることができる。

本発表では想定される ASIC を用いた電子分析器の概念設計を示し、今後の開発計画を示す。